IAN HORSFALL

STAB RESISTANT BODY ARMOUR

COLLEGE OF DEFENCE TECHNOLOGY

SUBMITTED FOR THE AWARD OF PhD

CRANFIELD UNIVERSITY

ENGINEERING SYSTEMS DEPARTMENT

SUBMITTED FOR THE AWARD OF PhD

1999-2000

IAN HORSFALL

STAB RESISTANT BODY ARMOUR

SUPERVISOR
DR M. R. EDWARDS

MARCH 2000

ABSTRACT

There is now a widely accepted need for stab resistant body armour for the police in the UK. However, very little research has been done on knife resistant systems and the penetration mechanics of sharp projectiles are poorly understood. This thesis explores the general background to knife attack and defence with a particular emphasis on the penetration mechanics of edged weapons.

The energy and velocity that can be achieved in stabbing actions has been determined for a number of sample populations. The energy dissipated against the target was shown to be primarily the combined kinetic energy of the knife and the arm of the attacker. The compliance between the hand and the knife was shown to significantly affect the pattern of energy delivery. Flexibility and the resulting compliance of the armour was shown to have a significant effect upon the absorption of this kinetic energy.

The ability of a knife to penetrate a variety of targets was studied using an instrumented drop tower. It was found that the penetration process consisted of three stages, indentation, perforation and further penetration as the knife slides through the target.

Analysis of the indentation process shows that for slimmer indenters, as represented by knives, frictional forces dominate, and indentation depth becomes dependent upon the coefficient of friction between indenter and sample. Analytical models are demonstrated to provide a reasonable estimate of energy absorption during and after penetration for a wide variety of knives and armour materials. The key armour parameters are shown to be the frictional interaction with the blade and the strength of the target material. The performance of knife blades is shown to increase with increasing sharpness, slimness, and surface finish. No single knife design performs best against all types of armour, and no single armour is best against all knife blades.

ACKNOWLEDGEMENTS

I would like to acknowledge the support of the Police Scientific Development Branch of the Home Office (PSDB) for supporting this work under contracts PITO 96/17/206/2/c, 98/17/038/2/c, and 99/17/139/2/c, with particular thanks to Gill Tan, Martin Pettit, John Croft, and Tim Thomas for their advice and encouragement. I would also like to thank the director of PSDB, Brian Coleman, for his kind permission to reproduce the PSDB Stab Resistance Standard For Body Armour in appendix 1 of this thesis.

I am indebted to Celia Watson, for her persistent and unending technical and moral support of both me and this research. I would also like to thank Steve Champion and Ian Harrod, for their help in completing this work.

I would like to thank David Sim of the University of Reading for his help and advice with the historical section of chapter 3.

Numerous students have contributed to related areas of this research, and I am grateful for their contributions. In particular, I would like to thank Stephanie Pollitt who started the original work, which led to this programme and without whose enthusiasm this work might never have started.

I would like to thank Mike Edwards for his extremely thorough and timely supervision of this thesis and for his help in its final preparation and presentation.

Finally I would like to thank my wife Jackie for her encouragement and patience during the long gestation period of this thesis.

CONTENTS

LIST OF FIGURES

CHAPTER 2

CHAPTER 3

List of figures continued

CHAPTER 4

List of figures continued

CHAPTER 5

List of figures continued

CHAPTER 6

CHAPTER 7

List of figures continued

CHAPTER 8

LIST OF TABLES

List of tables continued

CHAPTER 7

CHAPTER 8

APPENDIX 1

LIST OF SYMBOLS

A	Acceleration
E	Energy
E_{KE}	Kinetic energy
E_m	Energy derived from muscular effort
F	Force
F_F	Frictional force
P	Mean indentation pressure
P_0	Intrinsic yield pressure
S	Knife perimeter
V	Velocity
W	Work
Y	Measured hardness value
a	Radius of hole in plate
b	Distance from blade edge to blade axis
c	Ratio of intrinsic yield pressure to measured hardness
d	Diameter of indenter
h_0	Plate thickness
k	Shear strength
l	Depth of cut into plate edge
m	Mass
n	Sticking fraction
x	Displacement
α	Semi-angle of conical indenter or wedge
β	Sticking fraction
δ_t	Dimensionless crack opening displacement parameter
ϕ	Angle between cutting wedge motion and plane of plate
μ	Coefficient of friction
σ_0	Flow stress
σ_Y	Yield stress
τ	Shear strength

To my father, Sydney Thomas Horsfall (1933-1997),
for teaching me the value of engineering.

CHAPTER 1

INTRODUCTION

Knife attacks on police officers are not a new problem, but it was the murder of PC Keith Blakelock during the Broadwater Farm riots of 1985 which prompted official recognition of the need for protective measures. Although police fatalities from stabbing are thankfully rare the incidence of attacks on officers is sufficient to be considered to be almost routine. Anecdotal evidence suggests that there is at least one knife attack involving a police officer reported in the press each day. Official statistics indicate that there are approximately 18,000 assaults on police officers each year of which 8% are with weapons.

The knife threat is inherently variable in that the knife is propelled manually, by people with a wide variety of abilities and techniques. The definition of edged weapons may cover a wide variety of knives, tools, swords and other implements, many of which may be designed to perforate or cut specific materials or structures. Unlike ballistic armour it is difficult to specify a typical weapon which represents a worst case threat; it is only possible to determine the range of weapons and attacks which may be expected.

The field of knife resistant armour has not been the subject of many scientific studies but an extensive body of work does exist on related areas including ballistic penetration and metal forming. Some medical and forensic studies also exist on the incidence and effects of stabbing injury. These areas are reviewed in chapter 2.

Edged weapons have almost certainly been used in combat since prehistoric times. This has led to extensive development of stab, cut and impact resistant armour systems which persisted until high velocity rifles became common on the battlefield. A huge breadth of technology was developed in ancient times to combat edged weapons and this is of considerable use to the modern armour designer. Chapter 3 reviews the technology of knife resistant armour materials in two parts. In the first

part the history and technology of military armour systems is reviewed. The second part deals specifically with current commercial armour systems by reviewing recent patents in the field of personal armour.

The subject of light ballistic armour has been well studied and the interactions between these systems and typical ballistic threats are well understood. However bullets are generally blunt projectiles and are often deformed considerably upon impact. Knives differ in their extreme sharpness and small contact area. Consequently a large part of the scientific base for ballistic armour will not be relevant to stab resistant armour.

Due to the paucity of scientific knowledge on the specific case of knife penetration it is necessary to determine the key effects and mechanisms which occur in the interaction of a knife with an armour. Care needs to be exercised in order to produce conclusions that are generally applicable to the complete range of weapons and armour materials. For this reason, a study needs to be made of a variety of materials and weapons. This study is described in chapter 4 in which a drop tower test is used as the primary analytical tool. This was supplemented by stabbing tests done by hand, by an air cannon and by quasi-static tests.

There is an urgent need to determine the nature of the threat to police officers in both statistical and mechanical terms. The frequency, type and pattern of assaults need to be determined in order to identify and quantify the threat. This should include some identification of types of weapons that might be faced and their performance against candidate armour systems. Having identified the chance of an attack, it is then necessary to quantify the threat in terms of energy, velocity or momentum. Alongside this there needs to be an understanding of the medical effects of stabbing in order to determine the probability of injury or death. Chapter 5 examines the threat in terms of the stabbing ability of a number of sample populations. This is supplemented by an analysis of the characteristics of energy delivery on to the target.

A knife blade is rigid and sharp so its behaviour against a target may be similar to an indentation process. Indenter theory is well developed and might allow a prediction of the initial interaction based on the mechanical properties of the target and a knowledge of the knife tip geometry. It is not clear to what extent fracture properties such as toughness play a role in perforation resistance. In chapter 6 an attempt is made to apply indentation theory to the initial stages of knife interaction with a target

As the energy absorbed by an interaction is the product of the force and the distance over which it acts, it becomes clear that in order to maximise energy absorption the interaction distance must be maximised. This can be accomplished in two ways, the knife can be allowed to perforate and then partially penetrate the target such that energy is absorbed during the penetration process, or the armour can be allowed to deflect rearwards without perforation occurring. The latter case is particularly complex to analyse as it involves knowledge of the elasto-plastic characteristics of both the armour and its support. Although the properties of synthetic support materials could be characterised, in reality any analysis would have to account for the various different mechanical properties of parts of the human torso. The difficulty of the problem is such that it is the author's belief that it should be left for later analysis when other stages of the interaction are better understood.

The approach that will be adopted will be to examine the post perforation response of relatively rigid homogeneous armour materials. In chapter 7 the experimental results obtained in chapter 4 will be compared to analytical solutions. This is of value both in elucidating the absolute performance of armour and its response to being overmatched by the threat – a situation made more likely by the wide variety of threats from edged weapons.

The work covered in this thesis has been used by the Police Scientific Development Branch of the Home Office to develop a new test standard for stab resistant body armour (Appendix 1). It is necessary to determine the key variables which need to be addressed in a test standard and to provide data for later analysis. This is addressed in

chapter 4 which is an empirical study to examine the interaction of various armours and knives. In order to set a test standard it is necessary to quantify the threat. Chapter 5 will examine the stabbing ability of a sample population in order to determine the threat to police armour.

The main intention of the following chapters is to develop an understanding of the principal factors which affect the performance of stab resistant armour such that it will then be possible to develop armour and test systems on a scientific basis.

CHAPTER 2

LITERATURE REVIEW

2.1 INTRODUCTION

Relatively little directly applicable scientific work exists on stab resistant armour. This is particularly so when compared to ballistic armour, which has been widely studied for military purposes. Stab resistant armour is however in current service with the police forces in the United Kingdom and consequently there is at least some practical and commercial experience in the field. Despite the scarcity of scientific work in the specific field of stab resistance it is possible to identify a number of areas in which useful information may exist.

Prior to the use of firearms, soldiers were subject to stabbing attacks from swords, arrows, daggers, and spears. This led to the adoption of stab resistant armour from the very earliest periods of organised warfare. Although the scientific basis of ancient armour may be limited, the vast experience gained over the centuries has undoubtedly produced very capable and technologically advanced solutions. Consequently, many current patents show a clear line of descent from ideas which are thousands of years old.

Ballistic armour has been the subject of detailed scientific study for more than 200 years and although the penetration mechanics of high velocity projectiles may not be fully understood there is a plethora of empirical and theoretical work on the subject. Within this field there are a number of useful studies which may be at least partially relevant to knife armour.

The metalworking industry has a considerable knowledge of the mechanics of the punching, stamping and indentation of plates and sheets that may also be applied to the case of knife armour. This is complemented by studies of aspects of vehicle crashworthiness and damage resistance that may have some application to the present

work. However, it is first necessary to examine the threat to which the armour must be designed to respond.

2.2 THE THREAT

2.2.1 Patterns of stabbing incidents

There are no detailed statistics of injuries to UK police officers, but fatalities are sufficiently rare that they are all well documented. Over the period 1985-1995 a total of 29 police officers were killed in the line of duty in mainland Britain. Of these 9 were due to road traffic accidents or incidents, 8 shooting, 7 stabbing and 5 from other causes [1]. These data should not be taken to indicate the ratio of these types of incidents. For instance shooting is likely to result in a fatality in a higher proportion of cases than for other types of assault. Some studies [2,3] have shown a rising trend of stabbing injury and death over the last 30 years and concern over this increase dates back at least as far as 1966 [4]. However, more recent work [5,6] shows that over the period 1989-1997 assaults (of all types) on police officers were relatively constant (at 18,000 per year) and have in fact fallen slightly since 1991. Of the 18,000 assaults per year approximately 1000 are classed as serious, typically resulting in fractures, serious lacerations and bruising, or concussion. Approximately 1500 assaults per year involved the use of a weapon of some type although the proportion involving edged weapons is unknown.

The purpose of body armour should be to guard against injury as well as death, so it is necessary to examine the data from stabbing injury in more detail. Although no specific work exists to date on the threat to police officers or other security personnel from knife attack, there is a more general body of work on knife wounds and patterns of knife related incidents involving the general public. Rouse [7] looked at the patterns of fatal stab wounds in terms of wound types and the age of victim. A stab wound is defined as “having a greater penetration depth than surface wound width with penetration beyond the subcutaneous fat”.

A number of studies have been made of the type and location of stab wounds and particularly fatal wounds. Rouse [7] examined stab wounds according to site and found that out of a total of 69 single fatal wounds 50 were to the chest, 12 to the head and neck, and 7 to the abdomen and lower limbs. For multiple fatal wounds (81 cases), the wound causing the fatality was to the chest in 61 cases. Murray and Green [2] stated that of 27 single fatal wounds 18 were to the chest. It can be concluded from these studies that fatalities from stabbing are in the majority of cases due to chest injuries. Therefore protection of the chest will carry the highest priority if the aim is to prevent fatal stabbing attacks. A study of 92 mainly non-fatal injuries by Fligelstone [8] showed that 37 resulted in injury to the abdomen and 29 in injury to the chest. It was stated that the majority of injuries reported in the study were minor and only one fatality had occurred.

Bleetman [9,10] performed a number of studies of the medical consequences of stabbing and the consequent protection requirement for police body armour. The first study [9] analysed the injuries presented in hospital emergency admissions by ordinary members of the public and examined the likely requirement of stab resistant armour in preventing stabbing injuries. Knife wounds were analysed using the Injury Severity Score (ISS) system which is used in emergency medicine to determine the total severity of multiple injuries to a particular casualty [11]. Injuries are rated according to the Abbreviated Injury Scale (AIS) [12]. The three highest scores are squared and then summed in order to produce an ISS score. An ISS score of 16 or over is classed as major trauma and equates to a probability of survival of less than 10%. Examples of individual AIS and ISS scores are given in table 2-1.

Bleetman found that the injury mechanism of stabbing was primarily blood loss and associated complications, or punctures to the chest leading to respiratory failure. Hence lacerations to the liver, spleen, lungs or outer parts of the gut cause bleeding which has an ISS of 9. Punctures to the chest wall leading to lung collapse have a score of between 9 and 25 depending upon the exact nature of the injury. Damage to the heart and associated major arteries scores at least 16 and in some cases may be almost immediately fatal. It should be noted that the significant mechanism is the

profuse blood loss and its associated complications rather than direct organ failure. It was determined that protection should extend over as much of the torso as possible and should also cover the upper legs and pelvis if possible.

Table 2-1 Examples of AIS and ISS scores - a combined ISS of 16 is equivalent to a probability of survival of 10% or less.

Injury	AIS score	Individual ISS score
Shoulder pain (no injury specified)	0	0
Sprained wrist	1 (minor)	1
Fractured wrist (Colles fracture)	2 (moderate)	4
Head injury (unconscious less than 1hour)	3 (serious)	9
Major liver laceration	4 (critical)	16
Laceration of the brain stem	6 (maximum)	36

In a later study Bleetman [10] investigated the depth of penetration required in order to cause damage to vital organs and arteries. Whole body computer tomography scans were used to determine skin to organ distances for a group of 71 subjects. It was found that the minimum distance of vital organs from the skin surface was approximately 10mm whilst median distances were of the order of 20mm. Ultrasonic scans were performed on a group of 25 subjects in different postures (erect, supine and bent forward at the waist at 45°). Subjects were also scanned at various times in the breathing cycle. It was found that the position of internal organs could change by up to 80mm due to breathing cycle and posture. The worst case was found to be for a person in an erect posture and breath fully inspired. In this condition the lower edges of organs such as the kidneys and liver were typically 100mm below the bottom of the rib cage. Therefore armour on the torso should extend at least this far in order to provide full protection against serious injury to these organs.

One other aspect of stabbing injuries to receive attention is the presence of defensive wounds. These are wounds predominantly to the hands and arms due to the natural tendency of a victim to protect the upper body. Katkici *et al* [13] made a study of these wounds in 195 autopsies in which death was due to stabbing. Defence wounds were seen in about 50% of cases and were most often on the left hand and forearm.

In 1995 the United Kingdom Association of Chief Police Officers (ACPO) set up a study group in to investigate the requirements for national police officers uniform. The Uniform Project Group reported in October 1996 [14] after a wide ranging study of all aspects of police uniforms. In a survey of 10% of officers in England and Wales almost 82% felt a need to improve the personal protection offered by the uniform.

A further factor in police use of body armour in the UK has been the extension of the Health and Safety at Work Act 1974 to cover police forces. This imposes a duty of care upon the chief constable of each force towards individual officers, civilian employees and members of the public. This brings the police forces under the scrutiny of the Health and Safety Executive and requires police forces to carry out generic risk assessments, to apply the Personal Protective Equipment at Work Regulations 1992 (PPE), and the Reporting of Injuries Diseases and Dangerous Occurrences Regulations 1995 (RIDDOR)[6]. The PPE regulations require that suitable equipment should be issued on the basis of an objective risk assessment. Although there is still some discussion of the detailed implementation of this to the police it has had the effect increasing awareness of body armour amongst senior police officers and the staff associations representing the various ranks of police officers. The implementation of RIDDOR should have the effect of producing much more detailed information on the circumstances of assaults on police officers, which will in future allow a better assessment of the need for body armour.

2.2.2 The mechanics of stabbing

The previous section identified the statistical aspects of the knife threat to police officers. The next stage is to quantify the threat in mechanical terms as a terminal ballistics problem. One of the few directly applicable studies to have been carried out so far was that by Knight [15] in which a knife incorporating a spring balance was used to record the forces required to penetrate the skin of human cadavers. The purpose of this work was to provide evidence of the degree of effort required by an assailant. The primary aim was to determine whether it was likely that an injured

person might have caused the wound by falling on a passively held knife, a commonly used defence following homicidal stabbing.

The knife consisted of a blade attached to a transparent handle into which the blade could move against the action of a spring. This apparatus was calibrated so that the visible compression of the spring could be used to determine the axial load on the knife. This arrangement did not allow dynamic stabbing actions to be recorded so tests were performed either with the knife being pushed slowly through the skin or the cadaver being dropped onto the knife. The force required to cause a penetrating wound with a sharp knife was shown to be between 5N and 30N. It was found that skin that was tightly stretched, such as that across the ribs, required about half the force needed to cause penetration into slack skin. Once the skin was perforated the resistance to further penetration was found to be negligible. The most decisive factor in determining ease of penetration was found to be the sharpness of the blade tip. The effect of this far outweighed the effect of all other factors.

This area was further investigated by Green [3] and Jones *et al* [16], who used more sophisticated measurement techniques to confirm the earlier work, and also examined the effect of clothing. It was confirmed that blade sharpness was extremely important and that only sharp blades could penetrate clothing. Small rigid blades were found to be more penetrative than larger commando and dagger blades.

These studies of penetration showed that the skin offered a substantial resistance to penetration but once punctured the subcutaneous fat and other underlying tissue was easily cut. This has been confirmed by studies of the cut resistance of skin, [17] which were carried out in order to provide calibration data for crash test dummies.

2.3 TEST STANDARDS

The need for stab resistant armour has led to the adoption of a number of procurement standards for police body armour [18,19,20,21,22,23]. The general form of these tests is to specify a typical stab energy, and to deliver this to the target through a standard

penetrator. It is a measure of the uncertainty in this field that the 'typical' stab values adopted range from 15J to 210J, and that all the standards use different penetrators. Figure 2-1 shows some of blades currently in use in different test standards. One area in which all the methods agree is that performance is assessed in terms of penetration through the armour and/or backface deformation at a specified energy level. Unfortunately the scientific basis of these standards is often either limited or untraceable.

Figure 2-1. Various test blades, from the top PSDB N^{o}5, PSDB N^{o}1, Metropolitan Police spike, American icepick, and double sided dagger of the type used in Swiss and German tests.

2.3.1 Police Scientific Development Branch 1993 standard [18]

The Police Scientific Development Branch (PSDB) of the UK Home Office has set a standard that is widely accepted by UK police forces. This test, usually referred to as the KR42 standard, was originally defined in a study by Parker and Tan [24]. A small number of volunteers were asked to stab a high-density foam block. The terminal velocity and penetration of the knife into the block were recorded. The test was then reproduced using an air cannon launched knife to achieve the same velocity, and the mass of the knife missile was adjusted to achieve the same penetration into the target.

It was found that the maximum penetration achieved with a manual stab was replicated using a 0.4kg projectile at 14ms^{-1}; this equates to an energy of 42J. A variety of knives were tested and from these, two were selected as being the most penetrative. These were a small pocket knife blade (N^{o}1 blade, figure 2-1 second from top) and a heavy 'Bowie' knife blade (N^{o}5 blade, figure 2-1 top).

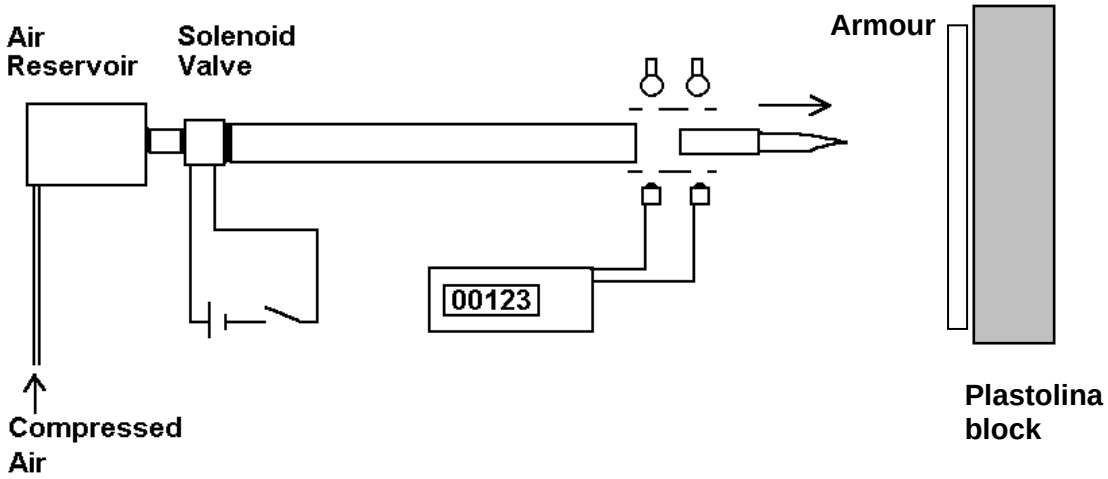

Figure 2-2. Diagrammatic representation of the PSDB (1993) test system which using an air cannon launched knife**.**

The knives are held in sabots, which allow them to be fired from the air cannon. The total weight of the projectile is 0.4kg for both blade types and a new blade is used for each firing. The muzzle velocity of the projectile is measured by optical gates and the test panel is situated 0.75m from the muzzle. The target is rigidly held against a Plastolina® block, which is conditioned according to the United States National Institute of Justice (NIJ) ballistic test procedure [25]. After the test penetration is measured directly as the blade is held in the target panel if penetration has occurred. Roma Plastilina® N^{o}1 is a soft modelling clay specified for use in the NIJ ballistic test standards, which is used in virtually all military and civilian ballistic test standards throughout the world. It is specifically not a flesh simulant but is used in ballistic tests as it approximates to the support afforded to an armour by the human body. Impacts upon the armour leave a permanent depression in the Plastolina® that can be measured as part of the test.

The standard test procedure is to fire a number of knives of the two types at the target with impact energies of 20-65J. Penetration is then plotted as a function of impact energy and must lie within a defined envelope as shown in figure 2-3. In practice there is little to be gained from test with energies below 42J as the allowable level of penetration does not decrease below 42J.

In addition to the air cannon test the armour is also subjected to an angled attack performed by hand. This is designed to test armours which utilise separate plates, the aim of the hand test is to attempt to perforate at the position and angle of attack which is most likely to defeat the armour.

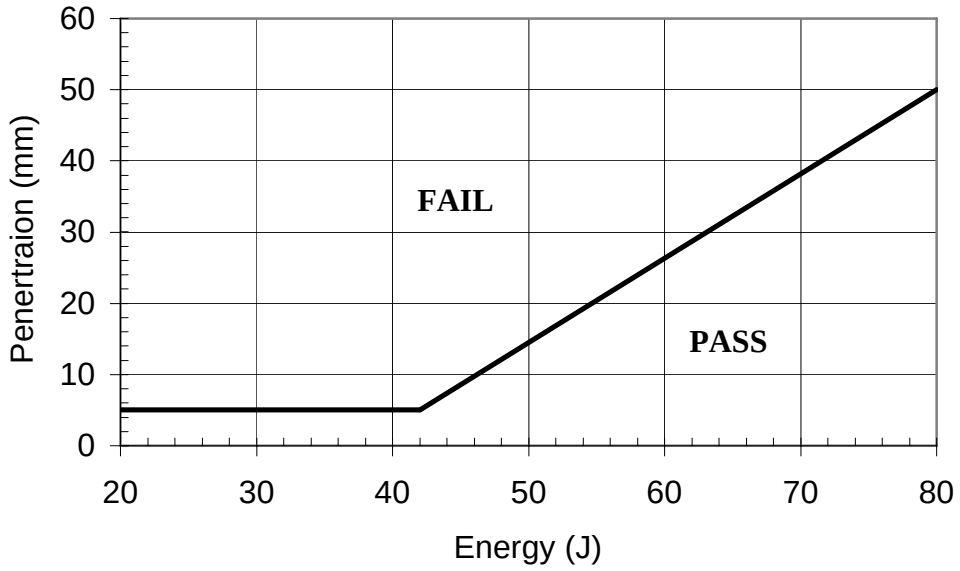

Figure 2-3. The performance criteria for the PSDB (1993) test.

2.3.2 Police Scientific Development Branch 1999 standard [23].

The 1993 PSDB standard was superseded in 1999 by a completely new test standard that was designed as a more realistic, traceable and reproducible test. The primary purpose of the new standard was to provide a scientifically based approach with both the test procedure and performance levels based on traceable data and research. The work described in this thesis formed a major part of the background for the standard. The standard is attached as appendix 1 and is preceded by a summary of the specific contributions of this thesis.

The test uses a gravity drop to propel each of two knife blade types into the target. The knife blades are manufactured by machining without hand finishing in order to minimise variability. Prior to the test the sharpness of the knife is quantitatively assessed by an indentation process that was developed from the work covered in chapter 6 of this thesis. The drop weight assembly consists of two masses connected by a sponge rubber spring that is designed to reproduce the kinetic energy delivery of a manually produced stab. The background to the development of this dual mass drop weight is given in chapter 5. Plastolina® backing was abandoned in favour of a multi-layer sponge rubber pack designed to simulate the support of a human torso. The test incorporates three protection levels to accommodate the need for armour in a variety of tactical situations. The protection level is designated by an impact energy level at which no more than 7mm of penetration is allowed. The armour is also tested at 150% of this energy level at which 40mm of penetration is allowed. The three protection levels are KR1-24J (for everyday use), KR2-33J (higher risk patrols), and KR3-43J (public order operations, forced entries etc).

2.3.3 Metropolitan Police test

This test is not an officially published standard but is used internally by the Metropolitan Police for procurement purposes. It uses a swinging arm to propel a sharp spigot into the armour sample supported on a Plastolina® backing. The spigot (figure 2-1 third from top) is a triangular section blade with each face having an included angle at the tip of 30°. The blade was designed to be reproducible, and can be manufactured to close tolerances by machining with no hand finishing. The three-sided design was adopted as it allows a very sharp tip to be produced; a conventional dagger blade has four faces at its tip, which will tend to form a chisel rather than a point. The spigot is propelled at the target material in order to provide an impact energy of 25J, the allowable penetration is 20mm at this energy level [26]. Both the energy level and allowable penetration levels are under review.

2.3.4 H. P White test [19]

This is a drop weight test, which uses the North American ice pick (a tool similar to a bradawl) as the threat. The ice pick (figure 2-1 second from bottom) is 7" (178mm) long and 0.163" (4.1mm) in diameter, the end profile is not specified but is conventionally relatively blunt. This is attached to a 40.5lb (18.37kg) mass and dropped from sufficient height to give an impact energy of 1886 inch pounds (213J). The armour test sample is supported on a Plastolina® backing conditioned in a similar manner to NIJ ballistic test procedure [25]. The impact must not penetrate the armour or cause a blunt trauma (permanent backface deformation into the Plastolina® block) of greater than 44mm. The greater impact energy in this test equates to a two handed overhead blow rather than a single-handed blow which is the basis of all the other tests.

2.3.5 Swiss and German Police tests [20,21]

These two standards are essentially the same with only minor differences in procedures. The test blade is a double-edged 'commando' style dagger blade. This is dropped onto the armour to give an impact energy of 35J with the total drop mass being 2.6kg. The armour is supported on a Plastolina® type backing block. Failure is defined as a knife penetration of more than 20mm into the backing or a blunt trauma of more than 40mm. The German standard differs in that the blade is greased before use and it is specified that the faces of the cutting edge must meet at an angle of 20°.

2.3.6 CEN draft standard [22]

This test is still in its draft form and is likely to undergo significant changes before reaching its final form. It is currently specified as a drop test using three impact energy levels of 15J, 25J and 40J respectively. Initially it was proposed to use two existing knife designs, the PSDB No1 blade and the Swiss dagger blade but this was later changed to a single sided machined blade as illustrated in figure 2-4. An unusual feature of this blade is that in order to attempt to achieve a reproducible tip shape the point has been truncated to small chisel edge.

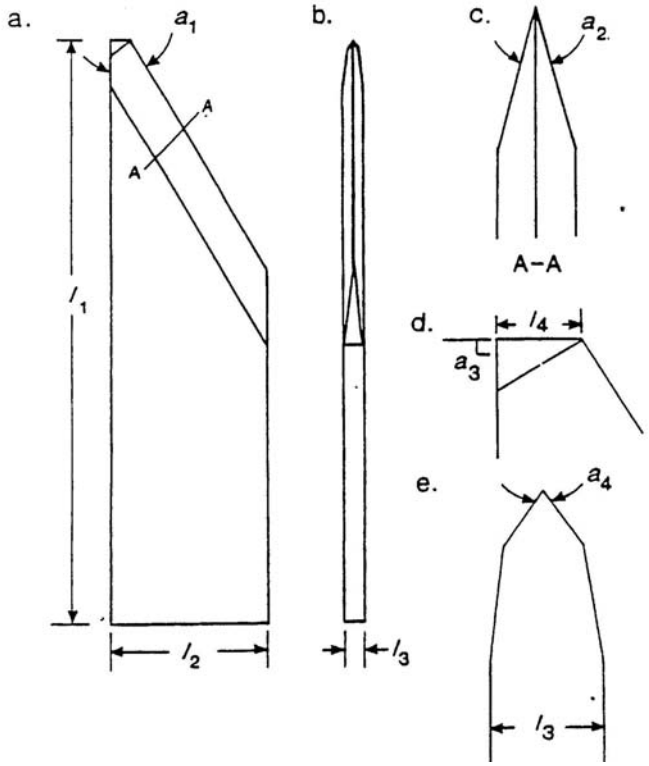

Figure 2-4. The test blade proposed in the current revision of the CEN stab resistance standard. The blade has a truncated tip that is designed to allow a specific sharpness to be achieved. (After [22]).

2.4 METAL FORMING PROCESSES

In considering the penetration mechanisms of sharp projectiles, parallels can be drawn with a number of well-documented metalworking processes. The hardness test in all its forms has been extensively studied, and parallels exist between sharp projectile penetration and the mechanics of various indentation hardness tests. Indentation mechanics have been reviewed by Tabor [27]. He showed that for spherical indenters the degree of plastic deformation and plastic zone size increases with indentation depth. However, for pyramidal or conical indenters the plastic zone size is constant relative to the indentation size. Hence indentation by conical indenters is not scale sensitive and is primarily a measure of flow stress of the indented material. Of particular interest is Tabor's analysis of the work of Bishop *et al* [28] and Hankins [29], who investigated the effect of surface friction on indentation.

Tabor showed that the force resisting penetration F by a conical penetrator is given by

$$F = \frac{P_0(1+\mu\cot\alpha)\pi d^2}{4} \qquad \text{.....(1)}$$

where

P_0	is the intrinsic yield pressure
μ	is the coefficient of friction
α	is the semi-angle of the cone
d	is the diameter of the indentation

It was noted that although a good fit to experimental data is observed the equation shows inconsistencies at very large angles. It neglects the effects of plastic flow, which would in practice lead to a non-uniform distribution of force over the cone.

For indenters with tip semi-angles in the range 45°-75° the intrinsic yield pressure P_0 can be related to the measured hardness value Y by a simple ratio denoted c. Tabor [27] showed that using the Vickers pyramid hardness test for materials that work harden the ratio P_0/Y was equal to 3.0. The intrinsic pressure can be equated to the stress at a point on the tensile stress strain curve which is representative of the average strain induced in the indentation. The best agreement of indentation hardness with tensile test data was shown to be for the stress at 8% strain[1] multiplied by the factor c. For materials which do not work harden P_0/Y =3.3 and it was suggested that the ratio c might increase as a function of decreasing cone angle or increasing friction.

Tabor and Atkins [30] performed a more detailed investigation of the effect of cone angle and showed that both c and the representative strain varied with cone angle. It was shown that for a 30° semi-angle cone c=2.87 and the representative (true) strain was 0.3, whilst for a 60° semi-angle c=2.42 and the representative strain was 0.17. These functions were found to vary in a complex fashion due to a change in deformation mode with cone angle.

[1] It is not clear from the original text whether this is true strain or engineering strain; however the difference between the two measures of strain be negligible.

For the case of a knife indenting a surface it might be expected that the applied load would increase as a function of blade cross section. However, for slim blades (analogous to a sharp indenter) the frictional loads are likely to lead to this being an underestimate by a factor of between two and three. Blades having a large and consequently rapidly increasing cross section would be expected to show larger increases in force due to indentation but less frictional effects. The opposite would be true for slim blades. Figure 2-5 shows the effect of friction on the force resisting penetration for a range of conical indenters. It can be seen that the effect of friction is to substantially increase the resistance as the cone angle decreases.

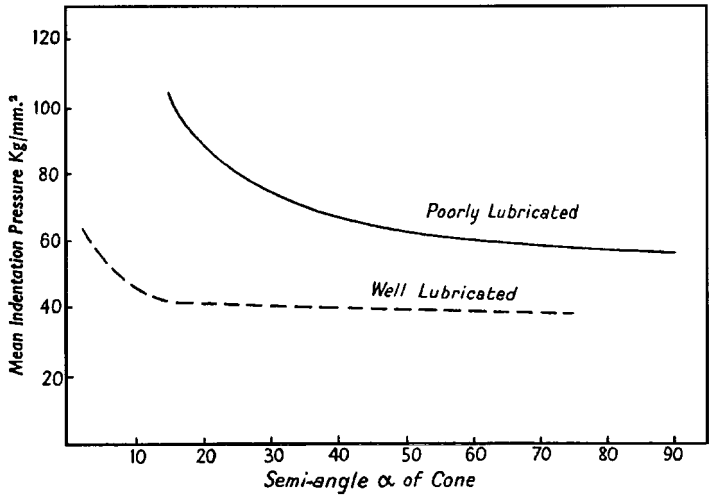

Figure 2-5. The effect of indenter sharpness on the force resisting indentation of a metallic plate. (After [27]).

Tabor [27] found that the resistance to indentation of a metal was critically dependant upon the indenter sharpness (included angle of conical indenter), and friction between the indenter and test material. Removing frictional loads by lubrication was shown to increase indentation by up to 60% for very narrow indenters. The tip of a knife blade may be regarded as an extremely narrow indenter and consequently will be subject to large effects from friction.

Another related area of metalworking technology is in the drawing and piercing of metallic sheet. Johnson and Mamalis [31] investigated the perforation of metallic sheet by sharp indenters. They found that perforation could be divided into several stages, indentation, combined indentation and localised bending, then petalling

failure, and finally sliding of the punch through the hole. It was found that for pyramidal punches with semi-angles of 45° or less, petalling, rather than plugging (shear failure of a plug of material), always occurred. This agrees well with the work of Ghosh and Travis [32] in which a conical indenter was used to pierce lead, copper and aluminium diaphragms.

A significant body of work exists on the subject of plate cutting by wedges [33,34,35]. This work is primarily used to model ship collisions particularly the case where the prow of one ship slices through the deck plates of another. The geometry which has been subject to the most study is illustrated in figure 2-6. A wedge of semi-angle 10-30° is forced through a plate from one edge. Typically the wedge is forced in at a small but finite angle to the plane of the plate such that the plate peels in one direction only. Certain assumptions are made, namely that the cut length is large compared to the plate thickness, deformation is not limited by or does not reach the edge of the plate, and the wedge is non-deforming.

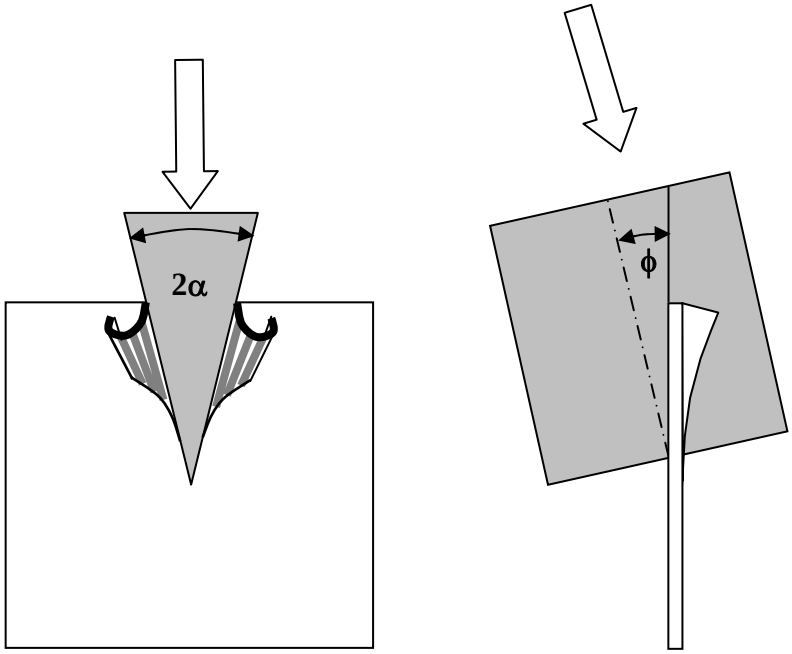

Figure 2-6. Typical geometry for wedge cutting of plate by a wedge of semi-angle α at an angle ϕ to the plane of the plate.

It is thought that, as the wedge is forced into the plate, energy is absorbed by three mechanisms, far field plate bending (usually described as global bending in ballistic work), various mechanisms at the crack tip including fracture and membrane bending and finally friction. Wierzbicki and Thomas [35] suggested that for the above geometry plate bending might account for 24% of total work, membrane work (fracture and local bending) 36% and friction 40%. Lu and Calladine [33] showed similar division of work between bending 60% and friction 40%.

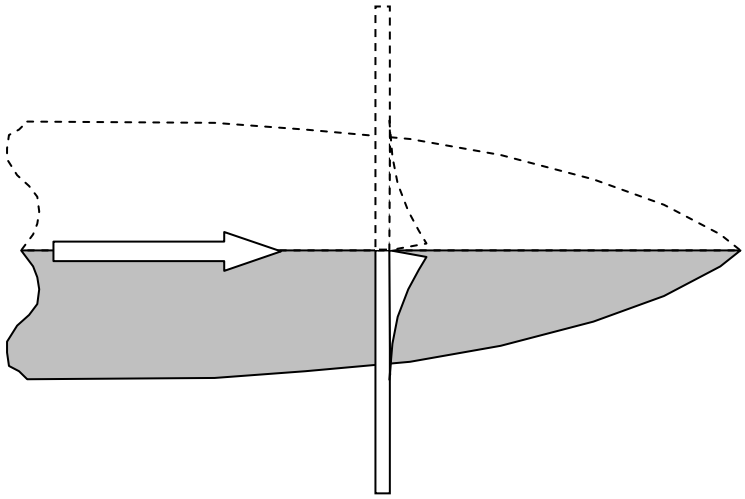

Figure 2-7. The relationship between the wedge cutting geometry (figure 2-6) and knife penetration.

This approach can be applied to the knife penetration case as the geometry is in fact similar and most of the assumptions are still valid. It is possible to consider the wedge cutting geometry (figure 2-6) as the one side of a knife piercing a plate such that the wedge action is created by the increase in knife cross section as illustrated in figure 2-7.

2.5 BALLISTIC PENETRATION

A very large body of work exists on the mechanics of ballistic penetration by projectiles. Standard texts in the field include “Impact Dynamics” by Zukas *et al* [36], whilst numerous reviews such as those of Backman and Goldsmith [37], and Corbett *et al* [38] cover the experimental and predictive techniques in the field. Of particular interest is the broad range of analytical and numerical models which have been developed for ballistic penetration; a useful review of these has been produced by Anderson and Bodner [39].

Terminal ballistics covers a very wide range of conditions, so experimental approaches have to be confined to particular regimes, whilst models almost universally rely on simplifying assumptions which have the effect of confining them also to restricted regimes. For a knife acting against a typical body armour it is possible to identify the applicable regimes and assumptions. This allows the similarities with specific ballistic regimes to be realised. For the knife armour case the following assumptions could be made;

the target is thin (relative to the penetrator diameter)
the projectile is for the most part non-deforming
the projectile shape is important
the target mechanical properties are important
the impact is at a moderate speed, therefore;
dynamic and momentum effects may occur but
dynamic effects are unlikely to dominate the process

Using this list of assumptions it is easiest to identify first those areas within ballistics which are not of immediate use. These include, the hypervelocity impact regime, approaches based on thick or semi-infinite targets, those using blunt or deformable projectiles, and momentum balance approaches. Therefore it is possible to limit an examination of ballistic studies to those which apply to thin targets and which take into account the target materials properties and projectile shape.

Some areas of ballistic penetration show clear similarities with the metal punching processes described earlier. Both fields make extensive use of work by Taylor [40] and Thomson [41] who investigated the problem of hole flanging in thin sheets. This approach was extended by Woodward [42] in order to account for the combination of different mechanisms occurring during the combined radial stretching and bending which occurs in the ballistic penetration of thin sheet.

A model has been proposed by Woodward [42] for the penetration of thin plates by pointed projectiles. This model takes the approach of Taylor [40] for ductile radial hole expansion and adds to this an extra term for the dishing behaviour (localised bending) of the plate. The original work of Taylor showed that the work done in penetrating a target was due to a purely radial material movement which formed lips on the front and back of the target (figure 2-8). Thus for a sheet of material of flow strength σ_0 (at a representative true strain = 1.0), and thickness h_0, the work done in forming a hole of radius a is given by

$$W = 1.33\pi a^2 \sigma_o h_o \qquad \text{.....(2)}$$

This model was slightly improved by Hill [43] by the application of a more accurate integration of the work done. This results in an equation for the work done in radial hole expansion

$$W = 1.92\pi a^2 \sigma_o h_o \qquad \text{.....(3)}$$

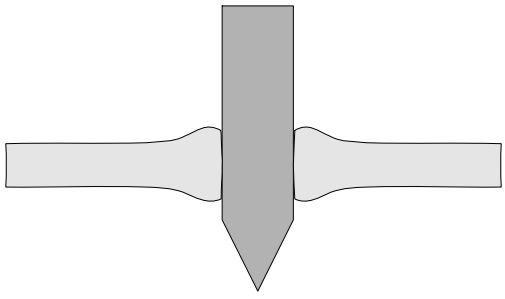

Figure 2-8. Symmetrical hole expansion as described by Taylor.

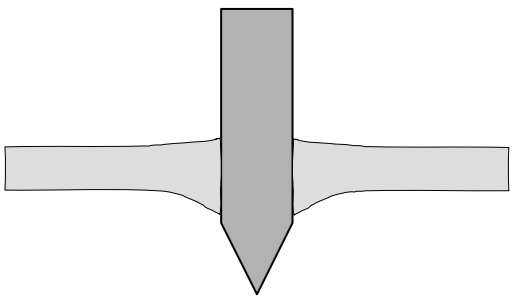

Figure 2-9. Asymmetric radial flow and hole expansion as described by Thomson.

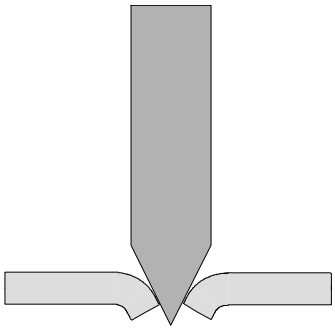

Figure 2-10. Bending and hole expansion as described by Woodward.

The Taylor model assumes that the material is both radially symmetrical and symmetrical about the plane of the target as shown in figure 2-8. However, in practice a thin target will tend to flow in the direction of projectile motion as shown in figure 2-9, and this will result in slightly different energy absorption characteristics. Woodward [42] proposed that for this dishing failure the model derived by Thomson [41] was most appropriate. This model calculates the energy absorbed in a dishing failure as

$$W = \frac{1}{2}\pi a^2 \sigma_o h_o \qquad \text{.....(4)}$$

The Thomson model describes the energy absorbed by primarily radial flow of material towards the rear target face and does not take account of any local bending of the target. Woodward proposed an extension to the Thomson model in which the energy absorbed in bending to the final form as shown in figure 2-10 was calculated. This assumed that the dish could be approximated to a beam of width $2\pi a$ and thickness h_0 with a flow stress of σ_0 such that

$$W_B = \frac{\pi^2}{4} a \sigma_o h_o^2 \qquad \text{.....(5)}$$

This was then added to the work required in dishing given by the Thomson model to give the total work in dishing of the target as

$$W = \frac{\pi}{2} a h_o \sigma_o \left(a + \frac{\pi}{2} h_o \right) \qquad \text{.....(6)}$$

Woodward showed that there was a transition from the Taylor mode (radial hole expansion) to the Thomson mode (dishing) when the hole radius became greater than 1.81 of the sheet thickness. For perforation of a thin sheet by a large penetrator the initial (Taylor mode) stage will be short-lived compared to the later (Thomson mode) stage when dishing occurs. Therefore for the purposes of knife penetration the initial stage could be disregarded without causing significant error and the Woodward version of the Thomson equation could be used for the entire process.

Although these models do not explicitly include projectile shape it is possible to account for this by calculating the work done in penetration on an incremental basis for a complex penetrator shape. This approach seems likely to yield useful results for knife penetration and will be examined in more detail in chapter 7.

The work of Zhu *et al* [44] on the ballistic penetration of aramid panels shows considerable similarity with sheet punching as discussed by Johnson and Mamalis [31]. Both these papers describe a multi-stage penetration process of three stages; indentation, perforation, and exit (sliding through) of the penetrator. In further work by Zhu *et al* [45] an analytical model was developed which calculated the forces acting on the projectile during each of these stages. The indentation stage was modelled using Tabor's method [27] as described in the section 2.4. The application of these three stages to knife penetration is illustrated in figure 2-11.

In the initial stage the knife produces an indentation in the armour and the process may be likened to that of an indentation hardness test. The resistive load at this stage will be a function of indenter shape (principally tip angle), frictional interaction with the armour, and the flow stress of the armour.

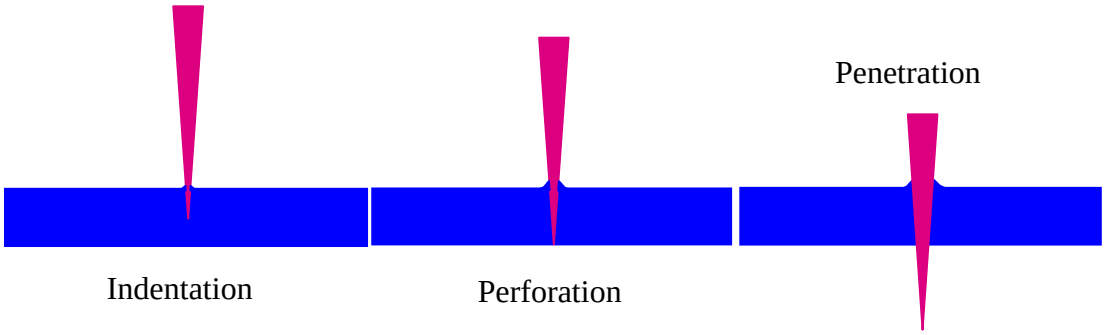

Figure 2-11. An illustration of the three stages of interaction between a knife and armour.

In the second stage the blade perforates the rear face of the armour. It has been suggested [46] that this phase starts when the plastic zone surrounding the indenter first impinges upon the rear face. This causes a reduction in the confinement of the target material so that the stress state changes from plane strain to plane stress and the plate material is able to move in the direction of the impact forming a bulge. In ballistic impacts it is generally assumed that significant energy is absorbed in forming and fracturing this bulge on the rear face of the armour. Atkins and Tabor [30] showed that for indenters with tip a semi-angle of more than 50° the deformation mode was one of radial compression concentrated below the tip of the indenter. Therefore for a projectile such as a bullet, with a nose semi-angle typically greater than 50°, deformation ahead of the projectile will form a bulge. A relatively blunt penetrator is likely to be embedded up to its full diameter in the target when the bulge is formed so the bulge is relatively large and the energy absorbed in both forming and fracturing the bulge is significant.

Examination of the tip profile of the blades shown in figure 2-1 shows typical tip angles are less than 45° in plan view and less the 20° in the plane of the blade. Atkins and Tabor [30] showed that for tip semi-angles of less than 50° there was a transition in deformation mode from radial compression below the indenter to a classical slip line deformation mode. In this mode deformation is by ‘cutting and pushing’ in which the plastic zone is confined to the sides of the indentation. As the indentation approaches a free surface the lack of deformation ahead of the indenter would result in little significant bulge formation and hence the perforation process would require

little energy. The analogy between indentation and knife penetration will not be perfect as the former is for a fully constrained system into a semi-infinite block. However, for a very slim indenter such as a knife, the result is likely to be that the perforation stage will not represent as important a part as it does in ballistic impacts.

2.6 PREVIOUS EXPERIMENTAL WORK (RMCS)

The paucity of published work on penetration by sharp projectiles has led to a requirement to determine the key experimental parameters. Therefore a long-term test programme, of which this thesis forms a part, was instituted to gather data on a number of aspects of stab resistant armour. The study included the effect of key variables, including projectile velocity, projectile sharpness, edge effects, and impact orientation. The experimental work was directed at proving the methods for data collection and determining the key experimental variables, which might effect the testing of protective clothing.

2.6.1 Drop tower

An initial study in 1993 by Horsfall *et al* [47] investigated the use of an instrumented drop tower as a method of examining the penetration process. This work concentrated on the use of thermoplastic matrix glass fibre composites although a wide variety of materials were tested, the complete work being given by Pollitt [48]. This work was subsequently re-analysed and some additional tests performed. These are reported as the initial study covered in chapter 4 of this thesis.

The first part of the work by Pollitt was to develop a dynamic test method. A dagger blade (figure 2-14, top) was selected as the test standard as it had a simple shape and was relatively sturdy. The blade was located in a Rosand IFW-8 drop tower, which allowed measurement of axial force during impact with sheet targets at speeds of approximately $3ms^{-1}$. The blade was dropped onto a target consisting of the test material clamped to the top of a plastic tube containing a ballistic simulant. This arrangement allowed relatively small samples to be used and the results were shown

to be repeatable. After the test, the ballistic simulant could be sectioned to allow penetration measurement. Quasi-static tests were also performed using the same geometry and forcing the knife through the target at a velocity of $1.6x10^{-4}ms^{-1}$ (10mm/min). Further details of these test procedures are given in chapter 4.

The test materials included a range of E-glass-epoxy composites and E-glass-Nylon composites. Glass-epoxy composites were fabricated by hot pressing of unidirectional laminates in a $[0/90]_{nS}$ layup with a fibre volume fraction of 30%. Some panels contained a single [0/90] array of tungsten wires situated centrally within the thickness of the composite. The wires were 100 micron diameter and spaced at intervals of approximately 3mm. Nylon matrix composite panels were fabricated by a proprietary process in thicknesses from 2mm to 8.8mm using a $[0/90]_{nS}$ layup of unidirectional E-glass fibres. The fibre volume fraction was approximately 50%. Further panels were of a similar construction but also contained a single [0/90] layer of tungsten wires approximately 1mm from each surface of the panel. The wires were of the same type as in the glass-epoxy composites but were at 1mm spacing.

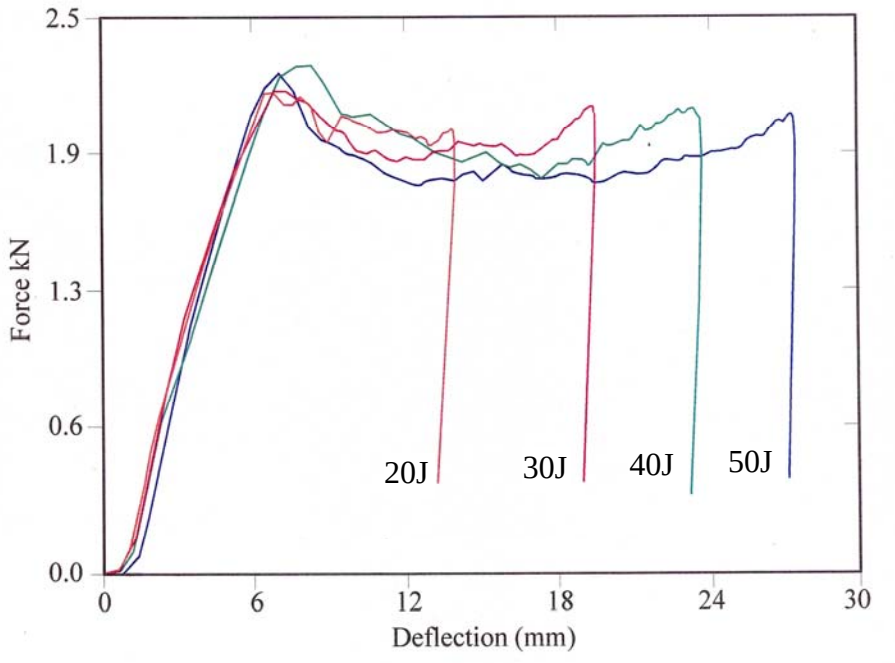

Figure 2-12. Force vs. deflection plots for impact tests on 5.8mm thick glass-Nylon composite at impact energies of 20J - 50J. After [47]

The dynamic response of the glass-Nylon composite is shown in figure 2-12. It was shown that the effect of increasing impact velocity and hence energy was to extend the force vs. deflection curve.

Quasi-static tests were performed on the same specimens and using the same geometry. It was shown that the force vs. deflection behaviour under quasi-static conditions approximated the envelope defined by the higher energy impact tests. Table 2-2 shows the correlation between penetration achieved at specific impact energy levels and the energy to achieve the same displacement under quasi-static conditions. From table 2-2 it can be seen that a good agreement is obtained between the two types of tests for the thicker panels. For thinner panels the quasi-static tests show significantly lower energies although a comparison is still possible.

The similarity of dynamic and quasi-static data was useful as it meant that armour performance could be established initially using widely available static test equipment. A single quasi-static test could be used to determine the approximate depth of penetration for a given input energy.

Table 2-2. A comparison of penetration achieved during impact tests and that achieved in quasi-static tests for various target materials. After [47]

Material	Impact energy (J)	Impact penetration (mm)	Quasi-static energy at equivalent penetration (J)
2mm Glass-Nylon	20	45	14
1.8mm Glass-epoxy	20	30	16
3.3mm Glass-Nylon	42	27	26
5.8mm Glass-Nylon	45	16	46
5.8mm Glass-Nylon-tungsten	41	11	45
4mm Glass-epoxy	40	20	43
4mm Glass-epoxy-tungsten	42	15	35

The processes occurring during penetration were similar to those observed by other workers [31,44] in which the failure processes followed a pattern of indentation, perforation then penetration. It was shown that the initial peak in the force vs. deflection plot coincided with perforation of the target.

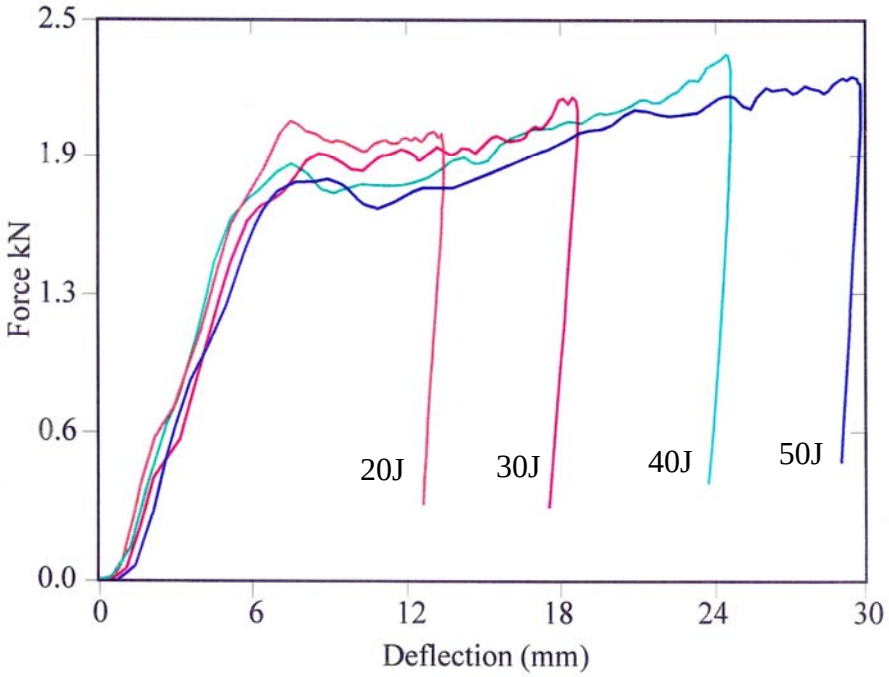

Figure 2-13. Force vs. deflection plots for impact tests on 5.8mm thick glass-Nylon composite containing tungsten wires at impact energies of 20J - 50J. After [47]

In an effort to provide better perforation resistance in the armour, tungsten wires were incorporated into panels of both the glass-epoxy and glass-Nylon composites. The presence of wires was shown to significantly reduce penetration for only a small weight penalty. The force vs. deflection plots for a glass-Nylon composite containing tungsten wires is shown in figure 2-13. Comparison of figures 2-12 and 2-13 shows that the primary effect of the wires was to increase resistance to penetration after perforation had occurred. The tungsten wire reinforced sample (figure 2-13) shows an increasing resistance force with penetration whilst for the glass-Nylon (figure 2-12) alone the penetration resistance peaks at perforation. It was suggested that post perforation resistance was a function of the force required to enlarge the perforation and frictional interaction between the knife and target, the so-called cutting and gripping modes respectively.

Comparison of glass-epoxy composites with Nylon-epoxy composites shows little difference in efficiency. The performance scales approximately with mass. However, composites containing tungsten wires do perform significantly better than the standard composites of equivalent thickness. For the glass-epoxy material, the 2x1.8mm layers had a very similar performance to a single layer 4mm thick. For the glass-Nylon composite, 2x2mm layers had a performance which lay approximately midway between that of a single 3.3mm and a single 5.75mm panel. This would tend to indicate that for these materials there is no significant performance difference between a single thick panel and multiple thinner panels of the same total thickness.

2.6.2 Air cannon

During the course of this work it became apparent that a higher velocity test would be required in order to reproduce the hand propelled stabbing action, and it was decided to adopt the air cannon method as developed by Parker [18]. Although it has been shown that for the limited range of materials there was little effect of strain rate variations (table 2-2), it was unlikely that this was true for higher velocities and for all likely stab resistant materials.

Parker [18] had determined that a typical stab velocity was 14.5ms^{-1}, and for a projectile mass of 0.4kg, this relates to a kinetic energy of 42J. The air cannon provided a suitable launch method as the velocity required is too high to be conveniently attained by a gravity drop. In most tests the air cannon was used to launch blades specified in the PSDB rest standard [18]. These blades are illustrated in figure 2-14 middle and bottom.

The air cannon was developed in a separate study by Kenyon [49]. The initial design used a 38mm calibre, which was later modified to 50mm in order to standardise with the test equipment of other workers. The study also set out to compare the air cannon with the drop tower and quasi-static tests. Two test materials were used, a 5mm thick glass epoxy composite (Fibredux-G-12-50) and a 7mm thick proprietary aramid thermoplastic composite. It was shown that the glass epoxy gave similar results on the drop tower (2-4ms^{-1}) and air cannon (10-18ms^{-1}) but showed a considerably

poorer performance in quasi-static tests ($1.6x10^{-4}ms^{-1}$, 10mm/min). During the quasi-static tests, cracking noises from fibre failure were heard, and continued even when the test was stopped. It is probable that stress corrosion processes weaken the glass fibres during relatively slow loading leading to a poorer penetration resistance.

The aramid-thermoplastic composite showed a similar pattern with the quasi-static performance being poorer than the drop tower and air cannon data. It is unlikely that this material is subject to stress corrosion and more likely that the difference was due either to viscoelastic relaxation of the matrix or variations in the coefficient of friction with strain rate.

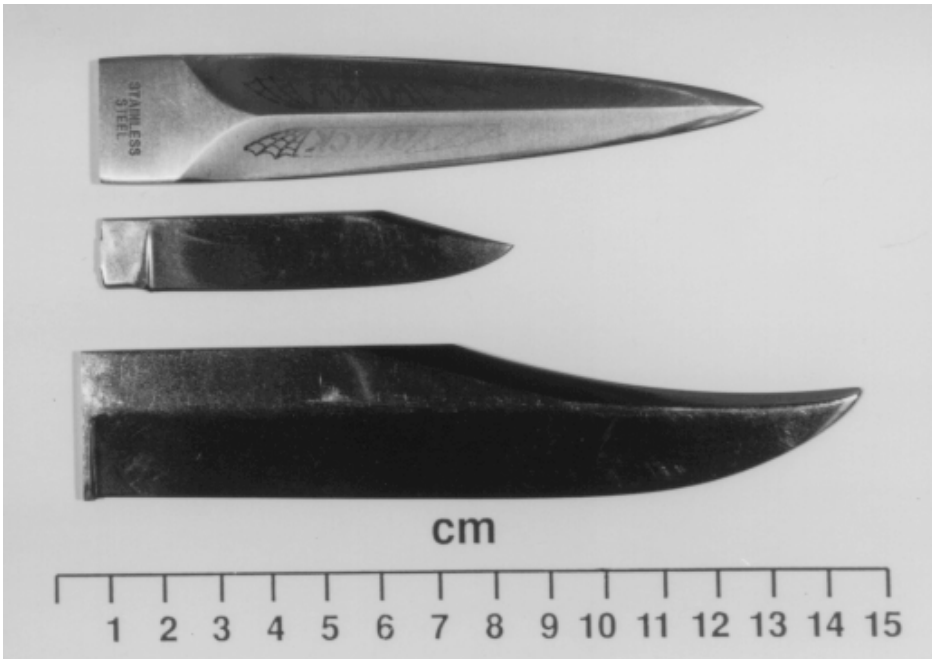

Figure 2-14. Knife types used in armour testing. From the top, these are the dagger used in drop tower testing, and in the middle and bottom, the two knife types used in the PSDB test method.

In a later study Prosser [50], used the air cannon to deliver three projectiles of different mass, but equivalent geometry, on to a proprietary aramid-elastomer composite. The velocity was varied with the mass in order to achieve the same impact energy and it was shown that with projectiles of mass from 0.4kg to 1.7kg the penetration of decreased only slightly with increasing mass.

However, the main aim of Prosser's work was to determine the stabbing capability of a sample population. An instrumented knife was produced which allowed the force and acceleration on a knife to be measured during hand delivered impact. These measurements allowed a quantitative assessment to be made of the energy, velocity and force history of a manually generated impact. The primary aim of this was to validate the energy levels and general form of test used in armour procurement standards. It was also useful in revealing more detail of the armour penetration process. This work was subsequently expanded to quantify fully both the magnitude and form of the energy delivery and is covered in chapter 5 of this thesis.

2.7 CONCLUSIONS

Based upon the work reviewed in this chapter it is possible to identify a number of areas for further study.

The threat facing stab resistant armour is not well characterised in terms of the weapon or its delivery. It would be useful to determine the magnitude of impact forces and energy during the impact. More detailed information on the characteristics of energy delivery, the variability of the threat and the effect of human factors including age, weight, height, and sex, would aid in an understanding of the requirement for stab resistant armour. This will be investigated in chapter 5 of this thesis.

The effect of weapon variables such as shape, sharpness and surface finish should be assessed as this will determine the validity of test methods and show the range of threats that an armour should resist. An experimental programme to provide data on a range of knife blades and armour materials is described in chapter 4.

The performance of stab resistant armour is generally assessed in terms of resistance to penetration, but small levels of penetration are allowed in several test standards and it is also customary to determine the performance over a range of energy levels.

Hence it is important to understand each stage of the interaction process. It would appear that the interaction follows several stages; indentation, followed by perforation then further penetration as the knife slides through the armour. Each of these stages needs to be studied with a view to gaining an understanding of the critical parameters controlling both knife and armour performance.

In chapter 6 the indentation and perforation stages are investigated further, whilst the later stages of penetration are examined in chapter 7. The penetration process will be investigated and compared to analytical models based on wedge cutting of plates and the ballistic approach of Woodward [42].

2.8 REFERENCES

1. UK Roll of Honour, http://www.ps2.com/jm/ukroll/honour.htm, 1998.

2. L. A. Murray and M. A. Green, Hilts and knives a survey of ten years of fatal stabbings, *Med. Sci. Law*, **27**, 3, 182-184, (1987).

3. M. A. Green, Stab wound dynamics-a recording technique for use in medico-legal investigations, *J. Forens. Sci. Soc*, **18**, 161-163, (1978).

4. C. G. Stalker, Stabbings, *J.Law Soc Scotland*, January (1966).

5. B. Brown, Assaults on police officers: An examination of the circumstances in which such incidents occur, Police Research Group, No 10, Home Office Police Department, London, (1994).

6. Officer Safety: Minimising the risk of violence, Her Majesty's Inspectorate of Constabulary, (1997).

7. D. A. Rouse, Patterns of stab wounds: a six year study, *Med. Sci. Law*, **34**, 1, 67-71, (1994).

8. L. J. Fligelstone, R. C. Johnson, M. H. Wheeler and J. R. Salaman, An audit of stab wounds in Cardiff, *J. R. Coll. Surg. Edinb*, **40**, 147-170, (1995).

9. A. Bleetman, Safety standards for body armour, Police Federation of England and Wales, Public Order Working Group, (1996).

10. A. Bleetman, Determining the protective requirements of stab-resistant body armour: The vulnerability of the internal organs to penetrating edged weapons, *Proc.Sharp Weapons Armour Technology Symposium*, Cranfield University, Shrivenham, (1999).

11. D.W.Yates, Assessment of the severity of injury, *In Scientific Foundations of Trauma*, (Ed G. C. Cooper, H. A. F.Dudley, D. S. Gann, R. A. Little and R. L. Maynard), Butterwoth Heinemann, Oxford, 448-455, (1997)

12. J. D. States, The abbreviated and the comprehensive research injury scales, In *Proc, 13th STAPP Car Crash Conference*, Soc. Auto. Eng, Warrendale, 282-284, (1969) in [11]

13. U. Katkici, M. S. Ozkok and M. Orsal, An autopsy evaluation of defence wounds in 195 homicidal deaths due to stabbing, J. Forens. Sci. Soc, **34** , 4, 237-240, (1994).

14. Uniform Project Group, Report to ACPO Autumn Conference, October (1996).

15. B. Knight, The dynamics of stab wounds, *Forensic Science*, **6**, 249-255, (1975).

16. S. Jones, L. Noakes and S. Leadbetter, The mechanics of stab wounding, *Forens. Sci. Int*, **67**, 59-63, (1994).

17. C. M. Careless and P. R. Acland, The resistance of human skin to compressive cutting, *Med. Sci. Law*, **22**, 2, 99-106, (1982).

18. G. Parker, PSDB Stab resistant body armour test procedure (1993), Police Scientific Development Branch, Publication No 10/93, (1993).

19. Sharp instrument penetration of body armour, H.P White Laboratory, HPW-TP-0400.02, (1988).

20. Technical guidelines for lightweight personal armour, Schweizerische Polizeitechnische Kommission, (1992).

21. Technical guidelines for personal armour, Technical Commission AK11, Research and Development Department for Police Technology, Munster, (1994).

22. Protective clothing -Body armour-Part 3:Knife stab resistance – Requirements and test methods (ISO/DIS 14876-3:1999).

23. M. J. Pettit, J. Croft, PSDB Stab resistance standard for body armour (1999), Police Scientific Development Branch, Publication No 6/99, (1999).

24. J.Tan, G.Parker, Stab resistant vests (Part 2), Police Scientific Development Branch, Publication No 20/92, (1992).

25. Ballistic resistance of police body armour, National Institute of Justice Standard 0101.03, US Department of Justice, (1987).

26. P.Fenne and S. Winslade, Metvest – the customer aspects, *Proc. Sharp Weapons Armour technology Symposium*, Cranfield University, (1999).

27. D. Tabor, *The Hardness of Metals*, Clarendon Press, Oxford, 95-114, (1951).

28. R. F. Bishop, R. Hill and N. F. Mott, The theory of indentation and hardness tests, *Proc. Phys. Soc*. **57**, 3, 147-159, (1945).

29. G. A. Hankins, Hardness tests research, report on the effects of adhesion between the indenting tool and the material in ball and cone hardness testing, *Proc. Instn. Mech. Engrs*, **1**,611-645 (1925).

30. A. G. Atkins and D. Tabor, Plastic indentation in metals with cones, *J. Mech. Phys. Solids*, **13**, 149-164, (1965).

31. W. Johnson and A. G. Mamalis, The perforation of circular plates with four-sided pyramidally-headed square-section punches, *Int. J. Mech. Sci*, **20**, 849-866, (1978).

32. S. K. Ghosh and F. W. Travis, An investigation into the static and dynamic piercing of diaphragms, *Int. J. Mech. Sci*, **21**, 1-22, (1979).

33. G. Lu and C. R. Calladine, On the cutting of a plate by a wedge, *Int. J. Mech. Sci*, **32**, 4, 293-313, (1990).

34. W. Q. Shen, K. W. Fung, P. Triantafyllos and N. M. Wajid, An experimental study of the scaling of plate cutting, *Int. J. Impact Engng*, **21,** 8, 645-662, (1998).

35. T. Wierzbicki and P. Thomas, Closed-form solution for the wedge cutting force through thin metal sheets, *Int. J. Mech. Sci*, **35**, 3/4, 209-229, (1993).

36. J. A. Zukas, T. Nicholas, H. F. Swift, L. B. Greszczuk and D. R. Curran, In *Impact Dynamics*, John Wiley and Sons, New York, (1982).

37. M. E. Backman and W. Goldsmith, The Mechanics of Penetration of Projectiles into Targets, *Int. J. Engng. Sci*, **16**, 1-99, (1978).

38. C. G. Corbett, S. R. Reid and W. Johnson, Impact loading of plates and shells by free-flying projectiles: A review, *Int. J. Impact Engng*, **18**, 2, 141-230, (1996).

39. C. E. Anderson and S. R. Bodner, Ballistic impact: The status of analytical and numerical modeling, *Int. J. Impact Engng*, **7**, 1, 9-35, (1988).

40. G. I. Taylor, The formation and enlargement of a circular hole in a thin plastic sheet, *Quart. J. Mech. Appl. Math*, **1**, 103, 103-124, (1948).

41. W. T. Thomson, An approximate theory of armour penetration, *J. Appl. Phys*, **26**, 80-85, (1955).

42. R. L. Woodward, The penetration of metal targets by conical projectiles, *Int. J. Mech. Sci*, **20**, 349-359, (1978).

43. R. Hill, Plastic deformation of non-uniform sheets, *Phil. Mag, Ser*. 7, **40**, 971-983, (1949).

44. G. Zhu, W. Goldsmith and C. K. H. Dharan, Penetration of laminated kevlar by projectiles-I. Experimental investigation, *Int. J. Solids Structures*, **29**, 4, 399-420, (1992).

45. G. Zhu, W. Goldsmith and C. K. H. Dharan , Penetration of laminated kevlar by projectiles-II. Analytical model, *Int. J. Solids Structures*, **29**, 4, 421-436, (1992).

46. S. N. Dikshit and G. Sundararajan, The penetration of thick steel plates by ogive shaped projectiles – Experiment and analysis, *Int. J. Impact Engng*, **12**, 3, 373-408, (1992).

47. I. Horsfall, S. M. Pollitt, J. A. Belk and C. Angood, Impact Perforation Testing of Stab Resistant Armour Materials, *Impact and Dynamic Fracture of Polymers and Composites*, ESIS 19, (Ed. J. G. Williams and A. Pavan), Mechanical Engineering Publications, London, 433-442, (1995).

48. S. M. Pollitt, An investigation into body armour to protect against knife attack, 45 Degree Course Student Project, Royal Military College of Science, (1993).

49. R. Kenyon, An investigation into body armour to protect against knife attack, 46 Degree Course Student Project, Royal Military College of Science, (1994).

50. P. D. Prosser, An investigation into body armour to protect against knife attack, 48 Degree Course Student Project, Royal Military College of Science, (1996).

CHAPTER 3

SURVEY OF KNIFE ARMOUR TECHNOLOGY

3.1 INTRODUCTION

Although the scientific understanding of stab resistant body armour is somewhat limited a wide variety of commercial designs is being sold and used at the present time. In addition to this body armour designed to resist edged or pointed weapons has been used by warriors since prehistoric times [1]. Therefore it is useful to review the available technology in both contemporary commercial products and historical records. In this chapter a review of ancient armour is conducted based upon historical and archaeological records, while current technology is discussed on the basis of published patents.

3.2 HISTORICAL TECHNOLOGY

The use of historical data in the development of modern armour systems is not without precedent. During the First World War the United States Government formed the Helmets and Body Armour Division under the command of Dr Ashford Dean, the first curator of the Department of Arms and Armour, Metropolitan Museum of Art, New York. His chief assistant was Carl Otto Kretzschmar von Kienbusch, probably the foremost American collector of arms and armour of his time. Their knowledge of historical systems was used in the development of ballistic armour for American soldiers [2].

Armour has been a feature of soldier's equipment since the earliest periods of organised warfare. The first records of armour use in warfare date back to the third millenium BC but there is evidence of offensive weapons in the eighth millenium BC [1] and it is likely that the history of armour is of similar antiquity. Although the development process was almost purely empirical, the vast experience gained over

thousands of years has led to a variety of highly effective armour systems. The protection required by a contemporary British police officer can be compared first to that required by soldiers in the classical Greek period. Tactics adopted during the 4th century BC led to a requirement for armour capable of resisting attack from short stabbing spears [3]. This led to the development of both armour and tactics to counter such a threat. Records exist of a wide range of different armour designs; Herodotus [4] documents the armour of the army of Xerxes in some detail. This included a wide range of armour materials including articulated metal plates, a variety of woven materials, and animal skins. Thus, aside from the invention of mail by the Celts [5], the main structural types of all subsequent armour had by this time already been defined. The following two and a half millennia of development has simply resulted in refinement of designs and the application of better materials.

Some caution is required when examining the historical evidence of ancient technology. There are surviving examples of solid plate armour from as long ago as the second millennium BC [5] but most other types of armour which embody natural materials such as leather have not survived. Therefore the historical evidence relies heavily upon funerary monuments, illustrations, carving, and some ancient texts, the accuracy of which is unknown. It should also be remembered that writers such as Herodotus were to some extent entertainers and accounts may have been embellished for the entertainment of the audience. Attempting to reconstruct or analyse ancient technology from such sources might be compared to attempting to determine current motor vehicle technology from television advertisements. For instance numerous illustrations and carvings from the Middle Ages show what is called banded mail [6]. This is shown in some illustrations to be extremely flexible and probably highly penetration resistant judging from its widespread usage. However, no examples of any such system exist and no reconstruction has successfully reproduced the illustrated appearance and properties. Significant effort has been put into recreating and analysing banded mail [6,7], although it has been suggested [8] that banded mail does not actually exist but is simply an artists representation of normal mail.

The first documented use of body armour was by the ancient civilisations of Mesopotamia from approximately 2500BC [1]. Development of armour to resist sharp weapons was more or less continuous from that time up until the 17th century AD when the widespread use of the firearms made body armour temporarily obsolete. From that time until the present day the military research shifted towards ballistic body armour which has become commonplace again only in the last decade. In the following section the major technical advances in body armour are traced for the five and a half millennia over which it has been developed.

Figure 3-1. Part of the `Standard of Ur` a lapis lazuli and shell inlay on the sound box of a lyre from the third millenium BC. The foot soldiers are wearing studded cloaks and lamellar skirts probably of cured leather or metal plates. (The British Museum, WA 121201)

3.2.1 Mesopotamia and Assyria, 2500BC-500BC

The historical record of armour extends back to approximately 2500BC to the earliest civilisations of Mesopotamia and the Middle East. 'The Standard of Ur' (Figure 3-1) shows troops wearing studded cloaks and wearing copper or bronze helmets. They also appear to have armoured skirts which may be composed of metallic or leather

lamellae. These plates hanging from the waistband are sometimes referred to in later texts as lambrequins [6]. These are very similar to examples of lamellar armour which were used by the Assyrian civilisations and later the by Romans (figures 3-2 and 3-3). It is also interesting to note that the use of armour in the third millenium BC was accompanied by the first development of armour piercing weapons with battle axes being constructed with blunt edges to cause shear failure of armour. Armour technology was only slightly refined over the next 1000 years and it was not until the rise of the Assyrian civilisations towards the end of the second millenium BC that significant developments occurred.

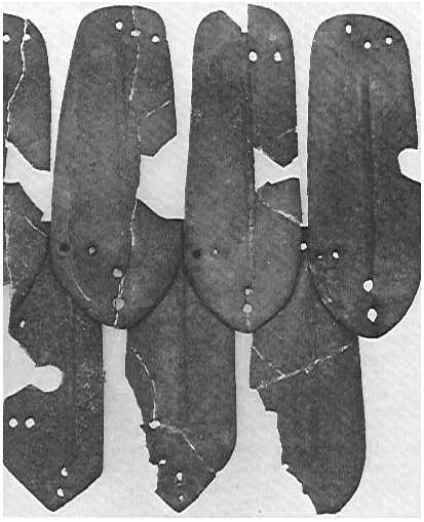

Figure 3-2. Egyptian bronze lamellar armour segments 14th century BC. (The Metropolitan Museum of Art, New York from [10])

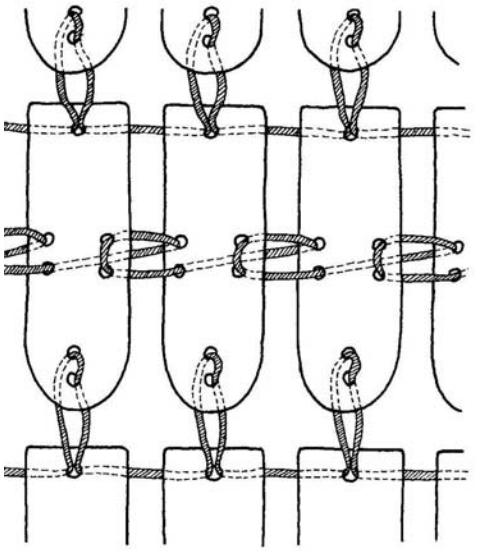

Figure 3-3. Method of joining lamellar armour, cords would be drawn tight to close the gaps in the finished armour. (After Bengt Thordeman from [12])

The Assyrian empire was the predominant power in the Near Middle East from the 10th until the 7th century BC, and under the rule of Tiglath-Pileser III (745-727BC) formed what was probably the first standing army the world had ever seen. During the relatively early period of the Assyrian civilisation the use of lamellar armour became common. This consisted of rectangular bronze plates riveted to a leather backing garment, and examples of these plates still survive as shown in figure 3-2 and a similar system is depicted in figure 3-4. The use of small plates joined to or

embedded in a flexible backing was a major advance and was retained by various armour designers until the Middle Ages. Variously known as scale, lamellar, and jazeraint armour this pattern was also adopted in the Brigandine of the 15th century AD. The scales could be riveted on the inside or the outside of the garment or sandwiched in quilted pockets.

Figure 3-4. Bas relief of an Assyrian cavalryman in the reign of Tiglath-Pileser III wearing a tunic of lamellar armour. (The British Museum, WA 118907)

3.2.2 Greece 1500BC – 500BC

During the classical Greek period metalworking technology and the armourer's craft made significant advances. An appreciation of this period is helped by the wealth of contemporary texts, illustrations and artefacts which have survived. Primitive tubular bronze breastplates are known to have been fabricated from the middle of the second millenium BC but they are likely to have been too unwieldy for battlefield use.

A more refined breastplate (cuirass) is shown in an illustration from a 6th century BC amphora (figure 3-5). The illustration shows Penthesilea Queen of the Amazons being killed by Achilles. Achilles is wearing a metal cuirass and a full helmet, and carries a shield. The shaped cuirass depicting torso musculature, known as the muscle cuirass, is known to have existed since the 8th century BC and was subsequently used by the Romans. It seems likely that the intricate work and advanced technology required to produce such artefacts made them extremely valuable and they were

probably made to measure for high ranking individuals. Likewise it is probable that the flexible lamellar armour and later mail designs were often generic and could be fitted to any soldier. Hence a rich individual would have a rigid but perfectly fitting armour whilst the ordinary soldier would have a flexible but more universally sized tunic.

Figure 3-5. Illustration from an amphora (530 BC) showing Achilles killing the Queen of the Amazons. Achilles is wearing a shaped metal cuirass. (The British Museum, BM 210)

From the 7th century BC through to the 5th century BC the use of the shield supported along the arm was introduced, and together with the use of well-drilled infantry in the phalanx formation this reduced the need for body armour. The best-drilled infantry such as the Spartan Hoplites appear to have discarded metallic body armour in favour of light but often voluminous cloaks. It has been suggested [9] that such cloaks might form an effective barrier against lighter blows, some designs being pleated or laminated to increase their strength. During the 4th century BC body armour again started to appear in Athenian service although it is conspicuously missing from

illustrations of Greek mercenaries fighting in the army of Alexander the Great, possibly due to the hotter climates in which operations were conducted.

During the same period there is evidence [6] that the Assyrians used quilted linen armours and similar designs are known to have been worn widely by Egyptian soldiers [10]. Quilted armour has little effectiveness against a strong thrust from a point but should act as a good energy absorber, thus it would be effective against slashing blows or purely light kinetic energy input such as from an arrow at extreme range. In the Middle East the archer was still a major part of an army whilst spears of various sorts predominated in Greece. Therefore it might be argued that lightweight armour was retained for defence against arrows whilst heavy plate armour was retained for the greater protection required against spears. There is a reference to the Assyrians using helmets of an interlaced or interwoven form at the battle of Marathon, which might be either mail or a basket weave of plates.

3.2.3 Rome 400 BC – 200AD

In terms of armour technology the next main advances occurred with the rise to power of the Roman civilisation from the 4th century BC onwards. The Romans were particularly adept at assimilating their enemy's technology and the best ideas of Rome's adversaries were gradually absorbed into the equipment of the Roman army. It is thought that the first mail was probably produced by the Celts possibly during the 4th century BC and was standard equipment in the Roman army by the middle of the 3rd century BC. Figure 3-6 shows a fragment of Roman mail, each link consisting of a circular piece of iron wire which has been hand riveted at its join. This can be compared in figure 3-6 to a modern welded stainless steel mail from a current stab resistant armour.

During the period of Rome's dominance from the early republican era (6th – 1st century BC) to the later imperial era (1st century BC - 4th century AD) armour technology gradually evolved. In addition to this, the type of armour used by Roman soldiers appears to have varied according to their particular role on the battlefield, the region (and climate) of service, and their individual wealth.

During the early republican period body armour primarily consisted of the cuirass (or Lorica) which consisted of both front and back plates joined by straps over the shoulders and sides. Below this lamellar armour plates were suspended to protect the pelvis and thighs. However this degree of armour was probably only worn by heavy units such as cavalry and spearmen who were generally the wealthier individuals. During the latter part of the republican era the lower order troops appear to have adopted the mail shirt whilst scale armour supplanted the cuirass of higher ranking individuals. Also during this period it appears that bronze was gradually replaced by iron.

Figure 3-6. An example of 2nd century Roman mail found at Arbeia Fort, South Shields (top right) compared to a modern stainless steel mail (bottom left). The Roman fragment is of riveted construction whilst the modern example is a welded type. (Roman mail example courtesy of D.Sim.)

During the imperial period the soldier's armour changed to a segmented plate type (Lorica Segmenta). This consisted of a number of metal plates joined by leather straps and hinges to form a segmented tubular covering of the torso with overlapping plates at the arms and shoulders as shown in figure 3-7 [11]. This design is to some extent the forerunner of all subsequent articulated armour systems.

Figure 3-7. A section of Trajan's column showing troops in Lorica Segmentata. (Victoria and Albert Museum from [11])

3.2.4 European armour 200 AD 1200 AD

During the first millenium AD relatively little development of armour technology appears to have occurred. Mail, lamellar and quilted textile armour were variously adopted by a succession of powers in Europe and the Middle East. The ordinary foot soldiers were often equipped with a padded tunic known variously as a Gambeson, Byrnie, Aketon, Haqueton, Wambais, or Wams as shown in figure 3-8. These employed a similar technology to that of earlier Egyptian types, usually based on quilted linen with a fibrous filling such as wool or flax. Some Byzantine cavalrymen (900 –1100AD) wore padded jackets over lamellar armour [12] which appears to be the reverse of normal practice.

The Norman period is of interest as it is relatively well documented particularly in the Bayeux tapestry in which at least 8 types of armour are represented. During the 11th century AD the long coat of mail or Hauberk became popular. This was usually worn over the quilted Gambeson which provided protection against blunt trauma.

Mail was produced in a variety of forms for both protective and decorative purposes. Most mail is of the riveted variety as illustrated in figure 3-9. Each link is produced from a circular segment of wire which was flattened and pierced at its ends and then riveted together. This is a laborious process and there is considerable debate over how such apparently large quantities were produced. However mail is likely to have been an expensive item which was probably recycled from earlier garments where possible.

Figure 3-8. The author wearing replica armour from the 15th century. The gambeson has a leather outer cover with wool padding and a linen lining. The coif is of riveted mail and is shown with a contemporary skull cap helmet. (Replica armour courtesy of D.Edge, The Wallace Collection)

Mail is primarily used to resist slashing attack and possibly arrows. Against a sharp point such as a sword tip or slim arrow tip it is less effective as it does not spread the load beyond the single link which is struck. A point acts as a wedge when striking the chain links and tends to force open and break the individual links. Heavier links allow larger gaps making the armour vulnerable to slimmer knives and arrowheads. In order to achieve good protection against slim blades or arrowheads the individual

links need to be small and hence are made from relatively thin wire that is easily cut or broken.

Figure 3-9. The bottom edge of a 15th century German coat of mail showing brass links along the lower edge and iron links above. (The Wallace Collection, A2)

Most mail is of a four-link type in which each link passes through four others. It is possible to produce a stronger variety by passing each link through six others but this significantly increases the difficulty of manufacture and the weight. An alternative method of increasing the strength of the mail is to increase the relative thickness of the link material as shown in figure 3-10 [8]. In it heaviest form, called double mail, the holes within links are mostly obscured. Mail of this type is often constructed from flat washer-like links rather than wire.

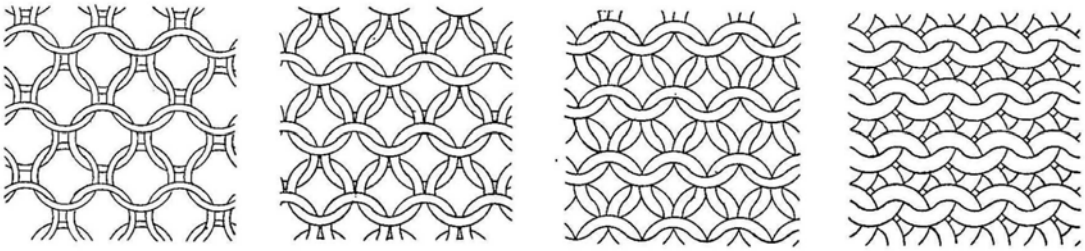

Figure 3-10. Increasing ring thickness with a constant outside diameter (from left to right) so that the gap within each ring is reduced. The rightmost picture shows a thick wire or washer type ring which is sometimes known a double mail and which has no visible apertures. (After [8])

It is also possible to reinforce mail by a variety of methods including threading of bars or wire between links, using rings incorporating cross bars (Indian bar link or theta mail), or substituting bars and plates for links (Japanese mail figure 3-11). It is generally thought that Japanese mail and similar types from India were designed to allow better cooling than the standard four-link mail commonly used in Europe.

The armour of the Far East should not be ignored. Bronze casting was introduced to China in the second millenium BC and was used for both monolithic breastplates and various scale armour designs. The remarkable finds of the terracotta army, dating from the 3rd century BC, have provided a significant amount of information on armour designs of the period. The majority of the terracotta warriors wear scale armour consisting of relatively large overlapping plates joined by silk cord. It is known that armour consisting of bronze plates was extensively used, as was armour of cured leather. One other unusual Chinese armour system was composed of multiple layers of rhinoceros hide and was used in the 9th century BC.

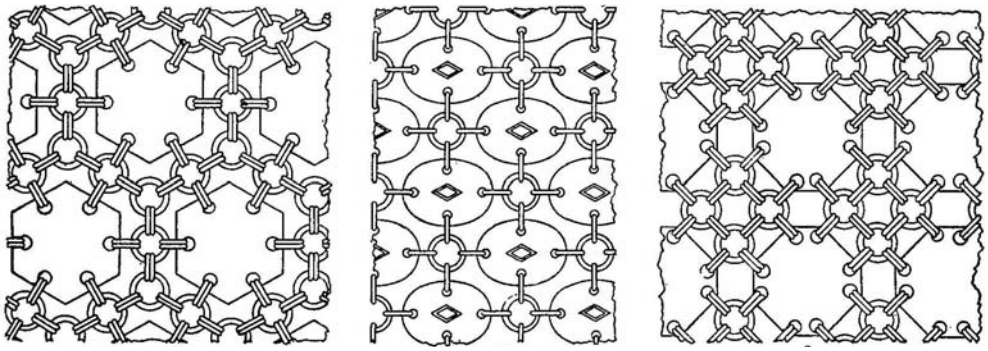

Figure 3-11. Japanese mail consisting of plates joined by mail links. (After [8])

3.2.5 The medieval knight 1200 AD – 1600AD

The most common view of ancient armour is of the medieval knight clad in all encompassing plate armour. By the 12th century AD mail garments often covered the entire body except the face. A surcoat or jupon was often worn over the armour and some sources suggest that this may have been padded to provide increased slash protection. From the 12th century onward there was a trend to reinforce this mail by

the addition of plate armour in either iron or cuir broulli. Cuir brouilli is cured leather which is formed to shape whilst wet, and then hardens upon drying. Such armour is known to have existed since at least the second millenium BC as it was recognised as an effective and readily formable plate material. The use of steel in place of iron and bronze allowed highly penetration resistant armour to be produced at a manageable weight. Therefore during the 12th and 13th century the amount of plate armour increased. In Europe by the end of the 14th century almost complete coverage of the body by plate had been achieved. Such suits of armour, or harnesses, were worn by the mounted knights whilst footsoldiers continued to wear either quilted, jazeraint, or scale armour or mail. One observation made of armour in general was that the knights armour of one period became the foot soldiers' armour of the next, armour being handed down or captured in battle and re-used by the less wealthy.

Plate armour of the 14th century generally aimed to make the left side of the knight impenetrable to weapons of the period whilst the right side was slightly less well protected in order to preserve movement and save weight. Considerable skill was exercised in producing armour which not only covered the body well but also used shape, and reinforcements to maximum effect. Plate edges were protected or designed to deflect blades and all gaps in articulation were closed by mail or so well mated as to prevent penetration[6].

By the 16th century the use of both handguns and cannon made the armourer's job more difficult and full armour became confined to the tournament. Although it was possible to produce musket resistant armour, the weight penalty was excessive and armour became limited by practicability rather than aiming for impenetrability. The lighter troops were protected by a brigandine whilst the breastplate alone was retained by pikemen and heavy cavalry. During the 17th century the Cromwellian army returned to one of the oldest armour types, the buff coat being the contemporary parallel to the hide armour of prehistoric warriors. The buff coat was often supplemented by a breastplate to provide additional protection to the torso.

Although some armour was retained in military service well into the 20th century, body armour was largely abandoned during the 18th century as rifle and artillery technology increased. Plated armour was issued to some troops or bought privately during the First World War and the Nylon-fibre based flak jacket was issued to aircrew during the Second World War. Current body armour to resist handguns is made from high strength polyethylene and aramid textiles although the garment design is not dissimilar to that used by Greek infantry of three thousand years ago.

3.3 A REVIEW OF PATENTS

In order to examine current body armour technology a search was conducted on patents in the areas of stab protection and body armour. Most of the patents discussed are intended for stab resistant body armour with some having been developed for protective gloves or containment of debris from explosions. All relevant entries for knife armour have been included while ballistic systems have only been included where they have unusual or notable technology. These entries are tabulated in table 3-1 at the end of this chapter.

3.3.1 Plate Armour

The simplest type of armour consists of one or more rigid plates. These have the advantage of high levels of protection against both penetration and blunt trauma. However their lack of flexibility reduces comfort and useable coverage area. Large armholes are required to give full shoulder movement to the wearer and most of the abdomen has to be left uncovered if the armour is to allow the wearer to sit down.

Monolithic ceramic or composite plates are often used for rifle protection and most military armour is provided with pockets on the chest and back to take such plates. The coverage of such plates is usually restricted to the centre of the chest and back. This covers the vital organs and also marks the centre of mass of the torso, which is the usual aim point of an attacker. Although monolithic plate armour is known to have been marketed as a stab resistant system, very little has ever been used and none has been officially issued to police forces.

Flexibility can be introduced by using several plates with hinges or some other form of articulation along their edges. Figure 3-12 shows a design [13] consisting of titanium metal plates bonded to an aramid cloth. Figure 3-13 [14] shows a similar concept which utilises a protected hinge arrangement at the plate edges.

3.3.2 Scale Armour

Scale armour consists of numerous small rigid plates that are flexibly joined to produce some degree of flexibility in the garment. A large proportion of knife armour patents refer to methods of articulating these plates in order to produce flexible systems. Individual plates may be loosely riveted together [15][16] as shown in figures 3-14 and 3-15. This may be compared to figure 3-4 which shows Assyrian scale armour

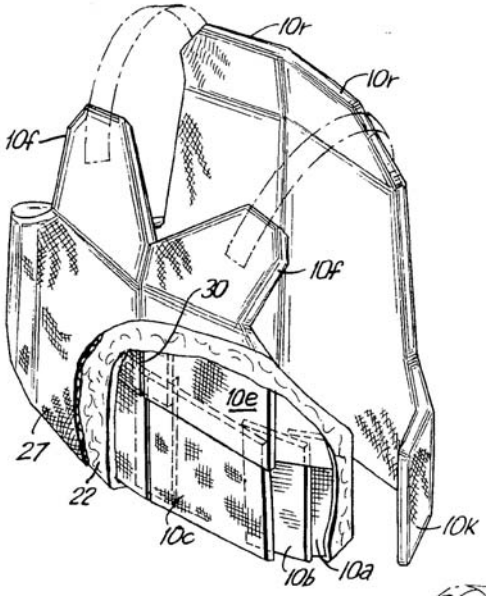

Figure 3-12. Plate armour consisting of titanium panels bonded to flexible aramid backing [13].

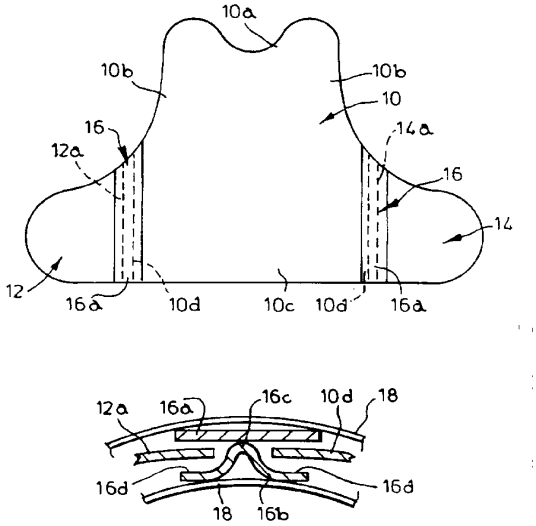

Figure 3-13. Plate armour design using multi-layer protection over hinges at plate edges [14].

Figure 3-15 also illustrates the use of a flexible backing material to provide additional location and support to the plates. The backing, typically an aramid textile, has an additional function of providing ballistic protection. Aside from the use of an aramid backing this appears to closely resemble the description of scale armour described in section 3.2.

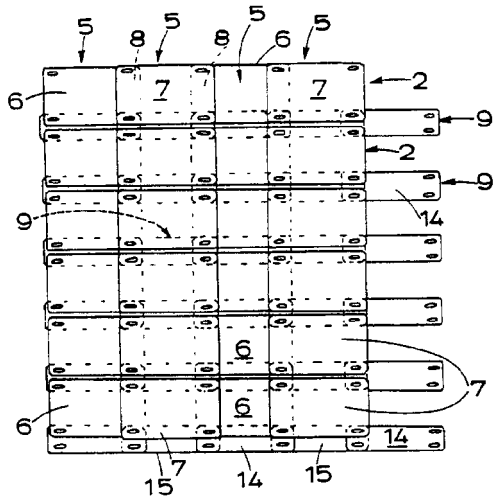

Figure 3-14. Scale armour consisting of small plates joined loosely by rivets [15].

Articulation can also be provided by placing the plates in pockets within a textile carrier [17]. Figure 3-16 shows a design that utilises small plates in pockets formed between several layers of fabric. This arrangement provides flexibility to the armour system but does not allow in-plane compression. When the wearer adopts a seated position the armour will be forced up into the neck by the wearer's thighs unless it can be compressed. One method of providing this compressibility is to hang the individual plate in staggered pockets so that they may slide over each other [18]. Figure 3-17 illustrates a system of relatively large titanium plates held in individual pockets. The main disadvantage of pocketed systems is the poor protection provided against angled strikes.

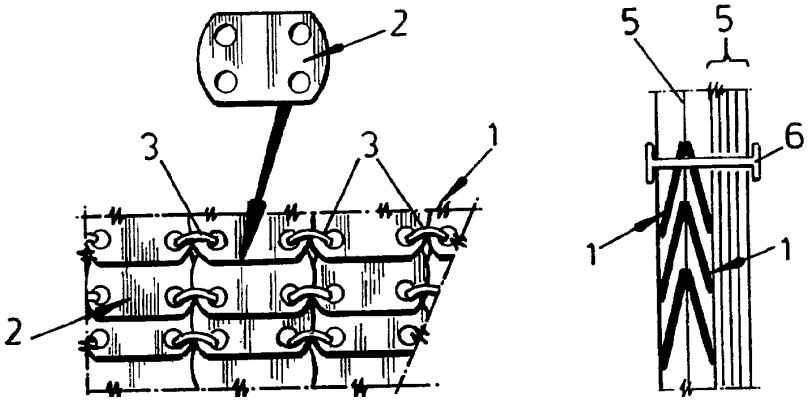

Figure 3-15. Scale armour of small plates joined to each other and to a flexible backing [16].

The main limitation to scale armour is the vulnerability of the plate edges. Multiple layers have to be used in order to provide an impenetrable array [19]. Figure 3-18 shows a typical arrangement of square plates to screen all the gaps. Simply screening the gaps is not sufficient to prevent penetration of the armour. There is a tendency for a knife to tilt each plate as it is struck and to defeat each successive layer of plates. This can be avoided by providing turned up lips on the plate edges as illustrated in figure 3-19. This illustrates an armour consisting of discs riveted to both sides of a textile panel.

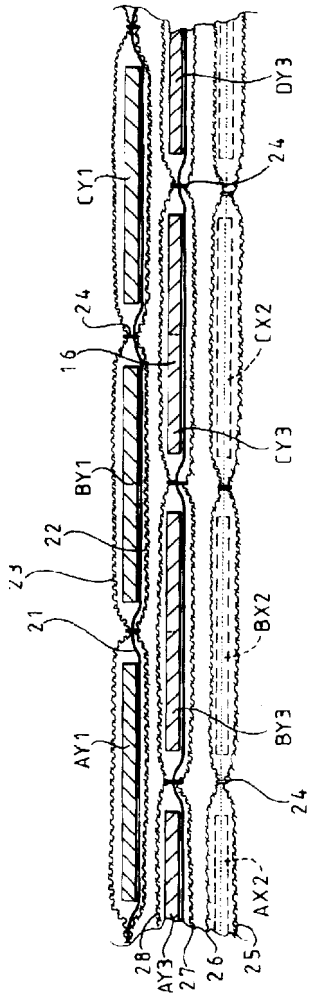

Figure 3-16. Rigid plate sewn into pockets formed between textile layers. A plan view of this armour is shown in figure 3-18 [17].

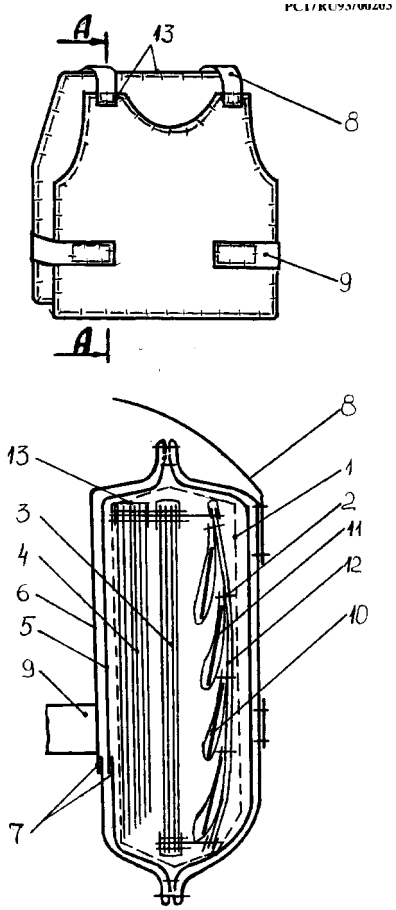

Figure 3-17. Plates hung in pockets so that the pack can concertina as the wearer bends forward [18].

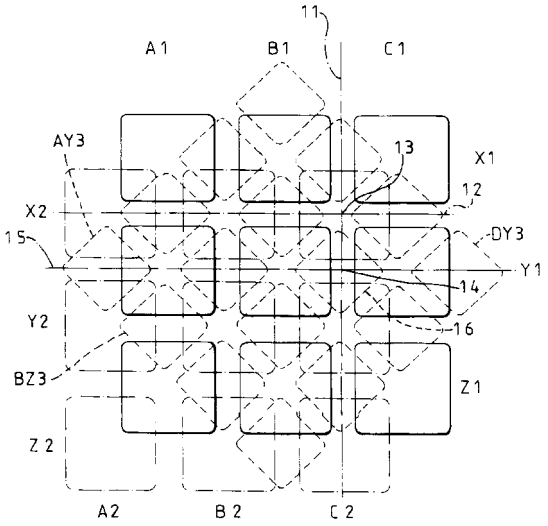

Figure 3-18. Plan view of the armour in figure 3-16 showing how 3 layers are required to provide full coverage.

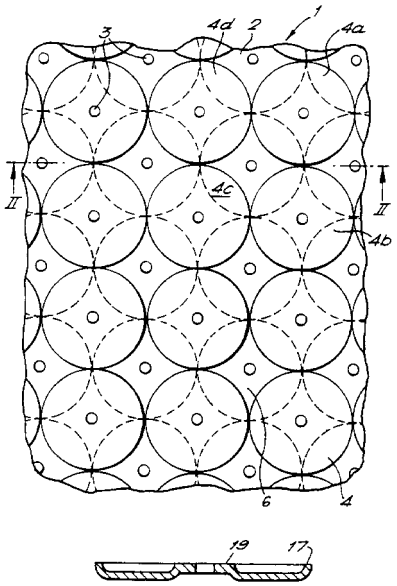

Figure 3-19. Disc shaped armour elements riveted to each side of a textile carrier. Disc edges are lipped on their forward edges to capture a blade tip.

There are also systems which lock the plate edges together mechanically [20] shown in figure 3-20. This is one of several similar designs that use hexagonal aluminium plates with pegs and holes combined with overlapping edges. This locking only allows the plates to bend in one direction, concave towards the wearer. This produces a very trauma resistant system, but with limited flexibility.

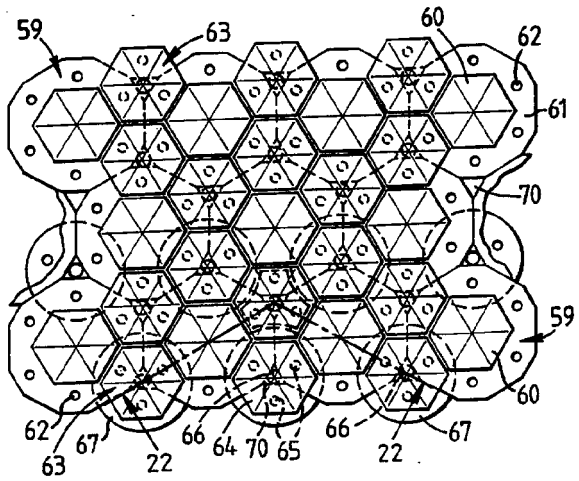

Figure 3-20. Scale armour consisting of two types of hexagonal aluminium plates which mechanically lock together to provide good edge protection [20].

In all plate armour designs the plate edges are particularly vulnerable. There is a tendency for a knife to slide across the plate surface until it reaches an edge, so that the blade is steered towards the weakest part of the armour. A novel approach to this problem is to wrap the individual plates with a cut resistant fibre or wire so that the knife is trapped and prevented from sliding [21] as illustrated in Figure 3-21. A similar effect can be provided by drilling small holes in the armour plates so that the blade tip is trapped and prevented from sliding across the plate surface [22]. This has the added bonus of decreasing the armour weight and introducing some possibility of breathability in the garment.

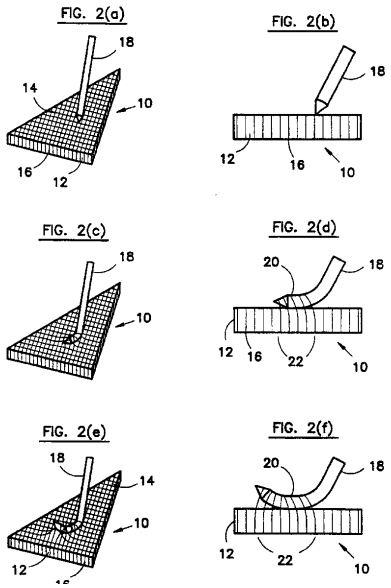

Figure 3-21. A fibre wrap over the individual plates traps the tip of a knife blade [21].

3.3.3 Flexible armours

Several patents show methods of producing intrinsically flexible armour. One method is to use fabric of cut resistant threads or wires [23,24,25 ,26]. This may also be used in multiple layers to increase protection or in order to reduce orientation dependent weaknesses in the fabric. Most of these designs feature metallic threads or woven cords which incorporate metallic threads such as that illustrated in figure 3-22. A particularly novel approach is to use interlocking spirally wound wires [27] as illustrated in figure 3-23.

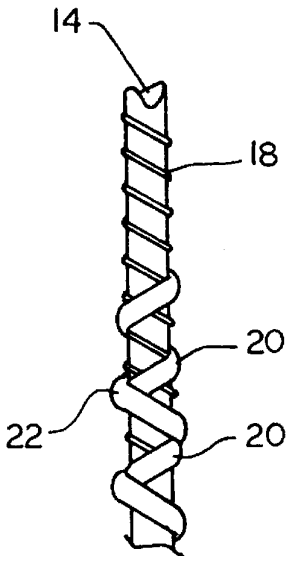

Figure 3-22. A cut resistant fibre consisting of a core strand 14 and outer wrap 20, 22 of aramid or polyethylene fibre with an inner wrap 18 of stainless steel wire [24].

A further approach is to take a conventional fabric and coat it with or embed it in a flexible matrix. This has the effect of constraining the fibres or other cut resistant elements so that the weave is not parted by a sharp implement. Systems have been proposed which use fibres coated with an elastomer [28], and mail [29] or small platelets [30] embedded in an elastomer. There are also patents for fabric covered with layers of abrasive particles [31,32] to further increase penetration resistance and cause damage to the weapon.

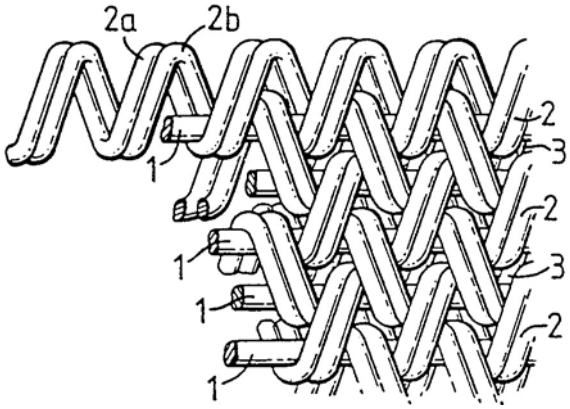

Figure 3-23. A design for a flexible explosion debris barrier consisting of interlocking spirally wound wires or rods [27].

An alternative method of introducing flexibility is to use thin flexible metallic sheets [33,22,34] which may be of stainless steel or titanium. This obviates the need for protection of joints but the flexibility is in only one axis at a time so double curvature is not possible. Foil may also be incorporated by producing a plain weave of foil strips [35], which significantly enhances flexibility over monolithic foil armour.

3.3.4 Mail

A few systems using mail have been found in the patent survey [36,29] although it is probably difficult to suggest an invention of sufficient novelty to gain a patent. Mail armour has been covered in some detail in the preceding section on historical technology. The primary difference between modern mail armour and its ancient predecessors is the use of materials such as stainless steel or titanium as well as the use of welded links.

3.4 DISCUSSION

From the preceding sections it can be seen that stab resistant body armour has a considerable technology base both historical and contemporary. A wide variety of systems exist which offer different answers to the compromise between protection and comfort. The majority of armour designs now available have existed since the second millenium BC and it is surprising that some of the patents have been granted given their obvious resemblance to ancient systems.

In examining the technology and use of armour in ancient civilisations it is possible to draw a number of conclusions which are of relevance today. When armour was used the first area to be protected was always the head; protection was next afforded to the front of the torso and then to the back. The limbs were generally the last area to be protected. This is in good agreement with current medical opinion [37,38], and both military and police practice, as the protection is afforded in the order of likely severity of injury to that area.

Where ultimate protection was required it was achieved by using solid plates. There was a considerable comfort and mobility penalty but this can be alleviated if the armour fitted well. Articulated plates offer probably the next best solution and a wide variety of types have been used which allow plates to hinge or slide over each other with movement of the wearer. Small plates attached to a flexible backing have been shown to offer both penetration resistance and blunt trauma protection. It seems not to matter whether the plates are in front, behind or within the textile layers and the choice seems to have been mainly determined by fashion. Mail offers a good compromise of flexibility and protection but it needs to be heavy to afford good protection and it is expensive to make.

It appears to have been recognised by armourers since the earliest of times that padding can play an important role in armour. Apart from improving comfort to the wearer, padding behind the armour spreads impact loads and may increase penetration resistance. The aim of the armour is to absorb energy and this is the product of the resistive force and the displacement of the armour in the direction of impact. Therefore it is possible to improve the energy absorption by allowing greater displacement. Taken to its ultimate degree this means that armour of low penetration resistance can be effective against some threats providing that it can deform sufficiently. Armour consisting of padding alone has been used since the very earliest times. Where greater protection was required padding was often used both behind and in front of mail and scale armour.

Cloaks and surcoats have been used throughout most of history. Although aimed partly to entangle sword slashes, these may also have been be effective kinetic energy traps designed to absorb the energy of an incoming missile or sword. A modern embodiment of the surcoat is shown in figure 3-24 [39] but it is unclear how this might be integrated with current police uniforms.

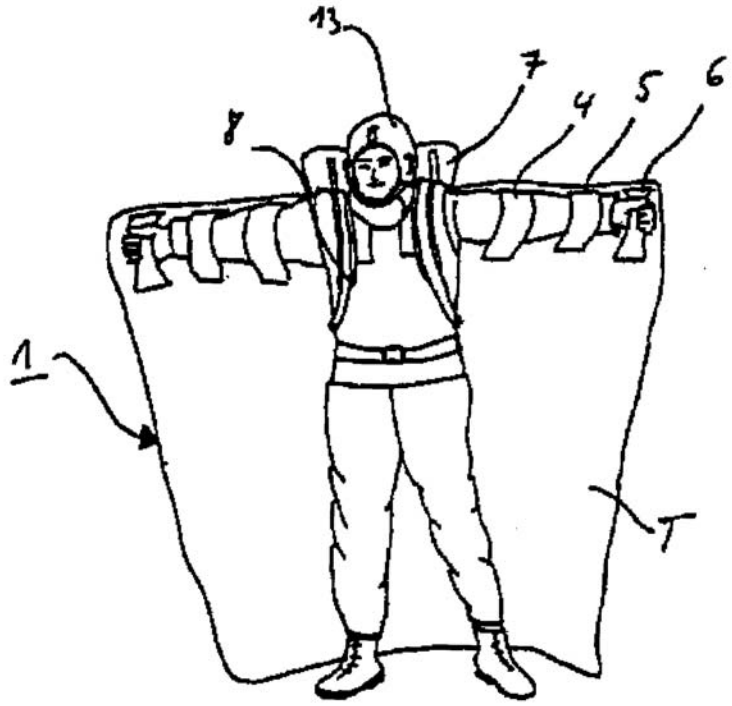

Figure 3-24. A proposed ballistic armour system (circa 1996) embodying some of the features of the medieval surcoat [39].

In the patented technology there is a number of plate, scale and padded systems similar to those described in the historical section. Plates and scales have been manufactured from a number of metals including titanium, aluminium, and various steels, although exposure to body fluids and moisture tends to favour the use of stainless steel. The exact grades and alloys used are not usually given but ease of fabrication and price is likely to be a major deciding factor. Titanium alloy such as Ti-6Al-4V is known to be used in some systems whilst commercial purity grade 2 titanium is often favoured on cost and formability grounds even though its strength is lower than that of Ti-Al-4V. No information is given on choice of aluminium or stainless steel grades.

A number of coated or embedded fabric systems have been patented. The main reason for this approach appears to be to restrain the fibrous elements from movement in order to force the knife to cut rather than displace the weave. Given the earlier

discussion on the effects of flexibility on energy absorption it can be seen that a careful balance must be achieved between in plane constraint and out of plane flexibility. Of particular note are the textiles coated with abrasive particles. Any system that can maximise frictional forces on a penetrating knife is likely to reduce penetration. Surface damage to the knife its cutting edge and point will also significantly reduce the penetration into the backing layers.

3.5 CONCLUSIONS

A study of stab resistant materials should cover a sufficient breadth of systems as to show how stab resistance varies with material and structure type. The materials of interest should include metals such as aluminium alloys, stainless steel, or titanium, and a fabric armour of some type. Purely textile armours seem unlikely to offer sufficient resistance to penetration but coated systems, which restrain strong fibres in a flexible matrix, may be of use.

From the investigation of injuries covered in chapter 2 and the use of ancient armour it is possible to deduce that the torso and lower abdomen should be provided with protection against stabbing. This protection will minimise the risk of death or serious injury with a minimum mobility penalty. If the aim is to prevent injury then almost all the body needs to be protected. Particular attention has to be given to the arms as these are likely to be injured whilst attempting to protect the rest of the body.

Some investigation of armour flexibility and or backing stiffness should be carried out. It appears that flexibility may be a major asset to armour for reasons of comfort and penetration resistance. The effect of flexibility will however be determined partially by the support afforded to that armour, be it padding, the human body or a test material such as Plastilina®. The combined effect of support and armour flexibility should be investigated providing that sufficiently flexible and penetration resistant armour can be obtained.

3.6 LISTING OF KNIFE ARMOUR AND RELATED PATENTS.

The following table lists patents relevant to stab resistant armour technology. It is not an exhaustive list but does cover most of the designs that are or have been in recent production. Only one patent is listed where multiple patents from different national bodies apply and patents of the same technology with minor differences have been omitted. The table lists the year of publication, number, assignee and inventors. The main subject of the patent is then specified as K-knife, B-ballistic or O-other. Those entries in bold are referred to in the text of section 3. A note is made in the last column of technology from companies or organisations thought to be armour manufacturers and therefore likely to have produced commercially available products.

Table 3-1. Patents relevant to stab resistant armour.

Year	Number	Assignee/ Inventor	Type	Description and comments
1989	GB2235929	ICI/Savage, Rogers, Taylor	K/B	Rigid material- Composite material composed of unidirectional fibres in a polymer matrix (Probably APC2)
1989 [23]	JP 1-244299	TEJIN Ltd	K/B	Flexible material Knitted fabric of stainless steel wires with polymer sheet between layers
1996 [19]	US 5,515,541	Sacks, Jones	K/B	Scale Flexible sheet with discs attached to each side
1994	US 5,364,679	Groves	B	Flexible material Material containing hemispheres
1992	US 5,087,516	Groves	B	Flexible material Layers of beads confined between textile
1996	CA 2152663	Pacific Safety Products/ Field, Soar		Soft body armour The assignee is an armour manufacturer
1995	GB 9519467	Lorica Logistics Ltd	K	Body armour The assignee is an armour manufacturer
1997 [14]	GB 2,303,534 A	TBA Textiles Ltd		Hinged plate armour The assignee is an armour manufacturer
1994	GB 9416356	Pentith GRO	K/B	Body armour
1994	GB 9411077	Windridge		Body armour, pocketed plates
1994	GB 9401716	Courtney		Body armour for lower torso

Table 3-1 continued

Year	Number	Assignee/ Inventor	Type	Description and comments
1992	GB 9225708	Buchanan	O	Fastening for armour The assignee is an armour manufacturer
1992	GB 92722	Dowty Armour -shield		Body armour The assignee is an armour manufacturer
1981	GB 81197	Lightweight Body Armour Ltd		Body armour The assignee is an armour manufacturer
1993 [17]	EP 611943	Meggitts Ltd/Davey	K	Knife armour material The assignee is an armour manufacturer
1992 [15]	WO 92/13250	Munyard/Buchanan		Riveted plate armour The assignee is an armour manufacturer
1986	EP 230702	PA Consulting/ Petty-Saphon	O	Improved silk based material
1997 [24]	US 5,632,137	Kolmes, Plemmons	K	Cut resistant yarn including metal wires.
1997 [25]	US 5,628,172	Kolmes, Plemmons	K	Cut resistant yarn, non metallic
1993	US 5619748	Safariland/ Nelson, Price	B	Polyethylene ballistic armour The assignee is an armour manufacturer
1997	FR 2738996	Cie Euro Dev Ind Sarl/ Le Carpentier	K/B	Flexible body armour using textile and plates
1996 [26]	EP 0,769,671 A2	Meggitts Ltd/ Mcallen	K	Flexible material of unidirectional metal strands on flexible support The assignee is an armour manufacturer
1995	US 5614305	Virginia Tech/ Paine, Rogers	B	Composite material containing shape memory wires.
1997 [28]	GB 2304350	Aegis/ Bold, Borham, Jenkins	K/B	Fibres embedded in a flexible matrix The assignee is an armour manufacturer
1997	GB 2303534	TBA Ltd/ Meadowcroft	K	Hinged plate system The assignee is an armour manufacturer
1997	GB 2302794A	T&N/ Allen, Murden	K	Hinged plate system The assignee is an armour manufacturer
1996	SE 503294	Majorin	K/B	Multi-layer polymer sheet
1995	RU 2046271	Reshetov	B	Scale armour curved plates threaded on string

Table 3-1 continued

Year	Number	Assignee/ Inventor	Type	Description and comments
1994 [33]	DE 44,13,969,A1	Schmoelzing	K	Flexible multi-layer metal foil armour
1994	US 5373582	Point Blank/ Borgese, Ditchfield, Dragone	B	Body armour with resilient straps to retain shape The assignee is an armour manufacturer
1994	US 5306557	Madison	K/B	Composite material of oriented fibres and metal foil
1994 [18]	WO 9404047	Jus-tandem Ltd /Orlov	K/B	Plate armour in textile pockets, probably Russian military type The assignee is an armour manufacturer
1993 [21]	US 5,254,383	Allied Signal/ Gerlach, Harpell, Prevorsek	K	Plated armour with fibre wrap The assignee is an armour manufacturer
1993	EP 544561	Etat Fr Min Interieur	K/B	Honeycomb with polyethylene outer layer
1992	WO 9220519	Allied signal/ Harpell, Prevorsek	K/B	Scale armour of rigid plates with flexible seams
1992	WO 9213250	Munyard/ Buchanan	K/B	Scale armour of multiple rows of plates with flexible connectors (plastic rivets)
1993	US 5,187,023	Allied Signal/ Harpell, Prevorsek	K/B	Scale armour of triangular plates sewn onto textile The assignee is an armour manufacturer
1992	US 90520815	Sullivan	O	Puncture resistant textile relying on fibre fibrilated by abrasion to fill pores in weave
1992 [20]	EP 541563	PPI Ltd/ Morgan	K	Hexagonal aluminium plates see also GB 915233 and GB 2285209 The assignee is an armour manufacturer
1991 [16]	GB 2,238,460	Personnel Armour Designs Ltd/ Lee	K	Scale armour of small plates linked to each other and fabric backing The assignee is an armour manufacturer
1988 [22]	RD 290012	Anonymous	K	Flexible perforated steel sheet or scale armour
1988	GB 2198824	UK MoD/ Marsden	K/B	Flexible textile of felted aramid fibre

Table 3-1 continued

Year	Number	Assignee/ Inventor	Type	Description and comments
1988	GB 2198628	UK MoD/ Shephard	K/B	Improved penetration resistance by using slip resistant fibre
1987 [13]	US 4,660,223	Point Blank/ Fritch	K/B	Scale armour of felted layers with titanium plates The assignee is an armour manufacturer
1987	EP 208499	Groves	B	Flexible material of beads constrained within textile
1984	GB 2130073	Personnel armour designs Ltd/ Lee	K/B	Scale armour of aramid fabric with ceramic tiles The assignee is an armour manufacturer
1961	GB 915 345	Lonza Ltd	K/B	Scale armour of plates between foam layers
1995 [31]	WO 9603277	Akzo Nobel NV	K/B	Textile armour with plasma sprayed abrasive coating. The assignee is an armour manufacturer
1995 [29]	EP 670466	Mehler Vario Systems	K	Mail embedded in polymer matrix The assignee is an armour manufacturer
1995 [39]	EP 740125	Mehler Vario Systems	K/B	Armoured cloak The assignee is an armour manufacturer
1997 [34]	US 5,697,098	Betencourt, Kenneth, Bain	K/B	Armour of multiple layers of titanium foil
1998 [32]	WO 9845662	Zefex BV / Breukers	K/B	Textile coated with abrasive particles The assignee is an armour manufacturer
1997 [36]	WO 9724574	Safeboard/ Granqvist	K	Mail enclosed in fabric with padding on the rear face. The assignee is an armour manufacturer
1996 [30]	US 5200263	Gould, Nichols	K	Small platelets embedded in elastomer
1995 [35]	EP 640807	Kuhn/ Tissu Rothrist	K	Plain weave of 2cm wide titanium foil strips
1992 [27]	WO 9200496	Passive Barriers Ltd/ Macwatt	K	Flexible material of interlocking spiral wound wires

3.7 BIBLIOGRAPHY

G. C. Stone, *A Glossary of the Construction Decoration and Use of Arms and Armour*, Jack Brussel, New York, (1961)

D. Edge and J.M Paddock, *Arms and Armour of the Medieval Knight*, Saturn Books, Leicester, (1996).

S. Bull, *An Historical Guide to Arms and Armour*, (Ed. T. North), Cassel, London, (1991).

Men at Arms Series, (Ed. M. Windrow), No 39, 89, 109, 137, 157, 166, 218 Osprey Military, London, (1980-1990)

C. H. Ashdown, *European Arms and Armour*, Barnes and Noble, New York, (1995) (reprint from earlier undated edition probably late 19th or early 20th century)

Studies in European Arms and armour: The Otto Kretzschmar von Kienbusch collection in the Philadelphia Museum of Art, (Ed J. Watkins), The Philadelphia Museum of Art, Scolar press, Aldershot, (1992).

De Cosson and W. Burgess, *The Catalogue of the Exhibition of Ancient Helmets and Examples of Mail at the Archeological Institute London 1881*, Arms and Armour Monographs, Ken Trotman, Cambridge, (1985).

Warfare in the Ancient World, (Ed. J. Hackett), Sidgwick and Jackson, London, (1989).

3.8 REFERENCES

1. T. Watkins, The Beginnings of Warfare, in *Warfare in the Ancient World*, (Ed. J. Hackett), Sidgwick and Jackson, London, 15-35, (1989).

2. A, d'Harnoncourt, Preface, in *Studies in European Arms and armour: The Otto Kretzschmar von Kienbusch collection in the Philadelphia Museum of Art*, (Ed J. Watkins), The Philadelphia Museum of Art, Scolar Press, Aldershot, 7-9, (1992).

3. P. H. Blyth, Energy absorption in Greek and Roman armour, *Proc. Light Armour Systems Symposium*, Cranfield University, Shrivenham, (1995).

4. Herodotus, History VI, Section 112, (340BC).

5. S. Bull, the Greeks and Romans, in *An Historical Guide to Arms and Armour*, (Ed. T. North), Cassel, London, 18-38, (1991).

6. C. H. Ashdown, *European Arms and Armour*, Barnes and Noble, New York, 134-138, (1995) (reprint from earlier undated edition probably early 20th century).

7. De Cosson, W. Burgess, *The Catalogue of the Exhibition of Ancient Helmets and Examples of Mail at the Archeological Institute London 1881*, Arms and Armour Monographs, Ken Trotman, Cambridge, (1985).

8. G. C. Stone, *A Glossary of the Construction Decoration and Use of Arms and Armour*, Jack Brussel, New York, (1961).

9. N. V. Sekunda and A. Mcbride, *The Ancient Greeks*, Elite Series, (Ed. M. Windrow), No 7, Osprey Military London, (1986).

10. T. Wise and A. Mcbride, *Ancient armies of the Middle East*, Men at Arms Series, (Ed. M. Windrow), No 109, Osprey Military London, (1981).

11. B. Dobson, in *Warfare in the Ancient World*, (Ed. J. Hackett), Sidgwick and Jackson, London, (1989).

12. I. Heath and A. Mcbride, *Byzantine Armies*, Men at Arms Series, (Ed. M. Windrow), No 89, Osprey Military London, (1979).

13. United States Patent, No 4,660,223, (1987).

14. UK Patent, No GB 2,503,534, (1997).

15. International Patent, WO 92/13250, (1992).

16. UK Patent, GB 2,238,460, (1991).

17. European Patent, No EP 0,611,943, (1993)

18. International Patent, WO 9404047 (in Russian), (1994).

19. United States Patent, No 5,515,541, (1996).

20. European Patent, No EP 541563, (1992).

21. United States Patent, No 5,254,383, (1993).

22. Research Disclosure, RD 290012, (1988).

23. Japanese Patent, No 1-244299, (1989).

24. United States Patent, No 5,632,137, (1997).

25. United States Patent, No 5,628,172. (1997)

26. European Patent, No EP 0,769,671, (1996).

27. International Patent, WO 9200496, (1992).

28. UK Patent, No GB 2304350, (1997).

29. European Patent, No EP 670466, (1995).

30. United States Patent, No US 5200263, (1996).

31. International Patent, No WO 9603277, (1995).

32. International Patent, No WO 9845662, (1998).

33. German Patent, No DE 44,13,969, (1994).

34. United States Patent, No 5,697,098, (1997).

35. European Patent, No EP 640807, (1995).

36. International Patent, No WO 9724574, (1997).

37. D. A. Rouse, Patterns of stab wounds: a six year study, *Med. Sci. Law*, **34**, 1, 67-71, (1994).

38. L. A. Murray and M. A. Green, Hilts and knives a survey of ten years of fatal stabbings, *Med. Sci. Law*, **27**, 3, 182-184, (1987).

39. European Patent, No EP 740125, (1995).

CHAPTER 4

EMPIRICAL STUDY OF ARMOUR AND KNIVES

4.1 INTRODUCTION

Due to the lack of significant previous work on the subject of stab resistant armour it was decided to conduct an empirical investigation of knife penetration into armour. The following chapter describes the test methods used and then three successive studies that were conducted in order to investigate key variables and provide a database of knife-armour interactions.

4.2 TEST METHODS

In order to investigate the penetration of knives into the various test materials three test types were used. Quasi-static penetration tests were conducted on a conventional universal testing machine (Instron 4206), whilst dynamic penetration tests were performed using a Rosand Precision Ltd IFW 8 instrumented drop tower or an air cannon.

4.2.1 Drop tower tests

The primary analytical test used an instrumented drop tower as described by Pollitt [1]. The drop tower consists of a weight carrier of variable mass which is accelerated downwards by gravity with assistance from a bungee cord. The weight carrier is guided along vertical rails such that the drop position is fixed and rotation about the drop axis is constrained. In the base of the tower there is a large aperture into which a target array can be introduced. The operation of the drop tower is controlled by a desktop computer which also handles data collection and analysis. A suitable striker, in this case a knife, is attached to the bottom of the weight carrier via a threaded section which carries a piezo-electric load cell. Axial loads on the striker compress the load cell producing an electrical charge which can be converted to units of force

by suitable calibration factors. The load washer was calibrated using a procedure similar to that described by Money and Sims [2]. In this procedure a mass was suspended from the striker by a wire and the weight carrier was then dropped, allowing the assembly to go into free fall and thereby emulating a compression pulse at the transducer. The tower layout is shown in figure 4-1 and the weight carrier is shown in figure 4-2 and 4-3.

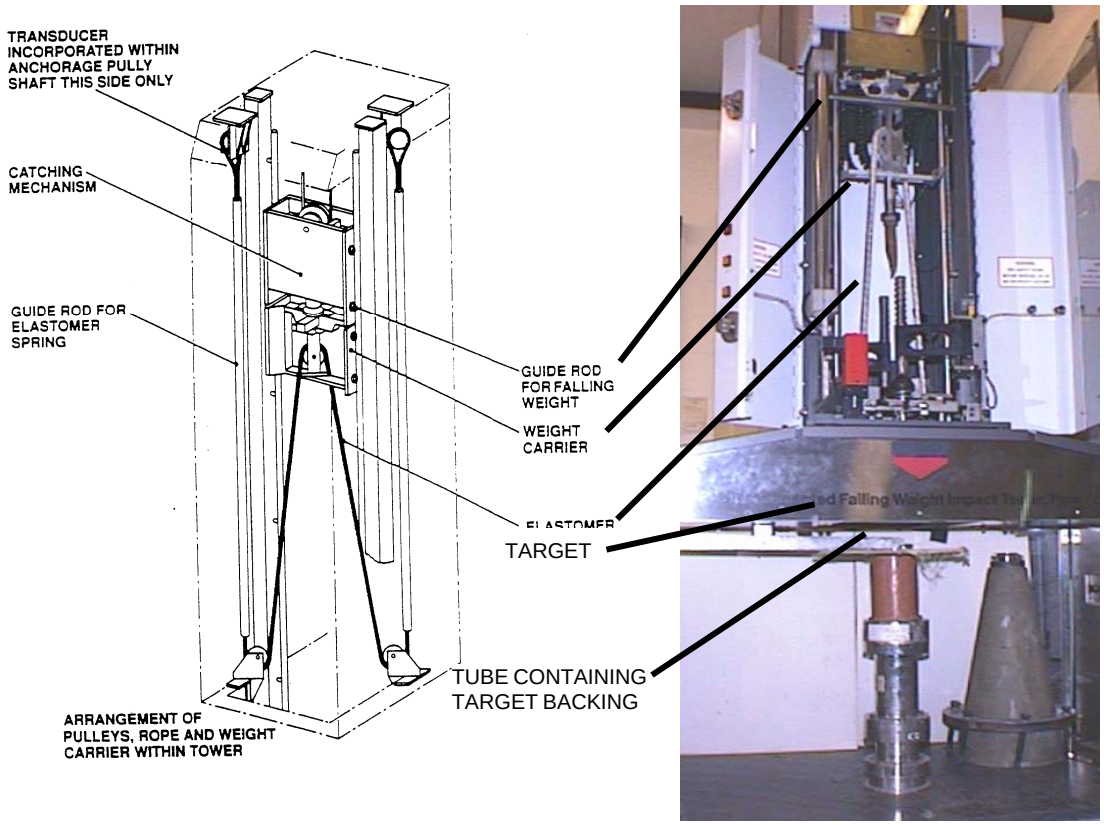

Figure 4-1. The drop tower layout showing to the left the upper part of the tower which contains the drop mass and accelerating bungee, and to the right the lower part of the tower and target.

As knife armour is designed to be worn on the body, the armour material will be supported by the wearer's body. In testing body armour it is customary to support the armour against a flesh simulant such as gelatine, or to use a clay based material such as Plastilina® which is conditioned according to the NIJ ballistic test procedure [3]. Roma Plastilina® N^{o}1 has become widely accepted as a ballistic target support in

which it provides both mechanical support and a means to measure armour deflection or blunt trauma into the wearer's body. Typically the Plastilina® is used in the form of a large block similar in size to an average male torso. The Plastilina® block has to be heated to approximately 35°C in order to achieve the required consistency.

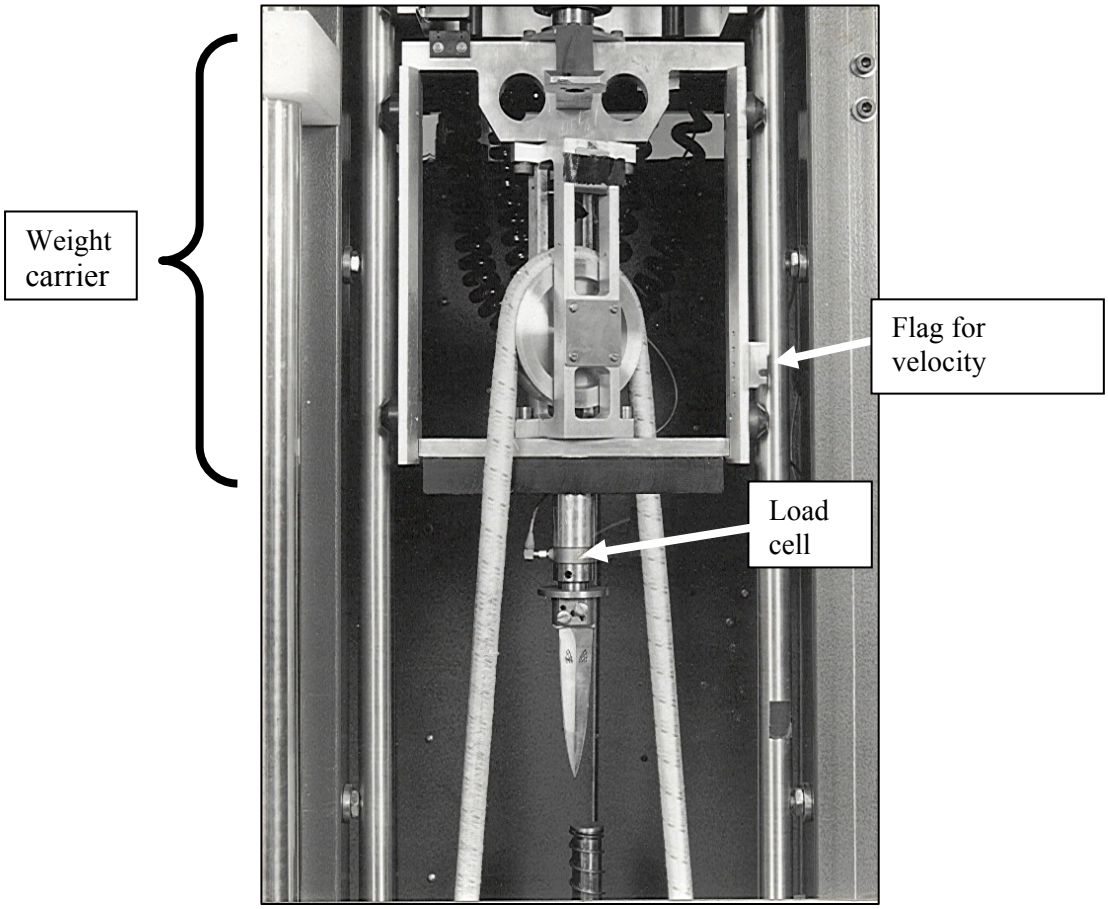

Figure 4-2. Layout of the weight carrier and instrumentation with a Black Widow knife blade attached.

For the purposes of the tests described in this chapter it was necessary to adapt the target support within the drop tower to allow more convenient testing and measurement. It was necessary to provide an accurate means of measuring penetration of the armour which was achieved by sectioning the backing block. Also the small size of some sample materials required that additional edge constraint was necessary to prevent them being pushed through the backing.

The targets were mounted on a rigid tube of 10mm diameter which was packed with the backing material. The backing material used was a flesh simulant clay manufactured by Peter Pan Playthings Ltd. This had the advantage that it had the required consistency at room temperature and therefore did not have to be maintained at an elevated temperature as is the case for Plastilina®. The test samples were clamped to the top of the tube by a load ring of 75mm inside diameter applied with a force of 690N by a pneumatic system in the drop tower. The test was then conducted and the backing removed for sectioning and measurement of penetration as shown in figure 4-4.

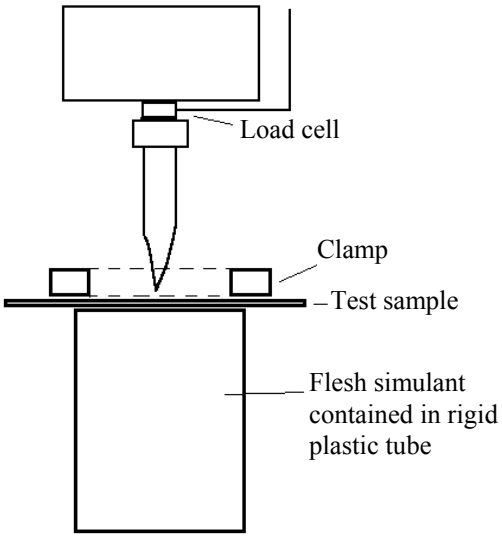

Figure 4-3. Diagrammatic representation of the weight carrier, knife, and target in the base of the drop tower in place.

The velocity of the weight carrier is measured immediately prior to impact by the passage of a metal flag on the carrier between two optical gates mounted 10mm apart on the tower frame. When the top gate is passed, a timer is started and when the bottom gate is passed, the timer is stopped and the data collection sequence from the force transducer is initiated. The position of the two gates is adjusted prior to each test so that the lower gate is interrupted as the target is first struck.

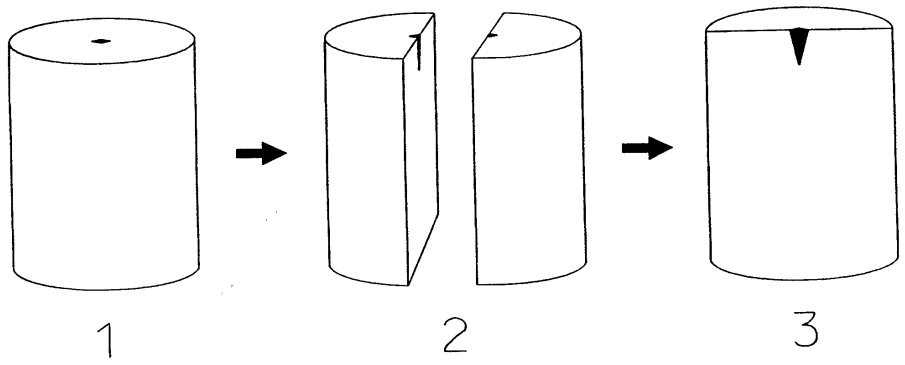

Figure 4-4. Procedure for measuring knife penetration by sectioning target backing (after Watson *et al* [4])

The data collection system then collects individual values of axial force at a fixed frequency. Data collection time was over a period of typically 50 milliseconds. For the earlier tests 300 data points were collected over this time interval, but during the course of the work the instrumentation was updated to allow up to 4000 data points to be collected during the test. From the raw data which are in the form of force vs. time it is possible to derive other data such as displacement velocity or energy from a knowledge of initial velocity and drop mass. This analysis was performed either with the proprietary drop tower software from Rosand Precision Ltd, or on a spreadsheet such as Microsoft Excel.

In practice there are some limitations to the impact geometry which are introduced by the timing and acceleration system. The lower timing mark (i.e. the impact position) must occur at a position after the bungee cord is slack otherwise additional energy will be imparted after the impact. The tower is equipped with sprung bump stops that start to arrest the weight carrier at a position approximately 100mm after the bungee becomes slack. Consequently the maximum useable penetration distance for a knife is 100mm from initial contact until arrest, otherwise some energy will be dissipated into the bump stops and the mechanical shocks produced by this will disrupt subsequent data.

Although the mass of the weight carrier can be varied the relatively low energy levels and high velocities over which stab testing is usually specified meant that the carrier

was always operated at minimum mass. For the initial study this minimum mass was 4.5kg but a weight carrier of lower mass was subsequently constructed specifically for stab testing, so later trials used this new 2.5kg carriage.

4.2.2 Quasi static tests

Some stab trials were conducted at quasi static rates in order to investigate rate effects and to allow direct observation of penetration mechanisms. These trials used the same geometry as the drop tower tests with the target mounted on a filled tube. The knife was rigidly attached to the crosshead-mounted load cell and then driven through the target at $1.6x10^{-4}$ ms^{-1} (10mm/min). Force vs. crosshead displacement data were collected and subsequently replotted in Microsoft Excel.

4.2.3 Air cannon tests

This method based upon the PSDB test procedure [5], uses an air cannon to propel various knives at velocities of up to $20ms^{-1}$. Compressed air is allowed into a reservoir and then discharged via a solenoid valve into the barrel. The knife is held in a Nylon or aluminium sabot and is propelled out of the barrel, its velocity being measured at the muzzle.

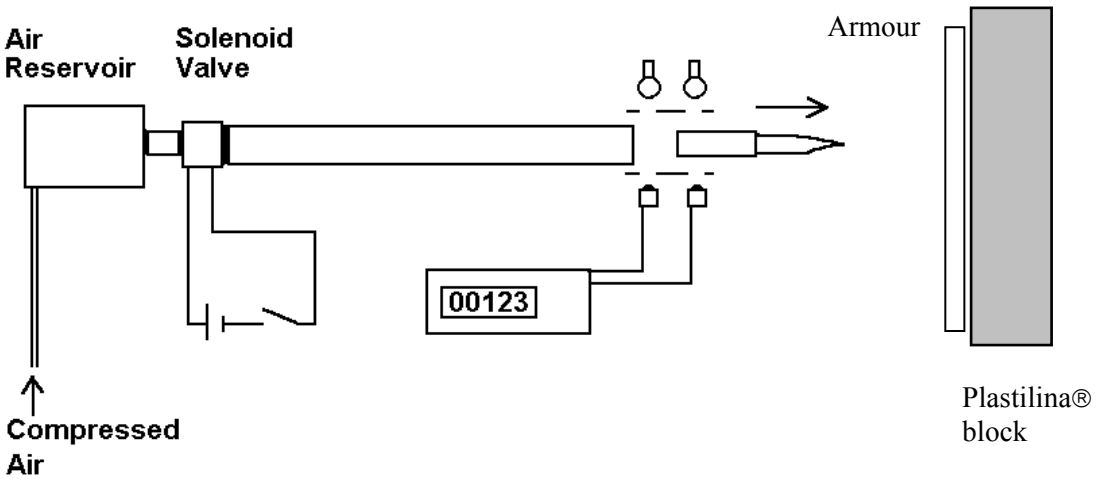

Figure 4-5. Air cannon systems layout.

In order to achieve a consistent trigger pulse, a piece of foam can be stuck on the knife tip. A more reliable method is to trigger the timer on the positive slope of the detectors so that the rear edge of the sabot is measured. This is better as the length of the missile is such that significant acceleration can occur during the time between the blade tip emerging and then the sabot rear emerging from the barrel.

The target is rigidly held against a Plastilina® block 75cm from the muzzle. The temperature of this block is adjusted to achieve the correct hardness in accordance with ballistic and knife test standards [3,5]. After the test, penetration is measured by removing the target with the blade still embedded and then directly measuring the protruding length of the knife.

4.3 INITIAL TRIALS

An initial study of knife-armour interactions was carried out by Pollitt [1], in which a diagnostic test was developed and some materials development was carried out. Some of these tests were repeated at a later date and further analysis was carried out as described by Horsfall *et al* [6]. It is these results which are covered in the following section, the complete work having been discussed in section 2.6.1.

The tests used a commercially obtained "street" knife called a Black Widow (see figure 4-2). This is a 105mm long, diamond section knife with an approximately straight taper. This shape was chosen in order to produce a relatively simple penetration vs. load response, as it was thought likely that both the magnitude and shape of the penetration vs. load curve would vary with knife shape. The knife was attached to a 4.5kg weight carrier and propelled into test materials with velocities between 3 ms^{-1} and 5 ms^{-1} calculated to give kinetic energies at impact of 20-50J. A piezo-electric load cell mounted immediately behind the knife blade provided a measure of force during the penetration event. A sampling period of 147μs was used and a low pass filter was applied at 8.4 kHz.

Panels of the test materials measuring 150mm x150mm were placed on a rigidly mounted open ended tube 100mm in diameter. The sample was clamped to the top of the tube by a pneumatic clamp ring with a load of 690N. The tube was packed with Peter Pan Ltd flesh simulant to support the sample. After each test this block was sectioned in order to measure the final penetration. All impacts were carried out with the knife blade orientated parallel to a fibre direction, i.e. 0° or 90° orientation. For comparison, quasi-static tests were performed using the same test geometry but with loading velocities of $1.6x10^{-4}$ ms^{-1} (10mm/min). This used a conventional Instron universal testing machine which recorded the force vs. deflection response via a load cell between the crosshead and the knife.

These methods allow not only the gathering of penetration data but also the analysis of the force vs. time or force vs. deflection characteristics of the penetration event. Energy dissipation can be measured by integration of these curves.

E-glass epoxy composites were fabricated by vacuum hot pressing of Fibredux 913-G-E-5-30 prepreg laminates. This unidirectional laminate has a resin content of 30% and a cured thickness of 0.125mm. This was laid up in $[0/90]_{nS}$ orientation with the number of laminae adjusted to give the correct thickness.

4.3.1 Results

Force vs. time curves were obtained for each impact, from which force vs. deflection curves were derived. In this case deflection was measured as the distance travelled by the knife after contact with the front surface of the test panel. Penetration of the blade was measured after each test, being taken as the distance from the rear face of the panel to the blade tip. Deflection values were in agreement with measured penetrations taking into account the thickness of the test panel.

Figure 4-6 shows a typical force vs. deflection plot for the 4mm thick glass-epoxy material over a range of impact energies. It can be seen that the start of the curve is similar irrespective of the impact energy but the latter portion extends further with

increasing impact energy. Also shown in figure 4-6 is the force vs. deflection curve recorded from the quasi-static test of the same 4mm thick glass-epoxy panel. This can be compared to the curves from the dynamic tests and again it is seen to be similar over the first 0.01m of displacement but thereafter shows a lower load.

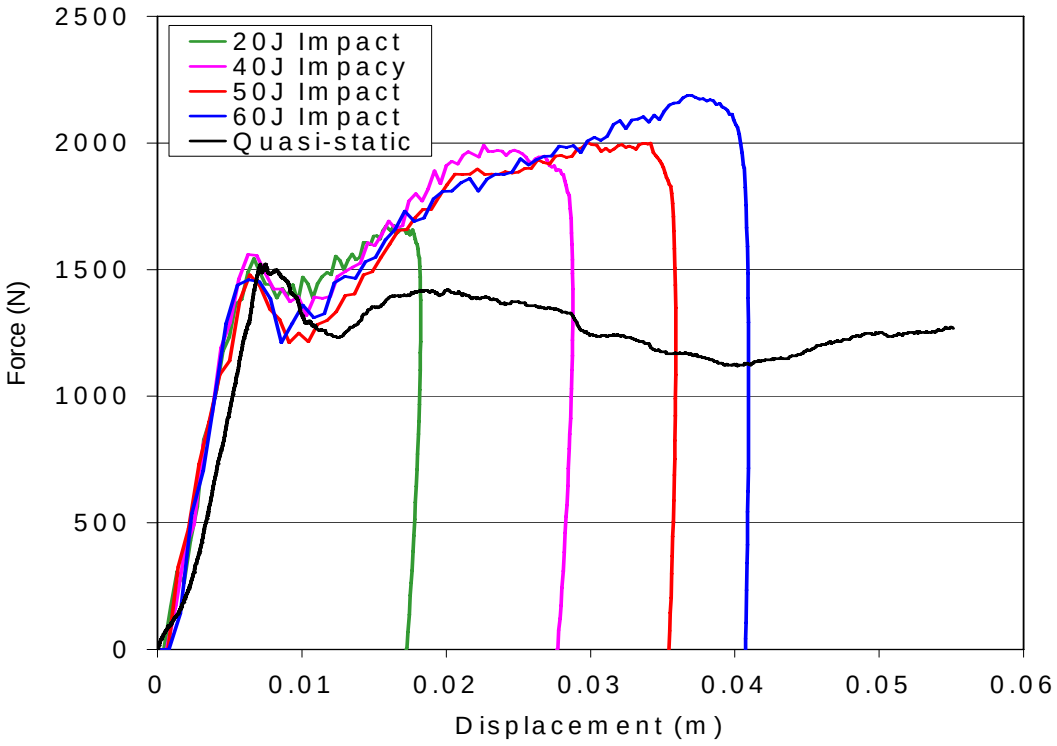

Figure 4-6. Force vs. displacement plots for impact tests on a 4mm thickness glass-epoxy composite panel at 20-60J; a quasi static penetration test is also shown.

4.4 SECOND STUDY – KEY VARIABLES

A further study was carried out into various aspects of the knife-armour interaction and a wider variety of armour materials were also assessed. The main variables investigated were lubrication of the knife, knife tip sharpness effects, target edge effects and target orientation effects. The drop tower method as described above was also compared to the air cannon method as used in PSDB body armour tests [5]. In addition to the Black Widow knife blade, tests were also conducted with the two blade types specified in the PSDB test and the spike used for armour testing by the Metropolitan Police.

4.4.1 Lubrication effects

This series of tests used the 4mm thick Fibredux® GFRP panel, which was tested at an impact energy of approximately 40J using the same type of dagger blade as used in the initial trials. Petroleum jelly was smeared on the blade and the impact was aimed to take place through a large blob of petroleum jelly on the target. These tests were compared to tests with the blade in its normal untreated state and with tests on a blade that had been degreased with methylated spirits.

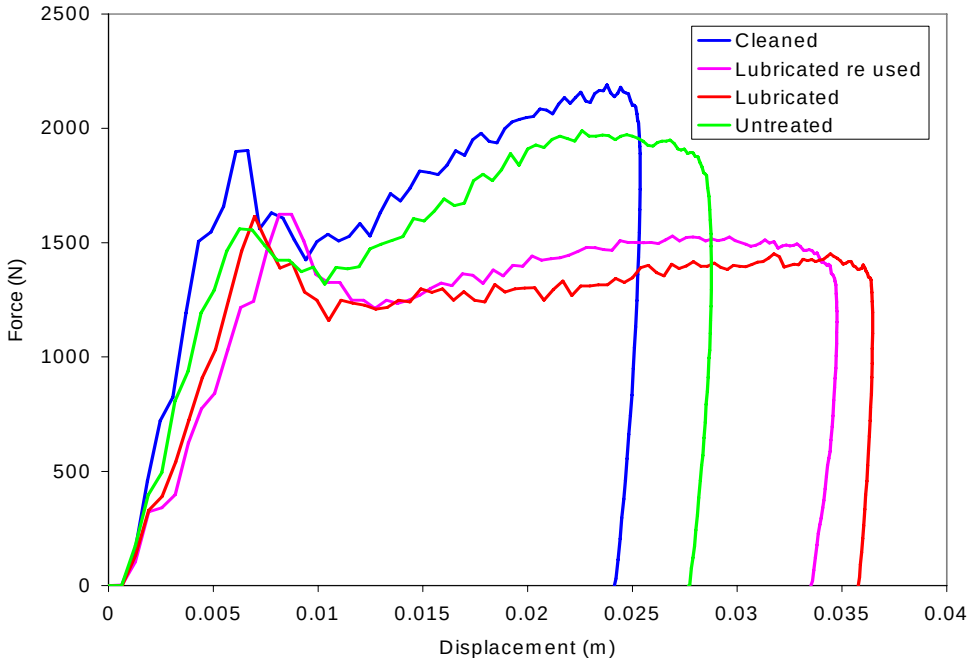

Figure 4-7. Force vs. displacement plots for blades with various degrees of

The data for the lubrication trials are shown in table 4-1. It can be seen that the depth of penetration averages 24mm for the lubricated blade and only 16mm when degreased, a reduction of 33%. Examination of the force profile of the events shown in figure 4-7 shows that the effect of lubrication is to decrease both the initial load (at perforation) and the load during further penetration of the target panel.

Table 4-1. The effect of lubrication on penetration through target.

Test No	Impact Energy (J)	Penetration (mm)	Condition
25	42	17	Control- as received
29	43	26	Lubricated
30	42	21	As above re used
31	39	16	Cleaned with IMS

4.4.2 Target edge effects

During some trials with the GFRP targets it was seen that cracking of the composite extended ahead of the blade edge and in some cases propagated to a free edge of the target. As this might significantly reduce the area of the target that could be tested it was decided to conduct a series of trials to investigate the edge effects.

Table 4-2. The effect of impact position relative to panel edges.

Test No	Average impact energy (J)	Average penetration (mm)	Orientation and spacing from edge (mm)
35,36	42.7	23.5	Centre
37,38,39	41.8	27.8	Normal (24)
40,41,42	41.3	26	Parallel (28)
45-47	65.4	44.5	Centre
48-50	63.4	45.6	Normal (27)

The dagger blade was used to conduct a number of impacts against a 4mm glass epoxy target. Impacts were placed within 25mm of one edge of the panel with the blade oriented normal or perpendicular to the edge. Tests were conducted at 40J and 60J impact energy levels. The results of these tests are summarised in table 4-2.

The results of this series were inconclusive. Despite using one of the more brittle target materials the edge effects seemed negligible. For the dagger-type knife, the edge effects are insignificant although for a thicker bladed knife a greater wedging action and hence splitting might be seen.

4.4.3 Sharpness effects

A number of tests were conducted against a 5.5mm thick aramid-thermoplastic target, with the blade in a sharp condition or after deliberate blunting, the blade tips are shown in figure 4-8. (Further details of this target type are given in section 4.5.1)

Table 4-3. The results of test with sharp and blunt knives.

Test Number	Impact energy (J)	Penetration (mm)	Knife
51,52,53,57	44.3	62	Sharp
54,55,56	44.6	60	Blunt

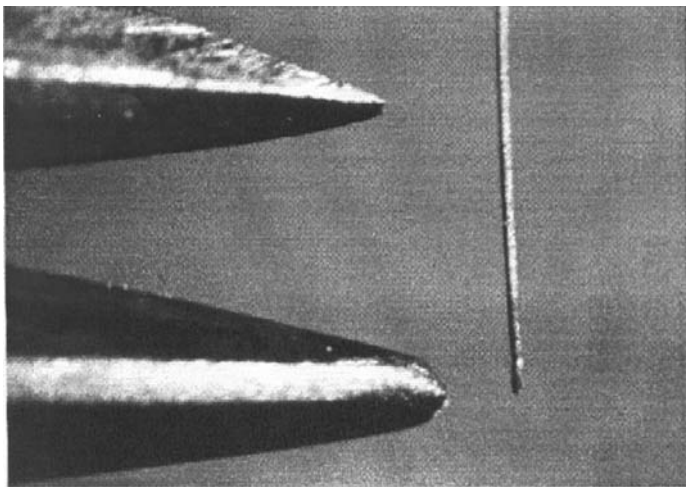

Figure 4-8. Macro photograph of sharp (top) and blunted (bottom) knife tips including a 50μm diameter wire for scale.

Penetrations were similar regardless of blade condition, but with the sharp knives the penetration was limited by the weight carrier reaching the limit of its travel. Therefore the penetration levels achieved from the sharp knives might have been slightly under-recorded. Figure 4-9 shows the force vs. displacement plots for one test each with a blunt and a sharp knife. It can be seen that the sharp knife produces a lower initial peak force, but the force resisting penetration actually climbs above that for a blunt knife after perforation has occurred.

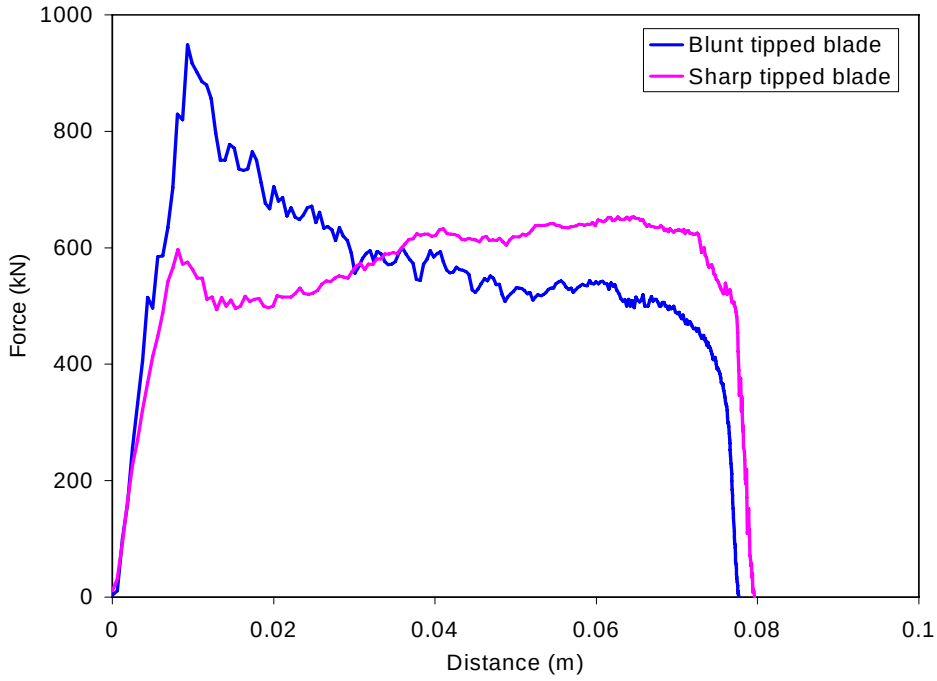

Figure 4-9. The force vs. displacement plots for blunt and sharp knives on 5.5mm thickness aramid-thermoplastic composite.

4.4.4 Orientation effects

A number of tests were conducted against a 5.5mm thickness aramid-thermoplastic target to determine the effect of weave orientation on penetration characteristics. The target used was the same aramid-thermoplastic matrix composite used in the sharpness tests. The test results are summarised in figure 4-10. In general the tests showed that the orientation effects were minimal. The penetration levels achieved were not significantly different between the three orientations tested and no

significant differences were observed in the force vs. displacement data. The only observed trend was that the intrusion of the target sample into the plasticine backing was greater for the 45° orientated tests.

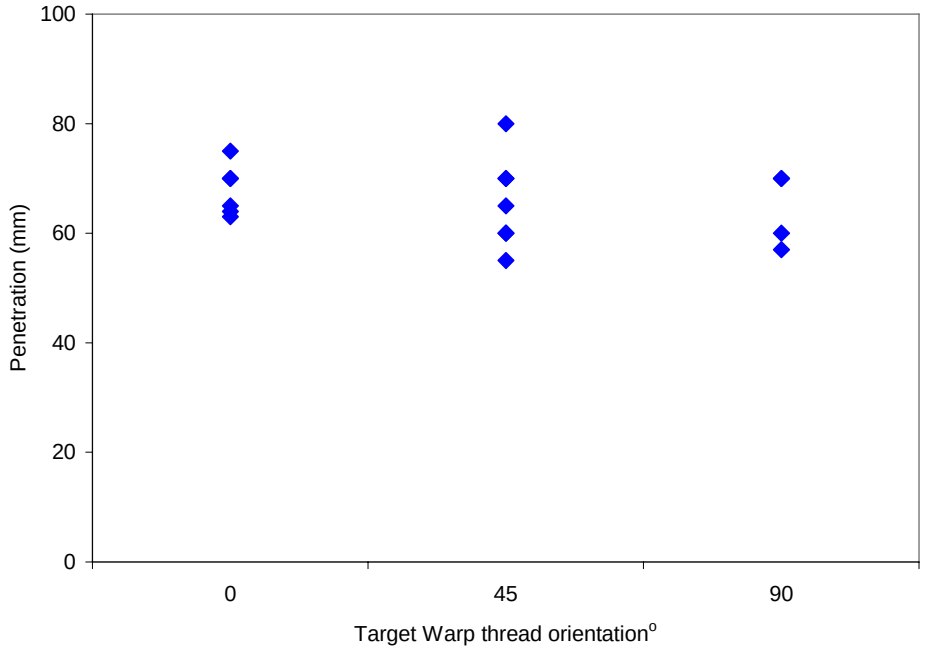

Figure 4-10. The effect of target orientation on blade penetration through target.

4.4.5 Shape effects

In order to investigate the effect of knife shape, a number of tests were conducted using a range of blades against a single target type. Initially tests were conducted against a 5.5mm thickness aramid thermoplastic composite target. However, the more penetrative knives fully penetrated this sample and ran in to the drop tower end stops. Therfore a second series was performed using 2 thicknesses of the target material. Three drops tests were performed at each condition and the average energy and penetration levels are shown in table 4-4.

The force vs. displacement plots for these four blades are shown in figure 4-11. The initial part of the curve is remarkably similar for all four knife types. However, following perforation at approximately 0.012m (equivalent to the thickness of the armour) the behaviour diverges.

Table 4-4. Test results for comparison of knife types, each result is an average of three tests.

Knife type	Energy (J)	Penetration (mm)
PSDB N°1	25	21
PSDB N°5	28	18
Black Widow	26	23
Met spike	24	11

After the armour is perforated the Black Widow blade shows a decreasing resistance whilst the Metropolitan police spike (met spike) shows a constant resistive force. Both the PSDB blades show perforation at lower initial loads but after perforation the N°1 blade shows an increasing load whilst the N°5 blade show a decrease followed by a constant load.

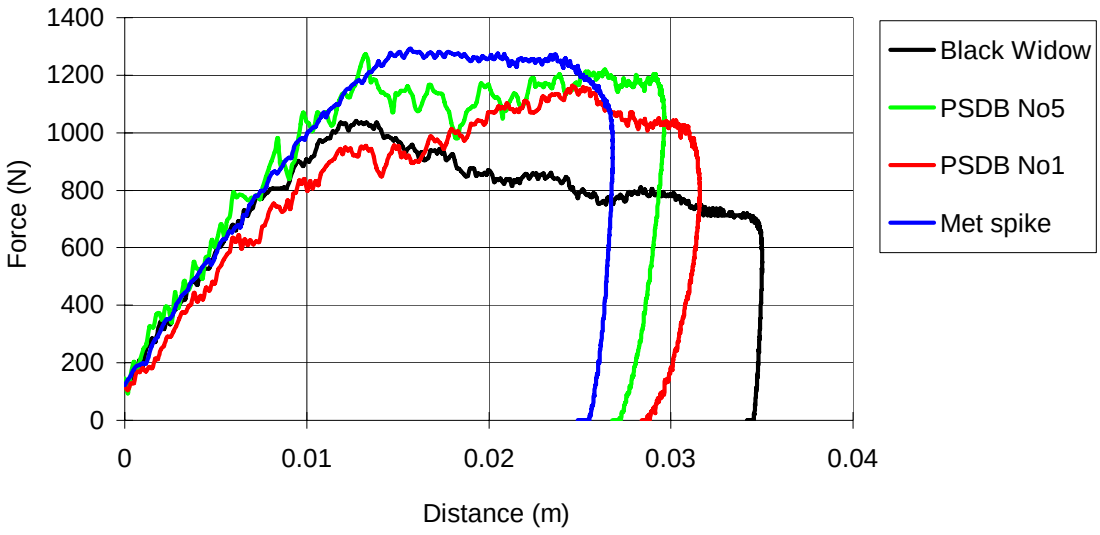

Figure 4-11. Force vs. displacement plots for four different blade shapes.

4.4.6 Bullet resistant textile armour

It was decided to test a bullet resistant textile armour with a knife in order to establish the variation in performance of textile systems between the ballistic and stab threats. Tests were conducted against a panel of commercially produced ballistic armour. This consisted of 21 layers of aramid textile and one layer of ultra high molecular weight polyethylene. The panel was subjected to a single impact from a 0.357" magnum projectile at an impact velocity of 400ms^{-1} giving an impact energy of 1200J. The test was carried out with the panel held against a Plastilina® backing block in accordance with the NIJ [3] ballistic test procedure.

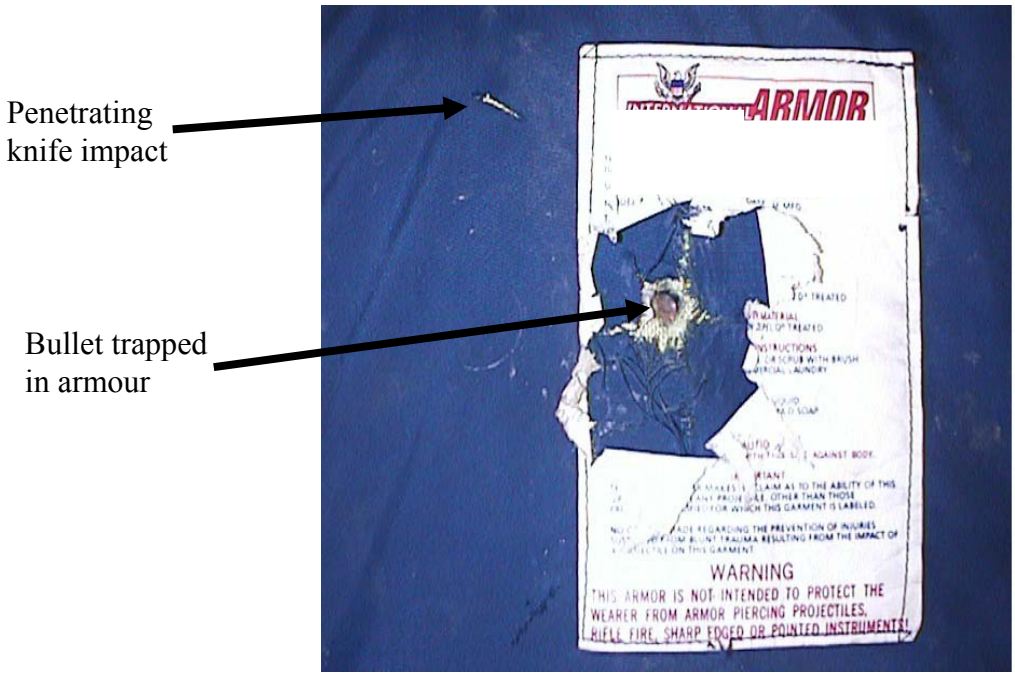

Figure 4-12. Bullet resistant textile panel showing captured 357 magnum projectile and penetrating knife cut, note warning on the bottom of the information panel ("This armour is not intended to protect the wearer from armour piercing projectiles rifle fire sharp edged or pointed instruments").

The projectile penetrated only the first few layers of the target and was then captured in the remaining textile layers. The same panel was then subjected to a knife impact using the PSDB N^{o} 5 knife blade launched from an air cannon in accordance with PSDB KR42 test procedure for stab resistant body armour [5]. The knife was launched at a velocity of 4ms^{-1} giving an impact energy of 40J. The knife penetrated

the panel by 50mm. The force vs. displacement profile is shown in figure 4-13. It can be seen that although there is a significant resistance to initial perforation with peak loads of approximately 1200N, after perforation the load decays rapidly.

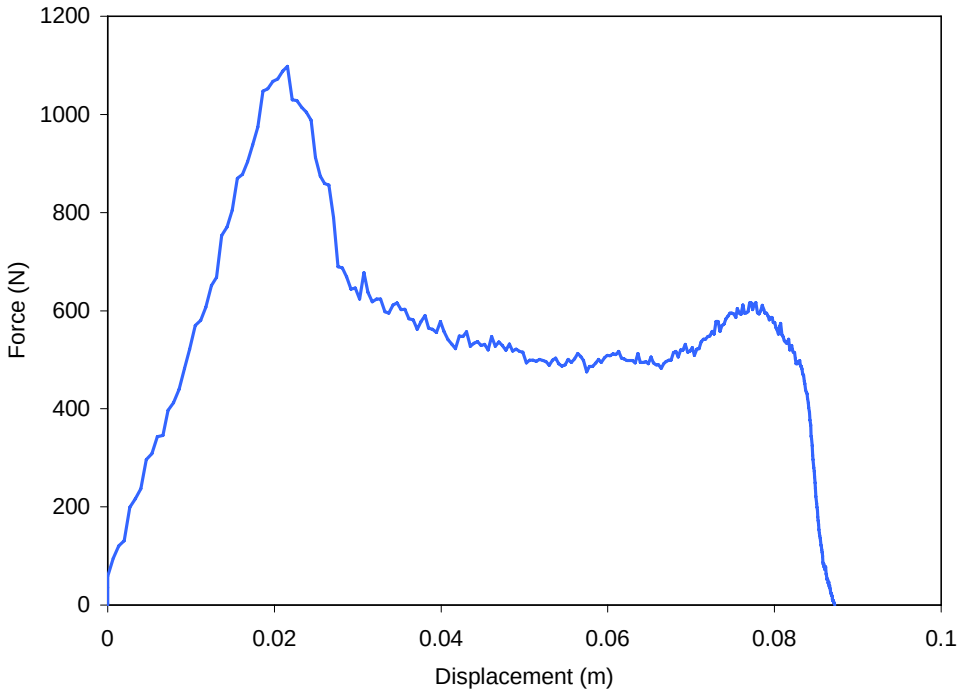

Figure 4-13. The force vs. displacement profile of a textile ballistic panel subject to knife attack.

4.5 THIRD STUDY – DATA GATHERING

In the third series of trials a more detailed study was carried out in which a matrix of tests was conducted for 4 different armour materials and 4 knife types. The aim of this series was to establish the penetration characteristics of both the knives and armour materials. Repeated tests were also made against some targets to assess blade damage during the test series. For this final series of tests a lighter weight carrier was developed for the drop tower, primarily in order to bring the test closer to the velocity regime predicted for manual stabs [7]. This new carriage had a total mass of 2.5kg and therefore allowed higher velocities to be used to obtain the desired range of impact energy levels. Previous tests had primarily used a simple dagger shaped blade,

but for this final series a number of blades used in test standards were employed, as shown in figure 4-14.

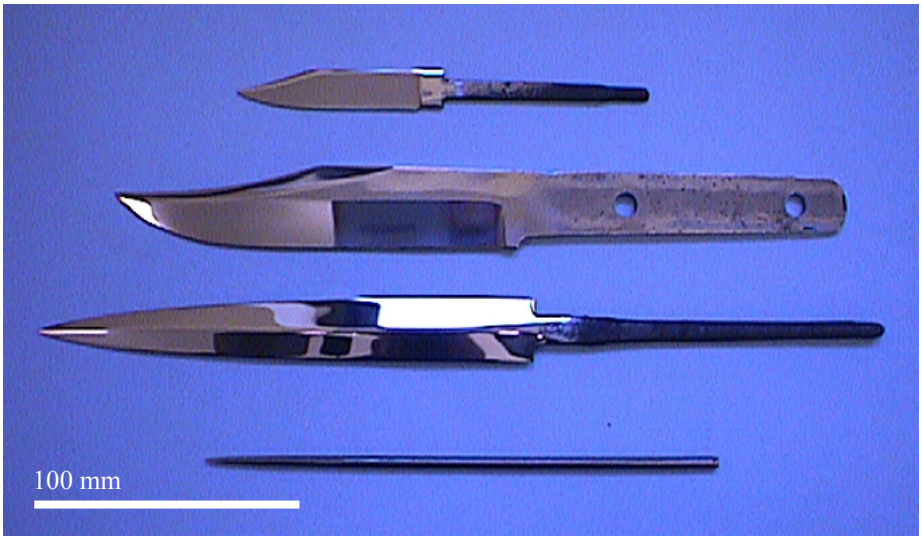

Figure 4-14. Test knives, from top to bottom PSDB No1, PSDB No5, commando, and icepick.

The PSDB N°1[1] and N°5[1] blades were from normal production batches, which are used for armour testing. The commando[1] blade closely resembles the blade used in the German and Swiss police test specifications. The icepicks were of 40-44 Rockwell C hardness supplied from H.P.White Laboratories USA. A harder variety was available but as no damage was observed to the softer type during testing it was not felt necessary to use the harder grade.

4.5.1 Armour Materials

Four armour materials were used in these trials, Aeroflex®[2] (an aramid reinforced thermoplastic), commercial purity titanium, and two grades of aluminium alloy. This set of materials was designed to simulate some of the actual and proposed armour materials for stab resistant garments. Mechanical tests were conducted to determine

[1] Supplied by H.M.Slaters Ltd, Sheffield, UK.

[2] Supplied by Aero Consultants UK Ltd, Cambridge, UK.

static mechanical properties and strain rate effects. Table 4-5 gives the material descriptions and table 4-6 lists the mechanical properties of the armour materials.

Table 4-5. Armour material descriptions.

Material	Description	Geometry
Aeroflex®	Plain weave Aramid fabric with a (rubbery) thermoplastic matrix.	6.5mm 14 layer 5.5mm 12 layer
Aluminium alloy	7075-T6 (Peak aged)	1mm sheet
Aluminium alloy overaged	7075 (As above then aged for 9 hrs @250° C)	1mm sheet
Titanium	Commercial purity titanium alloy Grade 2	0.5mm sheet

Aluminium alloy 7075 is a high strength heat treatable alloy. It was used in two conditions, the peak aged (-T6) condition and a softened condition obtained by overageing. The -T6 condition is the highest strength heat treatment condition giving the maximum level of both yield strength and ultimate strength but a relatively low ductility. This was softened by considerably over ageing the alloy. This produces a soft but stable heat-treated condition with lower strength but higher ductility.

The titanium used was commercially pure grade 2, which is a relatively low strength alloy of titanium and oxygen. This was used in the cold rolled condition. The strength levels achieved were very similar to that of the aluminium 7075-T6 but with considerably more ductility.

Mechanical properties were determined by tensile tests of specimens punched from sheet (laser cut from Aeroflex® sheet). Specimens were cut in the rolling direction from the metal sheets. Aeroflex® samples were cut in the longitudinal (warp), transverse (weft), and 45° orientations. Samples were tested at strain rates of between $3 \times 10^{-4} s^{-1}$ and $3 \times 10^{-2} s^{-1}$ corresponding to test speeds of $1.6 \times 10^{-4} ms^{-1}$ (10mm/min) and $1.6 \times 10^{-2} ms^{-1}$ (1000mm/min) respectively.

Table 4-6. Armour materials properties.

Specimen	Material	Strain Rate (s^{-1})	Yield Strength (MPa)	Ultimate strength (MPa)	Elongation to failure (%)	Hardness (H_V)
WA1	Aeroflex® Longitudinal	3×10^{-4}	262	383	-	-
WA2		1.5×10^{-3}	301	397	-	-
WE1	Aeroflex® Transverse	3×10^{-4}	284	408	-	-
WE2		1.5×10^{-3}	336	451	-	-
FF1	Aeroflex® Diagonal	3×10^{-4}	<2	22	-	-
FF2		1.5×10^{-3}	<2	31	-	-
Ti2	Titanium	3×10^{-4}	406	511	32	192
Na1	Aluminium 7075-T6	3×10^{-4}	489	544	11	203
Oa1	Aluminium 7075 soft	3×10^{-4}	136	250	10	79

The Aeroflex® samples exhibited variation in strength with orientation, and strain rate. Properties in the 45° direction were very poor although this is due mainly to the lack of edge constraint of the cut fibre ends. There is a marked strain rate effect over only half an order of magnitude in strain rate which is as expected for a thermoplastic material.

The titanium and aluminium 7075-T6 material show very similar levels of strength although the aluminium has only half the ductility. The softening treatment to the 7075 had reduced yield strength by approximately 75% and ultimate strength by 50%. The measured ductility of the softened 7075 was surprisingly low. This may have been due to the use of sheet tensile specimens, which did not allow significant necking to occur in the transverse direction.

4.5.2 Blade shape effects

For each test the penetration into the backing block was measured and the force profile during penetration was also recorded. In order to show the effects of different knife types it is useful to review the force vs. displacement data at a range of impact energy levels for each of the target types. Figures 4-15 – 4-18 show the force vs. displacement plots for each knife type against the Aeroflex® target.

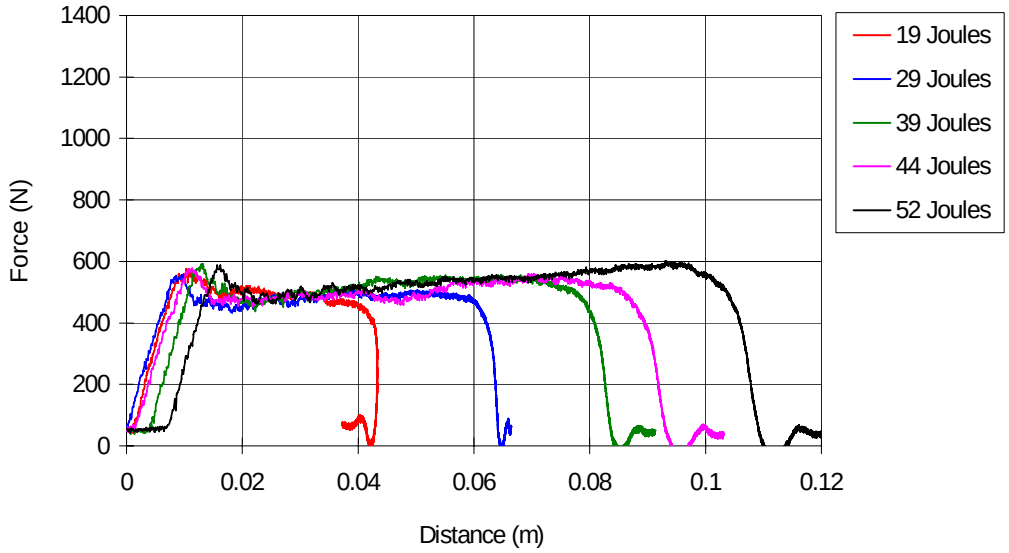

Figure 4-15. Commando knife blade against 14 layer Aeroflex® target.

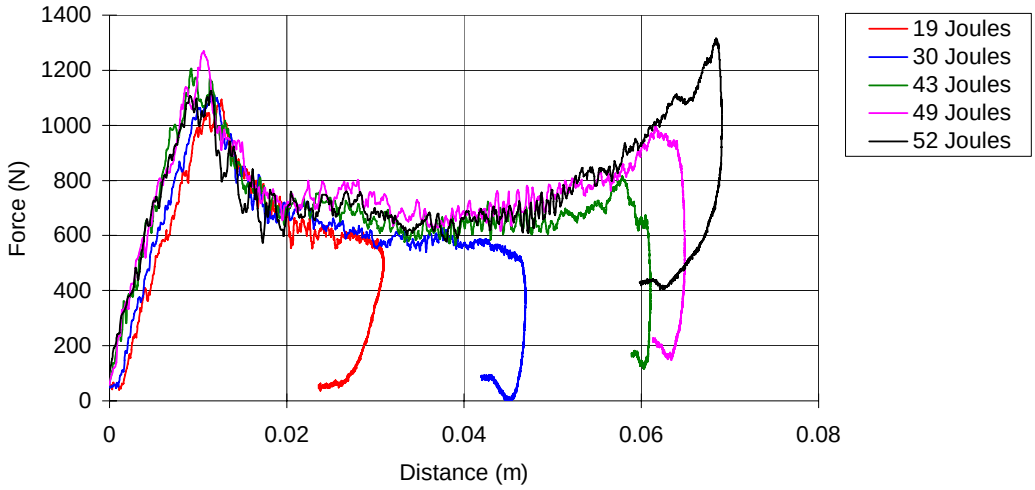

Figure 4-16. PSDB No5 blade against 14 layer Aeroflex® target.

Figure 4-15 shows the effect of impact energy over a range of energy levels for the commando blade against the Aeroflex® target. The load to perforate the target is approximately 580N. It can be seen that the initial part of the plot is similar in all cases and that the effect of increasing impact energy level is to simply extend the curves. Therefore the overall envelope is defined by the highest impact energy test and lower energy tests are truncated versions of this shape. Following initial perforation there is a load drop of approximately 100N, the force resisting penetration then increases slightly but steadily as penetration increases.

The force vs. displacement plots for the PSDB N°5 blade show a different form (figure 4-16). Over the range of impact energy levels studied there is a higher initial load on perforation of approximately 1200N. Following perforation the load drops by approximately 500N over the next 10mm of penetration and then climbs back with increasing penetration. As is the case for the commando blade, all curves overlay each other. It should be noted that there is a zero error of between 50N and 400N in the force signal at the end of each test. The unsharpened back edge of the blade cannot cut the target so the blade is forced off axis at higher penetrations producing bending loads on the knife blade and the force transducer. The bending loads produce an apparent axial load on the transducer which persists after the knife has halted. This manifests itself as a zero error in the force signal.

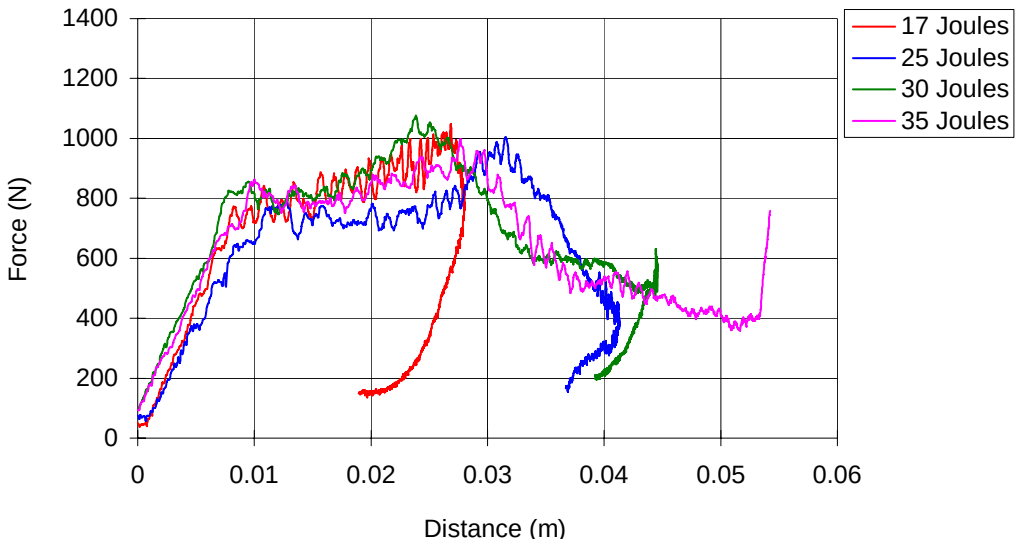

Figure 4-17. PSDB No1 blade against 14 layer Aeroflex® target.

For the PSDB N°1 blade (figure 4-17), the initial perforation load is approximately 600N, similar to that of the commando blade. Following perforation there is no load drop but a steady increase up to penetration levels of approximately 30mm. Beyond this the force decreases steadily. For the icepick against the Aeroflex® target (figure 4-18), the initial load at perforation is seen to be relatively constant at approximately 600N in all cases. This is followed by a slight drop then a steady rise in force up to a maximum level as the blade is arrested.

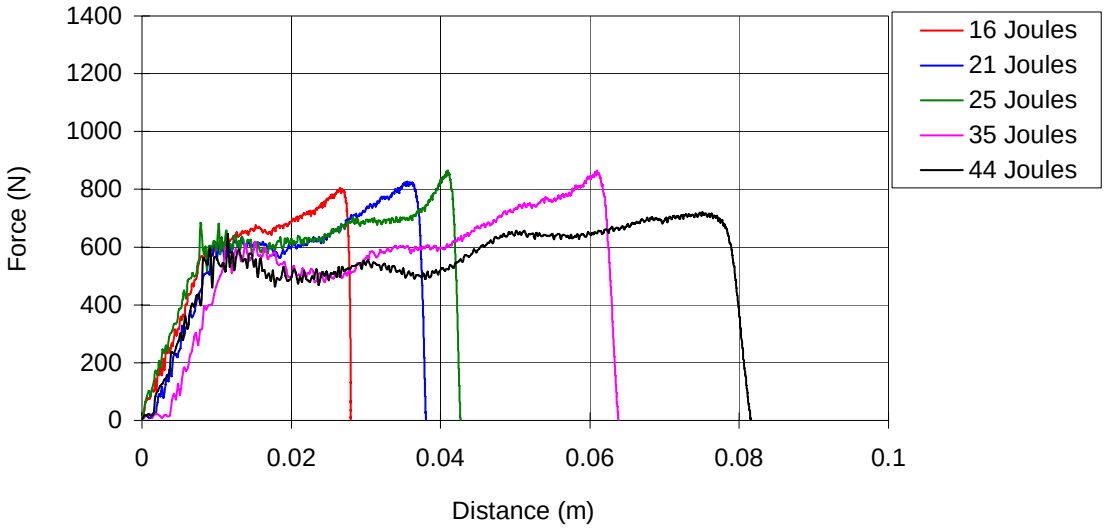

Figure 4-18. The icepick against the 14 layer Aeroflex® target.

The results of all the tests are summarised in tables 4-7 – 4-10. Figures 4-21 – 4-24 show the force vs. displacement data for the highest impact energy test against each target. For most target types the shapes of the force vs. displacement curves follow similar patterns to figures 4-16 - 4-18 in terms of variation with blade type or impact energy level. The only exception is for the titanium target, which for all knife types showed a difference in behaviour between tests below or above 20J.

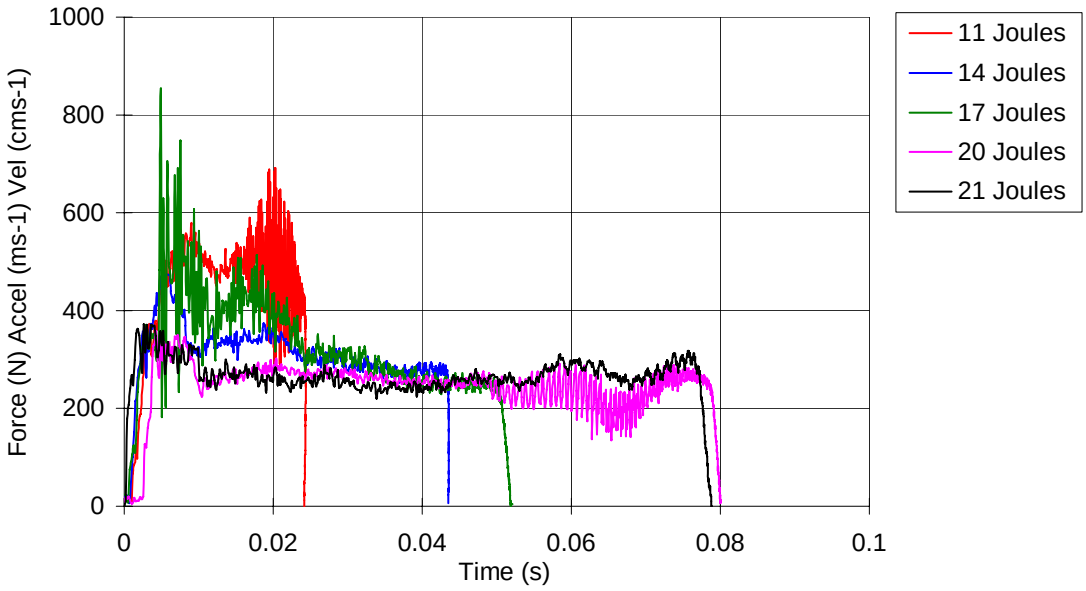

Figure 4-19. Icepick blade vs. titanium over a range of impact energy levels.

This effect is shown in figure 4-19, which is for the icepick weapon, the difference being most marked in tests with this blade type. It can be seen that at the higher impact energy levels (20J and 21J) the load at perforation is approximately 350N and is followed by a more or less steady resistance as penetration proceeds. However for the lower impact energy levels (11J – 17J) the target shows a similar initial load to perforation which then increases to approximately 500N followed by drop of 100N or more with increasing penetration. Figure 4-20 shows the initial parts of the force vs. displacement plots from figure 4-19 to which a moving average filter has been applied in order to filter the high frequency oscillation from the signal. The oscillation is seen to some extent in all tests on the titanium target and is probably due to the higher natural frequency of the target combined with a frictional stick-slip process during penetration.

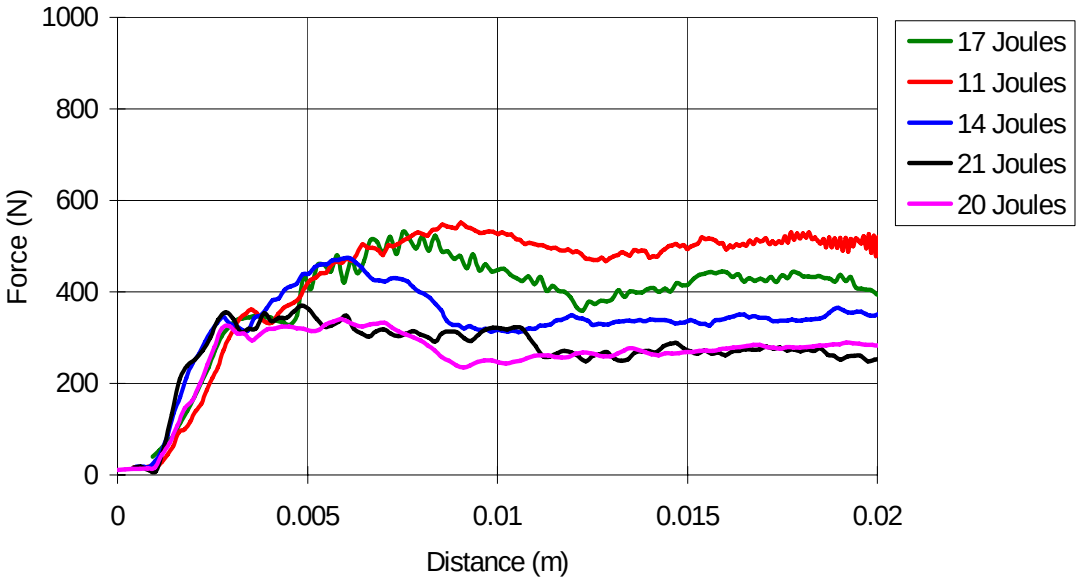

Figure 4-20. Icepick vs. titanium target showing only the initial part of the data. A four point moving average filter has been applied to the data to reduce high frequency oscillations.

Table 4-7. Summary of test results for the Aeroflex® target.

Knife type	Mean initial peak load (N)	Load drop after perforation (N)	Final peak load (N), (@ displacement)	Comments
Commando	600	100	600 (95mm)	All curves overlain
PSDB N°5	1100	500	1200 (65mm)	All curves overlain
PSDB N°1	800	none	1100 (25mm)	All curves overlain, peak load always at 30mm
Icepick	600	none	800 (76mm)	Curve shape dependent on impact energy.

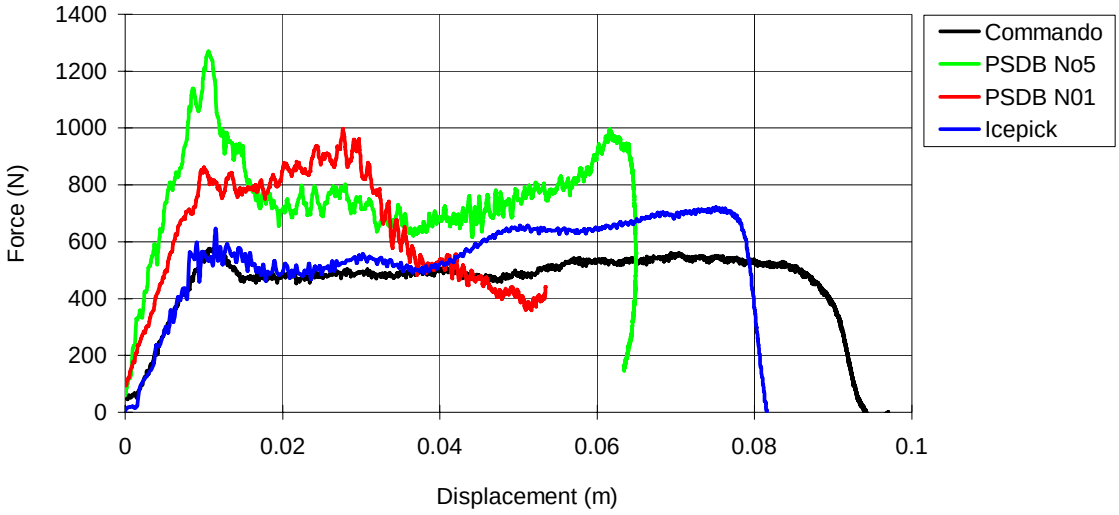

Figure 4-21. Force vs. displacement plots for the four test blade types against an Aeroflex® target.

Table 4-8. Summary of results for the aluminium 7075-T6 target.

Knife type	Mean initial peak load (N)	Load drop after perforation (N)	Final peak load (N) (@ displacement)	Comments
Commando	580	100	550 (95mm)	Similar to Aeroflex® target
PSDB N°5	700	200	900 (60mm)	Similar to Aeroflex® target
PSDB N°1	600	none	800 (25mm)	Similar to Aeroflex® target
Icepick	500	150	350 (70mm)	All curves overlain

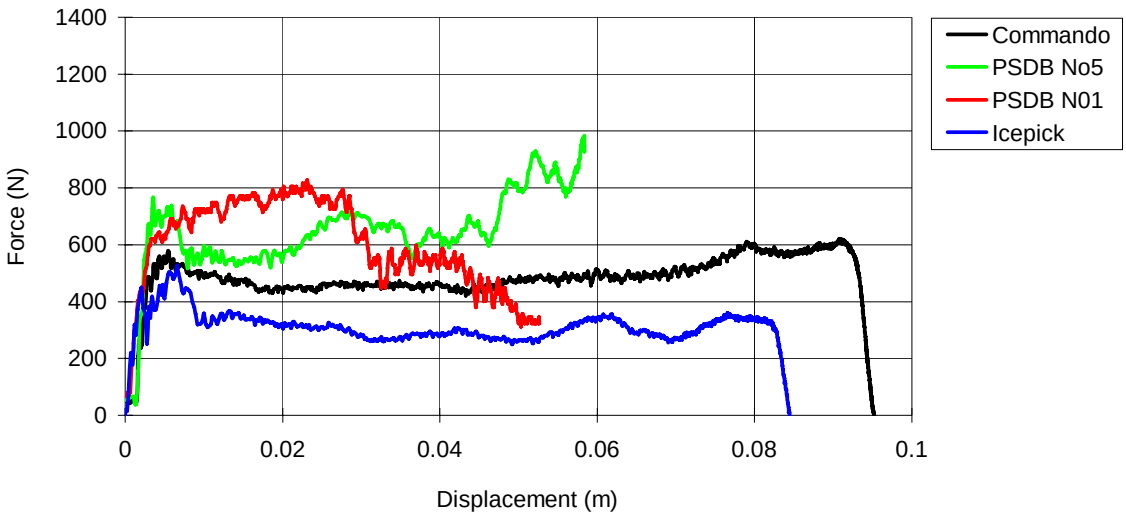

Figure 4-22. Force vs. displacement plots for the four test blade types against an aluminium 7075-T6 target.

Table 4-9. Summary of test results for the softened aluminium 7075 target.

Knife type	Mean initial peak load (N)	Load drop after perforation (N)	Final peak load (N) (@ displacement)	Comments
Commando	300	50	500 (80mm)	Similar to 7075-T6 and Aeroflex®
PSDB N°5	500	150	700 (60mm)	Similar to 7075-T6 and Aeroflex®
PSDB N°1	300	80	350 (30mm)	Similar to 7075-T6 and Aeroflex®
Icepick	550	100	550 (75mm)	Similar to 7075-T6 all curves overlain

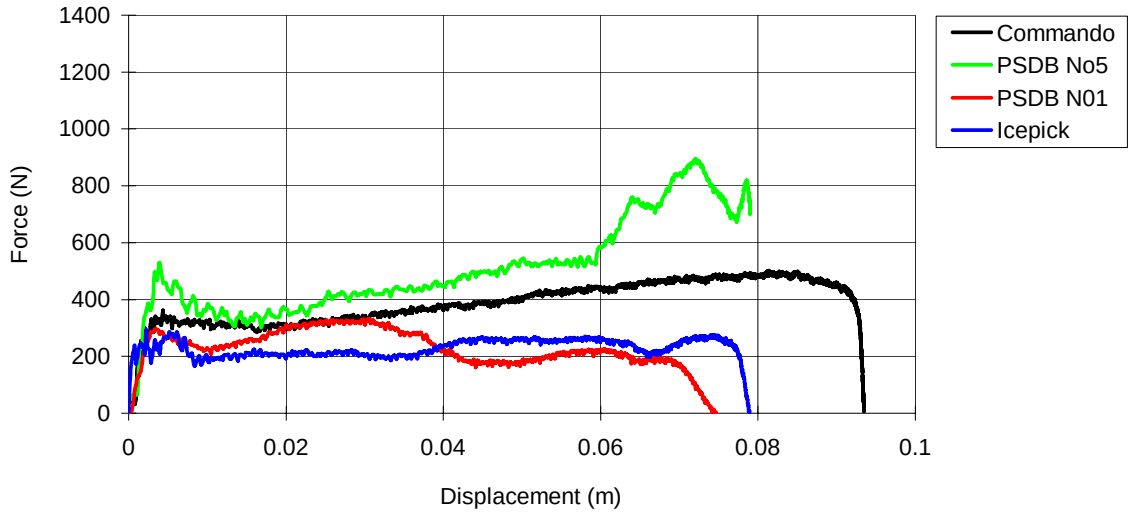

Figure 4-23. Force vs. displacement plots for the four test blade types against a softened aluminium 7075 target.

Table 4-10. Summary of results for the titanium target.

Knife type	Mean initial peak load (N)	Load drop after perforation (N)	Final peak load (N) (@ displacement)	Comments
Commando	500-600	none	600 (60mm)	Initial load higher for lower impact energy levels
PSDB N°5	500	none	650 (50mm)	Similar to previous targets
PSDB N°1	500	none	600 (30mm)	Similar to previous targets
Icepick	350-550	none	300-600 (variable)	Curve shape dependant on impact energy

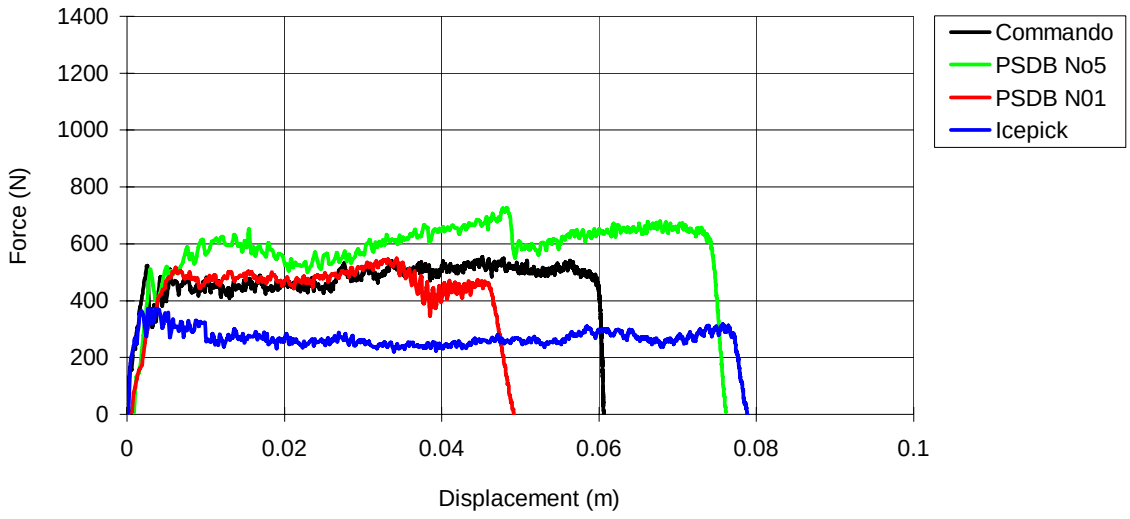

Figure 4-24. Force vs. displacement plots for the four test blade types against a titanium target.

4.5.3 Target material effects

Figures 4-25 – 4-28 summarises the results in terms of penetration as a function of impact energy for Aeroflex®, Aluminium 7075-T6, and softened Aluminium 7075 targets respectively. It can be seen that for the more penetration resistant target types (7075-T6 and titanium) the effect of knife type is negligible for impact energies below 20J. Above this level the commando blade is generally the most penetrative followed by the N°1 blade and the N°5 blade. For the poorer performing targets (softened 7075 and Aeroflex®) ranking is the same but persists down to low impact energy levels.

Figure 4-25 shows the data for the Aeroflex® target. The commando blade is seen to be the most effective followed by the PSDB N°1, and PSDB N°5, with the icepick performing least well. Penetration of this material relies upon cutting of the aramid fibres from which the material is made. The commando blade provides the best cutting performance as it is double edged.

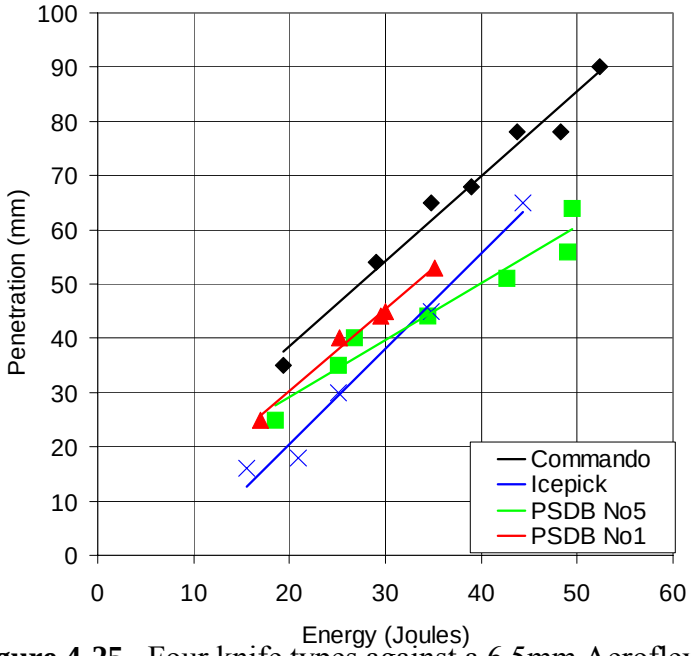

Figure 4-25. Four knife types against a 6.5mm Aeroflex target.

The two PSDB blades perform less well against Aeroflex® as the back of the knife cannot cut the fibres. This leads to considerable asymmetry in the forces on the knife given the rigid axial location afforded by the drop tower. For a free flying knife the resistive forces would be slightly less, however the off axis forces would tend to yaw the knife which would also reduce penetration. The icepick is surprisingly poor against this target, probably due to a relatively blunt point and a lack of cutting edges.

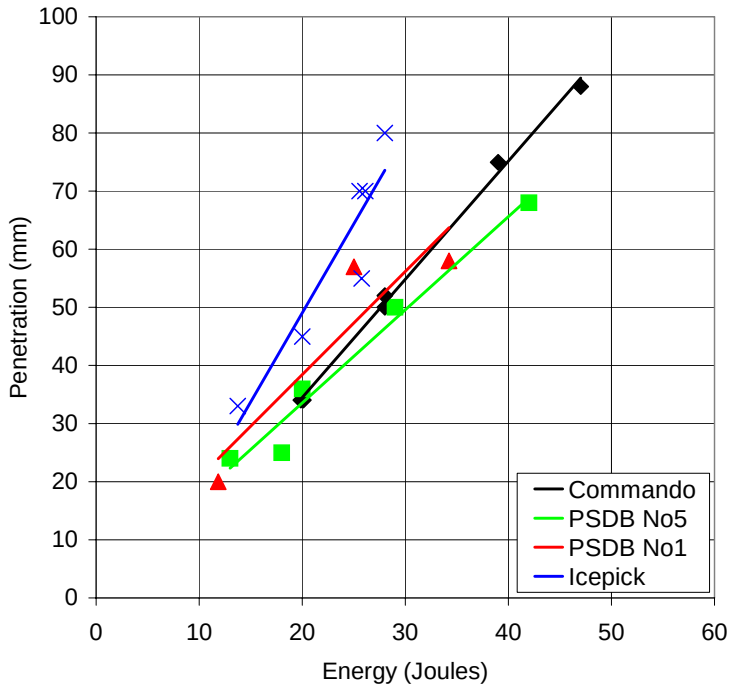

Figure 4-26. Four knife types against an aluminium 7075-T6 target.

Against the hard aluminium (figure 4-26) the blades all performed less well but the N°1 blade was least affected, and so became the second best performer after the icepick. The hard aluminium tended to crack ahead of the advancing blade so that the perforation was enlarged by wedging open rather than cutting. This removed the disadvantage of the single sided blades, resulting in the better performance of the N°1 blade.

Against the soft aluminium (figure 4-27), the icepick performs considerably better than the other blades. The PSDB N°5 and commando blades have similar performance whilst the PSDB N°1 blade is actually the poorest although by a relatively small margin. The poor performance of the N°1 blade is again due to having only a single cutting edge together with its small size making it difficult to clamp properly. Both the PSDB blades had a tendency to skew around during the test as the knife was forced towards the cutting edge by the ramp formed by its back. Although a similar effect was observed with the N°5 blade, its larger size meant that the effect occurred at a larger penetration value.

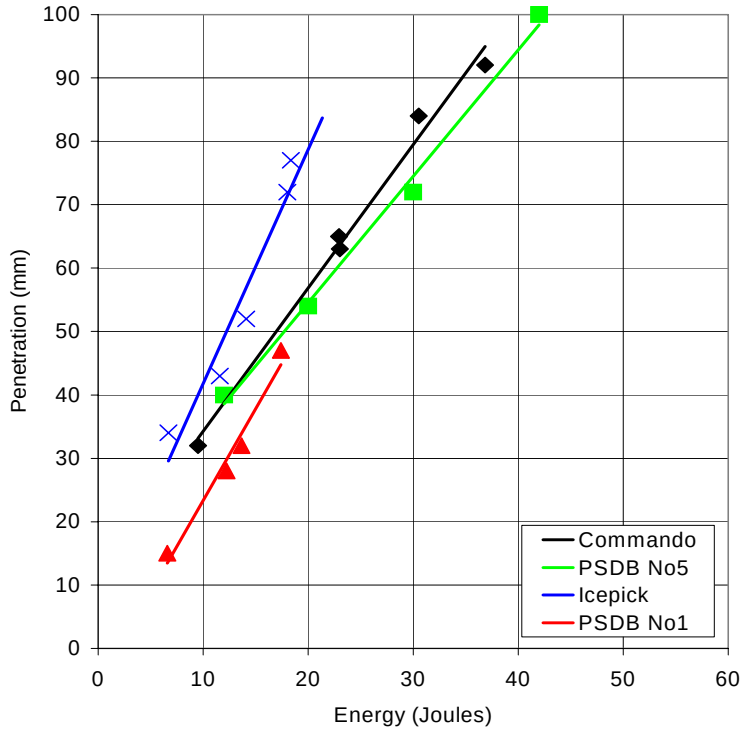

Figure 4-27. Four knife types against a softened aluminium 7075 target.

Against the titanium panel (figure 4-28) the performance of the icepick was better than against the hard aluminium, whilst the other 3 blades performed less well than against hard aluminium. The failure mechanism was generally similar to the soft aluminium and produced a similar pattern of results with a slightly wider spread. The No1 blade performed least well, and in one case was broken and did not penetrate the panel.

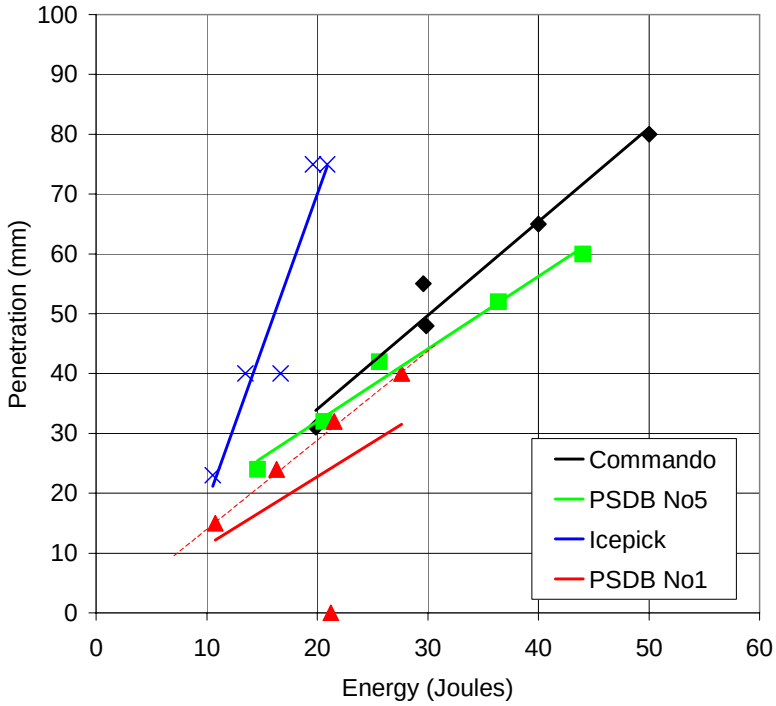

Figure 4-28. Four knife types against a titanium target. For PSDB N^{0}1 blade the solid line is for all data whilst dotted line omits zero penetration data point when blade buckled.

The icepick displayed an unusual characteristic against the soft aluminium 7075 armour. Figure 4-29 shows this data in more detail. In the first test the icepick performed relatively poorly compared with later tests. When a new blade was used the first test was again relatively poor. In both cases the first test produced approximately one third less penetration than subsequent tests at the same energy. Examination of the icepick's surface showed that in the 'as received' condition they

had a dull appearance. After one test against the armour the surface became polished. This radically reduced the frictional forces on the blades in subsequent tests. This effect appeared to be peculiar to this material and blade indicating that a relatively large part of the total energy is being dissipated by friction in this particular system.

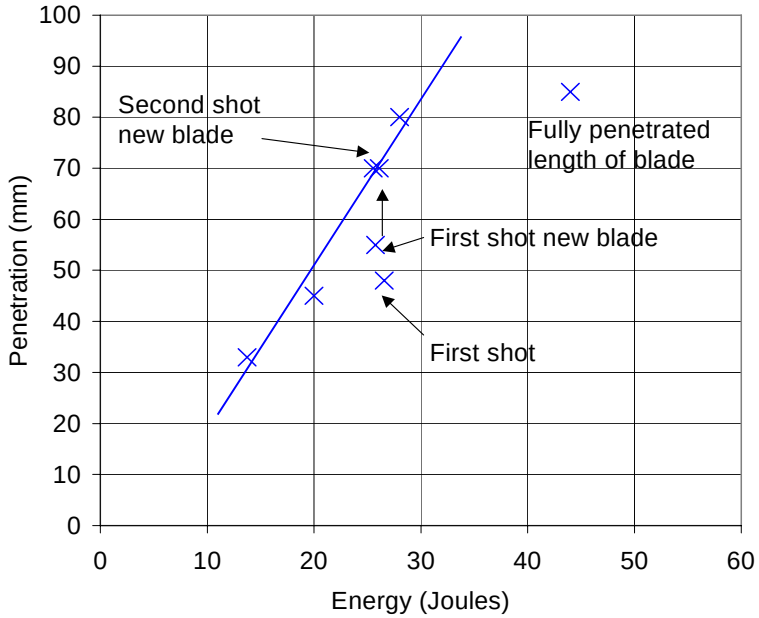

Figure 4-29. All data points for icepick tests against aluminium 7075-T6 showing the effect of blade surface scrubbing on first use.

4.5.4 Target failure morphology

The form of the hole in the armour varied as a function of material type and to a lesser extent blade type. Figure 4-30 shows the impact face of an Aeroflex® target subject to a 40J impact with the Black Widow blade at 45° to the weave direction. It can be seen that the hole has closed up after the blade was removed indicating that the deformation is largely elastic (or visco-elastic) in this material. There was no discernible difference in target appearance between the front and back faces.

Figure 4-30. Impact face of an Aeroflex® target subject to a 40J impact with the Black Widow blade at 45° to the weave direction. (3x magnification)

For the metallic targets the appearance of the perforation is similar for all targets with only slight differences. Figure 4.31 shows the impact and exit faces of a soft aluminium target struck at 31J with the commando blade. It can be seen that there is local dimpling forming an approximately circular depression. The depression extends only slightly beyond the cut ends of the hole and has a similar lateral dimension.

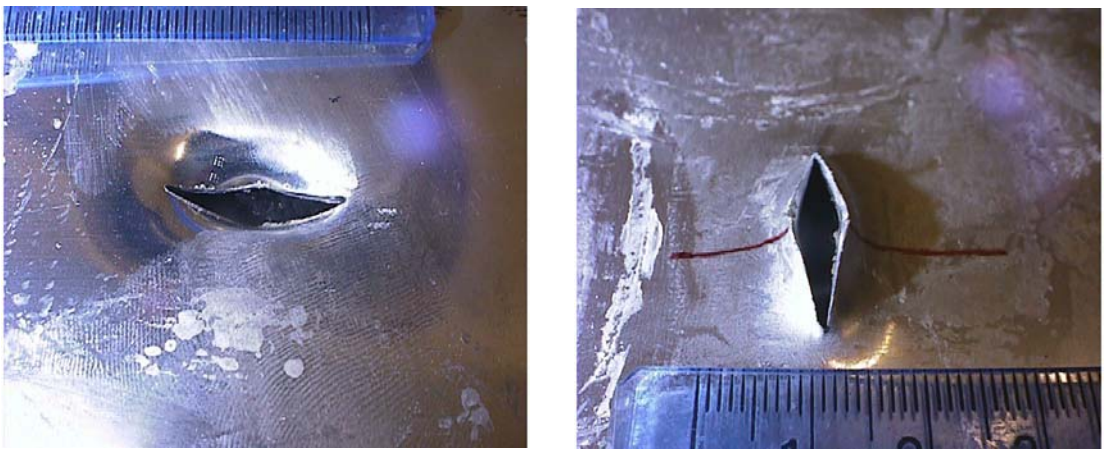

Figure 4-31. Impact and exit faces of a softened aluminium 7075 target struck with a commando blade at 31J. (2x magnification)

Figure 4-32 show two views of the same impact against a 7075-T6 target with the commando blade. The deformation is not symmetrical, one side of the perforation having significantly more bending and containing a single crack emanating from the mid point.

Figure 4-32. A perforation in 7075-T6 produced by a 47J impact with the commando blade. (2x magnification)

Figure 4-33 shows an impact against the 7075-T6 target with the PSDB N^{o}5 blade. The blade profile is clearly seen in the perforation which is slightly asymmetric. A single crack can be seen to extend from a position mid way along one edge. This position corresponds to the impact position of the blade tip.

Figure 4-33. Perforation (exit side) produced by a 40J impact on a 7075-T6 target by the PSDB No5 blade. (2x magnification)

Figure 4-34. Exit face of a 30J impact on a titanium target with the commando blade. (2x magnification)

The titanium target shows a similar appearance to the soft aluminium target. Figure 4-34 shows a perforation from a commando blade in which slight cracking can be observed extending from the mid point on one side only. As was common for all the metallic targets the perforation is slightly asymmetric.

4.5.5 Blade sharpness and wear effects

During the drop tests a number of standardised drops were conducted in order to assess blade degradation. The procedure was to perform 30J drops with the commando knife using Aeroflex®, or 7075-T6 targets. This was done with new blades and then repeated after the blades had been used in a number of tests and various other targets. The data are summarised in table 4-11.

The effect of repeated use of test blades is seen to be relatively small, and is comparable to the difference between individual blades of the same type. Use against the harder target types produced an increase in initial load of up to 20%. The effect of wear on final penetration level was not significant with both increases and decreases being observed.

Table 4-11. The effect of wear on blade performance.

Target	Knife Condition	Initial peak load (N)	Penetration (mm)
Aeroflex ®	New blade	476	50
Aeroflex ®	Same blade after 6 drops on 7075-T6	550	52
Aeroflex ®	New blade	492	48
Aeroflex ®	Same blade as above after 7 drops on titanium	547	47
7075-T6	Nearly new blade (1 drop on Aeroflex®)	561	50
7075-T6	As above after 9 drops on titanium	579	47

4.6 DISCUSSION

4.6.1 Initial study

The force vs. deflection curves in figure 4-6 show that there is an initial peak in the force at a deflection of 5-7mm during perforation of the panel. Observation of the quasi-static tests showed that this peak corresponded to initial perforation of the panel. Following this the knife slides through a steadily enlarging hole in the armour. The kinetic energy of the knife can therefore be absorbed by resistance to perforation of the armour and by providing resistance to further penetration after perforation.

During the stage after perforation the force resisting penetration can come from two distinct mechanisms. As the knife penetrates the panel the hole through which it is passing has to be continually enlarged by cutting or fracture of the armour material. Friction between the knife and the panel caused by gripping of the blade within the hole will provide a second mechanism resisting further penetration.

Although resistance to cutting and hole enlargement is desirable, it is only present if the cross section of the blade is increasing. Very slim blades will experience little resistance to penetration once initial perforation has been achieved. The gripping

mechanism is desirable as it provides a mechanism for absorbing energy from slim blades or relatively blunt ended non-tapering blades. A material exhibiting this property would produce force vs. deflection curves of the shape seen in figure 4-6 in which the force increases after initial penetration. Materials which provide less gripping of the blade or which have lower coefficients of friction in contact with the blade would exhibit a force vs. deflection response in which the force is more constant after penetration as shown in figure 2-12.

A comparison of the static and dynamic data in figure 4-6 shows that there is a generally good agreement between dynamic and quasi-static penetration tests in the initial stages of the impact and penetration event.

4.6.2 Second study

The aim of the second study was to determine key variables in the weapon and armour. The effect of blade sharpness, shape and lubrication are shown to be important. Lubrication of the blade by the use of petroleum jelly has an effect upon both the initial perforation load and upon the degree of subsequent penetration. A significant rise in initial perforation load was produced by cleaning the blade although there was no significant difference between a lubricated blade and one in an 'as received' condition. The degree of penetration achieved was more significantly changed by the presence or absence of lubrication.

The effect of tip sharpness is primarily seen in the variation in peak load at perforation although there appears to be a secondary effect on penetration. The sharpened blade produced a perforation load only 60% of that of a blunt blade but the subsequent penetration resistance was actually higher for the sharp blade. This may be likened to a well known carpentry trick; that splitting of wood is significantly reduced if blunt nails are used. It seems probable that a blunt blade may cause more damage in the material leading to a reduced penetration resistance. It should be noted that the two obviously different blade conditions visible in figure 4-8 were only barely discernible by handling. The variation in sharpness studied in these tests was

not significantly greater than that observed between apparently identical blades obtained for test purposes.

No difference in target performance was observed for impacts close to the edge of a target providing that the perforation was separated from the edge by a distance at least equal to the major dimension of the hole. It was also shown that axial orientation of the blade relative to the fibre direction did not significantly effect the result.

The effects of blade type and shape were significant. This appears to be due to a number of mechanisms including the number of cutting edges, the angle of edges to the blade axis (particularly blunt edges), and the change in cross section along the blade length. These factors determine the shape of the force vs. displacement curve after perforation.

4.6.3 Third study

For the Aeroflex®, and the two aluminium target types the force vs. displacement curves are seen to overlie each other. The overall response of the armour is given by the highest impact energy test and the effect of reduced impact energy is simply to truncate this curve.

From figure 4-15 it can be seen that when the commando blade is used against the Aeroflex® armour it produces a peak load at perforation then a slight drop. The force resisting penetration then lifts slowly but steadily with increasing penetration and all the curves overlie each other. The PSDB N^{o}5 blade shows a much larger drop in load on perforation but the load then increases rapidly as penetration increases. For the PSDB N^{o}1 blade there is no immediate drop in load on perforation but a change in slope. The load then increases up to a maximum at approximately 30mm penetration and then decreases. These effects appear to be linked to the blade shapes and in particular to the variation in cross section along the length of the blade.

In figure 4-35 the cross sectional area of each of the four blade types is plotted as a function of distance from the blade tip. From this it can be seen that the area of the commando blade increases steadily along its length. The area of the PSDB N°5 increases more rapidly up to a maximum at 90mm and that of the PSDB N°1 increases up to a maximum at 30mm.

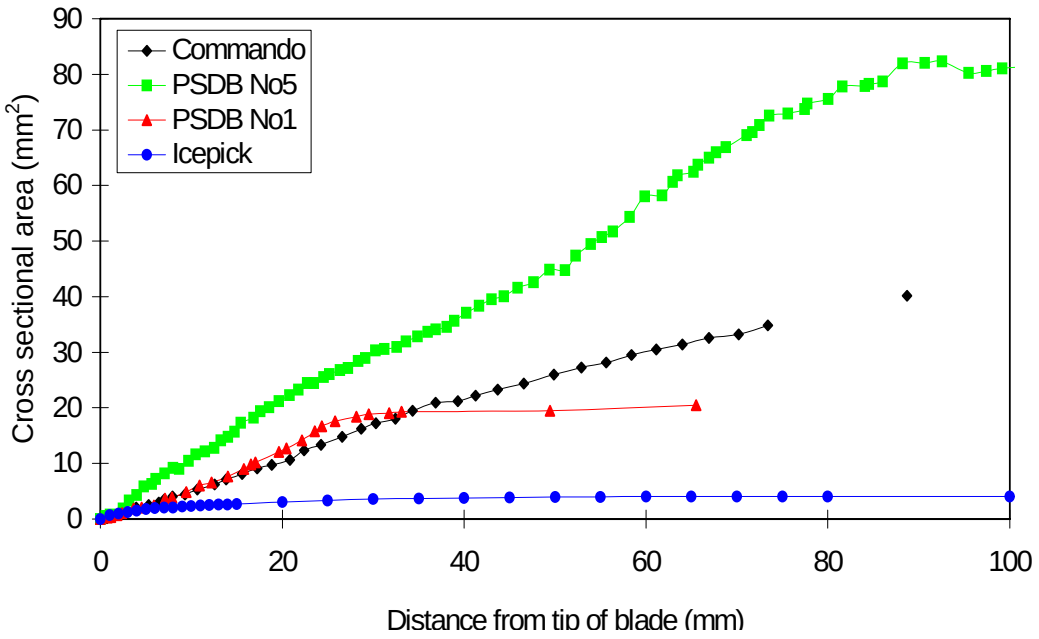

Figure 4-35. The variation in cross sectional area with distance from blade tip for the four test blade types.

For the N°5 blade the penetration levels do not extend past the part of the blade where its cross sectional area is a maximum. However for the smaller N°1 blade the levels of penetration often extend almost the whole length of the blade. Consequently for the N°1 blade the resistive force is seen to decrease once the blade penetrates past the point of its maximum cross section. This does not occur for the N°5 blade as this point is only just reached at the higher impact energy levels.

In addition to the cross sectional area of the blades, the shape of the blade and the type of cutting edge also play a part. The commando blade is symmetrical with two cutting edges, so slots in the armour can be cut by both edges as required to clear the

presented area of the blade. Both of the PSDB blades have only a single cutting edge. The PSDB N^{o}5 has a non-cutting edge which extends parallel to the axis for approximately 50mm after the tip and a major part of the growth in cross sectional area is a function of blade thickness. Consequently this blade shows a large drop in load after perforation and the force resisting further penetration only increases as penetration exceeds 40mm. In contrast the PSDB N^{o}1 blade has a non-cutting edge forming a significant angle to the blade axis. Therefore after perforation the slot in the armour can only be extended easily along one edge of the knife whilst the length of cut required is governed by both edges. Consequently there is little or no load drop on perforation and the load increases up to the point where the non sharpened edge becomes parallel to the blade axis.

The edged blades have relatively large cross sectional areas and it appears that the hole expansion required to accommodate this is the major factor resisting penetration after perforation. The icepick blade lacks any cutting edges and so the little expansion of the hole in the armour that is required has to take place by deformation of the armour. It can be seen from figure 4-18 that the load at the end of the test is the same irrespective of impact energy or penetration distance. This suggests that it is frictional resistance which is resisting penetration. The coefficient of friction generally increases with decreasing sliding velocity and this has the effect of increasing resistive force as the blade decelerates. Because the penetration of the icepick is governed by friction its performance is strongly influenced by surface finish so blade cleaning in the first test is seen to have a significant effect as shown in figure 4-29.

The titanium armour shows a different behaviour to the other target materials in that the shape of the initial part of the force vs. displacement curves is dependent upon the impact energy level. This effect is seen in all the blades and is illustrated for the icepick in figures 4-19 and 4-20. At low impact energy levels the load to perforate the armour is relatively high and extends over several millimetres of displacement. However, at higher impact energy levels the load is seen to be significantly lower and

perforation is seen to occur more suddenly. Titanium has a hexagonal crystal structure which is inherently more strain rate sensitive than the face centred cubic structure of aluminium. This would be expected to increase the strength of titanium as the impact velocity is increased. But the reduction in perforation load with increasing velocity suggests that there might be a reduction in ductility or a change in deformation mode at the higher impact velocities.

The hard aluminium alloy is particularly strong although relatively brittle. Against small sharp blades such as the PSDB N^{o}1 it is capable of inducing failure of the blade tip. However if the blade does not buckle, then the relatively brittle failure mechanism is not a good energy absorber and the resulting penetration levels are high. This behaviour is in keeping with the test performance of a number of commercial armour systems which show generally zero penetration resulting in broken blades interspersed with occasional catastrophic failure.

The soft aluminium is representative of typical formable and relatively cheap aluminium grades. Its failure mechanism is by petalling and cutting rather than the more brittle cracking seen in the hard aluminium. Its performance was relatively poor against all the blades but it was only slightly poorer than the other materials against the icepick. It seems likely that small and constant cross section of the icepick means that penetration is largely resisted by frictional forces. The soft aluminium does not crack and the petals formed during failure maximise the contact area with the blade. In addition the coefficient of friction of soft materials tends to be higher than hard materials as they can conform to the surface of the other material.

It is not clear why in tests of the icepick vs. aluminium 7075-T6 alone, there is a striking increase in icepick performance after the first test. Although this effect was not observed in any of the other systems in these tests, it would be expected in any armour which relied upon frictional loading of the blade. This might be the case for some of the coated textile systems that are currently on the market. If the icepick is to be used as a test blade then some consideration should be given to polishing the

surface. This would bring the performance closer to that which might be expected of a sharpened screwdriver.

The icepick is seen to be a very serious threat to the majority of armour materials even though its relatively blunt tip reduces its effectiveness against textile systems. This could be improved by specifying a sharper tip, but it would also have the effect of increasing the likelihood of buckling failure as seen in the N°1 blades. The commando continues to be the most reliable test shape as it is always either the best or second best performer. Although the PSDB N°1 blade does not perform particularly well in these tests it should be noted that the graphical results tend to emphasise the high energy performance. Close examination of the lower energy data and trendlines indicates that at 40J and below the N°1 blade is comparable to the other blades.

No significant loss of performance was observed during repeated use of blades. In a number of cases the measured penetration was greater for the used knives. This probably indicates that the effect of wear is limited or that the defeat mechanism changes. It is seen from section 4.4.3 that blade tip blunting increases initial loads but that this also increases target damage so that penetration then becomes easier. The overall effect is that penetration is independent of sharpness providing that the loads do not cause the blade to buckle. The main effect of wear or blunting is likely to be an increase in initial loads and hence increase the chance of the knife buckling. However, for a blade which is loaded close to its buckling limit, slight blunting might drastically reduce penetration by causing buckling of the blade.

4.7 CONCLUSIONS

The penetration of an armour by a knife follows a number of discrete stages with different parameters controlling each stage. Upon initial contact with the armour the force resisting the knife increases rapidly up to a point where perforation occurs. The

magnitude of the force at perforation is strongly dependent upon the tip sharpness of the test blade. Perforation occurs because the impact energy is dissipated over a very small area so that the armour is defeated locally before the impact can be absorbed in global processes such as bending.

Following perforation the resistive load of the armour generally decreases and the blade slides through the opening. The resistive load is a function of the force required to expand the hole and the frictional forces between the blade and the armour. The magnitude of the resistive loads after perforation is determined by the blade shape, surface finish and to some extent the target damage caused during perforation. Sharp cutting edges significantly decrease the load required to expand the hole particularly in the case of the textile targets. Minimising blade cross section also reduces penetration forces although this has to be balanced against buckling strength of the blade.

The perforation and penetration processes are generally independent of impact velocity and show good agreement with quasi-static penetration tests. Kinetic effects in accelerating armour material away from the perforation are negligible and strain rate effects are only apparent in the titanium armour.

The most notable factor revealed by these tests is that there appears to be no single best or worst blade type. Similarly, there is no single best or worst armour material, although this effect may be exaggerated to some extent by using test panels containing only one material. Commercial systems often contain combinations of materials particularly if they are dual purpose, i.e. ballistic and stab resistant. The test panels were chosen to give a range of different characteristics that to some extent match the materials which are seen in commercial systems. Therefore, there is every reason to expect similar variations in performance against current and future body armour systems

4.8 REFERENCES

1. S. M. Pollitt, An investigation into body armour to protect against knife attack, 45 Degree Course Student Project, Royal Military College of Science, (1993).

2. M. W. Money and G. D. Sims, Calibration of quartz load cells: An in-situ procedure for instrumented falling weight impact machines, *Polymer Testing*, **8,** 429-442, (1989).

3. Ballistic Resistance of Police Body Armour, NIJ Standard 0101.03, US Department of Justice, National Institute of Justice Technology Assessment Programme, (1987).

4. C. H. Watson, I. Horsfall, A. M. Robinson, Stacking sequence effects in multi-purpose body armour. *Proc Sharp Weapons Armour Technology Symposium*, Cranfield University, Shrivenham, (1999).

5. G. Parker, PSDB Stab Resistant Body Armour Test Procedure (1993), Police Scientific Development Branch, Publication No 10/93, (1993).

6. I. Horsfall, S. M. Pollitt, J. A. Belk and C. Angood, Impact perforation testing of stab resistant armour materials, *Impact and Dynamic Fracture of Polymers and Composites*, ESIS 19, (Ed. J. G. Williams and A. Pavan), Mechanical Engineering Publications, London, 433-442, (1995).

7. J. Tan and G. Parker, Stab Resistant Vests, Police Scientific Development Branch, Publication No 20/92, (1992).

CHAPTER 5

HUMAN PERFORMANCE

5.1 INTRODUCTION

Stab resistant body armour is now becoming a standard item of equipment for police officers in the United Kingdom. The armour is usually required to have a stab resistance as specified by the Police Scientific Development Branch KR42 standard [1]. This and all other test standards [2,3,4,5,6], specify that body armour must resist penetration by a specific blade type, delivered at a specific energy level or range of levels. However, the actual range of energy levels specified varies over more than an order of magnitude and the basis for these levels is not clearly defined.

This has led to some doubt over the validity of the specified test energy values. There is therefore a need to quantitatively assess the threat from knife attack. Previous studies have investigated the velocity achieved in stabbing [7], whilst the work in this chapter concentrates on the energy produced, as this is the key variable in test standards. This is a relatively complex task, as not only are there a wide variety of possible weapons but also a highly variable human element in powering the weapon.

This chapter describes tests to determine the energy range and characteristics of stabbing actions that might be directed against stab resistant body armour by an assailant. An initial study was carried out by Prosser [8] in which the energy and velocity achieved in different stabbing actions was determined for a small number of volunteers. In the following chapter this work is extended to a greater number of subjects from a number of sample populations, and characteristics of the energy delivery are analysed in detail. Some of the work covered in this chapter has been published previously and is attached as appendices 4 and 5.

5.2 EXPERIMENTAL TRIALS PROCEDURE

As all current standards define the energy of a blow that must be stopped by the armour, the primary measurement required is of impact energy. It is also useful to know the force and velocity history of the impact event. In order to assess the ability of a person to deliver a knife, it is necessary to measure a number of basic parameters, namely the force that can be applied and the rate at which it is applied. From this basic data it is possible to derive most of the required results including the total energy of the impact and the impact velocity. In this work it was decided to use an instrumented knife to measure the force and acceleration during an impact with a standardised target.

The instrumented knife is shown in figure 5-1 with a commando blade[1] which was used in all tests. The basic blade is a diamond section dagger of 120mm length, although this was cut down to 80mm for the tests. A new blade was used for each series of tests, although earlier substitution was sometimes required due to damage or blunting of the blade tip. The blade was held in a clamp on the front of the instrumented knife. A piezoelectric load washer positioned behind the blade measured the axial force on the blade during impact. On the rear of the hilt was a single axis accelerometer to measure deceleration during impact. A sabre guard was used to protect the hand of the subject. The transducers were connected to a transient recorder, in this case a Rosand Precision Ltd control unit.

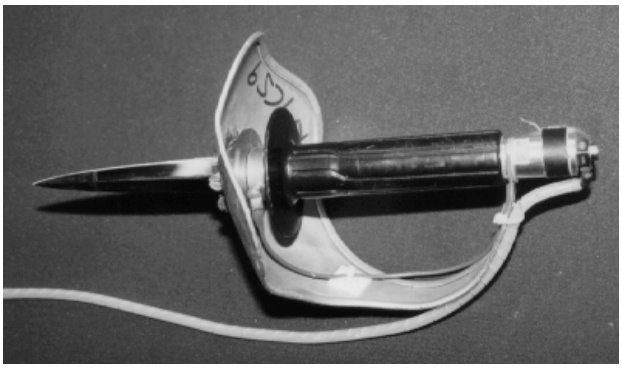

Figure 5-1. The instrumented knife.

[1]Supplied by H.M.Slaters Ltd, Sheffield, UK.

The force transducer was calibrated using a procedure similar to that described by Money and Sims [9]. A known mass was suspended from the blade clamp by a wire. The handle was then dropped, allowing the assembly to go into free fall and thereby emulating a compression pulse at the transducer. The accelerometer was supplied with a factory fixed calibration, although this was confirmed using a calibrated shaker table.

All tests used a standard target consisting of a 12 layer Aeroflex®[2] sheet. This is a semi-flexible aramid fibre composite consisting of plain woven layers in a thermoplastic binder and has been described in more detail in section 4.5.1. This material is not a candidate armour material, but was chosen to give a degree of resistance to penetration without actually preventing it. The target was mounted on a Plastolena® backing block of a type usually used for ballistic testing of body armour. This provided support to the target without interfering with the penetration process.

After each test the data was downloaded from the transient recorder to a personal computer spreadsheet for processing. The basic data consisted of instantaneous values for force, F and acceleration, A. For most tests 340 data points were recorded on each of the two measurement channels over a period of 50ms giving an interval Δt between data points of 147μs. Longer recording periods and high-speed video recording were used on some trials in which it was shown that the knife was arrested within 50ms. Therefore the impact velocity or the velocity at any point after impact was determined by summing the acceleration data from the last point backwards.

$$V_0 = \sum_{i=380}^{i=0} A_i \Delta t \qquad \text{.....(1)}$$

The instantaneous velocity V_i in metres per second, is then multiplied by the time interval between data points in seconds, to give the distance travelled in each time interval x_i in metres.

$$x_i = V_i . \frac{0.05}{340} \qquad \text{.....(2)}$$

[2] Supplied by Aero Consultants UK Ltd, Cambridge, UK.

The instantaneous energy in Joules, was then calculated as the distance travelled x_i multiplied by the force F_i. This was summed to determine the total energy of the stab E in Joules.

$$E = \sum_{i=0}^{i=380} F_i.x_i \qquad \text{.....(3)}$$

For each test it was therefore possible to determine total energy and impact velocity. It was also possible to show the force, acceleration (deceleration) and velocity history of the event. A typical result is illustrated in figure 5-2.

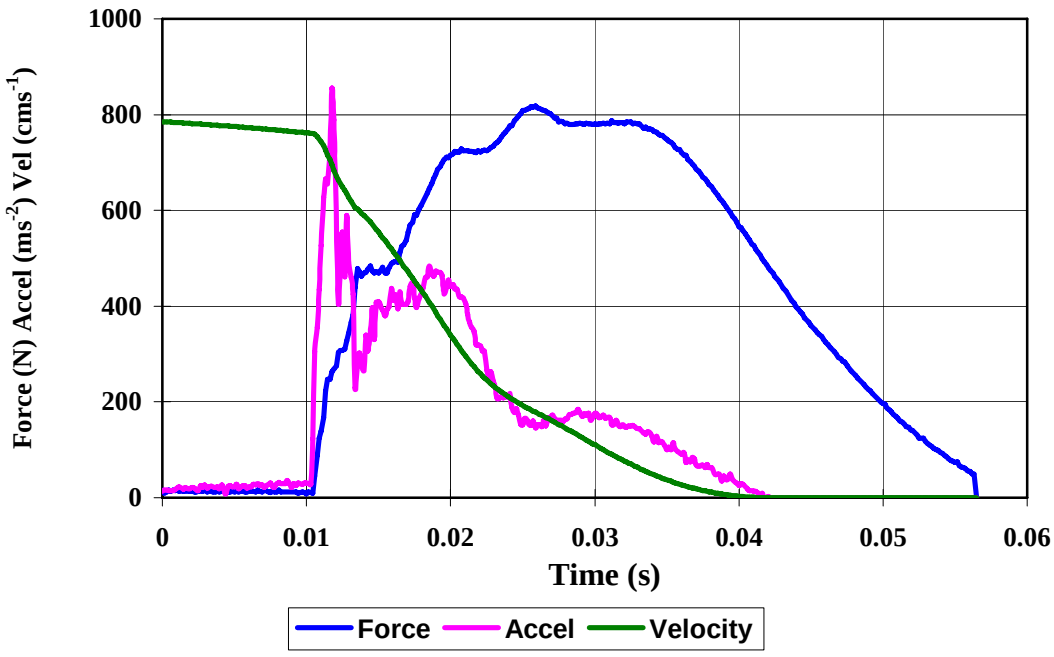

Figure 5-2. The velocity, force, and acceleration profile of a 42J underarm action stab.

In order to verify the calculations and assumptions the knife penetration into the target was measured after the test and compared to the total calculated displacement. These were found to be in agreement.

5.3 TRIALS RESULTS

Using the method described above an initial study was performed by Prosser [8] using a small number of volunteers including students at the Royal Military College of Science (RMCS) and serving officers and staff of Hertfordshire Constabulary. Penetration of the knife through the target was recorded together with the raw data. The results reported here include those of Prosser together with a larger sample of over 400 volunteers including more students from RMCS, police officers and staff from Gloucester Constabulary and visitors to the International Police and Security Exhibition 96. In most test groups each subject was asked to perform one underarm action stab (figure 5-3). In tests at RMCS each subject was asked to stab twice using an underarm action, and some subjects from each group were also asked to stab using an overarm action (figure 5-4). No other guidance on technique was given to the subjects.

Figure 5-3. An underarm action stab.

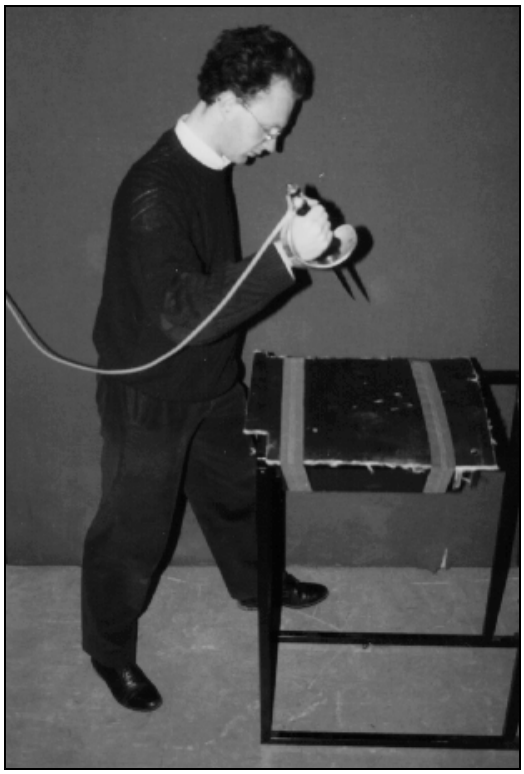

Figure 5-4. An overarm action stab.

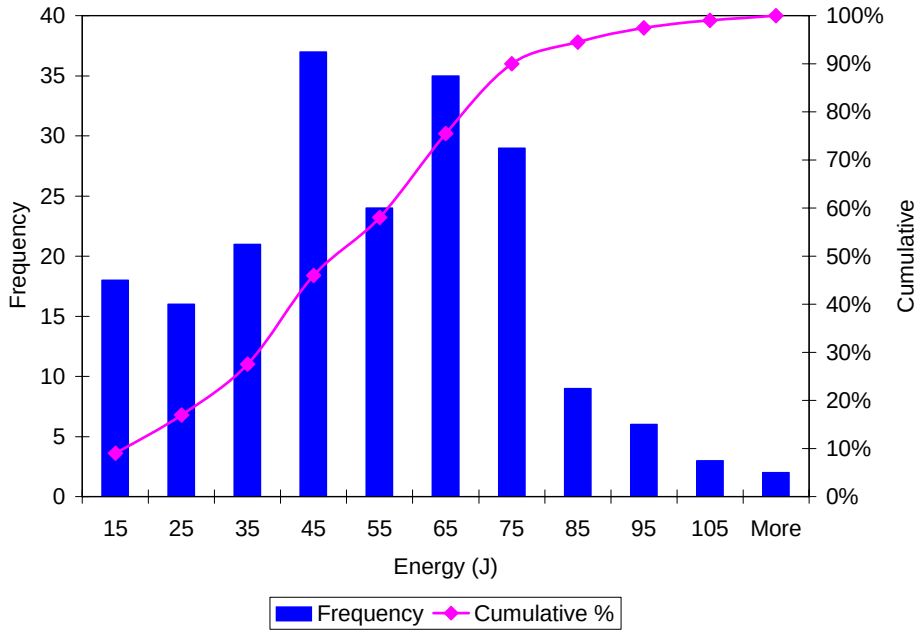

Figure 5-5. Histogram of stab energy for all underarm action stabs.

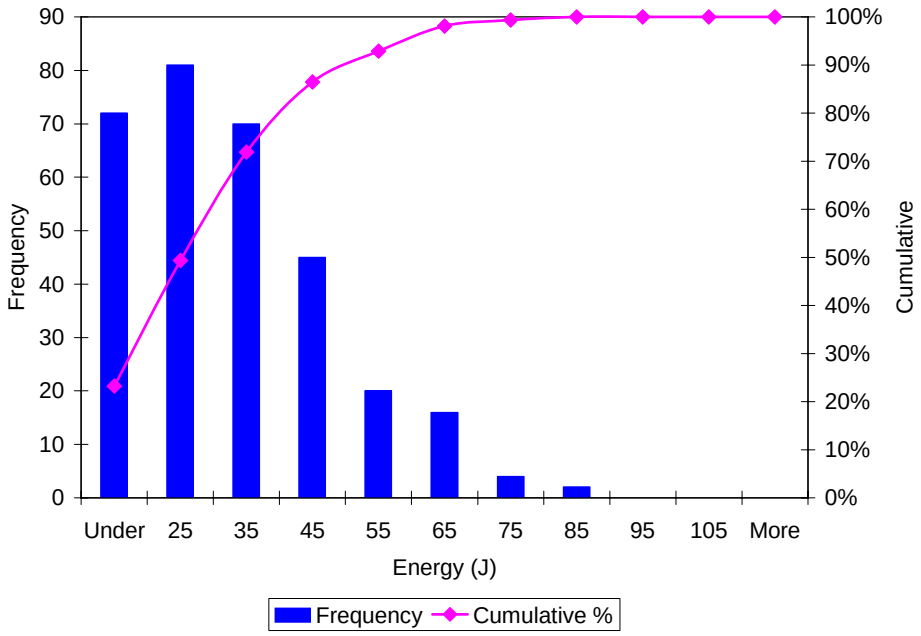

Figure 5-6. Histogram of stab energy for all overarm action stabs.

Figure 5-5 and 5-6 show the accumulated data for underarm and overarm action stabs respectively, and the data are summarised in table 5-1. The larger data set in figure 5-5 provides a more even distribution but it is possible to see a large difference between the two actions with the overarm action stabs showing higher mean and maximum velocities and energies.

Table 5-1. Summary of performance data.

Group	Number	Mean Energy (J)	95% Energy (J)	Maximum Energy (J)	Mean Velocity (ms^{-1})	Maximum Velocity (ms^{-1})
All underarm	310	27.5	57.5	83.5	6.1	11.5
All overarm	200	37.1	86.1	114.9	9.0	12.3
Male underarm	283	29.1	55.2	83.5	6.2	11.5
Female underarm	27	10.6	22.4	30.9	4.8	7.9
RMCS all underarm	32	26.8	50.9	57.5	6.1	9.4
Gloucestershire police all underarm	62	31.6	57	64	6.1	9.0

There was a significant difference between the performance of male and female subjects with the average energy for female underarm action stab being only 10.6J compared to 29.1J for males. Little significant difference was observed between different male groups, the RMCS students and Gloucestershire police groups performance being close to the overall values.

5.4 DISCUSSION OF TRIALS

The interaction between the knife and target is illustrated in some detail in figure 5-2. In this test the knife had an impact velocity of $8ms^{-1}$. On contact with the target it was rapidly decelerated leading to a peak deceleration of $800ms^{-2}$, whilst force rose more slowly to an eventual maximum of 800N. The actual shock loads to the test subject's wrist would be somewhat lower than this as the subject's grip onto the hilt was not completely rigid. However the loads are significant and in the case of more penetration resistant armour might lead to damage both to the knife and the wrist of the attacker. Most subjects were seen to continue pushing on the knife after impact which is indicated by the long tail of the force profile (figure 5-7). The muscular effort is in the region of 200N, but was insufficient to overcome the frictional resistance of the knife embedded in the target.

In this study the mean terminal velocity of the knife was $6.1ms^{-1}$ for underarm stabs and $9.0ms^{-1}$ for overarm stabs. These values compare well with results of Miller and Jones [7] who determined mean velocity values of $5.8\text{-}6.3ms^{-1}$ and $8.5\text{-}9.2ms^{-1}$ respectively. In a study by Tan *et al* [10] only the maximum terminal velocity was reported and this was found to be $14ms^{-1}$ although the maximum energy level measured was no greater than 42J. This velocity is significantly greater than the maximum recorded in both this thesis and in the work of Miller and Jones [7]. There is no clear reason for this, although as all three studies used different measuring techniques some discrepancy might be expected. One other possibility is that there might be some effect of knife mass. Assuming a similar muscular effort in accelerating the knife, a heavier knife will have a lower terminal velocity than a light knife but the same kinetic energy. The knife used by Tan *et al* [10] had a mass of 0.175kg whilst the knife used in this study was 0.6kg. However this does not explain the discrepancy with the data of Miller and Jones[7] who used a knife of mass 0.192kg.

The mean, 95-percentile and maximum values of energy and velocity are shown in table 5-1. The practical significance of the mean values is questionable as each group of volunteers contained some individuals who performed very poorly. Similarly the maximum values obtained were from exceptionally fit and well-trained individuals who may not be representative of the wider population. However, it may be that individuals willing to use a knife against a police officer may fall into a similar category. The 95-percentile value may give a realistic indication of maximum required armour performance. The value of most significance is probably the 95-percentile for all underarm stabs, which was 54.4J. This is significantly greater than that specified in the current UK test standards (42J) [1]. Only the USA (HP White) standard [2] specifies significantly higher energy levels and this was set against a double handed overarm action stab. There are a number of factors that effect the significance of the measured values to practical armour systems. The loads generated on the knife were approximately 1000N for the higher energy stabs. This was for armour that allowed 45mm of penetration at 40J. Practicable armour systems that meet current penetration limits would produce far higher loads so that the knife or attacker's wrist might be damaged. This may mitigate the effect of higher energy stabs.

The primary purpose of this study was to provide information on the energy levels required for testing stab resistant armour. Although both underarm and overarm action stabs were analysed, a greater importance has been placed on the underarm action for two reasons. Conventional designs of body armour afford poor protection from an overarm stab, as both the shoulders and the neck are difficult to protect. Also the overarm stab offers some chance of active defence whilst an underarm action can be relatively covert and is consequently more difficult to defend against. For this reason the underarm stab is seen as the major threat, and one that can be countered by wearing armour.

The validity of the data to the overall population and to potential attackers must be considered. A number of factors, both psychological and technical, will limit the

accuracy of the data. The volunteers in this these tests were operating under relatively relaxed conditions although the military and police volunteers might be expected to be able to produce reasonable levels of controlled aggression on demand. In addition, there was a considerable element of competition and peer pressure during the tests that were often conducted with groups of volunteers. The results of an individual's performance were known after each test and so there was an incentive to beat previous volunteers' scores.

The instrumented knife had a large hilt with a disc shaped guard at the front that allowed very good transfer of axial load from the hand. It has been stated [11] that the knives used in real assaults are often relatively small in order to allow concealment. This data might therefore represent an overestimate of the forces that could be generated with a more conventional knife hilt, particularly that of a small kitchen or folding knife.

It is necessary to consider the effect of the target on the measured stab energy. The target used in this study allowed typical penetrations of 45mm at 40J which is considerably greater than that which would be achieved in a commercial armour. However, a soft target was needed in order to eliminate the chance of injury to the test subjects which also allowed them to stab without fear of injury. This was felt to be important as a large number of body armour designs are covert and hence an attacker would not know that the target was armoured. It is therefore necessary to simulate the highest energy impact that might be generated.

In order to determine the effect of the target used on the measured energy the impact event must be analysed. It can be seen from figure 5-2 that very high loads are generated on the knife, which are greater than could be generated by direct muscular effort. These high loads are primarily generated by deceleration of the knife and later the hand and arm. An underlying and relatively small muscular effort is seen in the latter stages of the event once the knife has been arrested. Hence the energy measured during the impact event comes from two principal sources: the kinetic

energy of the knife-hand-arm system and the muscular force (work) expended during the penetration event. Armour of high penetration resistance might allow virtually no penetration, in which case only the kinetic energy component would be present, whereas a soft target that allowed large penetration would also receive energy due to manual work expended during the penetration event.

The manual work expended on the target will be the product of the muscular force and the total distance over which the knife travels during the impact. The knife travel will be the sum of penetration through the armour (typically 45mm), the target thickness (5.5mm), and target movement into the backing (10mm), giving a total of 60.5mm. Examination of the force data (figure 5-2) shows a residual force of approximately 200N, which can be taken as the underlying muscular effort during the impact event. If the total knife movement during impact were taken as 60.5mm and a constant muscular force of 200N then the muscular work done on the target would be 12J.

It can be seen that the measured ability of the subjects will increase with greater penetration into the target or greater blunt trauma (movement into the backing). It is not possible to test very effective armours in this way, as the impact forces on the knife would be likely to cause injury to the subject. Therefore a relatively low resistance material had to be chosen for these tests. Practicable armour systems must not allow more than 5mm penetration to meet current UK specifications [1]. These tend to be relatively flexible and consequently allow more movement of the armour into the backing material. Consequently the total energy which might be expended against an armoured target would not differ significantly from the range of values measured in this work. However, the energy values reported in this study may underestimate the maximum that might be achieved against a very soft or poorly supported target.

5.5 ANALYSIS OF HAND STABS

The preceding discussion shows that the load transfer into the armour was relatively complex. It is suspected that this is result of different parts of the moving mass (knife, hand, and arm) being brought to rest sequentially during the impact event. Figures 5-7 shows typical data sets recorded during the initial trials. From these trials it becomes apparent that although there are some differences in shape between each test there are also some common factors to all the curves.

1) There was an initial sharp deceleration followed by a more gradual deceleration to rest. The initial peak is probably caused by the initial sharp deceleration of the knife as it strikes the armour surface.

2) The force curve often showed two peaks approximately 20ms apart. This is produced as slack in the grip is taken up or as the hand is forced against the hilt guard when the knife is decelerated.

3) The force curve often rises to a fixed value at the end of the test. This is probably due to the volunteer trying to push the blade further into the armour.

4) Some curves show deceleration spikes in later parts of the test, probably because the knife hilt has struck the armour as the blade has penetrated to its full length.

Therefore it can be stated that the energy from the stab comes primarily from the kinetic energy of the knife, hand and arm. Because these components are not rigidly joined their individual contributions are separated to some extent. There also appears to be a muscular contribution particularly in the latter stages of the impact although this is most often observed after the knife has been arrested.

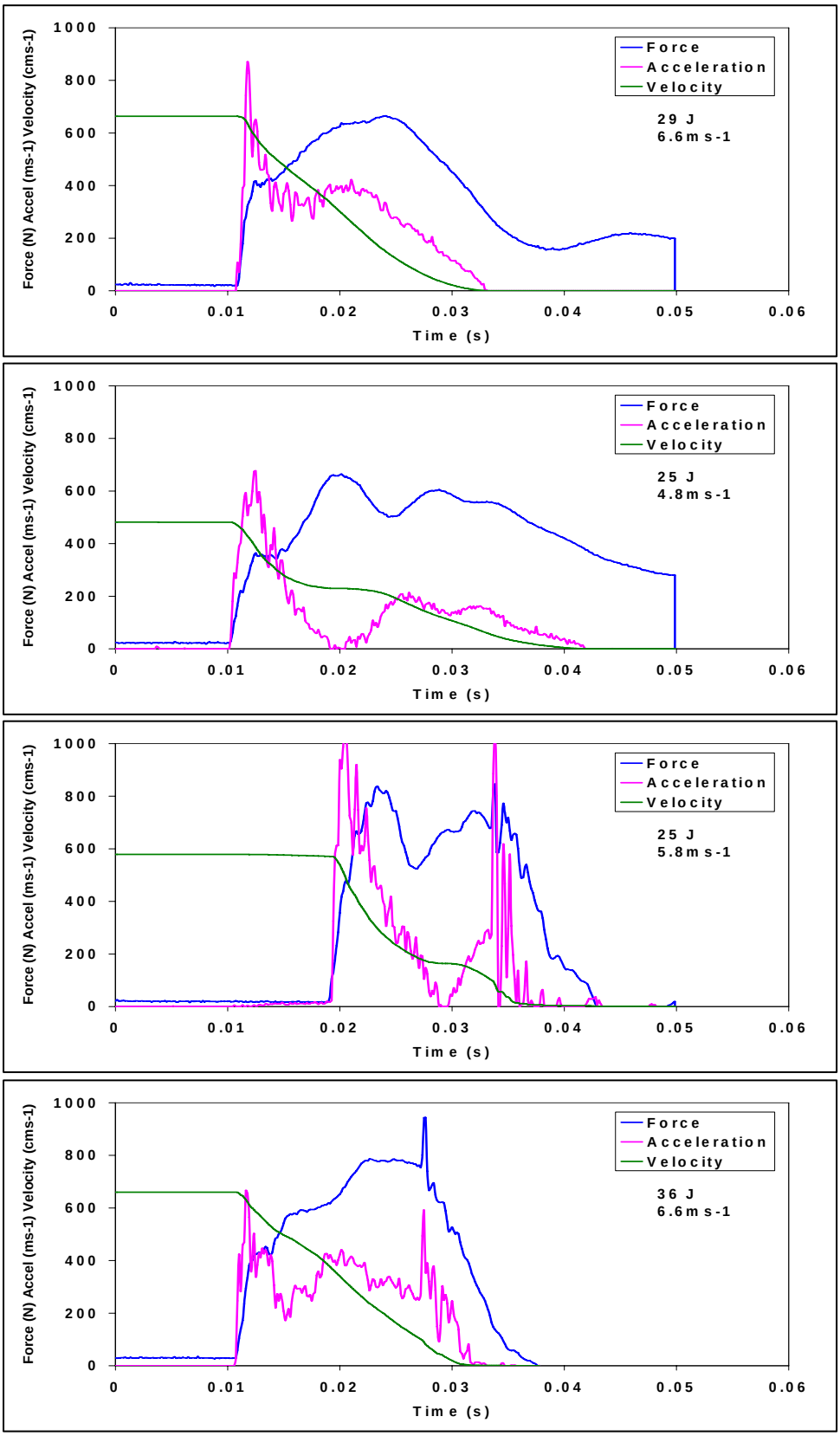

Figure 5-7. Four typical hand stab test data sets.

Using the data from the hand stab tests it was possible to make an estimate of the total mass involved during stabbing. If it assumed that the impact energy is purely a result of the kinetic energy of the moving masses then the effective mass of the knife-hand-arm system m_E can be estimated from knowledge of the impact velocity v and the total energy E_{KE}

$$E_{KE} = \frac{1}{2} m_E v^2 \qquad \text{.....(4)}$$

Taking the data from the tests in figure 5-7 and omitting the muscular effort, the effective mass is in the range 1.2-2.2 kg.

It is possible to make an estimate of the muscular effort E_m and to make an assessment of its effect on the stabbing event. An estimate of the maximum muscular contribution was made by assuming that a constant muscular force is exerted during the entire event. The measured force at the end of the test represents the magnitude of this force F_R after the knife had been halted. This muscular force was then multiplied by the penetration x expected for the impact energy. The penetration was known from previous hand stab and air cannon tests on the same target material. It was found that the energy derived from muscular effort can be derived from the muscular force multiplied by the penetration.

$$E_m = F_R . x \qquad \text{.....(5)}$$

The energy provided by the muscular effort is between 3.5-10.5J for the tests shown in figure 5-7. This is subtracted from the total energy and a new estimate of the mass is made. Taking the above figures as the maximum likely muscular contribution, the effective mass can then be estimated as 1.0-1.5kg.

The instrumented knife weighs 600g. For an average human body the hand is 0.6% of the body mass (typically 75kg) which equates to a mass of 0.45kg. For the forearm and hand the mass is typically 1.8kg. It can be seen that the nominal mass derived

from the hand stab tests (1.0-1.5kg) falls midway between the nominal mass of the knife and hand (1.05kg) and that of the knife, hand and forearm (2.25kg). The data shown in figure 5-7 were all from male subjects whilst the average mass data is for both male and females. Consequently it is likely that the actual hand masses would be higher than 1.05kg and would be within the range of values derived from the test data (1.0-1.5kg). It is therefore possible that the kinetic energy dissipated on impact with the target comes primarily from the arrest of the mass of the knife together with that of the hand.

From the above discussion it becomes clear that the recorded data from the hand stab trials show a complex interaction as a result of the relatively slack coupling between the hand and the knife. This has the effect of producing an extended series of energy transfer events and the characteristic double peak in the force data. It was decided to confirm this by high-speed video recording of further hand stab trials.

5.5.1 Video analysis of hand stab trials

In a study by Horsfall *et al* [12] volunteers were asked to stab into a target comprising of a panel of 14 layer AeroFlex®, supported on the foam rubber backing proposed for the new PSDB stab resistance test [6]. These trials were filmed using a high-speed video camera, with markers placed on both the knife blade and volunteer's wrist. Using image analysis software, the markers were tracked to obtain a distance vs. time plot of the stab event and record the relative motion of the wrist to the knife blade. Force and acceleration data were also recorded as in previous hand stab tests.

Figure 5-8 show a series of video stills of a test, used for the motion analysis of the hand and knife. It can be seen from figure that the wrist and arm rotate around the knife as the knife is slowed down. The angle between the arm and the knife axis increases after impact as the arm rotates around the handle and therefore decelerates at a lower rate than the knife.

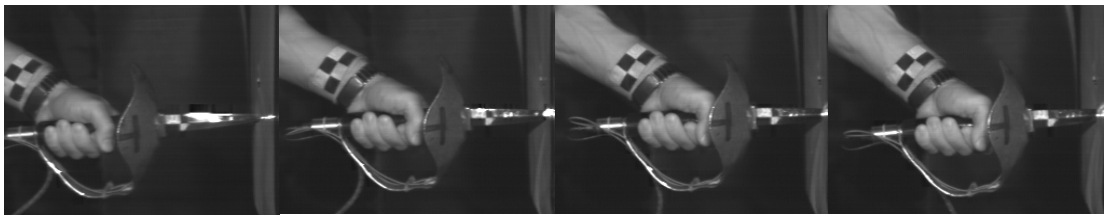

Figure 5-8. Still frames from high speed video of a hand stab. Note the relative position of the hilt and the thumb during the sequence.

The relative positions of the wrist and the knife blade were measured from the images in order to determine the movement of the grip. This data, shown in figure 5-9, indicates that there is a significant movement in the grip during the impact. For the test illustrated the wrist moves 27mm relative to the knife during impact. This data confirms the hypothesis that it is grip compliance that produces the characteristic double peak in the force curve.

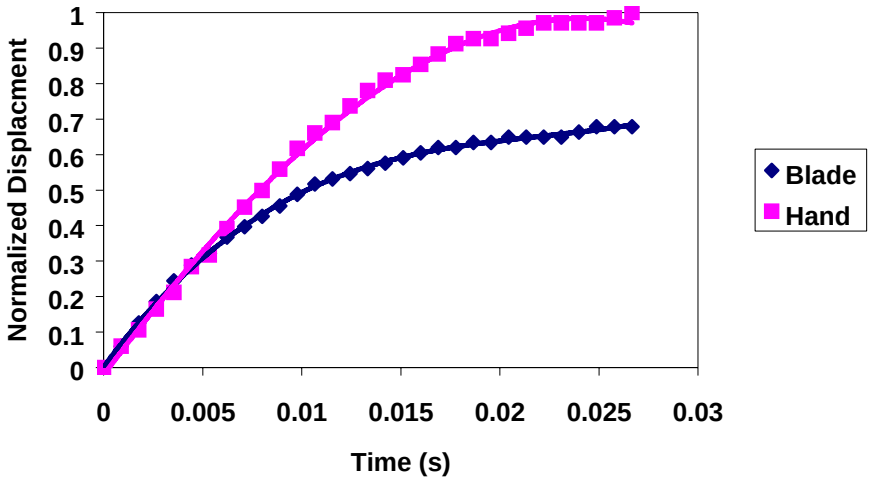

Figure 5-9. Displacement of the knife and wrist relative to the target [12].

In order to further investigate these effects a computer modelling package was used to simulate the motions of the knife, hand and arm.

5.5.2 Modelling of hand stabs

It would appear that the impact of a hand held knife could be seen as the progressive arrest of a number of connected masses. On impact with the armour the knife is first decelerated and its handle moves within the hand grip until any slack is taken up or the hand connects with the hilt guard. The hand is then decelerated, and as the wrist joint rotates the arm is decelerated. An underlying muscular force may also be superimposed on these deceleration forces.

A mechanical modelling software package (Working Model 3.0 by Knowledge Revolution) was used to produce a simple lumped mass model of this system. This package does not explicitly model material deformation but purely elastic collisions can be simulated. It was decided to model the hand stab with the assumption that the result would be used to design a drop tube test so a drop weight geometry was used. The system consists of a knife held in a two-part sabot with instrumentation to measure axial force on the knife blade. This is illustrated in figure 5-10.

The drop mass consists of a blade connected to a primary mass by a stiff spring. This spring simulates the force transducer in the instrumented knife. The spring tension is measured during the model run in order to provide equivalent output to the instrumented knife. The primary sabot mass is connected to the second sabot mass by two spring/dampers in series joined through a connecting block of negligible mass. The lower of these two spring dampers is relatively soft and is used to represent the slackness in the hand grip. It produces the delay between the initial peak and second peak in the force vs. time plots. The upper spring damper is relatively stiffer and is used to simulate the grip stiffness once the slack is taken up. This controls the rise time of the second peak in the force vs. time plot. A steady force is applied to the rear mass to simulate a constant muscular effort. The target which is struck by the knife consists of a block anchored to the background by a spring damper.

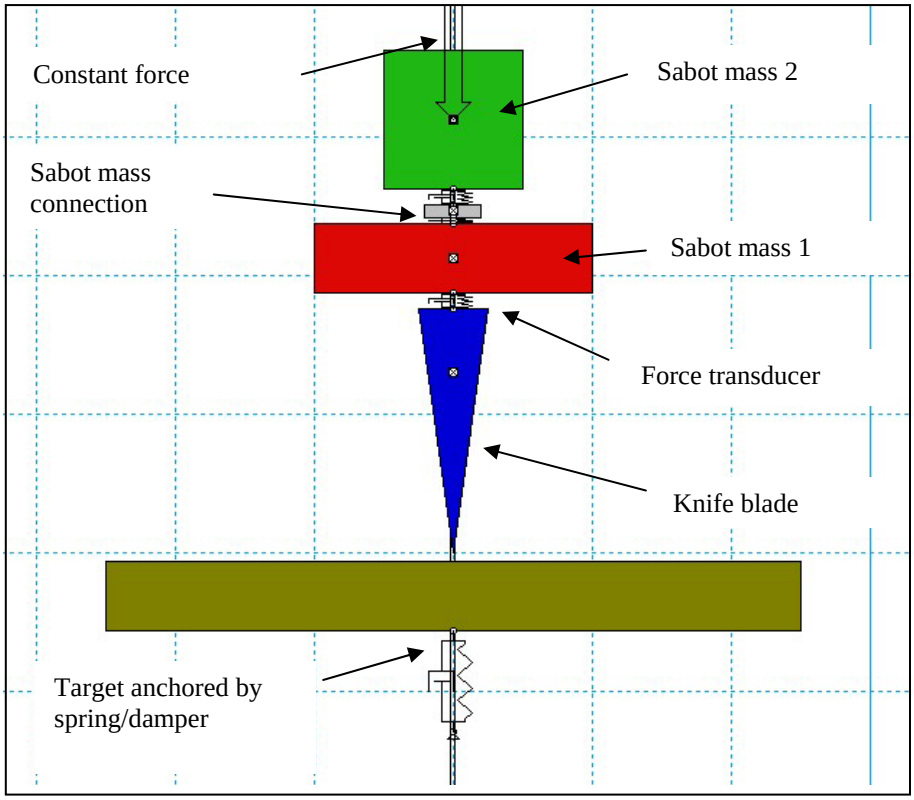

Figure 5-10. Drop mass arrangement in the computer model.

Table 5-2. Input parameter used in computer model of a hand stab.

Parameter	Value
Initial velocity of drop	4.0 ms^{-1}
Knife blade mass	0.1kg (mass in front of the transducer)
Sabot mass 1	0.5kg
Sabot mass 2	1.4kg
Grip slackness spring/damper setting	50Nm^{-1} 5$Nm^{-1}s^{-1}$
Grip stiffness spring/damper setting	7000Nm^{-1} 200$Nm^{-1}s^{-1}$
Constant force	200N

This model was used to investigate the effect of the various parameters and to produce output, which was similar to typical hand stab tests. Due to the wide

variation in the characteristics of the hand stabs it was decided to produce output which broadly matched the key features of the hand stabs. The targets were to match total event length (0.02-0.04s), peak loads (800N) and peak separation (0.01s). A single model run is illustrated in figure 5-11, using conditions as shown in table 5-2.

The model parameters were selected to replicate the hand stab data. There is an initial force peak of 800N followed by a broader peak of similar value. The delay between the peaks is 0.01s and the complete mass is brought to rest after 0.035s. It was found that a relatively complex combination of springs and dampers was required in order to simulate the hand grip. The system consists of a rising stiffness spring and a rising resistance damper to achieve the correct balance of travel and force. The spring value determined the overall width and magnitude of the resistive forces whilst the damping component provides control of the rise time of the forces. By adjusting all four parameters together with the spring damper length it was found to be possible to produce a wide range of impact characteristics.

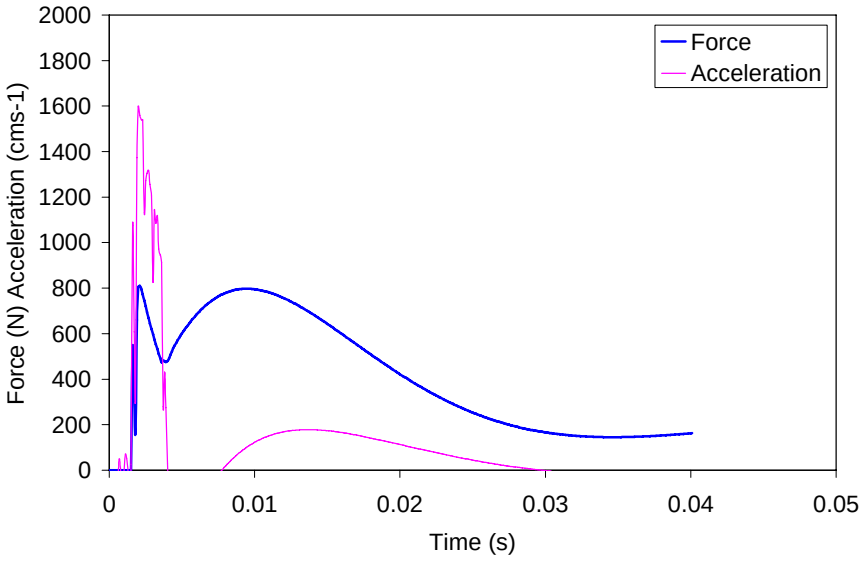

Figure 5-11. A plot of axial force on blade and acceleration of the primary mass, taken from the computer model using conditions from table 5-2. This plot should be compared with the hand stab trials data illustrated in figure 5-7.

The effect of various model parameters was investigated in order to show their effect upon the data. Figure 5-12 shows the effect on axial force of increasing the length of the grip slackness spring from 3mm to 12mm and 24 mm. This is to simulate the effect of a looser hand grip on the knife such that the hand slides further along the hilt before contacting the hilt guard. It can be seen that the effect of increasing grip slackness length is to increase the time delay between the initial force peak and the secondary force peak.

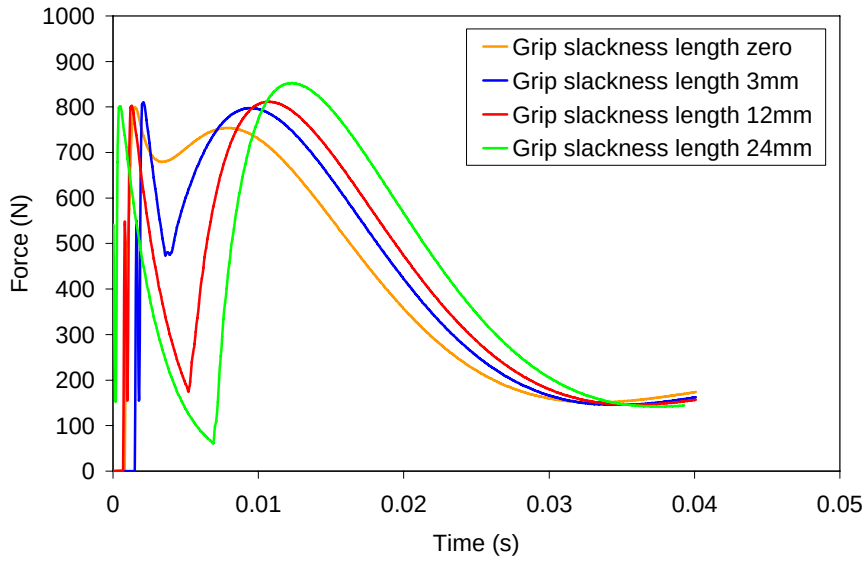

Figure 5-12. The effect of varying the length of the grip slackness spring/damper.

Figure 5-13 shows the effect of varying the stiffness and damping coefficient of the grip stiffness spring. This is to simulate the effect of a stronger or weaker hand grip on the knife. The effect of grip strength is to change both the magnitude and width of the second force peak with increasing grip strength increasing the magnitude and rise time of the peak whilst reducing its width. Figure 5-14 shows the effect of varying the ratio of the primary and secondary masses in order to simulate varying the mass of a knife or the mass of the arm and hand holding it.

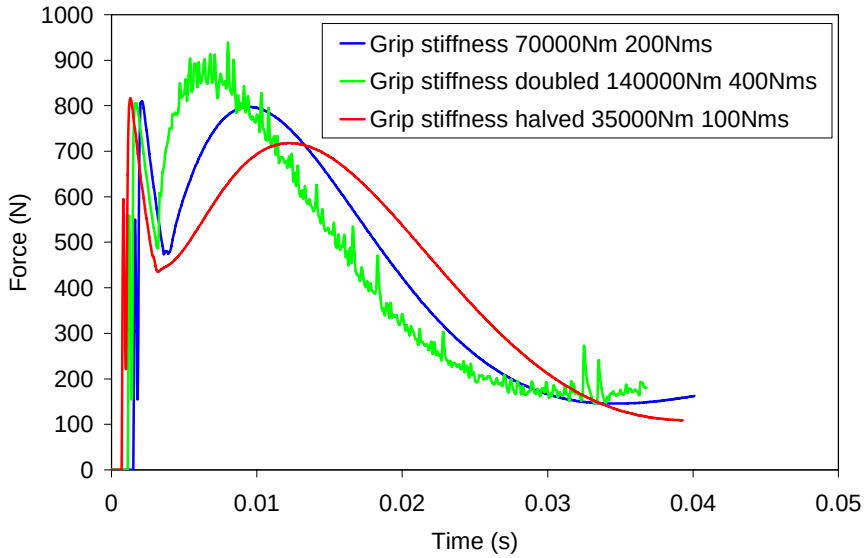

Figure 5-13. The effect of varying the stiffness and damping of the grip stiffness spring/damper.

Doubling the primary mass (blade and sabot mass 1) results in a relative broadening of the initial force peak and a reduction in the force drop between the two peaks. Halving the primary mass reduces the width of the first force peak and results in a greater trough between the force peaks.

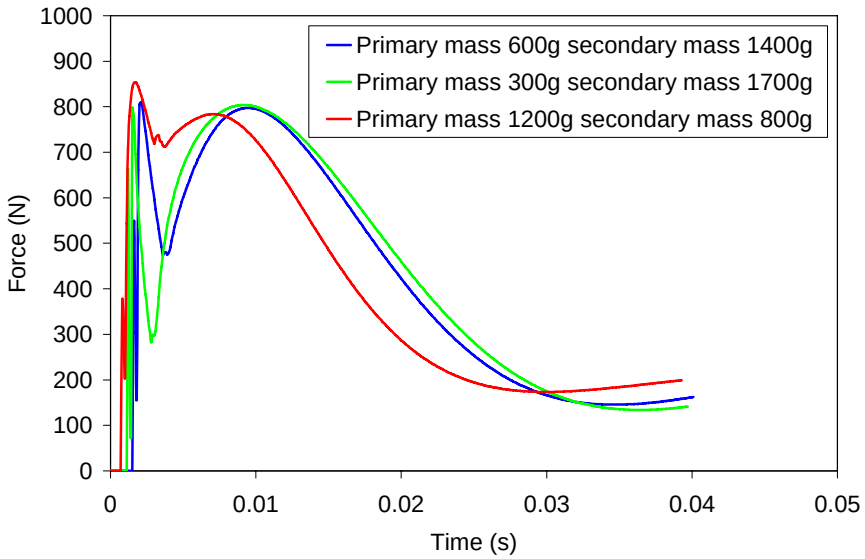

Figure 5-14. The effect of varying the ratio of the primary mass to the secondary mass.

The model is designed to provide a simple illustration of the effects of a series of lumped masses impacting a target. The force input is provided by the elastic collision of the knife blade and the target. The contact stiffness between these two bodies is considerably greater than the total compliance provided by knife indentation and bending within a real target. The sharp rise in input load produces a higher and narrower initial peak force than the experimental data. However the model does provide a useful tool for showing the effect of hand grip on the impact dynamics of stabbing and shows why a relatively complex force characteristic was observed in the hand stab data.

5.6 CONCLUSIONS

A method has been demonstrated for the measurement of the human ability in stabbing. This has produced data on typical stabbing abilities in terms of energy, velocity and force.

For the underarm stabbing action, the maximum energy achieved was 63J, the 95-percentile energy was 54J and the mean was 26J. For an overarm stabbing action the maximum energy was 115J, the 95-percentile energy was 77J and the mean was 46J. The typical terminal velocity of the knife was 6-10ms^{-1} although a higher velocity could probably be achieved with a more conventional and lighter knife. Impact loading on the knife often approached 1000N even against a relatively soft and easily penetrated armour.

The analysis of the hand stab characteristics show that compliance in the hand to knife grip is a major factor in the distribution of forces as a function of time during the impact. It is possible to estimate the effective mass of the human element at between 1.2 and 2.2kg for a purely kinetic impact and between 1.0 and 1.5 kg for an impact with the maximum likely muscular input. In practice, these values are similar to that of the typical hand and forearm mass (1.8 kg)

The analytical model run in Working Model 3.0 reproduces the characteristics of a hand stab impact. It is possible to produce a reasonable simulation of a hand driven stab using a dual mass system to represent the knife and the hand-arm combination. A pair of damped springs in series is able to simulate the hand to knife grip compliance. The spring stiffness and length is used to control the force distribution whilst the damping component controls the rise time of the force.

From the information given in this chapter it is possible to determine the required performance of a body armour in terms of the impact energy which must be resisted. Although it is possible to determine a specific energy level by direct examination of the cumulative probability data a more complex statistical analysis of the complete threat system is required.

The energy delivery from a hand propelled knife is relatively complex and is probably not well simulated by a simple falling mass or gun launched knife. A more realistic energy delivery can be achieved by using a dual mass system which simulates the coupled masses of the knife, hand and arm of an assailant.

5.7 REFERENCES

1. G. Parker, PSDB Stab resistant body armour test procedure (1993), Police Scientific Development Branch, Publication No 10/93, (1993).

2. Sharp instrument penetration of body armour, H.P White Laboratory, HPW-TP-0400.02, (1988).

3. Technical guidelines for lightweight personal armour, Schweizerische Polizeitechnische Kommission, (1992).

4. Technical guidelines for personal armour, Technical Commission AK11, Research and Development Department for Police Technology, Munster, (1994).

5. Protective clothing -Body armour-Part 3:Knife stab resistance – Requirements and test methods (ISO/DIS 14876-3:1999).

6. M. J. Pettit, J. Croft, PSDB Stab resistance standard for body armour (1999), Police Scientific Development Branch, Publication No 6/99, (1999).

7. S. A. Miller and M. D. Jones, Kinematics of four methods of stabbing: a preliminary study, *Forensic Sci.Int*, **82**, 183-190, (1996).

8. P. D. Prosser, An investigation into body armour to protect against knife attack, 48 Degree Course Student Project, Royal Military College of Science, (1996).

9. M. W. Money and G. D. Sims, Calibration of quartz load cells: an in-situ procedure for instrumented falling weight impact machines, *Polymer Testing*, **8,** 429-442, (1989).

10. J. Tan and G. Parker, Stab resistant vests (Part 2), Police Scientific Development Branch, Publication No 20/92, (1992).

11. P. Fenne and S. Winslade, Metvest – the customer aspects, *Proc Sharp Weapons Armour Technology Symposium*, Cranfield University, Shrivenham, (1999).

12. I. Horsfall, S. M. Champion, and I. C. Harrod, The development of realistic stab resistance test methods, *Proc Sharp Weapons Armour Technology Symposium*, Cranfield University, Shrivenham, (1999).

CHAPTER 6

PENETRATION MECHANICS - INDENTATION

6.1 INTRODUCTION

As stated previously the interaction between a sharp projectile and an armour can be broken down into a number of stages. The first stage is indentation in which the knife blade causes compressive yielding of the armour surface. Therefore it was decided to investigate the applicability of indentation theory to the initial stages of knife impact as this would provide a useful insight into the process and possibly provide a means for predicting the initial stages of the armour response.

6.2 INDENTATION THEORY

It is possible to produce a simple model of the indentation stage using the work carried out on indentation hardness testing. Hardness can be assessed by pressing a conical indenter into the surface of a material in which case the mean indentation pressure or hardness can be given by

$$P = \frac{4F}{\pi d^2} \qquad \text{.....(1)}$$

where

P is the mean indentation pressure (hardness)

F is the applied load

d is the diameter of the indentation

However, it is observed that this value increases with decreasing cone angle, due primarily to frictional forces on the indenter surface [1]. Bishop *et al* [2] proposed that the force resisting penetration F by a conical penetrator is more accurately given by

$$F = \frac{P_0(1+\mu\cot\alpha)\pi d^2}{4} \qquad \text{.....(2)}$$

where

P_0 is the intrinsic yield pressure

μ is the coefficient of friction

α is the semi-angle of the cone

d is the diameter of the indentation

Equating 1 and 2 gives the apparent mean indentation pressure

$$P = P_0(1+\mu\cot\alpha) \qquad \text{.....(3)}$$

Figure 6-1 shows data for indentation of an annealed copper by conical indenters. It can be seen that the mean indentation pressure increases sharply for the slimmer indenters but that this effect can be largely negated if friction can be eliminated. It is important to note the limitations to this approach. Although a good fit to experimental data is observed the equation shows inconsistencies at very large angles. It neglects the effects of plastic flow, which would in practice lead to a non-uniform distribution of force over the cone.

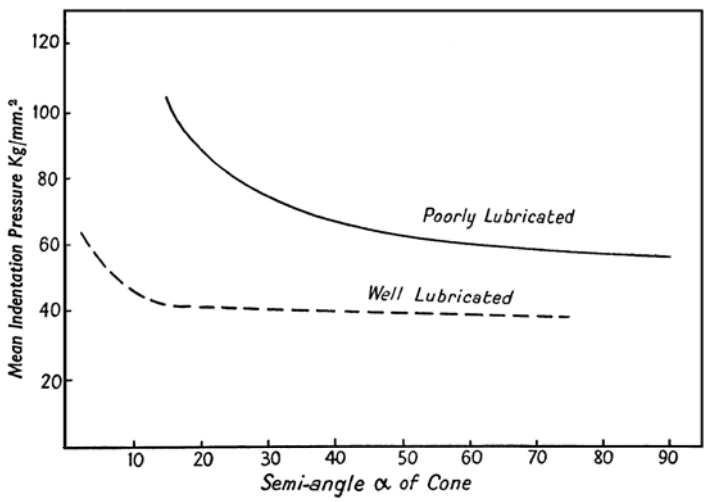

Figure 6-1. The effect of cone angle on mean indentation pressure. (After Bishop [2] in [1])

This approach can be applied to the case of a knife tip during the initial part of the impact process with armour. A sharp knife blade can be equated to a slim conical or pyramidal indenter. It should be possible to use this approach to examine the initial stages of the impact process.

6.3 EXPERIMENTAL

6.3.1 Polymer indentation tests

It was decided to repeat the work of Bishop [2]. The original work had used a series of steel indenters being pressed into an annealed copper block. However it was decided to use polymer substrates for initial trials, as this would be less likely to damage the indenters, and might even allow them to survive the dynamic tests.

A number of hardened steel conical indenters were fabricated. The included angle at the tip of the cones was 90°, 45°, 30°, 20° and 10°. These are illustrated in figure 6-2. The conical indenters were machined from EN24 steel and heat treated to give a hardness of 450 Hv. They were made with fittings to allow them to be used as indenters in a variety of test apparatus including a Vickers hardness testing machine, the Rosand Instrumented Falling Weight machine and an Instron universal test machine. Vickers hardness tests were also performed using the conventional Vickers indenter which had a 136° pyramidal indenter.

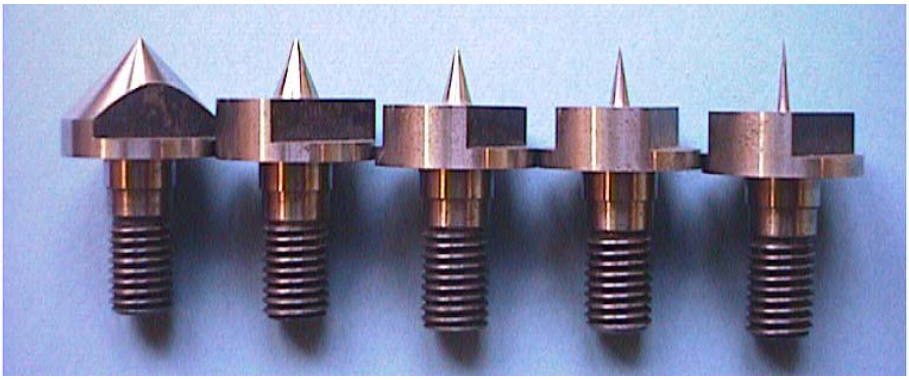

Figure 6-2. Conical steel indenters.

Three polymeric materials were selected, polyvinylchloride (PVC), Nylon and poly tetrafluoroethylene (PTFE). Bishop *et al* [2] had eliminated friction by re lubricating an indenter between subsequent applications to the same indentation until equilibrium was achieved. This technique was thought to be impractical for dynamic tests and the alternative was to use PTFE, which has an inherently low coefficient of friction. The materials were obtained in the form of sheet and rod. Typical mechanical properties for the three materials are given in table 6-1. The materials were stored and tested within a temperature range 18-22 °C and humidity 30-50% r.h.

Table 6-1. Typical quasi-static properties of the polymer types used in indentation trials.

Material	Tensile strength (MPa) [3]	Young's Modulus (GPa) [3]	Coefficient of friction [4]
PVC	40-60	2.4-3.0	0.5
Nylon	60-110	2.0-3.5	0.4
PTFE	17-28	0.35	0.06

6.3.2 Indentation experiments

Initial experiments used a Vickers hardness machine to press the indenters into the three test materials using a load of 9.8N. The diameter of the indentation was then measured manually using the ocular system of the hardness tester. The results of the static indentation experiments are shown in the tables 6-2, 6-3, and 6-4 and figure 6-3.

Table 6-2. Indentation test data for PVC sample.

Cone angle°	136 Pyramid	90	45	30	20	10
Width (mm)	0.574	0.412	0.375	0.358	0.335	0.29
Mean indentation pressure (MPa)	59.5	73.6	88.8	97.4	111.3	148.5
Depth (mm)	0.23	0.41	0.91	1.34	1.90	3.31

Table 6-3. Indentation test data for Nylon sample.

Cone angle°	136 Pyramid	90	45	30	20	10
Width (mm)	0.531	0.339	0.278	0.284	0.253	0.208
Mean Indentation pressure (MPa)	69.7	108.4	161.4	155.1	195.3	289.8
Depth (mm)	0.214	0.339	0.672	1.059	1.434	2.373

Table 6-4. Indentation test data for PTFE sample.

Cone angle°	136 Pyramid	90	45	30	20
Width (mm)	0.712	0.460	0.440	0.415	0.392
Mean Indentation pressure (MPa)	38.8	59.3	64.5	72.6	81.2
Depth (mm)	0.287	0.459	1.063	1.548	2.225

It was not possible to perform the indentation tests for the finest cone on PTFE as the penetration exceeded the travel of the hardness testing machine's indenter.

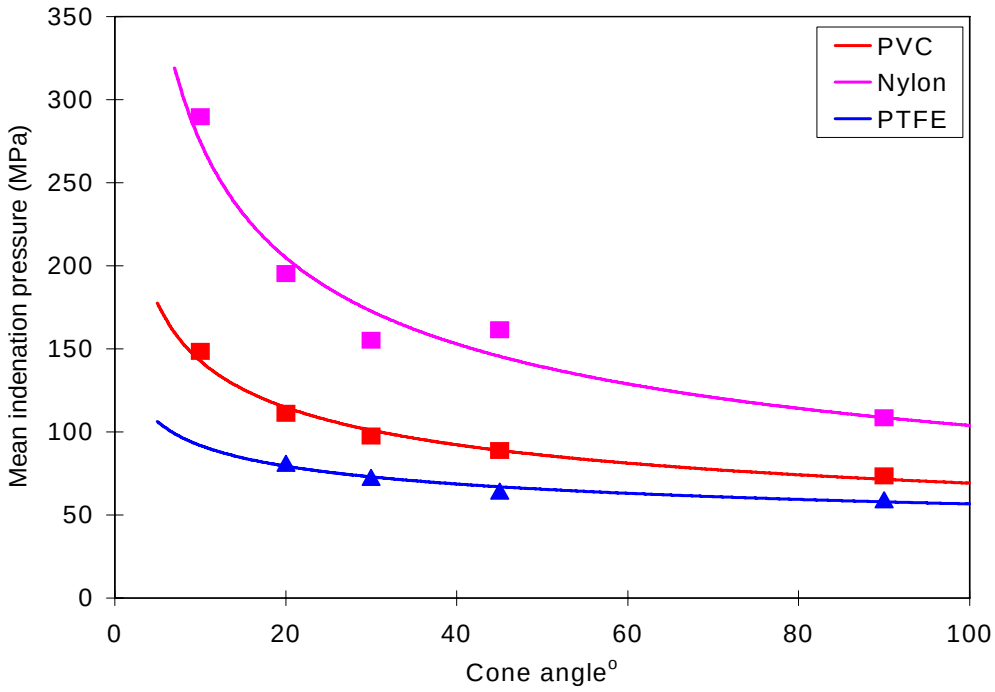

Figure 6-3. The effect of indenter cone angle on mean indenter pressure.

The data points shown in figure 6-3 indicate the mean indentation pressure for each material calculated from the indentation data. From this data it can be seen that the mean indentation pressure increases rapidly with decreasing cone angle. Figure 6-3 also shows best-fit lines calculated from equation 3. From these fitted lines it is possible to derive the values of the intrinsic yield pressure and coefficient of friction for each test material. These values are summarised in table 6-5.

Table 6-5. Summary of data used to generate best fit lines in figure 6-3.

Material	Intrinsic yield pressure (MPa)	Coefficient of friction
PVC	68.9	0.11
Nylon	98.8	0.18
PTFE	54.1	0.09

In order to check these derived values, a series of mechanical tests was performed on samples of the three polymers. Tensile tests were performed on specimens cut from the same sheets of material used for the indentation tests. Quasi-static compression tests were performed on cylindrical test specimens of 10mm (Nylon and PTFE) or 12.5mm (PVC) diameter and approximately 10mm in length. These tests used material of the same specification from the same supplier as the sheet material but in rod form so that a suitable specimen geometry could be used. Quasi-static tensile and compression tests used an Instron 4206 universal testing machine monitoring load and crosshead displacement with a cross head speed of $1.6x10^{-4}$ ms^{-1} (10mm/min). Dynamic compression tests were also performed using the same specimen geometry as the static compression tests. These tests were carried out on the Rosand drop tower used for knife testing (chapter 4).

For the three test types the maximum strain or strain to failure was measured directly from the specimens and used to check the accuracy of the displacement data. The force vs. displacement data was then converted to true stress vs. true strain.

The results for the quasi-static tests are illustrated in figure 6-4 in showing the response of each material in terms of true stress and true strain. Figure 6-5 shows the dynamic compression data for the materials. The PVC and Nylon specimens were impacted at $6ms^{-1}$ whilst the PTFE was impacted at $3ms^{-1}$ as it exhibited a transition to a brittle failure mode at the higher impact speeds. The PTFE and PVC samples deformed to a barrel shape whilst the Nylon specimens melted and formed annular shapes with the original end parts embedded within the annulus.

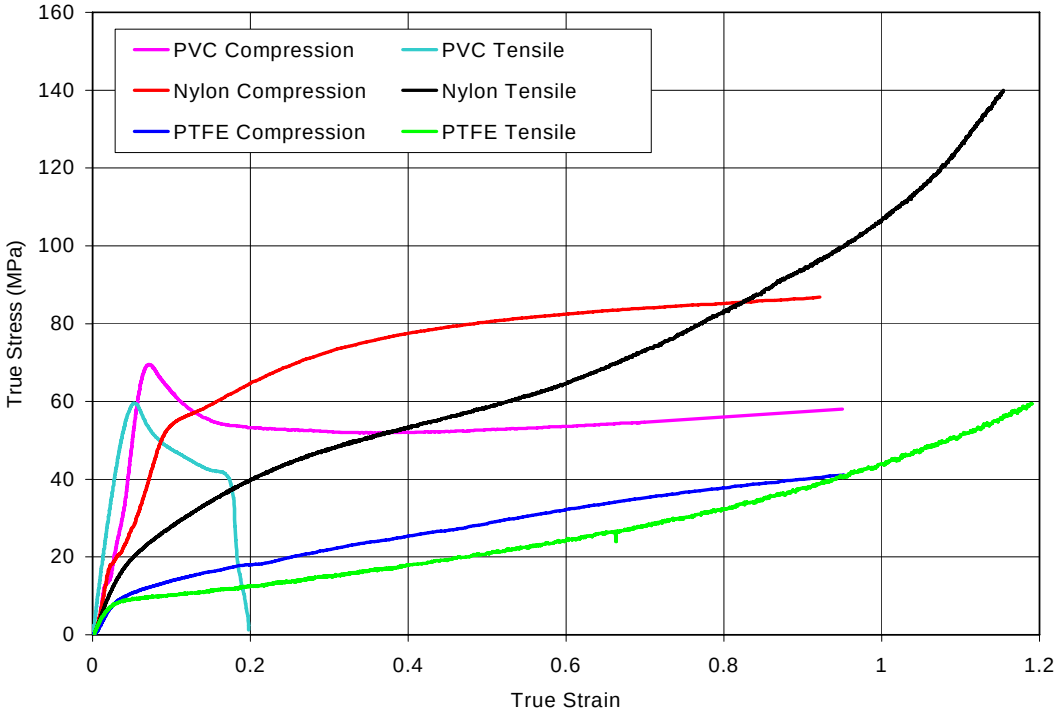

Figure 6-4. Quasi-static compression and tensile test results for the three polymer materials.

It is now possible to compare the materials properties from the various mechanical tests with the values of intrinsic yield pressure measured in the indentation tests. Test results from all the mechanical tests are summarised in table 6-6 in which it is possible to compare the intrinsic yield pressure with the more conventional materials property measurements.

From table 6-6 it can be seen that the intrinsic yield pressure derived from the indentation tests agrees well with the maximum stress up to a true strain of 1. The

maximum stress for PVC is the yield stress, whilst the stress at true strain of 1 is the maximum stress for the Nylon and PTFE. The agreement is equally good in compression or tension.

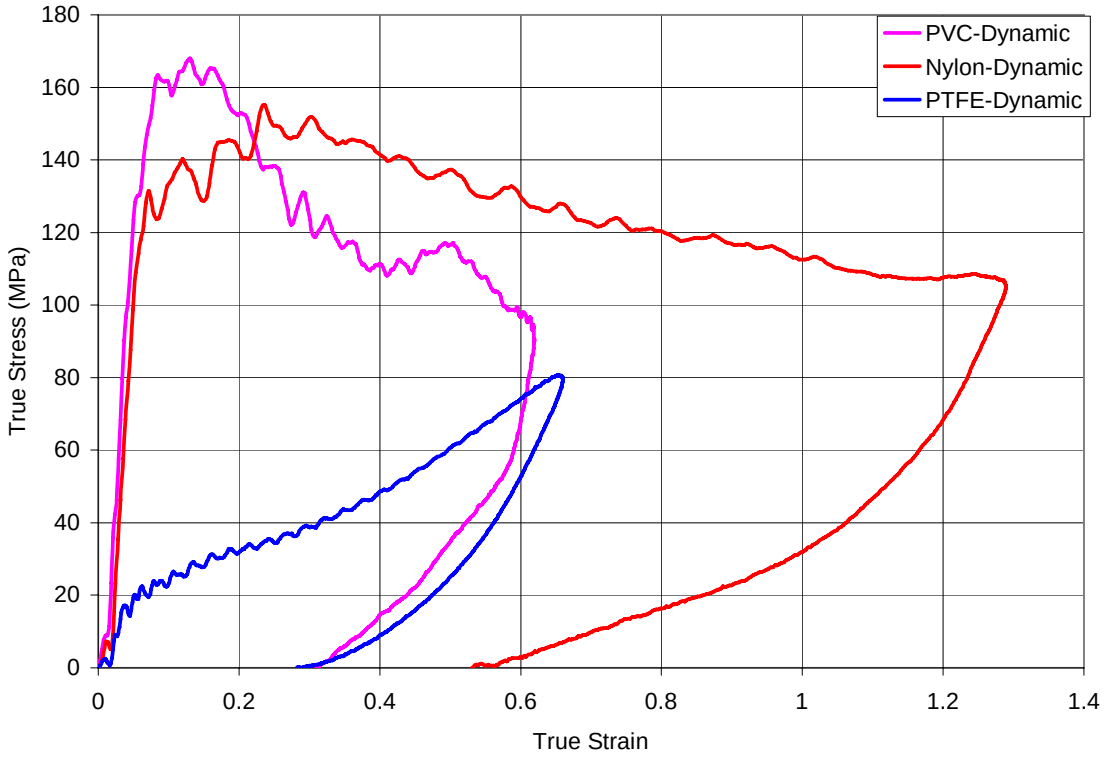

Figure 6-5. Dynamic compression test results for the three polymers.

The compressive and tensile yield stresses for Nylon and PTFE are relatively low, the tensile data showing that the lower yield stress seen in Nylon in compression is the correct value. Dynamic tests were carried out in order to provide data at the strain rates which might be seen in an knife impact. Both the PVC and Nylon show an elevated yield stress but exhibit (thermal) strain softening after yield; in the case of Nylon this is also evidenced by melting of the deformed specimen. The PTFE shows much enhanced strain hardening over the static tests although at impact speeds above $3ms^{-1}$ this caused a transition to brittle failure at low strain.

Table 6-6. Comparison of indentation data with mechanical test data.

Mechanical property and test type	PVC	Nylon	PTFE
Intrinsic yield pressure calculated from indentation tests (MPa)	69	99	54
Tensile yield stress (MPa)	59	15	8
Tensile 2% proof stress (MPa)	59	21	9
Tensile maximum stress up to true strain of 1 (MPa)	59 (Yield)	107	44
Compressive yield stress (MPa)	69	54 (13)[1]	8
Compressive 2%proof stress (MPa)	69	18	9
Compressive maximum stress up to a true strain of 1 (MPa)	58 (Yield)	87	41
Dynamic compressive yield stress (MPa)	162	131	17
Dynamic compressive maximum stress (MPa)	162 (Yield)	131 (Yield)	78
Hardness (Hv)	5.6	6.6	3.7
Hardness (MPa)	54.9	64.7	36.2
Flow stress derived from hardness (MPa)	18.3	21.5	12.0

It is known that the indentation hardness Y can be used to assess yield stress [1,5] according to the relationship

$$\sigma_Y = \frac{Y}{3} \qquad \text{.....(4)}$$

Therefore the hardness of the polymers was measured by a conventional Vickers hardness test with a load of 9.8N. The yield stress derived by this method agrees well with other test methods for the Nylon and PTFE but for PVC it is a factor of 4 lower than that derived by most of the other methods.

[1] The apparent yield stress from figure 6-4 is 54MPa, however a slight inflection can also be seen at 13MPa, this latter figure being in agreement with the tensile data.

6.3.3 Indentation depth effects

The data from the initial series of tests also revealed the effect of indenter cone angle on the depth of the indentation produced. This is shown in figure 6-6 in which the indentation depth has been calculated from the measured indentation diameter.

It can be seen that the indentation depth is sensitive to the cone angle particularly for small cone angles. This is of considerable interest as one of the known problems with testing of stab resistance is the measurement of the sharpness of the test knives. It has been shown that sharpness is a significant factor in both the characteristics and the magnitude of penetration (as seen in 4.4.3), but no standardised method exists for the evaluation of tip sharpness.

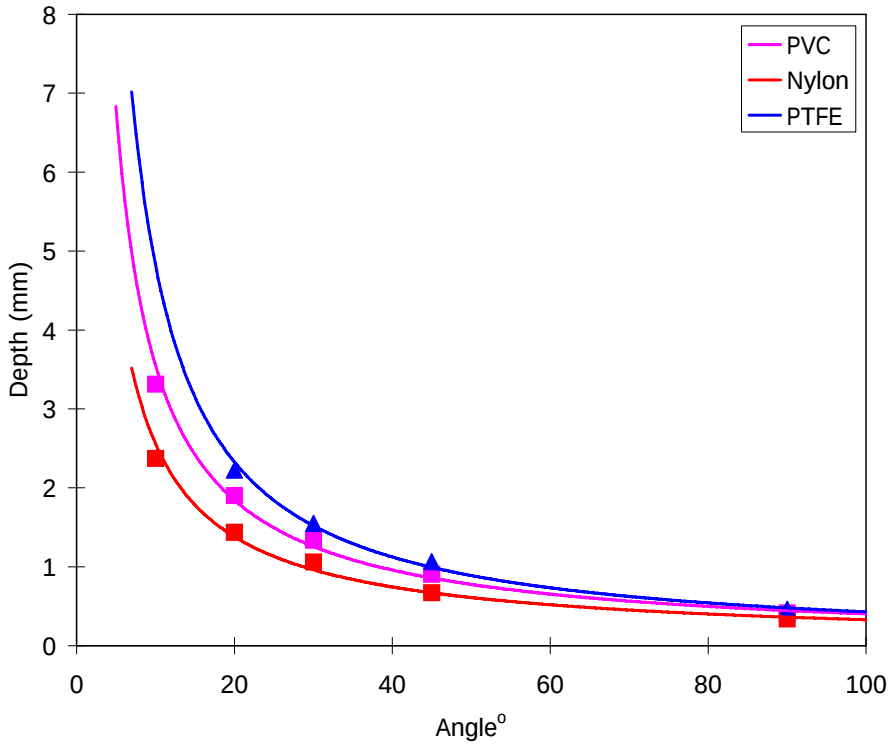

Figure 6-6. Indentation depth as a function of indenter cone angle.

Stemming from the knowledge gained in these trials it was concluded that indentation depth might give a good indication of knife tip sharpness. If indentation depth of a knife into a standardised substrate could be directly measured then it might offer a

convenient method of defining sharpness. Whilst it is possible to calculate the depth of indentation from the measured diameter it would be more convenient to directly measure indentation depth. This was found to be possible using an adapted Rockwell hardness machine in which a knife is used to produce an indentation into a soft aluminium sample. This test was subsequently developed as part of the PSDB stab resistant armour test standard [6], and is reported in appendix 6.

During the course of developing the knife sharpness test it was determined that polymeric substrates were unsuitable. When the depth of indentation was continuously monitored during a test it was found that equilibrium was not reached within a reasonable time. It was found that better results were obtained with very soft metallic substrates and an annealed 99.997% pure aluminium was eventually adopted.

With the adoption of a new substrate for indentation and the availability of a depth sensing hardness testing machine it was possible to investigate further the effect of indenter angle.

6.3.4 Indentation testing using knives

The conical indenters were used in a further series of indentation trials using a soft aluminium substrate. The tests were performed on a modified Rockwell hardness testing machine in which the indentation depth was directly measured. It should be noted that this technique measures the difference in indentation depth produced when the indenter load is increased and not the total indentation.

Figure 6-7 shows the measured indentation depth as a function of indenter cone angle. It can be seen that this is similar to figure 6-6 for the broader indenters but shows a deviation from the predicted behaviour for the 10° conical indenter. Also shown in figure 6-7 are the results of tests on several commando blades. Comparison of the knife data with the cones shows that the knives produce an indentation depth equivalent to cones with an included angle in the range 25°-45° with an average equivalent to a 30° angle cone.

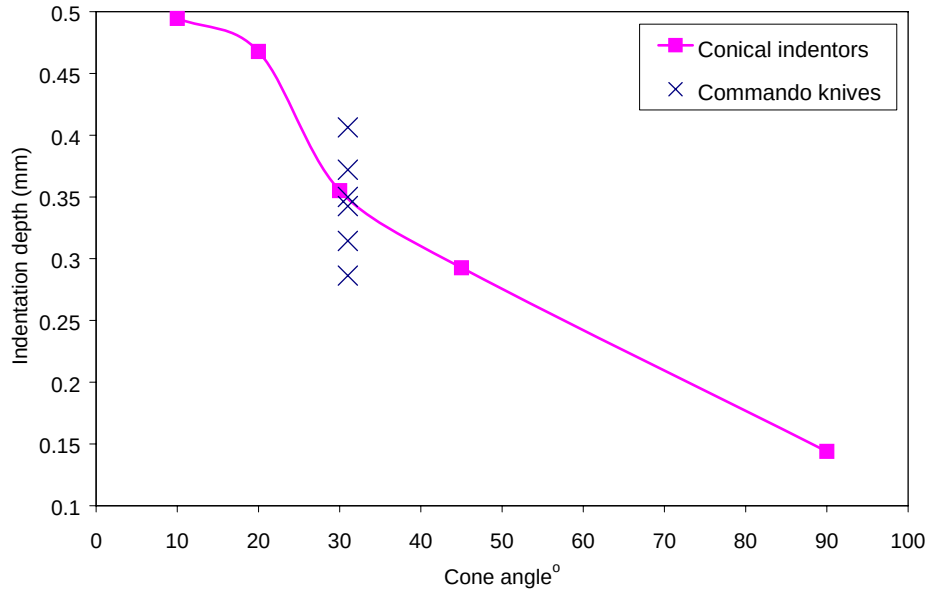

Figure 6-7. A comparison of the indentation depth into aluminium produced by conical indenters and commando blades.

6.3.5 Knife indentation into polymer samples

A commando knife was used to perforate the polymer sheet materials used in the indentation tests. The test method used was as described in chapter 4 with the sheet samples being mounted on a 100mm diameter tube filled with modelling clay. For each material a series of tests were performed with impact energy levels in the range 10J – 45J. Quasi-static penetration tests were also performed using the same geometry and at indentation speeds of 1.6 x $10^{-4}ms^{-1}$ (10mm/min) and 8.3 x $10^{-4}ms^{-1}$ (50mm/min).

The results are summarised in tables 6-7, 6-8, and 6-9 together with calculated values for initial perforation load. The dynamic force vs. displacement traces showed behaviour as described for most materials in chapter 4 in which the overall envelope was defined by the highest energy impact. Therefore only the 45J impacts are shown in figure 6-8 which may be compared to the static behaviour shown in figure 6-9.

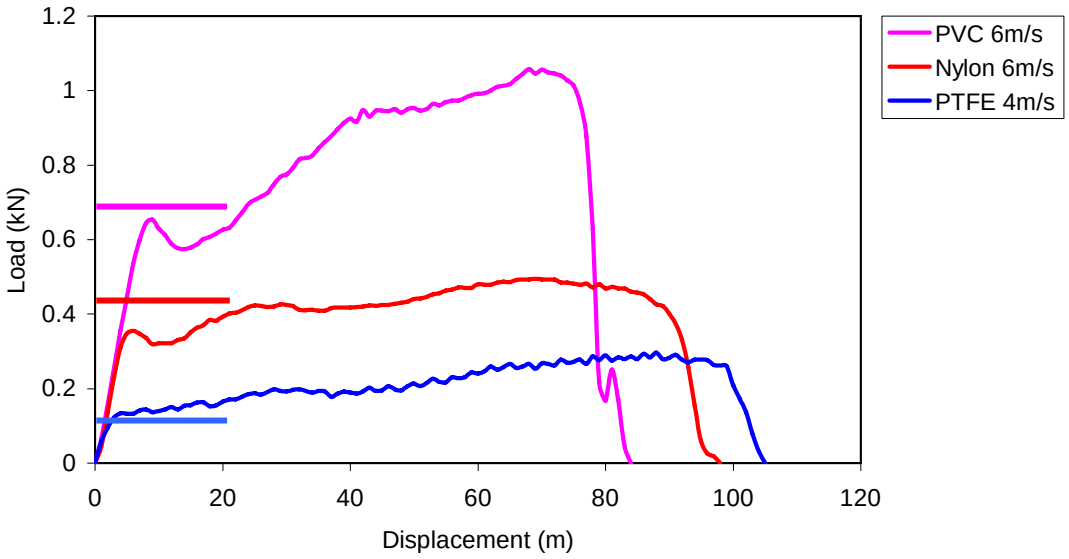

Figure 6-8. Force vs. displacement plots for impact tests of the commando knife against polymer targets. Solid bars indicate calculated perforation load.

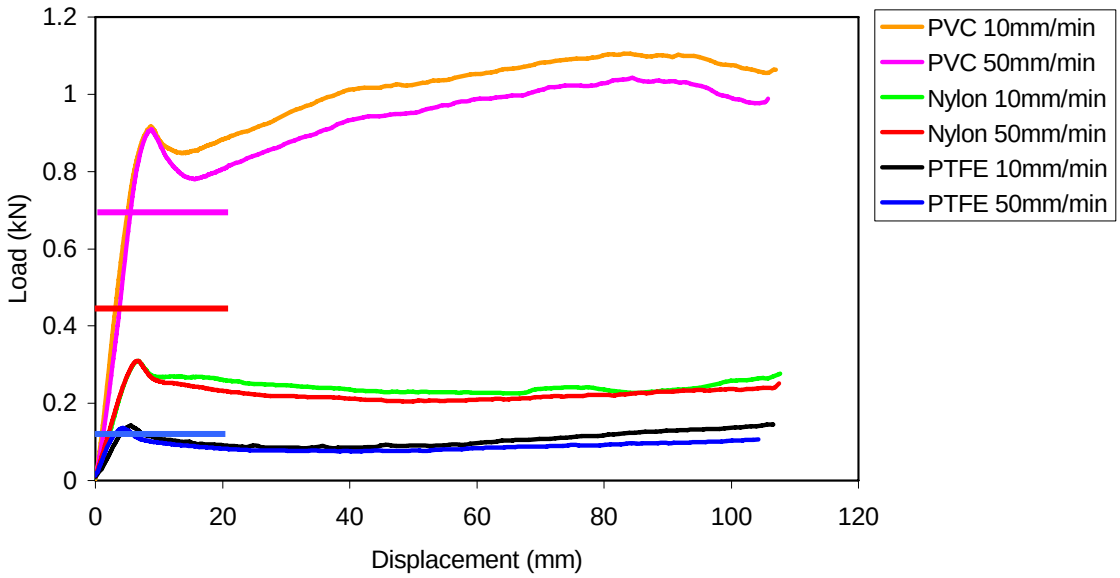

Figure 6-9. Force vs. displacement plots for quasi-static tests at two speeds for the commando knife against polymer targets.

The load required to just penetrate the sheet was calculated from equation (2) using the intrinsic yield pressure derived from indentation tests, these values being

indicated in tables 6-7, 6-8, and 6-9 and figures 6-8 and 6-9. The indentation depth was set as the sheet thickness and the included angle at the tip was estimated at 30° as described in the previous section. The actual perforation load is seen on the load vs. displacement plots as the initial peak or change in gradient of the curve and can be compared to the calculated values. It can be seen from figure 6-8 and 6-9 that the calculated perforation loads agree well with those shown on knife tests. In practice it is highly unlikely that perforation can simply be regarded as a truncated indentation process, but the good agreement with indentation theory suggests that indentation is the dominant process.

Table 6-7. Knife penetration tests for against PVC sheet**.**

Filename	Energy (J)	Penetration (mm)	Peak load (N)	Perforation load (N)	Calculated perforation load (N)
IHC-80	9.45	11	767	630	695
IHC-79	19.84	21	934	630	
IHC-78	30.82	31	985	620	
IHC-76	42.03	38	1050	660	
IHC-81	42.09	41	1060	630	
IHC-77	48.08	48	1060	620	

Table 6-8. Knife penetration tests against Nylon sheet.

Filename	Energy (J)	Penetration (mm)	Peak load (N)	Perforation load (N)	Calculated perforation load (N)
IHC-74	10.01	30	365	330	423
IHC75	14.97	40	387	360	
IHC-71	20.6	49	442	350	
IHC-72	31	70	442	330	
IHC-73	42.6	89	505	360	

Table 6-9. Knife penetration tests against PTFE sheet.

Filename	Energy (J)	Penetration (mm)	Peak load (N)	Perforation load (N)	Calculated perforation load (N)
IHC-67	6.72	50	209	140	125
IHC-68	10.2	60	238	150	
IHC-69	15.21	80	285	140	
IHC-70	17.56	87	300	130	
IHC-66	20	95	375	160	

6.4 DISCUSSION

The attempt to recreate the earlier work of Bishop has shown that indenter theory can be applied to the indentation of polymer samples by conical indenters. By using a range of indenters it is possible to derive mechanical property data for polymers which is shown to agree with data derived from conventional uniaxial compression tests. The intrinsic yield pressure derived from indentation tests is equivalent to the true stress at a strain of 1.

It is interesting to note that the indention method allows measurement of compressive strength without the need for machining of specimens and is to some extent non-destructive. As such, an indentation method as described here might allow the measurement of mechanical properties from specimens where conventional mechanical tests were not possible.

The data for coefficient of friction does not agree well with textbook values, although there may be a number of reasons for this. Conventional friction tests are not usually performed with contact loads in excess of the yield stress of one component. However in the indentation test the contact loads are by definition in excess of the yield stress. These high loads would cause the polymer to conform to the surface

texture of the indenters so that the actual measurement was derived from the shear strength of the polymer rather that a surface sliding mechanism.

In the derivation of equation 2 it is assumed that the substrate material is perfectly plastic and can therefore be represented by a single value of flow stress. However it can be seen in figure 6-4 that the materials used do not exhibit this type of behaviour. Although a more complex analysis could be used to more accurately represent the post yield behaviour of the materials a single value at a specified strain provides a more practical solution.

Table 6-10. A comparison of measured and calculated perforation loads for a commando blade penetrating polymer sheet targets.

Material	Mean Measured perforation loads (MPa)		Calculated perforation loads (MPa)	
	Static	Dynamic	Based on yield pressure	Based on stress at strain =1
PVC	905	632	695	594
Nylon	299	346	423	377
PTFE	129	144	125	97

Table 6-10 shows a comparison of the actual perforation loads from both static and dynamic tests. This can be compared to the calculated perforation loads using equation 2 based on both intrinsic yield pressure values and compressive strength values (at true strain =1). There is good agreement between the dynamic data and the calculated values based intrinsic yield pressure or stress at strain =1. The static penetration test data agrees less well particularly for the PVC target.

Indentation theory appears to give good agreement with the perforation resistance of sheet materials when penetrated by knives. This indicates that an indentation mechanism rather than elastic-plastic failure mechanisms control the perforation process. Most previous work on penetration of plates is based on the effect of blunt penetrators and assumes that perforation occurs due to tensile or shear failure of the

plate. This is based on the assumption of a deformable and relatively blunt penetrator. For the case of a knife impacting a polymer or thin metallic plate these conditions do not apply. The penetrator is non-deforming and is very sharp, which leads to very high contact stresses considerably in excess of the plate yield stress superimposed on cutting mechanisms around the penetrator. It has been shown [7] that for sharp indenters the plastic zone extends in a radial direction from the indenter. It seems likely that this restricts the size of the process zone ahead of the knife. Consequently this process zone does not interact with the rear face of the plate until just before perforation occurs. Therefore a calculation based upon a semi-infinite substrate applies even to relatively thin substrates as the surface effects are limited.

6.5 CONCLUSIONS

Indentation of polymers by conical indenters has been shown to be in good agreement with indentation theory. For indenters with tip angles of 40° or greater, the indentation behaviour is governed by yield strength. However, for slimmer indenters frictional forces dominate, and indentation depth becomes increasingly dependent upon the coefficient of friction between indenter and sample.

For small tip angles the depth of indentation is very sensitive to tip angle. Consequently it is possible to use depth of indentation as a measure of tip angle which is analogous to sharpness.

By using conical indenters of various tip angles it is also possible to use this technique to measure mechanical properties of the polymer materials.

By using mechanical property data from conventional or indentation tests it is then possible to estimate the force required to penetrate a sheet material with an arbitrary indenter - in this case a knife.

6.6 REFERENCES

1. D. Tabor, *The hardness of metals*, Clarendon Press, Oxford, 95-114, (1951).

2. R. F. Bishop, R. Hill and N. F. Mott, The theory of indentation and hardness tests *Proc. Phys. Soc*, **57**, 3, 147-159, (1945).

3. M. F. Ashby and D. R. H. Jones, *Engineering Materials Volume 2*, International Series on Materials Science and Technology, **39**, Pergmon, 206-207, (1986).

4. Metals Reference Book 5th, (Ed. C. J. Smithells), Butterworths, 1281, (1976).

5. H. E. Boyer, *Hardness testing*, ASM International, 1-16, (1987).

6. M. J. Pettit and J. Croft, PSDB Stab Resistance Standard for Body Armour (1999), Police Scientific Development Branch, Publication No 6/99, (1999).

7. A. G. Atkins and D. Tabor, Plastic indentation in metals with cones, *J. Mech. Phys. Solids*, **13**, 149-164, (1965).

CHAPTER 7

PENETRATION MECHANICS

7.1 INTRODUCTION

From the results presented in chapter 5 it is possible to accurately quantify the threat in terms of delivered energy. It has been shown in chapter 6 that it is possible to determine the initial penetration resistance of a given armour from a knowledge of the tip profile of a knife. However, the threat is specified in terms of delivered energy, and it is the absorption of this energy that must be quantified in order to determine the effectiveness of an armour material or system. One aim of this chapter is to analyse the data presented in chapter 4 by a number of approaches in order to determine the factors that affect the performance of various armour materials.

In real armour systems the ultimate goal is to achieve complete penetration resistance so that no perforation occurs, and indeed some proof tests require this. However it is difficult to qualitatively assess the performance of armour without penetrating it and for this reason the majority of test standards specify small allowable penetration levels. In addition to this a number of standards require testing at substantially higher energy levels in order to determine the failure mode of an armour system. In the work reported in chapter 4, test materials were chosen which allowed some penetration to occur in order that useful quantitative data be obtained. The data from these tests should provide information on the post perforation behaviour of the armour materials.

A number of approaches are possible in attempting to address the energy absorption of an armour system. A mechanistic approach could examine the various different absorption mechanisms and attempt to quantify these for one or more armour/knife systems. This has the disadvantage that there are numerous mechanisms whose relative importance varies as a function of both knife and armour type. A second approach would be a purely analytical approach in which the energy absorbing processes are disregarded, and instead an attempt is made to fit data such as that

discussed in chapter 4 to a simple formula taking into account only simple target and knife parameters.

The former approach would mean that only a limited number of systems could be studied and the practical relevance of any detailed analysis to armour systems in general might be negligible. It is the author's intention to provide as broad an approach as possible in order to address the majority of current and future systems. Therefore the approach taken in the following chapter is of a broadly empirical model which deals with the major mechanisms present for most armour and knife types

7.2 ANALYTICAL MODELS

From the examination of the literature in section 2.5 it appears that there are two methods which might provide an insight into the knife penetration process. These are the ballistic model as discussed by Woodward [1] and the wedge cutting approach. In the following chapter these two approaches will be modified to account for the particular case of knife penetration and compared to data from tests in chapter 4.

7.2.1 Ballistic penetration model

The Woodward [1] ballistic penetration model based on the work of Taylor [2] and Thomson [3] was discussed in 2.5. It was shown that the work done in penetrating a thin target could be equated to

$$W = \frac{\pi}{2} a h_o \sigma_o \left(a + \frac{\pi}{2} h_o \right) \qquad \text{.....(1)}$$

In considering the case of a knife penetrating a target of the types described in chapter 4 it can be seen that the behaviour of the targets is similar to that described by Woodward but with some significant differences. The knife shapes are relatively complex, they do not have radially symmetrical cross sections and they generally taper along their whole length. Frictional effects are large and must therefore be

included in any calculation of absorbed energy, and the velocity is relatively low so some global deformation may occur.

One of the assumptions used in assessing the bending work was to consider the final form of the target. It has been shown in chapter 4 that for the majority of cases the form of the force displacement curve is described by the highest impact energy test and to some extent by quasi static penetration. Therefore, the energy to penetrate a given distance could be calculated from the cross section of the blade at that distance from its tip. It would then be possible to incrementally calculate the energy displacement characteristic of the blade for each increment of penetration through the target. The blade cross section is described by the diameter of a cone of equivalent cross sectional area.

It has been observed from the earlier tests (figure 4-26 – 4-30) that the dish formed in the target is typically circular and of a diameter approximately equal to the major dimension of the blade cross sections. Therefore if the distance from the blade axis to each edge b is substituted for the projectile radius a in equation 1 then the total dishing work W_D would be

$$W_D = \frac{\pi}{2} h_o \sigma_O \left(a^2 + \frac{\pi}{2} b h_o \right) \qquad \text{.....(2)}$$

7.2.2 Plate cutting model

Another method for analysing knife penetration is to use an approach based on cutting of thin plates [4,5,6]. This work is primarily used to model ship collisions particularly the case where the prow of one ship slices through the deck plates of another. The geometry which has been subject to the most study is illustrated in figure 7-1. A wedge of typical semi-angle 10-30° is forced through a plate from one edge.

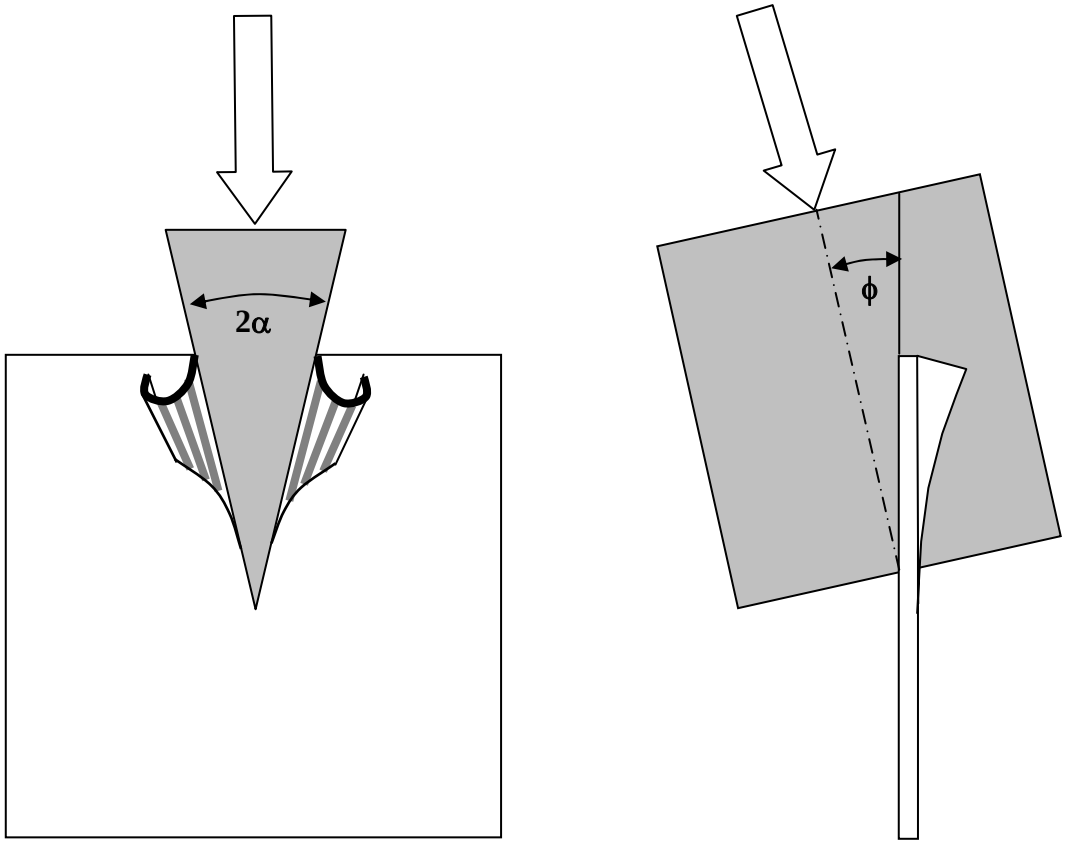

Figure 7-1. Typical geometry for wedge cutting of plate by a wedge of semi angle α at an angle ϕ to the plane of the plate.

Wierzbicki [6] has proposed that the force resisting the cutting of a plate of thickness h_0 to a depth l is given by

$$F = 3.28\sigma_O(\delta_t)^{0.2} l^{0.4} h_0^{1.6} \mu^{0.4} \quad \text{.....(3)}$$

where δ_t is a dimensionless crack opening displacement parameter and μ is the coefficient of friction. In order to adapt this to the case of knife penetration it is necessary to allow for the actual inclination of the wedge (cutting edge) to the plate and to allow for both cutting edges (i.e. the total force is doubled).

Therefore for a knife penetrating a plate the force resisting plate cutting becomes

$$F = 6.56 \sin\phi \sigma_O (\delta_t)^{0.2} l^{0.4} h_0^{1.6} \mu^{0.4} \quad \text{.....(4)}$$

where ϕ is the angle formed between the cutting direction and the plane of the plate.

7.2.3 Frictional effects – Coulomb friction

It is generally thought that the coefficient of friction decreases to almost negligible levels as the sliding speed moves above 500ms^{-1} [7], and consequently friction is ignored in most ballistic penetration analyses. However as discussed in chapter 5, the knife impact velocity is likely to be of the order of 10ms^{-1}. The results presented in chapters 4 and 6 show that for stabbing perforation friction is a significant part and may even be the major part of armour resistance after perforation. It is therefore necessary to make some allowance for frictional effects in calculating total energy absorption.

The indentation model developed in chapter 6 showed that it is possible to use a Coulomb friction model of the form

$$F_F = F_N \mu \quad \text{.....(5)}$$

such that the frictional force F_F is given by the product of the normal force F_N and the coefficient of friction μ. This could be implemented in a penetration model relatively simply since the friction force could be summed over the periphery of the blade cross section and the thickness of the target. Unfortunately the normal force is unknown, as only the axial force is measured and this is the sum of both the friction force and other forces.

In attempting to implement this approach into a penetration model it is therefore necessary to make a number of assumptions. The normal force is difficult to measure and the actual area of contact is also unknown. However an upper bound could be

achieved by assuming purely radial deformation and setting the normal force as equal to the flow stress σ_O. The frictional force would then be given by the instantaneous perimeter of the knife S, multiplied by the thickness of the target plate h_o

$$F_F = \sigma_O \mu S h_O \qquad \text{.....(6)}$$

Table 7-1 shows a comparison of frictional forces taken from penetration tests with forces calculated from equation 6. The values are for a commando blade at a penetration of 25mm through each material using data from figures 4-22 and 4-23 for the aluminium targets and 6 – 8 for the polymer targets. Mechanical property data is as measured in chapter 6 for the polymers and chapter 4 for the aluminium .

Table 7-1. A comparison of frictional forces calculated from equation 6 with measured total force resisting penetration.

Material	Coefficient of friction	Thickness (mm)	Total measured force (N)	Calculated frictional force (N)
PVC	0.105	5.5	707	795
Teflon	0.088	2.7	188	256
Aluminium 7075-T6	0.2	1.0	443	2314
Softened 7075	0.2	1.0	324	1098

The calculated value for the PVC target is close to the experimental value whilst for the both the aluminium 7075 targets the calculated value is too large by almost half an order of magnitude. The PVC target fails by a radial hole expansion as assumed in the derivation of equation 1, whilst the Teflon shows some dishing, and the aluminium targets show a dished and petalled failure. It would therefore seem that the actual contact geometry is a major influence and may effect both the contact force and contact area. The contact geometry appears to be influenced by the thickness of

the target. The softened 7075 has a maximum true stress of 285MPa and the 7075-T6 has a maximum true stress of 610MPa yet the difference in measured resistive force is a between 324N and 443N respectively. For the two aluminium targets the difference between the calculated and experimental data are similar. This indicates that target strength is only a second order effect, whereas the primary factor controlling friction is the target thickness.

7.2.4 Frictional effects – shear stress

It is also possible to use an interfacial shear stress approach, which has been successfully applied for the tearing and cutting of steel sheet [5,8]. This approach is generally applied to cases where the normal force is of a similar order to the material strength such that some degree of sticking is achieved between the sliding surfaces. Under these conditions the apparent frictional force becomes a function of the shear strength of the weaker surface and a slipping friction factor. The friction stress is then given by a term nk [8] (or $\beta\tau$ [5]) where n (or β) is the slipping friction factor and k (or τ) is the shear strength of the weaker component.

The cutting of metal plates by wedges has been extensively studied and the effect of friction is known to be significant. For the case of a wedge cutting into a plate from a free edge the frictional force has been estimated to account for up to 40% of the total resistance [5,8]. For this case Shen *et al* [5] suggest that the frictional force acting on one side of a wedge of semi angle α cutting a distance l into a plate is given by

$$F_F = \beta\tau\left(\frac{h_O l}{\cos\alpha}\right) \qquad \text{.....(7)}$$

The slipping factor $\beta\tau$ was found empirically to have a value in the range 0.04-0.14 with $\tau=\sigma_O/2$. If this approach is applied to a knife cutting into a plate then for the small angle between blade faces $\cos\theta=1$ and the distance l becomes the perimeter of the blade S, and equation 7 can be rewritten as

$$F_F = \beta\tau S h_O \qquad \text{.....(8)}$$

It can be seen that equations 6 and 8 are essentially the same particularly given that the terms $\sigma_0\mu$ and $\beta\tau$ are both essentially empirical constants.

7.2.5 Contact geometry

Another unknown variable is the actual contact area between a knife and the plate. It has been assumed that the knife penetrates the plate in a geometry similar to that shown in figure 7-2, such that the contact area will be the thickness of the plate multiplied by the perimeter of the knife cross section. The correlation between calculated and experimental data in table 7-1 for the polymer targets suggests that this approach may be correct for thicker plates, i.e. those in which only limited petalling occurs.

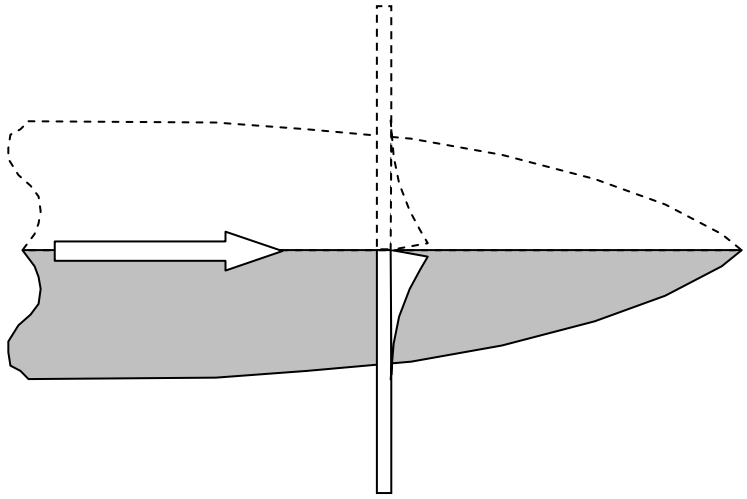

Figure 7-2. The relationship between the wedge cutting geometry (figure 7-1) and knife penetration.

For thin targets the situation is more complex and may be compared to work on wedge cutting of plate by as described by Wierzbicki *et al* [6]. This geometry is illustrated in figure 7-3 in which it can be seen that the plate is rolled into cylindrical flaps or petals with the wedge only being in contact for part of its length. The crack extends from a point G at the edge of the plate to a point C, which may be ahead of the tip of the wedge. The wedge is in contact with the bent surface of the petals for most of the contact length EG and is only in contact with the thickness of the plate at point E.

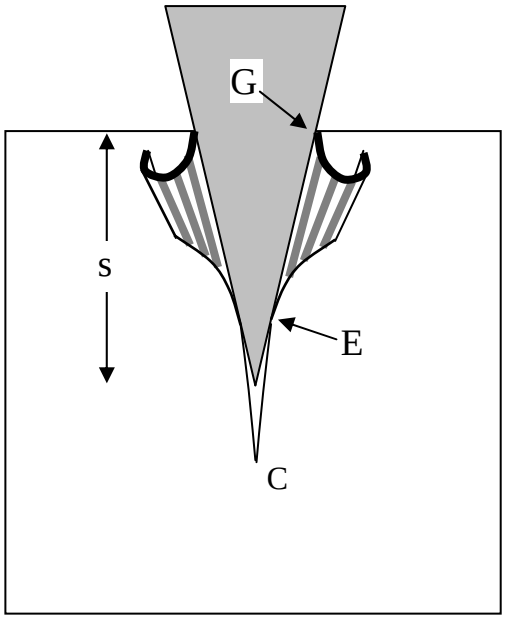

Figure 7-3. The geometry of wedge cutting of an inclined plate (after Wierzbicki [6]).

This may be likened to a situation at each edge of the knife where the knife is pushed into the plate as its cross section increases. Consequently the assumed contact area of a knife penetrating in a similar manner will be significantly less than the quantity Sh_0 (plate thickness multiplied by blade perimeter).

Both the Coulomb friction and shear stress models produce the same problems; the coefficients are difficult to measure under the specific conditions (or the conditions are difficult to specify), and the area of contact is difficult to determine. The indentation method described in chapter 6 can be used to determine μ, but can only be applied to soft materials as the sharp indenters required to achieve accurate measurements are too fragile to be used to indent strong materials. Typical values for μ are available from reference sources but due to variation with both sliding speed and normal force these would be only very rough estimates. The contact area will vary in a complex manner as a function of target material properties and knife geometry.

This leads to a situation as discussed in reference [8] where the coefficients become disposable parameters which can to some extent be varied in order to make theory and experiment agree. Some estimate of μ can be made but a correction factor is required to account for the combined effects of dishing geometry and sticking contact.

Therefore the frictional force could therefore be calculated from an equation of the form

$$F_F = \sigma_O \beta \mu S h_O \qquad \text{.....(9)}$$

Where the value of β would be in the range 0.04-0.14 as found by Shen *et al* [5]. This approach seems likely to give an estimate of the frictional forces acting upon a knife and parameters which can either be obtained experimentally or estimated within reasonable limits.

4.2.1 Summary of analytical methods

The penetration of a knife through a thin target can be likened to a ductile hole enlargement process as described by equation 2, or an approach based on wedge cutting can be adopted as given by equation 4. In either case it is also necessary to separately calculate the frictional resistance using equation 9. In order to make use of these equations it is necessary to know the flow stress of the target plate and the geometry of both the knife and target. Estimates must be made, or empirical fits are then required to determine the coefficient of friction μ, the slipping friction factor β and the crack opening displacement parameter δ.

7.3 VALIDATION OF ANALYTICAL MODELS

The data collected in the third trial described in chapter 4 and on polymer samples in chapter 6 was used to test the equations derived from the Woodward model (equation 2), the Wierzbicki model (equation 4), together with that describing friction (equation 9).

The mechanical properties of the target material were assessed by static tensile tests or by the indentation method as described in chapter 6. For the Aeroflex the flow stress and coefficient of friction used in calculations were derived by the indentation method. For the metallic targets the flow stress was taken as the maximum true stress measured in quasi static tensile tests (figure 7-4). The coefficient of friction was set as 0.2 for the metallic targets. The value of β was adjusted within the limits given by Shen [5] in order to obtain an optimum fit with experimental data. For all the materials the crack opening displacement parameter δ_t =1. The values used in calculations are denoted by * in table 7-2.

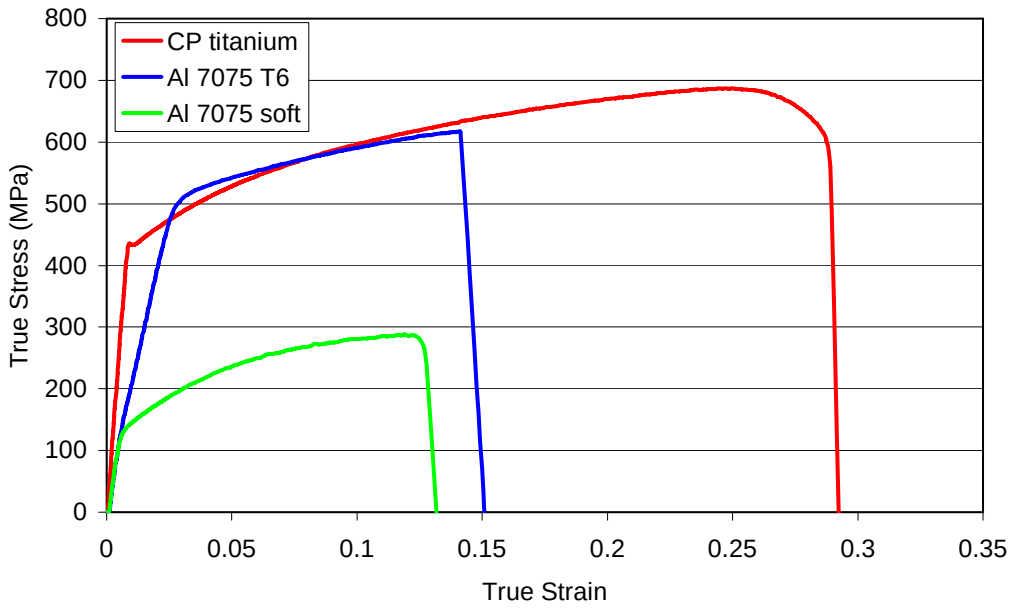

Figure 7-4. Quasi-static stress strain data for CP titanium grade 2, aluminium 7075-T6, and softened aluminium 7075.

The dimensions of each of the four blades (commando, PSDB $N^0$1, PSDB N^o5, and icepick) were measured in order to determine the profile along their entire length. This data was used to calculate the blade cross sectional area and perimeter as a function of distance from the tip. The projectile radius a in equation 2 was the radius of a circle of equivalent cross sectional area of the blade at a given point.

Table 7-2. Data for strength and coefficient of friction used in calculations.

Material	Slipping factor β	Ultimate tensile strength (MPa)	Mean yield pressure (MPa)	Coefficient of friction
Aeroflex	0.1*	22-383	23.5* (by indentation)	0.13* (by indentation)
Aluminium 7075-T6	0.04*	616*		0.2*
Aluminium 7075 soft	0.1*	289*		0.2*
CP titanium	0.14*	686*		0.2*

The blade geometry data and mechanical property data were then used to determine the work done in hole expansion of the target in a piecewise fashion for small increments of blade displacement according to equation 2. The frictional force and wedge cutting force were determined at similar increments and the work was then the product of the force and the displacement increment. This approach was used to determine the total work done in blade penetration of the target as a function of displacement of the blade tip from the front surface of the armour.

Figure 7-5 shows the work done against hole expansion and friction (equations 2 and 9) for the commando blade penetrating Aeroflex, aluminium 7075, and titanium targets. This can be compared to figure 7-6, which shows the work done in wedge cutting and friction (equations 4 and 9). As discussed in chapter 4, the force vs. displacement profile for any particular knife/target interaction can be described by the

highest impact energy test or a quasi-static test. Therefore, work done in penetrating a real target can be derived from a suitable force vs. displacement plot and compared to that predicted from the analytical models. Figure 7-7 shows the energy vs. displacement plots derived from impact tests with the commando blade on Aeroflex, aluminium 7075, and titanium targets.

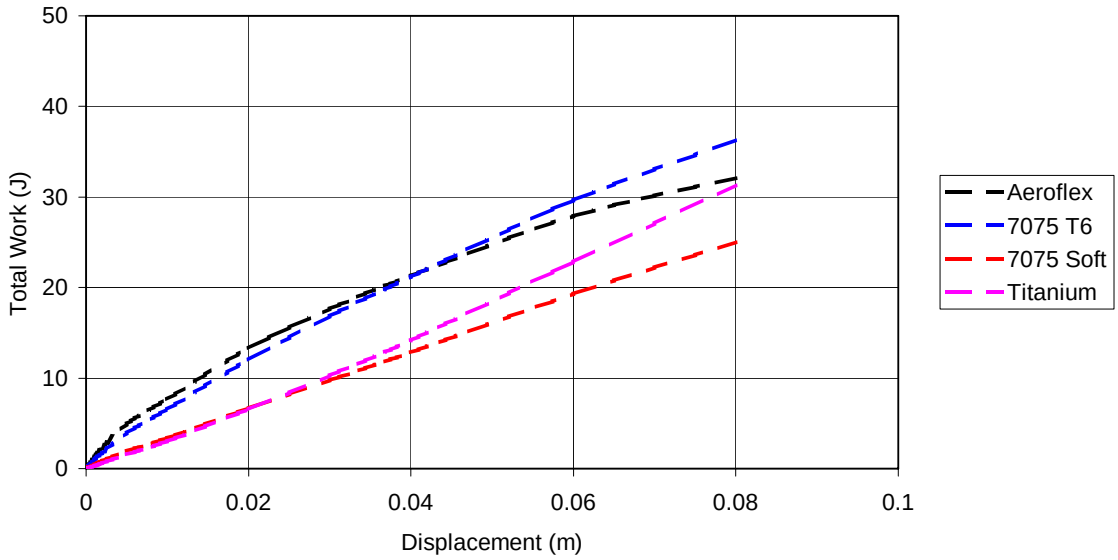

Figure 7-5. Total work done against ductile hole expansion and friction in penetrating various targets with a commando blade calculated from equation 2 and 9.

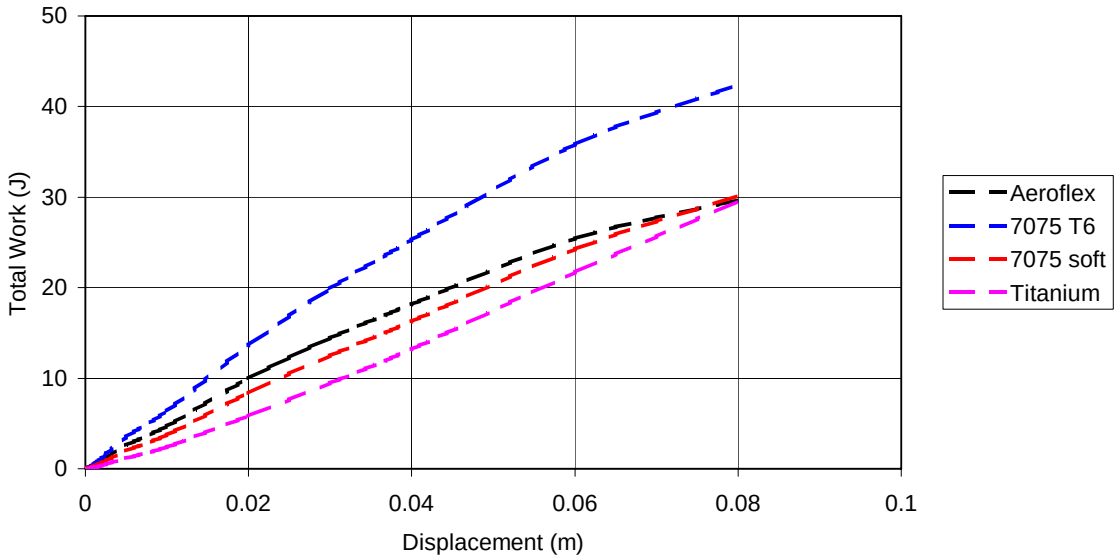

Figure 7-6. Total work done against wedge cutting and friction in penetrating various targets with a commando blade calculated from equation 4 and 9.

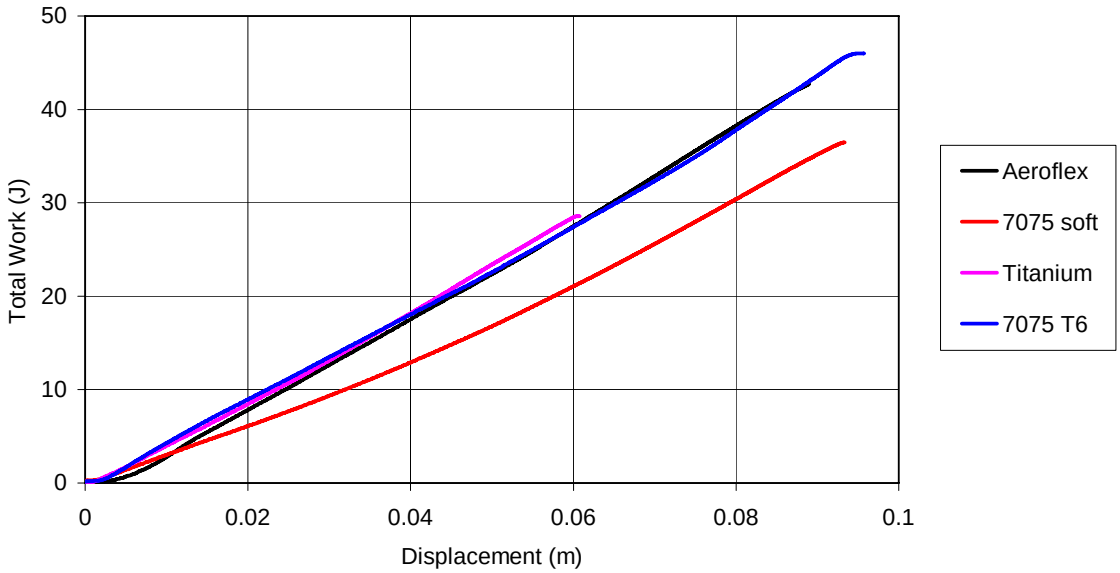

Figure 7-7. Work done in penetrating various targets with a commando blade, derived from impact test data.

The two methods of calculating the work done in penetrating the targets show remarkably similar results in terms of the magnitude ranking and shape of the work vs. displacement curves. The fit between the calculated and experimental data is reasonable, being of the correct magnitude, but the shape and ranking are not well predicted. It is perhaps unreasonable to expect the energy curves to overly each other as their absolute and relative positions will be affected by initial indentation and bending effects within the target, which are not accounted for in the calculations. It is more useful to compare the slopes of the curves. It can be seen that the experimental data show substantially linear increases in work with penetration. The work calculated for ductile hole expansion and wedge cutting both shows a decreasing slope with increasing penetration. If the frictional work alone is plotted as shown in figure 7-8, then the curve shapes and gradients are similar to that of the experimental data.

Whilst it is possible to optimise the fit of the predictions to the experimental data by adjustment of β, δ, and μ, the fit to a wider data set should be examined. It is also

necessary to examine the accuracy of the experimental data before proceeding further

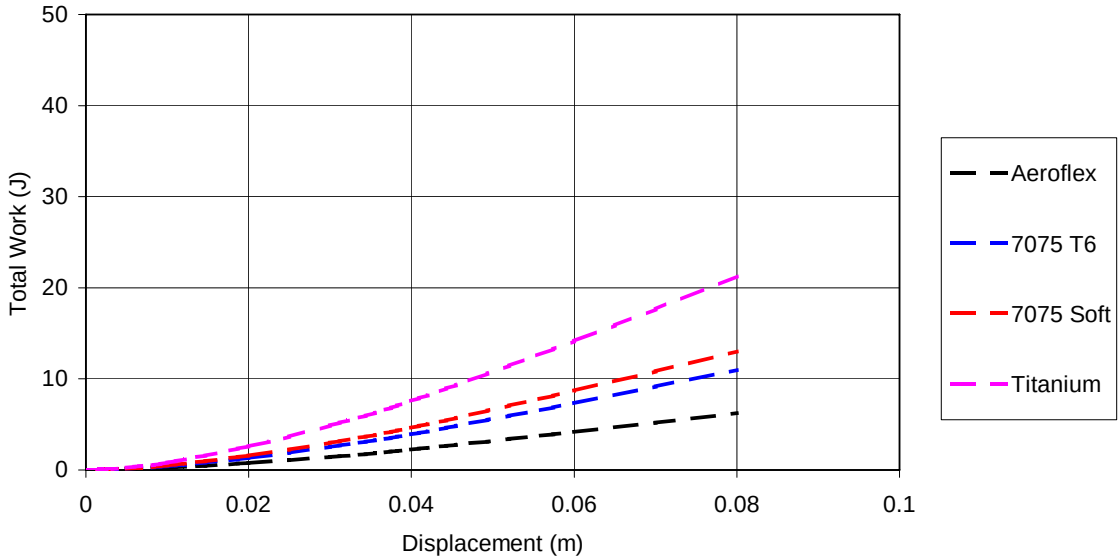

Figure 7-8. Total work done against friction in penetrating various targets with a commando blade calculated from equation 12.

with optimisation of the calculations.

Figure 7-9 shows a comparison of calculated work vs. displacement data and the directly measured blade penetration. It can be seen that the two data sets are in agreement for the softened 7075 and Aeroflex targets whilst there is a significant difference for the 7075-T6 and titanium targets.

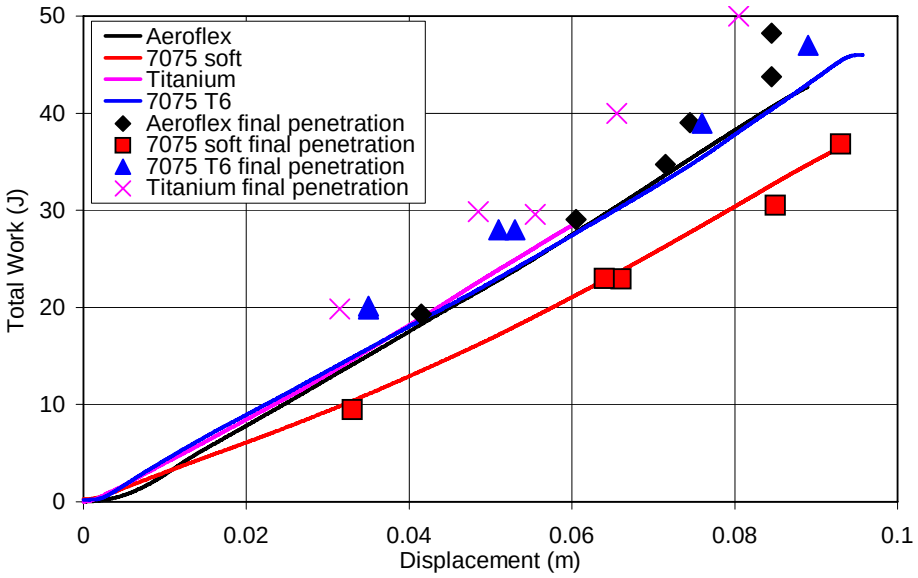

Figure 7-9. A comparison of experimentally derived work vs. displacement curves for a single test against each material with all the measured depth of penetration values for the same target. Tests were with the commando blade, and depth of penetration data has been corrected for target thickness.

The difference between measurements derived from force vs. displacement data and those from directly measured final penetration is comparable with the difference between either of these sets of data and that calculated from the analytical models. Although the fit between individual data sets and the calculated data could be achieved by varying the empirical constants this would not improve the overall correlation between the data sets. Therefore, it seems unreasonable to change empirical constants within the analytical models in order to obtain an exact fit with the experimental work vs. displacement data.

The figures 7-10 - 7-13 compare the calculated work done in hole expansion and friction for each target type. Each figure shows the calculated and experimental data for four blade types.

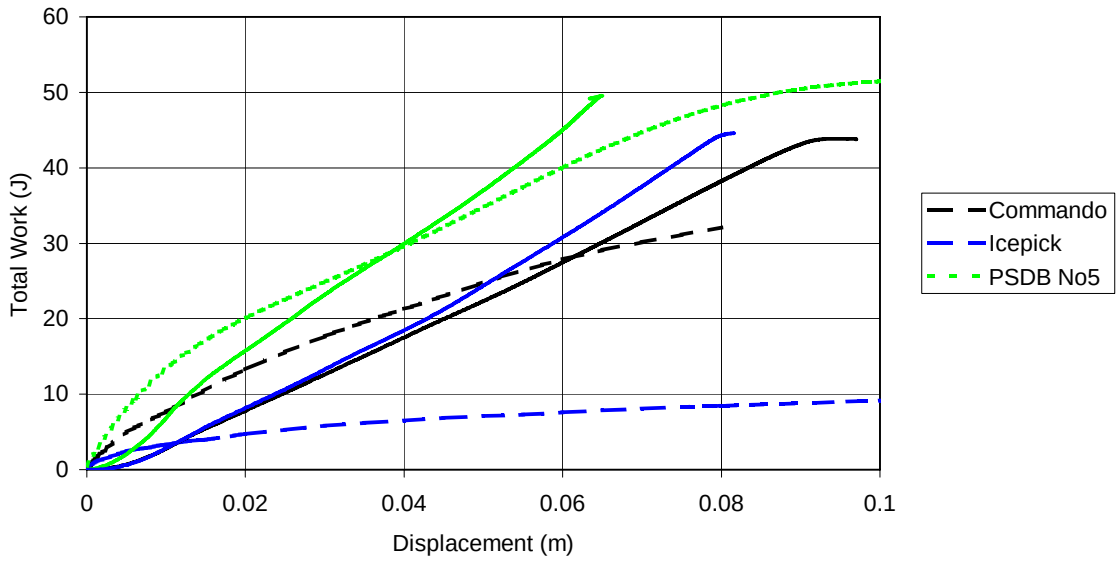

Figure 7-10. A comparison of calculated data for hole expansion and friction (dotted lines) with experimental data of total work done in penetrating a 6.5mm Aeroflex target.

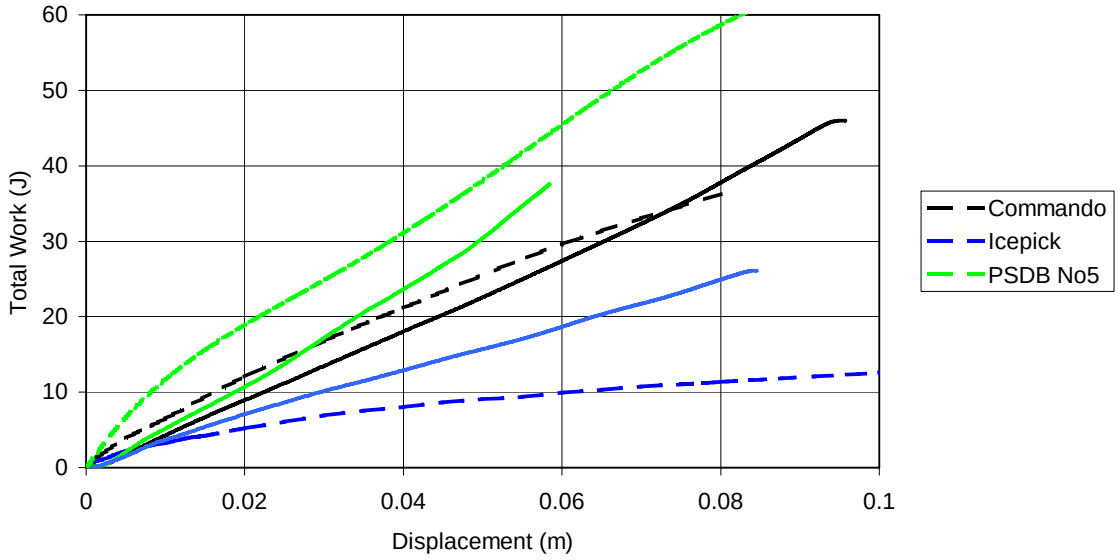

Figure 7-11. A comparison of calculated data for hole expansion and friction (dotted lines) with experimental data (solid lines) of total work done in penetrating a 1mm aluminium 7075-T6 target.

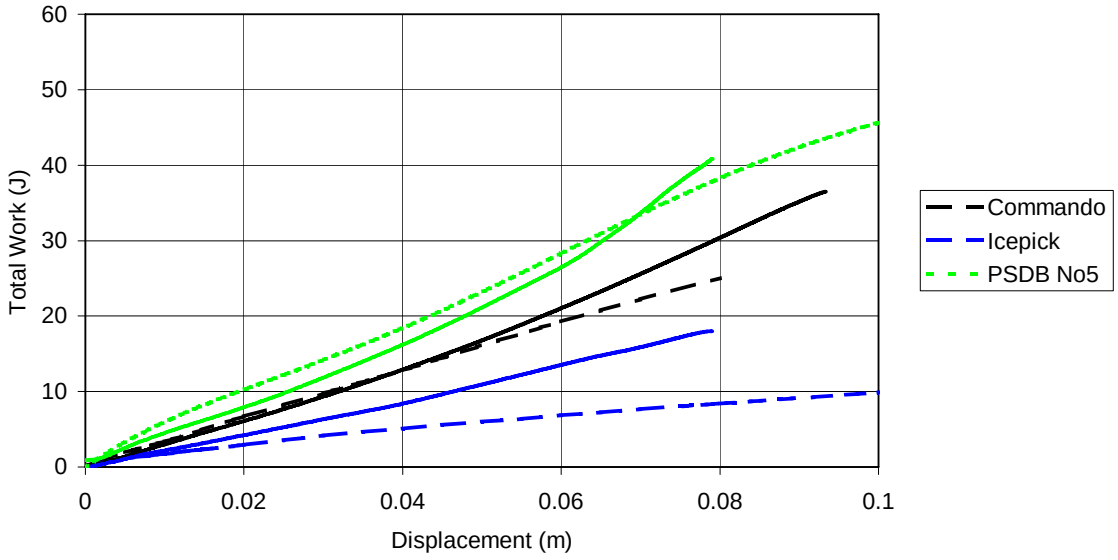

Figure 7-12. A comparison of calculated data for hole expansion and friction (dotted lines) with experimental data (solid lines) of total work done in penetrating a 1mm soft aluminium 7075 target.

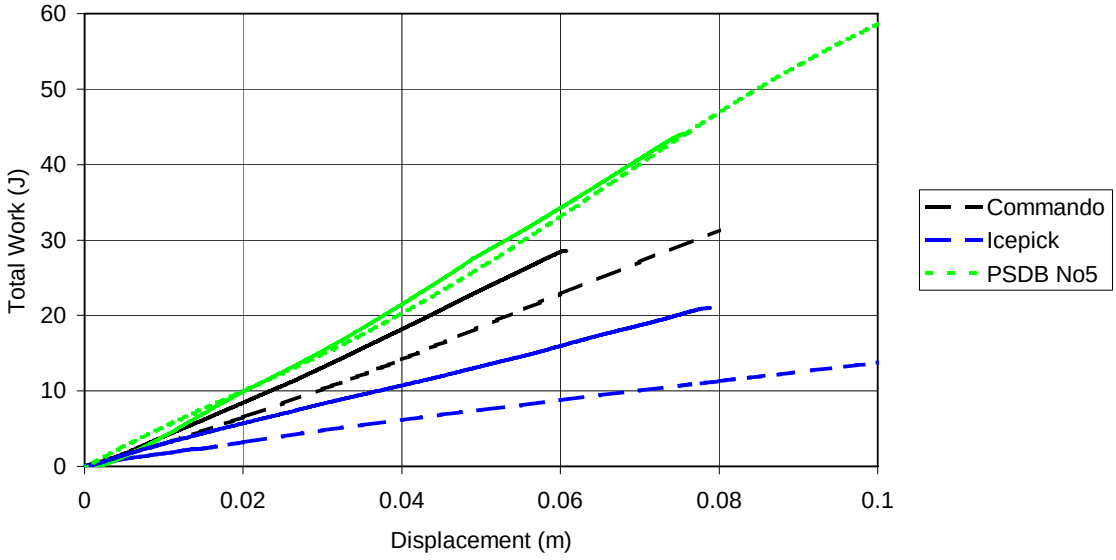

Figure 7-13. A comparison of calculated data for hole expansion and friction (dotted lines) with experimental data (solid lines) of total work done in penetrating a 0.5mm titanium target.

It can be seen from figures 7-10 – 7-13 that the overall match of experimental data to calculated data is reasonable although there are some cases where significant differences exist. Although it is possible to optimise the fit for a particular case by variation of materials properties, this does not result in an overall improvement in fit when all data sets are considered.

In general the calculated data for the commando blade is in reasonable agreement with the experimental data in terms of magnitude but the calculated curve shape is generally too steep at small penetrations and too shallow at higher penetrations. For the PSDB No 5 blade the calculated data fits very well with the experimental data in all cases. For the icepick the calculated data underestimates the work of penetration in all cases and for the Aeroflex target is only a quarter of the experimentally derived values.

Using the same methods to calculate the work done in penetrating the polymer targets reveals a similar set of results as shown in figures 7-14, 7-15, and 7-16. The

magnitude of the work is correctly predicted by sum of the hole expansion and frictional work whilst the curve shape is better reproduced by the frictional data alone. Again it can be seen from figure 7-16 that the frictional work does not reproduce the rankings of the targets achieved in experiments.

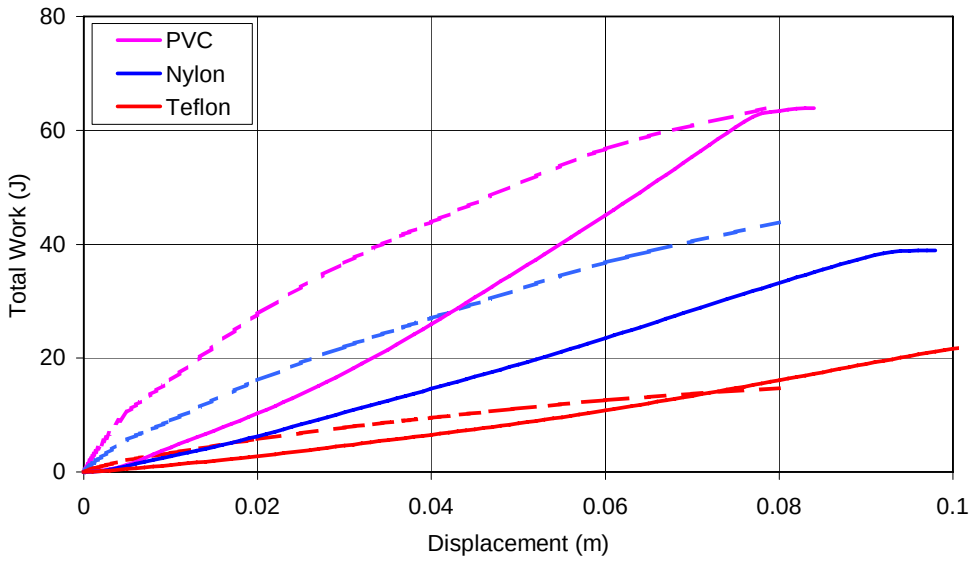

Figure 7-14. Total work done against ductile hole expansion and friction in penetrating polymer targets with a commando blade calculated from equation 2 and 9 (dotted lines) and experimental data (solid lines).

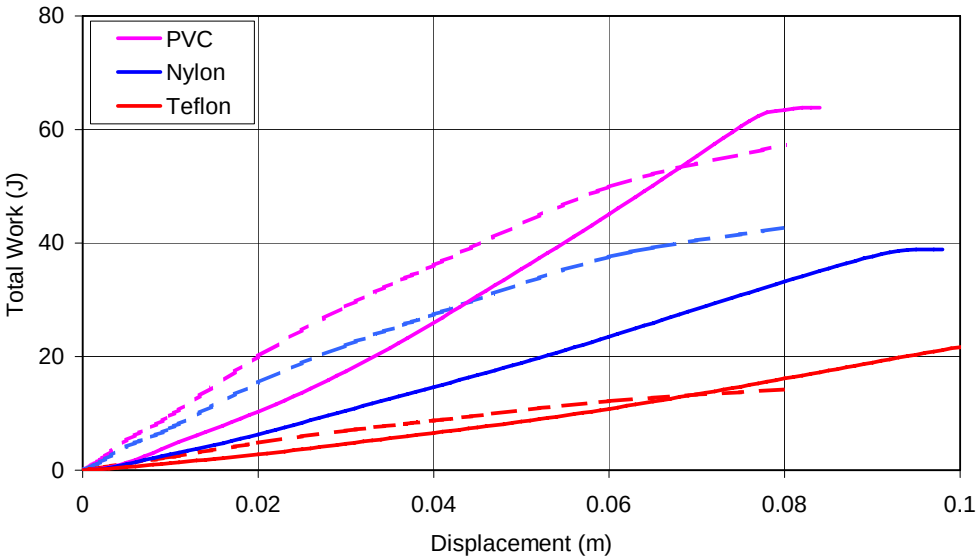

Figure 7-15. Total work done against wedge cutting and friction in penetrating polymer targets with a commando blade calculated from equation 4 and 9 (dotted lines) and experimental data (solid lines).

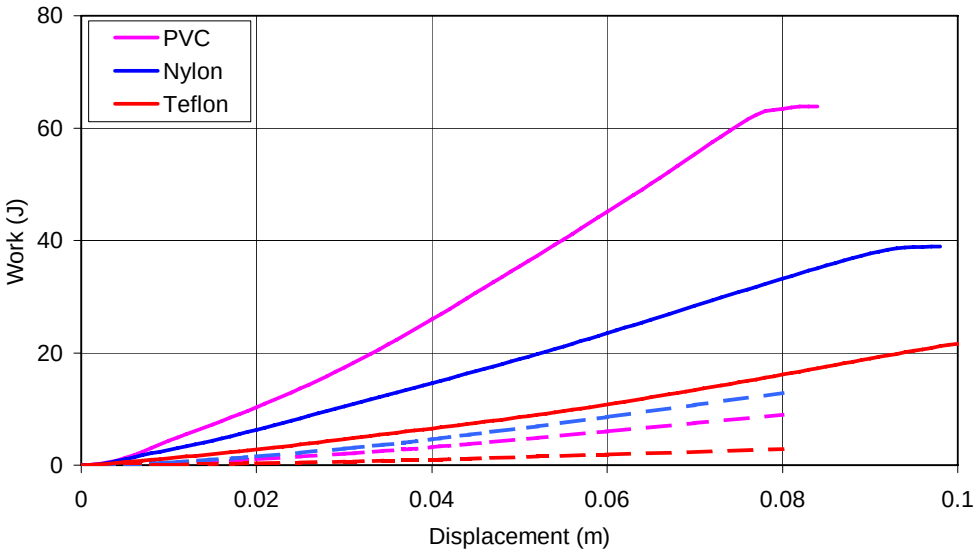

Figure 7-16. Total work done against friction in penetrating polymer sheet targets with a commando blade calculated from equation 9 (dotted lines) and experimental data (solid lines).

7.4 DISCUSSION

From a comparison of the various calculated and experimental data it appears that both a hole expansion based model or a wedge cutting model give a reasonable estimate of the work of penetration of a knife through various targets. The poorest estimate is for the icepick where both models significantly under predict energy absorption. The fit of the calculated data to experimental data appears to be better for the blades that have a larger cross sectional area.

It is generally observed that the shape of the curves derived from experiment is similar to that of the curve calculated for frictional work, i.e. initially concave upwards and then linear. However, the frictional work generally fails to predict the ranking of the targets which is arguably more important. The results suggest that the frictional component may be under estimated whilst the hole expansion or wedge cutting work is probably overestimated.

The slipping friction factor β has been adjusted to optimise the fit for the aluminium 7075-T6 and titanium target. Without this adjustment the work done against the aluminium 7075-T6 target is significantly over predicted, whilst the work done against the titanium target is under predicted. It seems likely that the primary reason for this is the relatively low toughness of the 7075-T6 target and the high toughness of the titanium target. The effect of toughness (or work of fracture) will be twofold, it will directly control the cutting work and indirectly control the normal force on the sides of the blade. A second effect will be that any cracking of the target will reduce the constraint afforded to the petals or flaps of material adjacent to the blade. It can be seen in figures 4-32 and 4-33 that cracking in the 7075-T6 target leads to triangular flaps supported along only one side. In this geometry the hole is enlarged by bending the flap. In the softened 7075 and titanium targets (figures 4-31 and 4-34) the cut edges remain intact so that deformation takes the form of both bending and stretching.

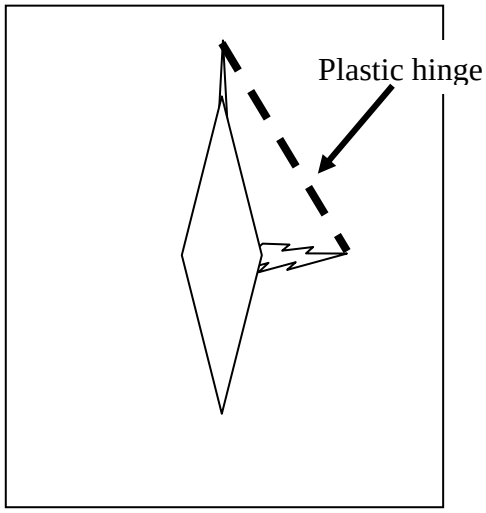

Figure 7-17. The deformation induced by a diamond section knife in a low toughness material (compare to figures 4-32 and 4-33).

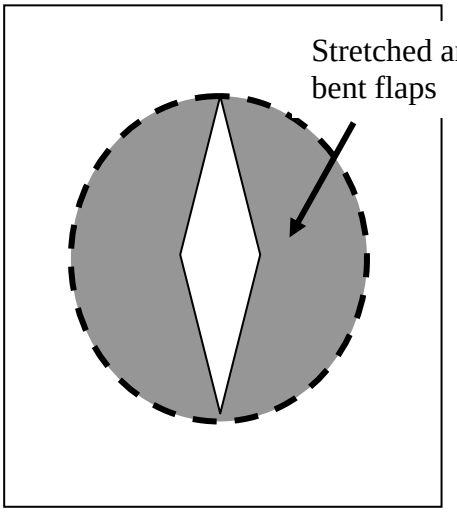

Figure 7-18. The deformation induced by a diamond section knife in a ductile material (compare to figures 4-31 and 4-

If a crack propagates significantly ahead of or to the side of the blade then the constraint acting on the petal or flap pressing against the side of the blade will be reduced. It should be possible to allow for this in the wedge cutting model by adjustment of the crack opening displacement parameter δ. However, as this is only raised to the power 0.2 its effect is limited. Figure 7-19 shows the effect of varying δ over two orders of magnitude for the titanium target.

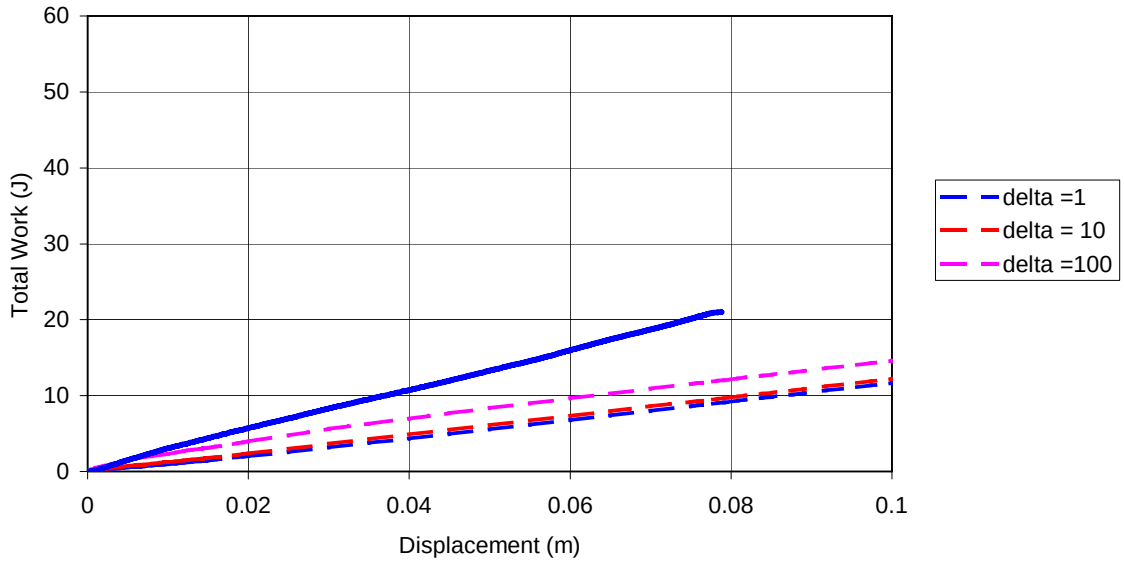

Figure 7-19. The effect of varying the crack opening displacement parameter δ_t on the calculated work to penetrate titanium target with an icepick using equations 7 and 12. The calculated lines are dotted and experimental data is the solid line.

The cross section of the icepick is small compared to the other blades which suggests that adjusting the cracking parameter is likely to have only a small effect. The effect of minor variations in surface finish on the performance of the icepick were discussed in section 4.5.3. This also suggests that the energy absorption during penetration with the icepick is dominated by frictional effects.

It is surprising that for the polymer targets the wedge cutting model gives such good agreement with other calculated data and experimental data, as the targets are relatively thick. The polymer targets were between 2.7mm and 5.5mm in thickness and the Aeroflex target was 6.5mm in thickness. In the derivation of equation 4

Wierzbicki [6] states that it is not valid for cut lengths of less than 6.7t, where t is the plate thickness.

7.5 CONCLUSIONS

The penetration of knife blades through plates appears to be relatively complex and involves a number of different mechanisms, the relative magnitude of which depend upon the knife geometry and target material and geometry.

The work done in penetrating a sheet target by a knife can be estimated by approaches based upon wedge cutting of plate or radial hole expansion. The two use similar parameters and both somewhat simplify the actual geometry, but the agreement with experimental data is good. However, there is little evidence that these approaches accurately follow the underlying mechanisms.

It is apparent that friction plays a major part in the energy absorption process and it appears that the current analysis probably underestimates the frictional contribution. The complexity of the contact geometry makes it difficult to distinguish whether a coulomb friction or shear stress model applies. It is probable that some parts of the interaction are controlled by one process and other parts, possibly simultaneously, are controlled by the other.

7.6 REFERENCES

1. R. L. Woodward, The penetration of metal targets by conical projectiles, *Int. J. Mech. Sci*, **20**, 349-359, (1978).

2. G. I. Taylor, The formation and enlargement of a circular hole in a thin plastic sheet, *Quart. J. Mech. Appl. Math*, **1**, 103, 103-124, (1948).

3. W. T. Thomson, An approximate theory of armour penetration, *J. Appl. Phys*, **26**, 80-85, (1955).

4. G. Lu and C. R. Calladine, On the cutting of a plate by a wedge, *Int. J. Mech. Sci*, **32**, 4, 293-313, (1990).

5. W. O. Shen, K. W. Fung, P. Triantafyllos and N. M. Wajid, An experimental study of the scaling of plate cutting, *Int. J. Impact Engng*, **21,** 8, 645-662, (1998).

6. T. Wierzbicki and P. Thomas, Closed-form solution for the wedge cutting force through thin metal sheets, *Int. J. Mech. Sci*, **35**, 3/4, 209-229, (1993).

7. S. C. Lim and M. F. Ashby, Wear-mechanism maps, *Acta metall*, **35**, 1, 1-24, (1987).

8. C. M. Muscat-Fenech, and A. G. Atkins, Denting and fracture of sheet steel by blunt and sharp obstacles in glancing collisions, *Int. J. Impact Engng,* **21**, No 7, pp.499-519, (1998).

CHAPTER 8

GENERAL DISCUSSION

8.1 INTRODUCTION

The penetration of knives or other edged weapons through an armour system is a complex and inherently variable event. A wide range of solutions have been proposed and marketed as knife resistant systems ranging from cumbersome solid plate designs to highly flexible fabric and mail systems. The mechanisms that control and affect the performance of a particular system are, to some extent, unique to the particular knife-armour combination. Consequently the study of armour systems and penetration mechanics is a broad one and must take note of the wide range of possible interactions.

Apart from the variability in the threat and the armour system, knife impact on armour has a number of aspects which make this a unique problem. At impact, a relatively small amount of energy is dissipated by a moving mass over a small area of the armour. The armour is not free standing but is in close contact with the body of the wearer, and the deformations produced within the armour may be large.

The combination of these latter points makes analysis of the problem particularly complex as they require a model which is dynamic but which can work with relatively slow events; involves several interactions between different bodies; has interactions on both a small scale and a large scale and involves large plastic and elastic deformations. This is a challenging and currently intractable problem even to modern computer based numerical analysis. Consequently the problem has to be broken down into a number of stages in order to provide tractable problems. In the current work the aim has been to characterise the input part of the system in terms of human performance and delivery characteristics, and to then examine the interaction of the knife and armour in a number of discrete stages.

The present study has attempted to cover the basic science and extant technology of relevance to stab protection. Care has been exercised to prevent a concentration on aspects of the subject which are not generally applicable, in an attempt to limit the field of study some areas have not been fully investigated. The experimental and analytical study has concentrated on the interactions between knives and relatively rigid single component homogenous materials. This has been pursued in the full knowledge that flexible systems and relatively complex constructions are used in many commercial and historical systems. However, the relatively simple systems which have been studied have produced useful pointers to the direction of development of all armour systems.

To a large part the work described in this thesis has been performed in support of the development of the PSDB 1999 stab resistant armour standard [1]. The aim of this standard was to provide a scientifically based test procedure with the best possible repeatability. Therefore one aspect of the work was to determine the threat in terms of both the weapon and its delivery. The second aspect was to gain an understanding of the penetration process and the factors which might effect the interaction of a knife an armour.

8.2 TECHNOLOGICAL AND HISTORICAL BACKGROUND

A wide range of related technology is of use in examining the problem of stab resistance. The hole flanging operation as originally studied by Taylor [2], has been applied to both armour and metal forming processes, provides a basis for investigating knife interactions. In comparing this approach with the wedge cutting of plates, it has been shown that there is little difference in the calculated result as both analyses depend on a similar set of variables. For both approaches, the main adaptation required for the analysis of knife attack is to account fully for the frictional forces generated over the length of the knife as it perforates and penetrates the armour.

Current stab resistant armour technology can be split into a number of fields, including articulated plates, mail and textiles. The first two of these provide numerous solutions, the majority of which can be seen to bear close resemblance to ancient military armour. Plated systems, whether of leather and metal, or polymers and composites offer a relatively simple and cheap method of providing protection. There is however an almost direct and inverse relationship between protection and flexibility. The use, in armour, of modern composites or metals with their wider ranges of toughnesses and hardnesses, has probably not yet been fully exploited.

Mail offers a degree of flexibility and protection that is difficult to match. This makes it an obvious candidate for resistance to edged weapons, but it requires careful construction and use if it is to be effective against knives. Ancient armour used riveted links whilst modern systems initially used open links and more recently welded links. Only the latter are capable of providing the strength required to protect against stabbing as well as slashing attack.

Mail was traditionally worn over a padded and quilted jacket known as a gambeson. Interestingly, the gambeson was known to have been worn both underneath and over mail. The purpose of the gambeson was to provide an elastic support for the mail in order to reduce blunt trauma from heavy impacts, but it was also known to improve armour penetration resistance against arrows. The effect of padding both behind and in front of flexible armour is worthy of further study.

The extent to which ancient military armour was adapted to meet the threat and the environment in which it was used can be examined. It is reasonable to assume that coverage and protection levels would have been based on experience. Therefore the armour should to some extent mirror the threat within the confines of available technology. The relative protection required by different parts of the body can be gauged by the order in which protection was applied to meet the threat or discarded to provide mobility. The head was always the first area to be protected, and apart from a relatively brief period during the 19^{th} century AD, soldiers have always worn armoured helmets. Breastplates and torso protection appears to be the next priority.

The absence of torso protection again covers only a brief period probably from the 18th century AD to the mid 20th century AD. In both cases this absence of protection was primarily due to a lack of practicable technology to meet the threat. Apart from head and torso protection the armour worn by soldiers has generally been limited but has extended further along the limbs when tactics and technology allowed.

In a number of cases the armour provided to soldiers has been designed against specific threats and tactics such that the degree of protection varied across the body. There are a number of examples of asymmetric protection. Medieval armour was often thicker or consisted of more plates on the left side whilst lighter armour was often applied around the right arm in order prevent hindrance of the sword arm. The opposite was often the case for jousting armour where the threat was always from the right. Possibly the most extreme example of this type of application was in armies which employ slingers and stone throwers in the rearmost ranks. Figure 8-1 shows an armour from the Gilbert Islands of the Pacific which is made from coconut fibres. The rear torso guard extends up high behind the head to protect the wearer from stones. The typical tactics of the islanders was for the men to form the front rank and engage in hand to hand fighting whilst the women stood back and threw stones at the opposition. The armour was therefore designed not to impede the wearers fighting ability whilst protecting him from the misdirected efforts of his own side.

This demonstrates the considerable ingenuity shown by the designers of ancient military armour in protecting the most vulnerable areas whilst preserving mobility. At least some of these lessons can be transferred to the development of stab resistant police armour. Police armour for normal patrol wear must provide protection against a wide range of threats and in most cases this will not be an organised battle. Therefore the threat direction is difficult to specify, and protection must address the vulnerable area rather than those parts of the body most likely to be injured. Assuming that helmets are worn, the next area for protection should be the torso. This will not protect the wearer from injury, as that is predominantly to the extremities, but it will protect against the majority of fatal and serious injuries. An optimum solution might apply rigid plates to immobile parts of the body whilst

providing flexibility (and lower protection) to the more mobile parts of the body. However it is not clear whether such a complex solution would justify the difficulty in specification, testing and the added cost.

Figure 8-1. Armour from the Gilbert Islands (Kiribati) consisting of coconut fibres. The large panel behind the head is to protect the wearer from stones thrown by his own troops. (After [3])

In comparing patent and historical information it is surprising how little of the modern technology is truly novel. Numerous patents relate to plate and scale armour that is clearly similar to historical examples, and there is little evidence to show that the modern significantly exceeds the performance of the ancient examples. The protection and flexibility afforded by late 14th century plate armour has not been surpassed by modern systems. Unfortunately the range of duties, aesthetic and psychological considerations, and the need for armour to be worn for long shifts

precludes against the use of such systems in the modern police force. However the pattern of protection, fit quality and ergonomic lessons incorporated in plate armour systems should not be ignored. Modern armour, in common with ancient systems, must allow a full range of movement of the limbs and torso and should not impose more than a moderate physiological strain on the wearer.

The use of various scale armour systems in ancient times has been copied in numerous modern designs. Armour composed of small plates loosely tethered together or in combination with a textile carrier provides a good compromise of protection and flexibility. However in order to produce a design with good protection it is necessary to resort to quite complex structures. The plate edges always remain vulnerable and it is difficult to protect them without a significant weight or flexibility penalty. A major part of the ancient armourer's craft was in the minimisation of the proverbial chinks in the armour without compromising flexibility.

Woven textiles do not perform well against pointed weapons as the weave is easily parted. Animal skins have often been used for armour as the individual fibres are entangles and partially bonded together. The effect of this is to require a penetrator to cut the fibres. The use of coated textiles goes some way to matching the fibre constraint achieved in leather without compromising the other useful properties of the textile such as ballistic resistance. The use of an abrasive coating on a textile [4], achieves both the mechanical stabilising effect together with an increase in frictional interaction with the blade. The use of a plasma sprayed abrasive coating applied to a high strength textile appears [5] at first to be one idea that has not developed from ancient armour. However the North American Pawnee Indians are known to have used an armour consisting of two layers of hide enclosing a layer of sand [3].

8.3 INDENTATION

In chapter 6, it was shown that it was possible to predict the perforation force of polymeric targets using an indentation model. This model has also been applied to

the metallic and composite targets investigated in chapter 4. It is first necessary to determine the relevant mechanical and physical properties of the target materials. For the polymeric and the composite targets the flow stress and coefficient of friction can be determined by the indentation method using a range of cone indenters. The indentation method using steel cones cannot be used on these harder materials. For the metallic targets the flow stress at a true strain of 1 would be the best strength measure to use. Tensile data was available but the strain to failure was less then 1 so the maximum true stress value was used. The coefficient of friction was set at 0.5 for all the metallic targets as no reliable data were available. The mechanical property data are summarised in table 8-1 and stress-strain plots for the metallic targets are shown in figure 8-2. Table 8-2 shows the calculated perforation load for all the target types tested.

For the polymeric targets the calculated perforation loads are, as previously discussed, in good agreement with the data for impact tests. However for the other target types the agreement is much poorer.

Table 8-1. Strength and friction property data used to calculate the perforation loads given in table 8-2.

Materials	Flow stress (MPa)	Test for determining stress and stress and friction.	Coefficient of friction
PVC	68.6	Indentation	0.105
Nylon	98.7	Indentation	0.175
Teflon	54.1	Indentation	0.088
Aeroflex®	23.5	Indentation	0.13
Aluminium 7075 T6	615	Maximum true stress	0.5
Softened 7075	289	Maximum true stress	0.5
CP titanium	686	Maximum true stress	0.5

Table 8-2. A comparison of average perforation load in impact tests and calculated load.

Material	Average perforation load (MPa)	Calculated perforation load (MPa)
PVC	631	695
Nylon	346	423
Teflon	144	125
Aeroflex®	583	352
Aluminium 7075 T6	568	417
Softened 7075	374	196
CP titanium	448	116

For the Aeroflex® target the calculated force is approximately 60% of the measured value. The flow stress derived from indentation tests was 23.5MPa. Comparison with the tensile test data shown in table 4-6 shows that this value is comparable with the lowest recorded strength, that for tests at 45° to the fibre direction. In the indentation test the cones are pressed into the surface to a depth of approximately 1mm, and the indentation diameter is then measured. For a material such as Aeroflex®, which is comprised of strong fibres in a rubbery matrix, it seems likely that significant elastic and visco-elastic recovery might take place upon removal of the indenter. It can be seen from the stab test shown in figure 4-30 that the target is capable of elastic recovery from even severe perforation. It therefore seems probable that the flow stress value of 23.5MPa is too low. Increasing this value to 39MPa produces a calculated perforation force equal to the average test value.

It is surprising that agreement is achieved using such a low value of strength. The tensile strength of Aeroflex® was measured in the range 400-450MPa along the fibre directions. Even allowing for the poor diagonal properties (22-31MPa), it would be expected that the representative flow stress for indentation would be considerably in excess of the 39MPa value which gives a best fit to the data.

It is notable that the stab test data for Aeroflex® (figure 4-21) shows that it performs very well against the icepick. The icepick is the most penetrative threat against all the metallic targets, yet is the least penetrative against the Aeroflex® target. This suggests that cutting may play a crucial role in penetration and perforation of the Aeroflex target whilst being less important for the other materials. Aeroflex would be expected to have a low compressive modulus as the overall value is dominated by the matrix. When struck by an edged sharp blade, fibre and matrix cutting allows passage of the blade. The low compressive and bending modulus would allow the cut ligaments to move and accommodate the blade with little resistance. However in the absence of cutting edges, as is the case with the icepick, tensile stresses may be generated around the indenter [6] and the high tensile modulus and strength of the fibre will dominate. These effects are probably the primary cause of the relatively low perforation forces measured for this target type.

For the 7075 T6 target the calculated perforation force is 73% of the measured value Again this could be due to a low value of flow stress (615MPa), although this is unlikely - a value of over 850MPa would be required in order to match the measured data. Examination of the stress strain curves (figure 8-2) shows only limited work hardening in this material, so it is unlikely that a compression test to a strain of 1 would produce a significantly greater stress.

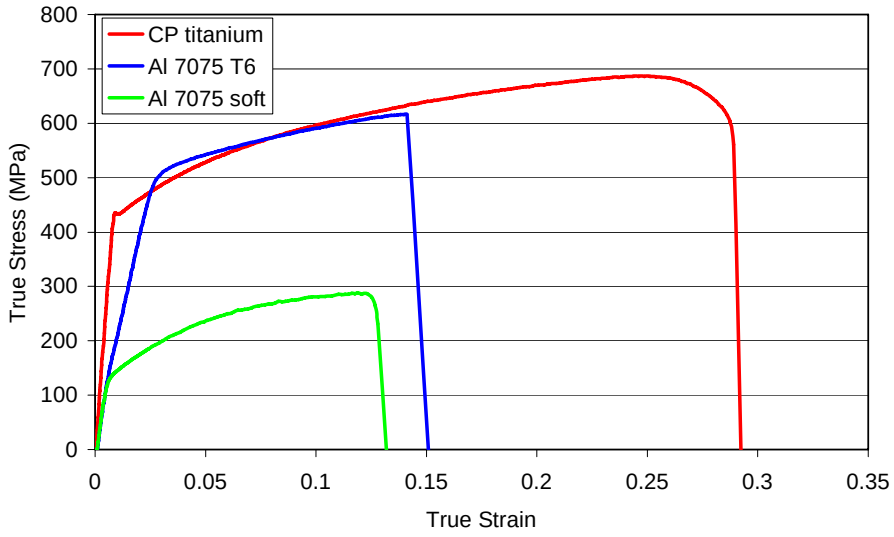

Figure 8-2. True stress vs. true strain data for tensile tests on metallic target materials.

For the soft aluminium and the titanium targets the calculated perforation forces are considerable underestimates of the measured forces. There are a number of possible explanations for the error in the calculated loads.

The flow stress values may be too low. This is possible for the soft aluminium, which does show significant work hardening; here the flow stress was measured at a strain of only 12%. However, the larger error is for the titanium target where the flow stress was taken at 25%.

It may be significant that the greatest error is for the titanium, which is the thinnest target. It may be that for thin targets the indenter tip radius is significant compared to the thickness. For indenter theory to be valid during and before perforation the plastic zone must be predominantly to the side of the indenter and not below it. If there is a significant plastic zone below the indenter then bulging and fracture of the exit surface would occur, with significant energy absorption taking place.

For a relatively sharp indenter (compared to the thickness of the target) it would appear that there is no significant contribution from fracture processes during perforation. The initial perforation and associated bulging is very localised and does not contribute significantly to the overall energy absorption. However for the relatively blunt tipped indenters (or a very thin target) there is probably a significant contribution from fracture at perforation. This effect may be one of the reasons for the use of multi-layer metallic foil armour systems as discussed in the review of patents [7].

The effect of sharpness on penetrative ability may also help to explain why textile ballistic armour is not resistant to knives. Textile armour is designed primarily to defeat soft and blunt projectiles such as those illustrated in figure 8-3. It can be seen that these projectiles are initially blunt and are further blunted and flattened during impact with the armour. Due to the blunt shape and deformable nature of handgun bullets, the energy could be assumed to be dissipated over an area equal to the projectile calibre. Although the knife has a lower energy and a lower velocity this is

concentrated at the tip of the blade. The cutting edges of a blade easily part or cut textile fibres such that the impact energy could be assumed to act over only the contact area of the tip or cutting edges.

Figure 8-3. Handgun projectiles used in the PSDB ballistic body armour tests [8], from left to right 9mm, 0.357" magnum and 0.44" magnum. Similar projectiles after impact with textile armour are shown to the rear.

Table 8-3 compares the threat from the 0.357" magnum projectile of the PSDB ballistic body armour standard [8], with that of the No1 knife blade of the stab resistant armour standard [9]. The energy intensity is calculated for the ballistic threat by taking the contact area over the original projectile calibre (lower bound) or the area of the deformed projectile, typically twice the original calibre (upper bound). The effective contact area for the knife blade is difficult to estimate. An upper bound figure might be the presented area at a distance from the tip equal to the armour thickness (typically 5mm). From figure 4-35 the presented area of the No1 blade 5mm from the tip is 2.5mm^2. A lower bound might be the presented area calculated from the tip radius. The actual tip radius is subject to some variation as shown in figure 8-4, which shows a selection of PSDB No5 blades. For a relatively blunt knife the tip radius would be approximately 250μm giving a presented area of 0.2mm^2.

Table 8-3. A comparison of the ballistic and knife threats to body armour.

Threat	Bullet 0.357” magnum (PSDB high handgun [8])	Knife PSDB No1 blade (PSDB KR42 [9])
Velocity (ms^{-1})	450	10
Energy (J)	1032	43
Shape	Blunt and deformable	Sharp – non deformable
Contact area (mm^2)	65 - 254	2.5 – 0.2
Energy intensity (Jmm^{-2})	4 - 16	17 - 210

The upper bound of the energy intensity of the ballistic threat can be seen to be approximately equal to the lower bound of the stab threat. So the energy intensity of the knife threat is generally greater than that of the ballistic threat and this provides an explanation as to why a textile ballistic armour does not protect against knives and edged weapons.

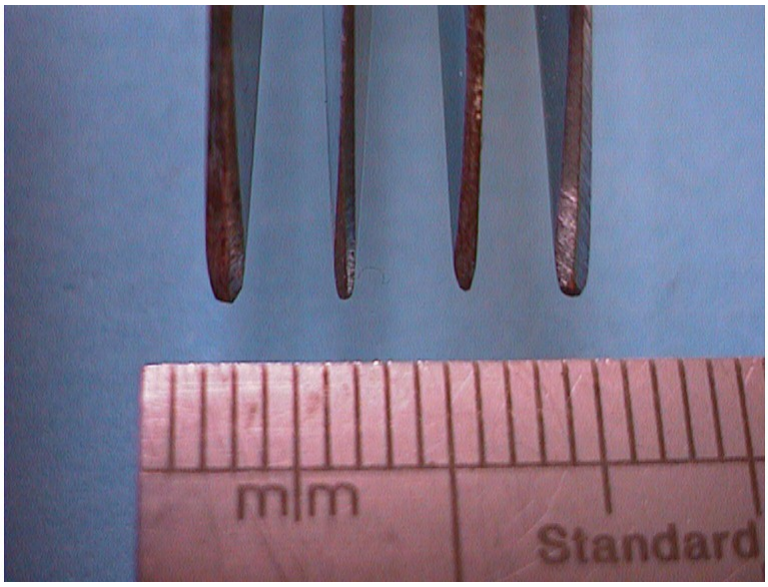

Figure 8-4. A macrophotographic view of the tips of PSDB No5 blades. It can be seen that the tip profile varies considerably despite these blades being from the same production batch.

One other aspect of the indentation part of the penetration process is its effect on test accuracy and repeatability. The blades shown in figure 8-4 show the typical variation in tip profile of ostensibly identical commercial hand-finished knives. From the preceding discussion of tip shape effects, it may be concluded that the tip sharpness, i.e., tip radius, and the angle formed between the faces near the tip, is likely to be a critical factor in blade performance. In section 4.4.3 the primary effect of tip sharpness was shown to be upon the perforation load. The effect on total depth of penetration is relatively small, apparently because blunter blades cause more damage during the perforation process; allowing easier penetration in the later stages. This effect will not however make tip sharpness unimportant. It must be stressed that the armour systems studied in this work were thinner or less penetration resistant than would be required to meet most armour test standards. As such, the loads imposed on the blades were somewhat lower than would be seen in a real armour system. For thicker or stronger armour systems the loads imposed upon the knife can easily be sufficient to cause buckling failure of the blade. Therefore, the effect of tip sharpness will be to determine whether or not buckling and defeat of the knife will take place.

The propensity of blades to buckle under severe loading means that the blade tip should be neither too sharp (resulting in a fragile blade) or too blunt (resulting in high loads). A number of methods have been used in test standards to attempt to standardise tip sharpness. These have included the use of machined rather than hand finished blades and even deliberately blunted blades. Directly measuring blade sharpness is a relatively difficult process, proof test against paper or other calibrated standards are possible, as is optical measurement of tip shape. But all these approaches have disadvantages in accuracy, cost or reproducibility.

Given that the primary requirement of tip sharpness is to minimise indentation loads, measurement of indentation load or a related parameter would provide a direct measurement of the blade tip effectiveness. Based on the work in this thesis, a tip sharpness test was developed which uses an adapted Rockwell hardness test [10] and now forms part of the PSDB stab resistance test standard [1]. In this test the blade is used as the indenter in a hardness test against a standardised soft aluminium block.

The depth of indentation is then measured in the conventional Rockwell procedure as the increase in indentation depth caused by an increase in the indenter load from 3kg to 8kg. This test provides a quantitative measure of blade tip sharpness and the measured value must lie within specified limits for the blade to be passed for use.

8.4 PENETRATION ANALYSIS

The post perforation behaviour of various knife-armour combinations was compared to theoretical predictions using an analytical model for ballistic penetration originally proposed by Woodward [11], and a second analytical model based upon wedge cutting as originally proposed by Wierzbicki and Thomas [12]. In both cases the frictional forces were calculated separately using an equation developed from the work of Shen *et al* [13].

The equation derived from ballistic studies shows that the work done in forming a hole through the target is given by

$$W_D = \frac{\pi}{2} h_o \sigma_O \left(a^2 + \frac{\pi}{2} b h_o \right) \qquad \text{.....(1)}$$

The wedge cutting model shows that the force required to push a blade into a target is given by

$$F = 6.56 \sin\phi \, \sigma_O (\delta_t)^{0.2} l^{0.4} h_0^{1.6} \mu^{0.4} \qquad \text{.....(2)}$$

while the frictional model shows that the axial force produced by friction between a knife and the target is given by

$$F_F = \sigma_O \beta \mu S h_O \qquad \text{.....(3)}$$

For all three models, the work done in forcing a knife blade through a target was calculated on an incremental basis.

These models require knowledge of the geometry of the target and knife, a flow stress for the target and two parameters relating to frictional interaction. These last two parameters, the coefficient of friction μ and the sticking fraction β, are not easily determined. It has been stated in chapter 7 that these parameters can be used as empirical factors in order to match experiment and calculation. It could be argued that the use of μ is misleading as in some parts of the knife such as the cutting edges, the contact stresses may be sufficiently high as to prevent sliding. In this case sliding resistance becomes a function of the shear strength of the weaker material. However this may not always be the case and it has been shown that a reasonable result is produced if realistic values of μ and β are used.

For softer materials it is possible to estimate the coefficient of friction by curve fitting of indentation data for a range of indenters of different cone angles. As steel cones were used in this work the technique could only be applied to softer materials. Although the use of harder materials such as diamond might allow stronger materials to be tested, it is necessary to use very small cone angles to achieve accurate data. Such cones would be extremely fragile, and it therefore seems unlikely that the technique could be usefully employed for all but the softest materials.

If a better estimation of the actual contact geometry during cutting could be obtained then a more realistic modifier could be used to replace the sticking fraction term β. This would allow the coefficient of friction to be discarded in favour of the product of the target shear strength and this new constant.

Examination of the data generated by the two penetration models shows little difference between the two. Both the ballistic and wedge cutting based models produce similar results that correctly determine the ranking of target materials and estimate the absolute values of the work done in penetration. The calculated data was compared to displacement vs. energy data derived from the force vs. displacement records of each test. However this experimental data is not absolutely reliable as it is also shown that these derived values differ to some extent from the penetration depth measured directly from the hole in the backing block. The difference between

experimentally derived displacement and measured penetration is of the same order as the difference between the measured and the calculated data. Therefore, both models can be said to produce reasonable estimates of the performance of the targets with errors which are of similar magnitude to those generated in the measurement process.

8.5 HUMAN PERFORMANCE

The energy and velocity that can be achieved in stabbing actions has been determined for a number of sample populations. Volunteers were asked to stab a target using an instrumented knife which measured the axial force and acceleration during the stabbing. The maximum energy obtained in underarm stabbing actions was 83.5J whilst overarm stabbing actions could produce 115J. The loads produced on contact with the target often approached 1000 N.

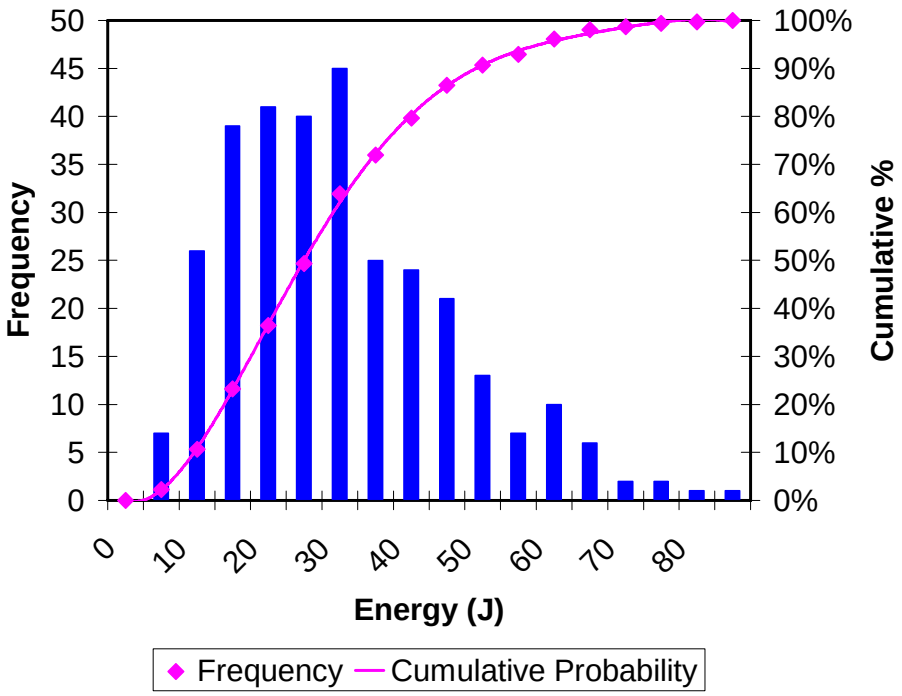

Figure 8-5. The impact energy achieved in underarm action stabs (all data for all groups), showing the frequency histogram and cumulative probability plot.

The PSDB 1999 test standard [1] specifies three protection levels for stab resistant armour (KR1, KR2 and KR3), in terms of the impact energy levels. The test energy levels were derived from analysis of a number of studies including the data discussed in chapter 5. It is possible to use the data generated in this study alone to estimate the effectiveness of armour in terms of a probability of protection (P_P) at a given energy level. From the human performance evaluation, discussed in chapter 5, it was determined that for the underarm threat the maximum delivered energy was 83.5J, the 95 percentile energy was 57.5J, and the mean energy was 27.5J. As previously discussed it is this underarm action stab threat which armour is designed to defeat. The cumulative probability (P_C) of the energy values obtained in tests is plotted in figure 8-5. The cumulative probability curve is in effect the probability of an attack achieving a given energy level. So that for instance it can be seen from the plot that the probability of achieving 57.5J is approximately 95%. However, this does not mean that armour capable of preventing penetration at 57.5J has a probability of protection of only 95%.

It has been found by Croft [14], that the majority of blades confiscated by the police are either relatively weak kitchen knives or are blunt. The weaker knives will bend when struck against armour whilst the contact loads generated by blunt knives will either prevent penetration or cause buckling of the blade tip. Less than 1% of confiscated weapons were found to meet both the strength and sharpness standards required of test blades. A similar finding was reported in a study by Fenne and Winslade [15].

In order for an armour to be defeated, the impact energy must be greater than that which the armour passed in testing and the weapon used must be as penetrative as the test blade. For instance, the PSDB KR3 protection level requires an initial test at 43J. The probability that an armour which just meets this standard can be defeated could be calculated as the product of probability of a delivered blow being above 43J and probability of the assailant being equipped with a good knife (1%). From figure 8-5 the cumulative probability of a blow being below 43J can be seen to be 85%.

Therefore the probability of exceeding this level is 15%. This gives an overall probability of failure of the armour of

$$P_F = 0.15 \times 0.01 = 0.0015 \quad (\text{or } 0.15\%)$$

and likewise a probability of protection

$$P_P = 1 - 0.0015 = 0.9985 \quad (\text{or } 99.85\%)$$

So an armour which has been tested to 43J should provide a probability of protection of 99.85%, assuming that the data is representative of the population of likely assailants. A similar calculation can be performed for any given energy level. The probability of achieving a given energy (P_C) can be read from figure 8-5 and the probability of protection (P_P) can then be calculated.

It is also necessary to take into account the definition of armour failure and its consequences. Each of the three protection levels of the PSDB 1999 standard (KR1, KR2 and KR3) specifies an initial energy level (E1) at which up to 7mm of penetration is allowed and a higher energy level (E2) at which 20mm of penetration is allowed. The higher energy level (E2) is 150% of the lower, and is used in order to test whether the armour undergoes a catastrophic failure at impact energies above the lower (E1) level.

Most armour is worn as outer clothing so some degree of penetration might be allowed without resulting in a blade reaching the skin. It must be remembered that the main purpose of armour is to prevent serious injury and there will be a significant flexibility, weight and comfort penalty in designing an armour impervious to knives. Bleetman's analysis [16], showed that although the minimum skin to organ distance (of any organ, on any subject, under any conditions) was 10mm, the average distance was of the order of 25mm. Therefore in order for serious injury to result at 10mm penetration, the armour must first be penetrated to this level, the penetration must be immediately over an organ such as the liver, and the armour must be worn by

someone of slim build who has their breath fully inhaled at the time of impact. Therefore, there is a very low probability of anything more than slight injury resulting from a penetration of 7mm.

The PSDB test standard specifies allowable penetration at two energy levels for each protection level. At the E1 energy level 7mm of penetration is allowed, and this is almost certain to result in either no injury or only a slight laceration of the skin. At the E2 level 20mm of penetration is allowed, which might produce a slight to moderate injury, but is unlikely to be serious. Therefore it is possible to calculate the probability of protection for the basic (E1) energy level at which injury is likely to be only slight and at the higher (E2) energy level at which injury is likely to be only moderate. From table 8-4 it can be seen that for the KR1 test standard, which is the lowest specification, the probability of the armour protecting against a 7mm penetration is 95.5% whilst the probability of protecting against a 20mm penetration is 99.75%.

Table 8-4. Estimated probability of protection of armour at PSDB 1999 test energy levels.

Test level	Energy level, E1 (J)	Probability of protection		Energy level, E2 (J)	Probability of protection	
		P_C %	P_P %		P_C %	P_P %
KR1	24	50	95.5	36	75	99.75
KR2	33	65	99.65	50	90	99.9
KR3	43	85	99.85	65	98	99.98

It has been shown that the energy dissipated at the target is delivered primarily as kinetic energy of the total moving mass of the knife, hand and arm of the person delivering the blow. These components are not rigidly joined so the energy is delivered in a number of stages as these masses are decelerated. As a result of these findings the PSDB 1999 test standard [1] has adopted a dual mass drop weight designed to replicate the energy delivery of a hand propelled knife [17].

Probably one of the most important findings of the human performance assessment is in the nature of the energy available to do work against the armour. As the major part of the available energy is from the kinetic energy of the total moving mass, it is the sudden arrest of this mass on contact with the armour which produces a contact stress sufficient to penetrate the armour.

From the work presented in chapter 6 it appears that the initial resistance to penetration provided by the armour is not subject to significant dynamic effects and can be treated as a static indentation problem. This is also shown in the post perforation data presented in chapter 4, which shows a lack of dynamic effects in all systems except titanium. The interaction of the primarily dynamic energy input with primarily static dissipation mechanisms may be of some significance and is examined in the next section.

8.6 DYNAMIC INTERACTIONS

The approach adopted in previous chapters has specifically excluded the investigation of target flexibility and the interaction of the target with its support. Historical data suggests that armour was almost always backed with heavily padded layers ostensibly to absorb impact energy and reduce trauma. Recent work by Watson *et al* [18] has shown that the presence of padding layers in front or behind the armour can significantly increase its penetration resistance. It is thought that such layers aid in the movement of the armour in the same direction as the impact such that the initial contact stresses are reduced and the interaction distance is increased.

An armour which is rigid must dissipate all of the input energy by the mechanisms discussed in previous sections. However an armour which has any significant flexibility can deform backwards into its supporting medium be it Plastilina® in a laboratory or the body of the wearer when in use. It has been shown [19] that the measured penetration resistance of an armour is substantially increased when a softer backing block material is used. In theory it should be possible to describe an armour

which dissipated no energy at all but simply transfers the input momentum onto its support where it is then dissipated in plastic deformation, or movement. The significance of this effect can be examined by investigating the effect of target support compliance.

The effect which is of interest is the deformation of the target into its support in the direction of knife travel. An explicit model of this process would be highly complex and require detailed descriptions of all the components materials and interactions. However it is possible to construct a simple 1 dimensional lumped mass model of the system which can allow some investigation of key parameters. This is a similar approach to that used in section 5.5.2 for analysis of the hand stabbing action.

In order to investigate the effect of target support and flexibility a model was implemented within the Working Model V3.0 computer package. This package is a mechanical and dynamic modelling package with graphical input and output which has already been demonstrated in section 5.5.2. The complete knife-armour-support is modelled as a number of masses connected by spring dampers and a programmable actuator as shown in figure 8-5.

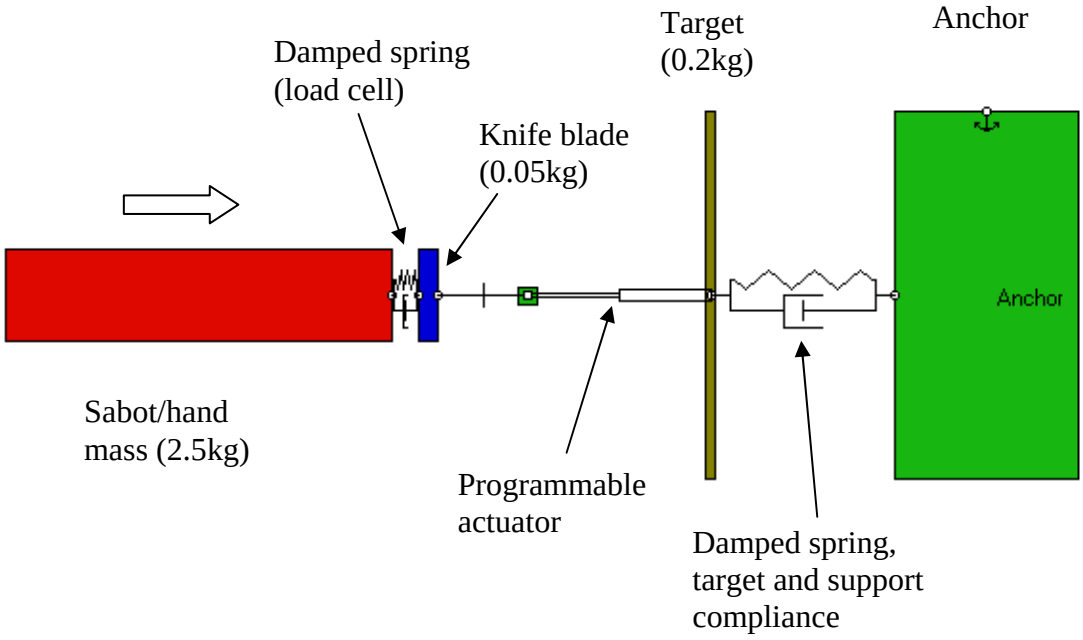

Figure 8-6. Diagrammatic representation of the target compliance model.

The model is set up to represent a generalised impact of a hand propelled or drop tower supported knife acting against a target such as Aeroflex®. The input to the system is a knife mounted onto a 2.5kg mass via a stiff spring damper which models the properties of the piezo load cell used in the drop tower or hand stab trials. This is connected to a programmable actuator, which provides a resistive force between the knife and the target. The length of the actuator is monitored and used to provide a resistive force to simulate the action of a knife penetrating the target. The penetration resistance of the target is determined from an idealised force displacement plot as shown in figure 8-7. This is a generalised form which has similar performance to the Aeroflex® or composite targets discussed in chapter 4. The peak resistance occurs at a displacement of 8.5mm, which simulates the effect of target thickness of approximately 6mm with 2.5mm of local dishing. The curve should be compared with typical experimental results in chapter 4.

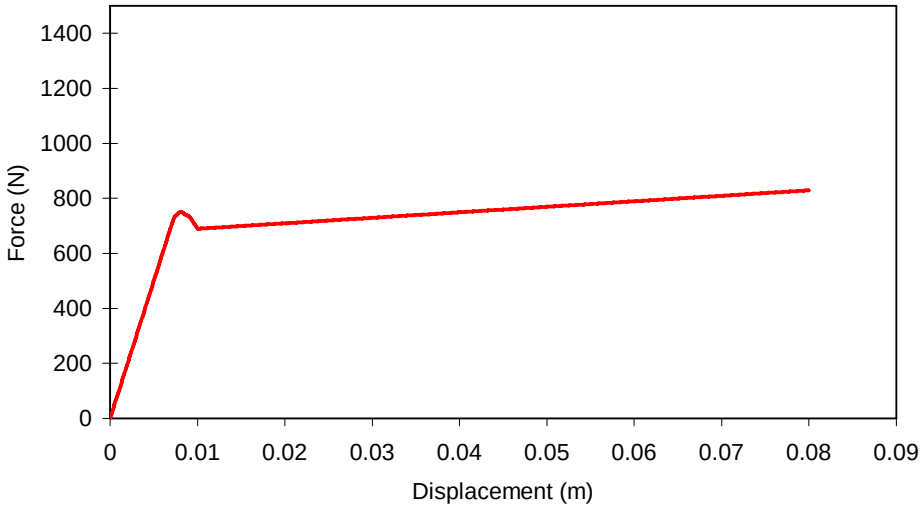

Figure 8-7. Generalised force vs. displacement plot used to program actuator.

The target, of mass 0.2kg is coupled to a rigid anchor via a spring damper. This spring damper provides a means to control the rearward movement of the target simulating the movement of a flexible target into its support medium. The moving mass consisting of the sabot and hand (2.5kg), the load cell (zero mass), and the blade

(0.05kg) is set in motion at 3.5ms^{-1} giving an impact energy of 15.6J. The blade mass represents the mass of that part of the knife which is forward of the load cell. The load cell output is monitored together with the moving mass position to give a force displacement plot of the impact event. It is also possible to monitor the actuator length (effectively penetration) and the target movement. The stiffness and damping of the target support spring was varied over a range of values. This support compliance embodies the momentum and stiffness of both the target and support materials. No attempt was made to provide realistic values as they are not known and would be difficult to estimate. The values used and a summary of results are given in table 8-4. The force displacement plot for each condition is shown in figure 8-8.

Table 8-5. Summary of results for variation of target compliance.

Spring constant (Nm^{-1})	Damping constant (Nms^{-1})	Blade displacement (mm)	Total penetration (mm)	Penetration into backing (mm)	Target displacement (mm)
50000	2000	26	24	15	1
10000	400	26	19	10	7
5000	200	27	12	3	14
2500	100	33	7	0	25

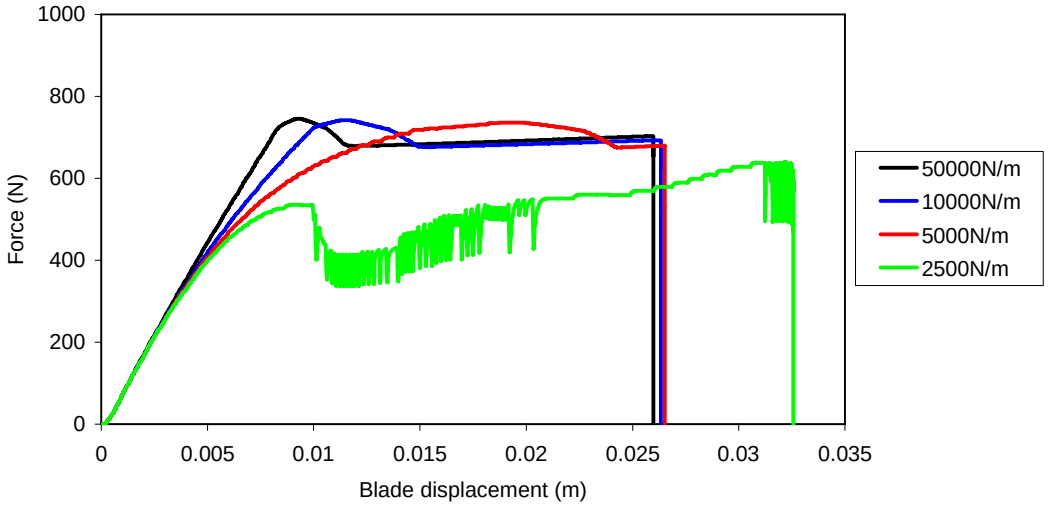

Figure 8-8. Force vs. displacement plots as a function of target mounting compliance.

Table 8-4 shows the spring and damper constants used together with displacement of the blade which is analogous to the displacement measured in drop tower tests. The total penetration is the effective penetration of the blade measured from the front face of the target. The penetration into the backing is the effective penetration measured from the rear face of the target. The difference between these two quantities being the effective thickness of the target and is equal to the displacement at perforation shown in figure 8-7. The target movement is analogous to the displacement of a flexible target into the backing material.

It can be seen from figure 8-8 that with a stiff mounting compliance ($50000Nm^{-1}$) the force displacement plot simply recreates the materials characteristics of the target as shown in figure 8-6. This simulates the situation of an armour which is rigid or mounted on a rigid backing. As the mounting compliance is reduced the target starts to move rearwards and the initial peak force is first displaced and then reduced in magnitude. In the case of the softest mounting ($2500Nm^{-1}$) the peak force is insufficient to penetrate the target and a significant amount of the energy is dissipated into the mounting. It should be noted that the area under the curve remains constant irrespective of mounting compliance as the total energy dissipated in the interaction is fixed.

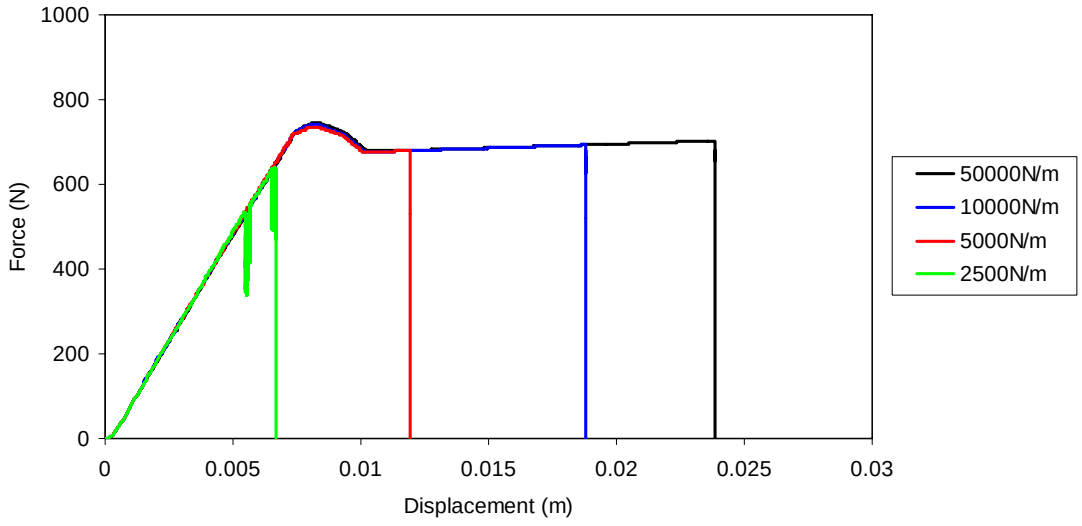

Figure 8-9. Force vs. armour penetration as a function of target mounting compliance. The area under the curve is seen to decrease with mounting compliance.

The effect of target compliance on the penetration of the armour can be seen in figure 8-9, and is summarised in table 8-4. In figure 8-9 the force on the blade is plotted as a function of actuator length i.e. penetration into the target. Now it can be seen that as the target mounting compliance is reduced the area under each curve, i.e. the energy dissipated into the target, is reduced. With a mounting stiffness of 2500Nm the penetration is less than the target thickness so perforation does no occur. It can be seen that whilst the area under the curve is constant for all conditions in figure 8-8 it decreases with decreasing mounting stiffness for the plots in figure 8-9. This demonstrates that as the mounting stiffness is decreased the armour is required to dissipate less of the input energy.

8.7 CONCLUSIONS

There exists a wealth of technology that can be applied to stab resistant armour although the scientific background to the subject is still limited. It has been possible to determine the key parameters that affect the performance of both armour systems and knives. The performance of armour improves as a function of its frictional interaction with a knife, its strength and to some extent its flexibility. The performance of knives, not unexpectedly, is largely a function of sharpness, slimness and surface finish. It should be noted that that sharpness does not directly effect penetrability but controls the likelihood of blade buckling.

The stabbing ability of a sample population has been determined together with useful information on the dynamics of knife delivery and terminal effects. The energy input from stabbing has been shown to be primarily a kinetic one and the interaction of this with the armour sheds light on both future developments in stab resistant armour and ancient military designs.

The interaction between a knife and armour is complex with a number of different mechanisms and stages. The impact and perforation of the armour occurs in three successive stages of indentation, perforation and further penetration. This sequence is

superimposed upon a complex interaction of the impacting mass of the knife and the person propelling it with the armour and its wearer. Significant compliance exists between each of these components such that any momentum transfer between the knife and the armour is complicated by the other parts of the system.

The main goal of armour designers is to increase wearer comfort and specifically flexibility in armour systems. From a technological viewpoint the main requirement will be to provide better flexibility without compromising protection. An examination of the effect of armour flexibility in the previous section shows that increased flexibility may also increase armour performance. This approach is useful but cannot be taken to extremes. A practical armour will be mounted against a wearer's body and the ability of the armour to deform will be limited over areas such as the ribs.

8.8 REFERENCES

1. M. J. Pettit, J. Croft, PSDB Stab resistance standard for body armour (1999), Police Scientific Development Branch, Publication No 6/99, (1999).

2. G. I. Taylor, The formation and enlargement of a circular hole in a thin plastic sheet, *Quart. J. Mech. Appl. Math*, **1**, 103, 103-124, (1948).

3. G. C. Stone, *A Glossary of the Construction Decoration and Use of Arms and Armour*, Jack Brussel, New York, (1961).

4. C. Bottger, Twaron SRM – a novel type of stab resistant material, *Proc Sharp Weapons Armour Technology Symposium*, Cranfield University, Shrivenham, (1999).

5. International Patent, No WO9845662, (1998).

6. A. G. Atkins and D. Tabor, Plastic indentation in metals with cones, *J. Mech. Phys. Solids*, **13**, 149-164, (1965).

7. United States Patent, No US 5,697,098, (1997).

8. G. Parker, PSDB ballistic body armour test procedure, Police Scientific Development Branch, Publication No 2/95, (1995).

9. G. Parker, PSDB Stab resistant body armour test procedure (1993), Police Scientific Development Branch, Publication No 10/93, (1993).

10. I. Horsfall, I. C. Harrod and C. H. Watson, Knife tip sharpness and its measurement, *Proc Sharp Weapons Armour Technology Symposium*, Cranfield University, Shrivenham, (1999).

11. R. L. Woodward, The penetration of metal targets by conical projectiles, *Int. J. Mech. Sci*, **20**, 349-359, (1978).

12. T. Wierzbicki and P. Thomas, Closed-form solution for the wedge cutting force through thin metal sheets, *Int. J. Mech. Sci*, **35**, 3/4, 209-229, (1993).

13. W. O. Shen, K. W. Fung, P. Triantafyllos and N. M. Wajid, An experimental study of the scaling of plate cutting, *Int. J. Impact Engng*, **21,** 8, 645-662, (1998).

14. J. Croft, PSDB stab resistance standard for body armour, *Proc Sharp Weapons Armour technology Symposium*, Cranfield University, (1999).

15. P.Fenne and S. Winslade, Metvest – the customer aspects, *Proc. Sharp Weapons Armour technology Symposium*, Cranfield University, (1999).

16. A. Bleetman, Determining the protective requirements of stab resistant body armour: the vulnerability of internal organs to penetrating edged weapons, *Proc. Sharp Weapons Armour technology Symposium*, Cranfield University, (1999).

17. I. Horsfall, S. M. Champion, and I. C. Harrod, The development of realistic stab resistance test methods, *Proc Sharp Weapons Armour Technology Symposium*, Cranfield University, Shrivenham, (1999).

18. C. H. Watson, I. Horsfall, A. M. Robinson, Stacking sequence effects in multi-purpose body armour. *Proc Sharp Weapons Armour Technology Symposium*, Cranfield University, Shrivenham, (1999).

19. M. J. Chiou, Development of protective body armour for puncture, stab and multi-threat protection, *Proc Sharp Weapons Armour Technology Symposium*, Cranfield University, Shrivenham, (1999).

CHAPTER 9

CONCLUSIONS

a) This thesis has provided a broad study of the science technology and application of stab resistant armour. This has provided an insight into the mechanisms that control the interaction of a knife with an armour.

b) From an analysis of both ancient armour and modern injury statistics it is possible to say that in order to minimise the risk of death armour should provide protection to the chest and abdomen. If the aim is to provide protection from injury then protection should extend over the limbs.

c) The 95 percentile underarm stab has an impact energy of 54J with typical impact velocities being in the range 6 – 10ms^{-1}. The impact energy is primarily the result of the deceleration of the knife, hand and arm of the assailant upon contact with the armour. The compliant connections between these components leads to a sequential energy delivery which can be simulated by a dual mass missile. The data from this study has been used to design such a missile for use in the PSDB (1999) test standard. This consists of a blade and primary mass of 0.65kg joined to a secondary mass of 1.25kg by a sponge rubber spring.

d) The interaction of a knife blade and an armour has been shown to follow three stages, indentation, perforation and further penetration. The indentation stage can be analysed using indentation theory and this allows the load required to indent the target to be calculated. Setting the indentation depth as equal to the target thickness d, it is possible to calculate the perforation load as

$$F = \frac{P_0(1+\mu\cot\alpha)\pi d^2}{4} \qquad \text{.....(1)}$$

Energy absorption during the perforation process is shown to be a relatively minor part of the total, although this appears to be less true for very tough and/or thin targets. The penetration stage following perforation can be analysed by either hole expansion or wedge cutting models. The hole expansion model shows that the work done in penetrating the target is given by

$$W_D = \frac{\pi}{2} h_o \sigma_O \left(a^2 + \frac{\pi}{2} b h_o \right) \qquad \text{.....(2)}$$

And the wedge cutting model shows that the force resisting penetration of a target is given by

$$F = 6.56 \sin\phi \, \sigma_O (\delta_t)^{0.2} l^{0.4} h_0^{1.6} \mu^{0.4} \qquad \text{.....(3)}$$

In both cases it is necessary to account fully for the effects of friction. A reasonable agreement with experimental data is obtained from the sum of either equations (2) or (3), and the frictional resistance given by

$$F_F = \sigma_O \beta \mu S h_O \qquad \text{.....(4)}$$

Both the initial indentation stage and final penetration stages of penetration are shown to be strongly dependent upon the frictional interaction of the knife blade and the armour.

e) The energy delivery is primarily dynamic whilst the penetration resistance of armour is shown to closely follow quasi-static behaviour. The interaction of these two systems provides a number of possible mechanisms for additional energy absorption. In particular it is shown that the use of flexible or flexibly mounted armour might allow significant energy to be absorbed by a backing, or the wearer rather than within the armour. A computer model has been used to show that reducing the mounting compliance of a flexible armour can dramatically increase penetration resistance.

f) It has been possible to determine the key parameters that affect the performance of both armour systems and knives. The performance of armour improves as a function of its frictional interaction with a knife, its strength and to some extent its flexibility. The performance of knives, not unexpectedly, is largely a function of their sharpness, slimness and surface finish. It should be noted that that sharpness does not directly effect penetrability but controls the likelihood of blade buckling. Against any particular armour there is likely to be an optimum sharpness which minimises perforation loads whilst providing sufficient strength to resist buckling.

g) Penetration of armour by pointed instruments is shown to be due to a concentration of impact forces on a small area of the armour. This allows initial indentation and then perforation to occur without significant energy absorption except in the immediate vicinity of the contact. The presence of sharp cutting edges is shown to provide a means for increasing the perforation size in soft armours, whilst in more brittle armour materials cracking can occur. Both these effects reduce the constraint on material close to the perforation and reduce the resistance to blade passage.

h) The interaction of a hand held knife and armour worn as clothing has been shown to be a complex problem. The inherent variability of almost every aspect of this system provides a difficult challenge to the armour designer. It is apparent that the perfect armour will never be designed, but neither will the perfect knife. Whilst it may never be possible to make the perfect armour it will always be possible to make better armour.

CHAPTER 10

RECOMENDATIONS FOR FUTURE WORK

The aim of this thesis has been to provide a broad understanding of the behaviour of the stab resistant body armour. This has necessitated a relatively shallow study of each area, consequently there may be merit in further more detailed investigation of most of the main themes of this thesis.

The human performance study is under further study in order to confirm the validity of the data for a wider range of weapons. Work is also in progress to extend the study towards slashing attack in addition to stabbing. The effects of a more compliant target on the energy dissipated in a manual stabbing action are worthy of further analysis.

Each of the stages of armour failure (indentation, perforation and penetration) together with the effects of global bending and dishing should be subject to further study possibly using numerical modelling techniques. At present, the analysis of such problems is just out of reach of desktop computing systems. However this restriction will almost certainly disappear with advances in computing speed and will then allow relatively convenient analysis of these problems.

The application and effects of flexible armour systems requires further analysis. When this thesis was started no truly flexible armour existed, but recent advances have lead to the development of much more flexible armour systems. The effect of increased flexibility is to allow momentum to be dissipated through the armour into the backing or wearer. Although a preliminary analysis of this has been demonstrated in previous chapters, it is worthy of further detailed practical and theoretical analysis.

The understanding of knife penetration mechanics developed in this thesis should be extended to cover textiles, mail, and other inhomogeneous structures that might be used in armour. It might be possible to relate indentation to some measure of weave

stability or resistance to parting. Similarly the characteristics of the frictional interaction with a flexible material should be investigated.

It is apparent that the effect upon an armour of being in close contact with the body of the wearer has received very little attention in the scientific literature. As armour becomes thinner more flexible and lighter the support and constraint afforded by the body becomes increasingly important. In both stab resistant and bullet resistant armour the effects of the wearer on the armour are crucial yet appear to be poorly understood. Further analysis should be carried out on the interaction between an armour and its wearer.